cy-8

MARTIN MARIETTA ENERGY SYSTEMS LIBRARIES
3 4456 0049753 0

CENTRAL RESEARCH LIBRARY
DOCUMENT COLLECTION

ORNL-2696
Reactors-Power

HOMOGENEOUS REACTOR PROJECT

QUARTERLY PROGRESS REPORT

FOR PERIOD ENDING JANUARY 31, 1959

OAK RIDGE NATIONAL LABORATORY
CENTRAL RESEARCH LIBRARY
DOCUMENT COLLECTION
LIBRARY LOAN COPY
DO NOT TRANSFER TO ANOTHER PERSON
If you wish someone else to see this
document, send in name with document
and the library will arrange a loan.
UCN-7969
(3 3-67)

OAK RIDGE NATIONAL LABORATORY
operated by
UNION CARBIDE CORPORATION
for the
U.S. ATOMIC ENERGY COMMISSION

Printed in USA. Price $4.00. Available from the

Office of Technical Services
U. S. Department of Commerce
Washington 25, D. C.

LEGAL NOTICE

This report was prepared as an account of Government sponsored work. Neither the United States, nor the Commission, nor any person acting on behalf of the Commission:

A. Makes any warranty or representation, express or implied, with respect to the accuracy, completeness, or usefulness of the information contained in this report, or that the use of any information, apparatus, method, or process disclosed in this report may not infringe privately owned rights; or

B. Assumes any liabilities with respect to the use of, or for damages resulting from the use of any information, apparatus, method, or process disclosed in this report.

As used in the above, "person acting on behalf of the Commission" includes any employee or contractor of the Commission to the extent that such employee or contractor prepares, handles or distributes, or provides access to, any information pursuant to his employment or contract with the Commission.

ORNL-2696
Reactors-Power
TID-4500 (14th ed.)

Contract No. W-7405-eng-26

HOMOGENEOUS REACTOR PROJECT QUARTERLY PROGRESS REPORT FOR PERIOD ENDING JANUARY 31, 1959

Project Director	R. B. Briggs
Associate Director	C. E. Winters
Homogeneous Reactor Test	S. E. Beall
Reactor Analysis and Research	R. N. Lyon
Engineering Development	R. N. Lyon
Reactor Materials Research	E. G. Bohlmann
Chemical Engineering Development	D. E. Ferguson
Supporting Chemical Research	H. F. McDuffie
Analytical Chemistry	M. T. Kelley

DATE ISSUED

APR 2 1959

OAK RIDGE NATIONAL LABORATORY
Oak Ridge, Tennessee
operated by
UNION CARBIDE CORPORATION
for the
U. S. ATOMIC ENERGY COMMISSION

MARTIN MARIETTA ENERGY SYSTEMS LIBRARIES
3 4456 0049753 0

SUMMARY

PART I. HOMOGENEOUS REACTOR TEST

1. HRT Operations

Most of November was occupied with completion of the inspection and maintenance activities which followed run 17. These activities included recovery of 12 more corrosion specimens from the core tank, installation of a new corrosion-specimen holder in the blanket region, and installation of a new inlet pipe from inside the core tank to the chemical plant. In addition, several changes in reactor instrumentation were made to provide additional reactor safety in case of sudden reactivity additions. The reactor piping was again hydrostatically tested at nearly 3000 psia without leakage; the container was retested at 30 psia, and the leak rate was satisfactorily low at 4 liters/min.

Reactor run 18 was designed to study the problems of fuel instability as indicated by loss of circulating uranium, sudden power excursions, or gradual changes in the composition of the fuel solution. These three factors were observed closely over the 1200-hr (350 Mwhr) operating period of run 18. Although the data scattered badly, there did not appear to be a loss of uranium inventory greater than 400 g at 1.5 Mw; no power disturbances were observed in any portion of the run; changes in solution composition were so small as to be inconclusive, although slight losses of uranium and copper were indicated.

2. HRT Processing Plant

Three hydroclone loop runs (more than 750 hr) have been completed in HRT run 18 with the newly installed take-off through the core dip pipe. Solids removal rates at low reactor power were slightly higher than in previous runs. In the first 106 hr--the D_2O portion of the run--273 g of corrosion products, analyzing 47% Zr, 21% Fe, and 3% Cr, were collected. The zirconium content of solids removed in the next 335 hr dropped to 38%, and a total of 613 g of solids was collected. Uranium and copper in the solids averaged about 4% and 1.5%, respectively.

The rotor of the circulating pump locked during rinse operations following the first 106-hr run. The pump was replaced with a spare, by normal underwater maintenance techniques.

Values for total zirconium corrosion through run 17, calculated according to three independent methods, are in reasonable agreement. By assuming that the hydroclone removes a representative portion of all corrosion-product solids present, zirconium corrosion can be related to known stainless steel corrosion rates. According to this relationship, and also by means of the direct measurement of a 40-mil reduction in core wall thickness, a total of 29 kg of ZrO_2 is calculated to have been produced. Also, if it is assumed that equal fractions of fission-product zirconium and corrosion-product zirconium are collected by the hydroclone, the total ZrO_2 formation may be calculated accordingly. Corrosion indicated by this third approach has differed from run to run by approximately 50 to 100% from that calculated according to the preceding methods.

3. HRT Reactor Analysis

Recent calculations indicate that small deposits of uranium on the core wall could lead to melting of the zirconium in contact with the uranium. At a core power of 6.4 Mw, the uranium-bearing-scale thickness required for the core to reach the melting point appears to be about 50 mils for a scale containing 2 g of U^{235} per milliliter and covering a wall area of about 3 in.^{2}.

The power response of the HRT following a reactivity addition has been calculated for various initial powers, on the basis that 40% of the reactor power is generated in the blanket. At an initial total power level of 1 Mw, the peak power following a reactivity addition of 0.5% Δk_e was about 4 Mw.

The critical mass in HRT-type reactors (blanket containing only moderator) was calculated for various core diameters and H_2O-D_2O compositions. The smallest core diameter which would permit a uranium concentration less than 10 g/liter at 280°C was about 29 in.; this minimum diameter occurred when the moderator contained 85% D_2O.

The effect of core and blanket temperature upon critical concentration was calculated for HRT-type reactors containing only moderator in the blanket. The critical concentration with the core at 300°C and the blanket at 250°C appears to be slightly less than the critical concentration with the core and blanket at 280°C.

4. HRT Design

Preliminary cost estimates indicate that an HRT replacement reactor-vessel assembly of all-welded design would cost about $500,000; the cost of a duplicate would be $326,000. A vessel design to allow removal of the core would cost $575,000, and an extra core and head would cost $186,000.

The thorium (0.01%) and natural uranium (0.001%) in Zircaloy-2 contribute less than 0.005 w/cc to the heating of the HRT core wall.

A projected-light viewer, capable of accommodating tools for remote maintenance, was designed for use at the HRT.

5. Development of HRT Components and Remote Operations

Testing of four prototype HRT feed and purge pump heads was continued up to a total of 14,000 to 16,000 hr per head.

Operation of the HRT core model with modified configurations indicated that reversal of the direction of flow would improve the heat transfer at the core wall and permit solids to be removed. Testing of the annular-inlet type of HRT replacement core was continued; to date it has not been possible to achieve a stable flow pattern which also permits complete removal of solids.

Design and testing work was started on a core-wall thickness gage, a radioactive solids sampler, a remote impression device, methods for removing the diffuser screens from the HRT core, and methods for patching the defect in the core-tank wall.

The HRT mockup, while continuing the test of a titanium pressurizer and feed heater, was operated for 1663 hr during the quarter on a fuel composition of 0.045 m UO_2SO_4, 0.036 m $CuSO_4$, and 0.025 m H_2SO_4. This solution has a heavy-phase formation temperature of 330°C.

The system was pressurized by boiling the solution in the pressurizer at temperatures from 313°C (1500 psi) to 336°C (2000 psi), and the heavy phase was formed and dissolved at will by controlling the temperature. Performance was satisfactory at all conditions.

A 0.021-in.-thick feed-pump diaphragm failed after 12,153 hr of operation. The titanium letdown heat exchanger and three titanium-to-stainless-steel transition flanges have been in service 6092 hr without leakage.

6. HRT Controls and Instrumentation

The present reactor letdown valve has now operated satisfactorily for 3000 hr. However, a smaller valve undergoing test in the HRT mockup loop has operated 3400 hr and is considered to be more suitable for the present reactor operating conditions. Both valves have 17-4 PH stainless steel plugs and integral 347 stainless steel seats.

A sample quantity of improved design end-seals for the mineral-insulated cable now used in the reactor power wiring system was purchased for evaluation.

An improved experimental shield-solenoid mechanism was fabricated in an attempt to improve the reliability of the remote-area radiation-monitoring sensors utilized to detect radiation leakage into reactor auxiliary systems.

A list of revisions to the instruments and controls system is given, and maintenance experience for some of the components is described.

PART II. REACTOR ANALYSIS AND RESEARCH

7. Research and Analysis

The effects of core-vessel thickness on the ratio of U^{235} to Th required for criticality (critical-mass ratio) and the reactivity worth of the reflector were calculated for several slurry-core reactors. For a reactor having a moderator composition of 90% D_2O - 10% H_2O, a pressure-vessel inside diameter of 5 ft, a core diameter of 2 1/2 ft, and a core thorium concentration of 400 g/liter, increasing the core-tank thickness from 3/16 in. to 1 in. increased the critical-mass ratio from 0.066 to 0.088 g of U^{235} per g of Th (200°C). For a 1/2-in. core-wall thickness, dumping the reflector would remove sufficient reactivity to cause the reactor to be subcritical at 20°C as a bare reactor.

The amount of natural boron required to decrease the critical temperature from operating conditions to 20°C was calculated for three slurry reactors. In a 12-ft-dia core-region thorium breeder (150 g of Th per liter), about 50 ppm of boron would decrease the critical temperature from 280 to 20°C; in a 4 1/2-ft-dia reactor containing 200 g of Th per liter, the corresponding boron concentration was 550 ppm; in a 2 1/2-ft-dia reactor containing 400 g of Th per liter, about 700 ppm of boron would decrease the operating temperature from 200°C to 20°C.

The tube diameter of the high-temperature (200°C) vertical-tube viscometer was successfully calibrated.

At room temperature the yield stress of a given thoria suspended in methanol was several times less than when the thoria was suspended in water at the same concentration.

Heat transfer under nucleate-boiling conditions was studied for ThO_2-H_2O slurries containing up to about 1000 g of Th per liter. For concentrations up to about 200 g of Th per liter, the presence of thoria does not appear to influence the rate of heat transfer; at a concentration of 1000 g of Th per liter, the maximum heat transfer rate (at "burnout" conditions) was 210,000 Btu/hr-ft^2 compared with 490,000 Btu/hr-ft^2 for water under corresponding conditions.

Thoria caking studies indicated that slurries have less tendency to form cakes and spheres at 50°C than at temperatures greater than 200°C, and also less tendency at a thorium concentration of 75 g per kg of H_2O than at concentrations greater than 100 g/kg. Cakes are more easily formed on surfaces exposed to low fluid velocities (5 fps) than on those exposed to high velocities (20 fps), but if cakes are formed on all surfaces, those formed in the higher velocity regions are more adherent.

The stress in a two-radii contour diaphragm pump was calculated as a function of the ratio of the two radii. A criterion was developed for calculating the largest possible displacement for a specified value of the diaphragm stress; for this condition an optimum ratio of the two radii exists.

PART III. ENGINEERING DEVELOPMENT

8. Development of Fuel- and Slurry-System Components

Following replacement of a Bourdon tube, the natural-circulation recombiner was operated at 1500 psi very satisfactorily.

Work on the Reliance 6000-gpm top-maintenance pump was stopped, pending further negotiations with the vendor, who may withdraw from the canned-motor pump field. A test stator has been irradiated to 2.8×10^9 rad without serious deterioration. The 300A pump circulated slurry satisfactorily for 1200 hr, testing various impeller vane shapes and aluminum oxide bearings. Startup of the 200Z slurry pump was delayed by a stator failure. Design and fabrication of hydraulic and bearing components for testing in slurry pumps was continued.

A three-stage compressor for contaminated oxygen passed its factory tests prior to being set up for endurance tests at ORNL. Two 2-gpm diaphragm heads continued to pump solution without incident. Except for check-valve wear, two diaphragm heads for slurry use operated without difficulty through the quarter. Foaming was observed in the slurry pump system as a result of the release of dissolved gas; control of foaming by boiling and its elimination with the addition of a small amount of phosphoric acid was demonstrated.

By use of a tungsten-carbide-trimmed throttling valve, 200 slurry samples were withdrawn from a 1500-psi loop before a valve leak occurred. Satisfactory continuous service was obtained from two throttling chokes which let slurry down from 1300 to 1500 psi.

It was not possible to produce permanent slurry plugs in an inverted-L tube bundle when circulating a flocculated slurry.

Tests of a 30-in.-dia core model having a conical bottom were made in order to maximize the wall shear as a function of the distance of insertion of the inlet nozzle.

The effect of a 100-v d-c potential applied to a settled bed of thoria was to attract and repel water from the electrodes; the slurry particles did not plate out on either electrode.

9. Development of Reactor Slurry Systems

The handling characteristics, rheological properties, attack rate, and stability of mixed thoria-urania slurry under conditions anticipated in a proposed experimental slurry-reactor were examined in run 200A-18, which operated for 1026 hr. The slurry appeared to be stable, was easily circulated, and exhibited almost negligible attack on the pump parts and loop piping. On completion of the run, the slurry drained freely from the loop, and the residue was easily washed from the loop.

The 200B loop was completed and placed in operation. It differs from the 200A loop in two respects:

1. Instead of a single, horizontal flow circuit, three parallel, vertical flow paths are provided from a horizontal discharge header. These lines are 1-in. sched-80, 1 1/2-in. sched-80, and 2-in. sched-160 pipes, approximately 12 ft long, and are equipped with valves.

2. The pressurizer is equipped to operate as either a gas or a steam pressurizer.

A heat-transfer meter located in the 1-in. leg provides information regarding the formation of slurry films or scale on the pipe wall, an important factor in the design of heat exchange equipment and the reactor vessel. The loop is operating with a slurry of mixed thoria-urania (210 g of Th per kg of H_2O) for comparison with the recently completed run 200A-18.

The 30-in.-dia experimental pressure vessel is being installed in the 300-SM loop for the study of slurry behavior under re-entrant flow at reactor operating temperature and pressure. A flowsheet of the high-pressure circulating loop is included. A low-pressure system containing a dump tank of new design is also under construction for use with the high-pressure loop. A flowsheet of the low-pressure system is also presented.

In order to obtain guidance as to the best initial flow pattern for the 300-SM pressure vessel, a series of flow and distribution tests was made in a 6-in. transparent model of identical shape. The tests were made with a rapidly settling thoria slurry, which showed that re-entrant flow at the bottom, with the top head-closure contoured to complete the upper hemisphere, was superior to straight-through flow in either direction and showed promise of meeting design criteria for a circulating-slurry reactor core.

Tests were continued on the measurement of slurry density by means of gamma-ray transmission, using modifications of commercial equipment. Room-temperature measurements on a rapidly settling slurry were reproducible and accurate. Measurements of the density of circulating water over the range of 20 to 200°C agreed with the known density at the temperatures of measurement.

The possibility of studying the nuclear criticality aspects of a low-power circulating-slurry system was investigated. The system is proposed for contruction in Building 7503.

10. Instrument and Valve Development

The differential transformers being developed for use at high temperature and in radiation fields were redesigned to reduce the effects of winding-form resistance and potting-insulation changes.

Two pressure transmitters which are now commercially available and incorporate a secondary pressure seal were evaluated as to suitability for HRP applications and found to be very satisfactory.

Life testing of two types of all-metal control-valve actuators (single, 40 in.^{2}; dual-stacked, 123 in.^{2}) was concluded. Both units proved satisfactory for HRP applications.

PART IV. REACTOR MATERIALS RESEARCH

11. Solution Corrosion

A number of tests were made during the quarter to study the deposition of uranium, copper, and nickel sulfates from dilute simulated fuel solutions circulated through a heated Zircaloy-2 pipe section in a 100A pump loop. With the heated pipe mounted in a nearly horizontal position, loss of salts from solution was observed in all cases when boiling of the solution occurred. When the dissolved oxygen concentration of the solution was reduced from 1000 to 20 ppm, loss of salts from solution was still observed under boiling conditions.

When the orientation of the heated Zircaloy-2 bypass was changed from its nearly horizontal position to a vertical position with the flow from top to bottom, no salts were lost from solution even under conditions of vigorous boiling and at metal wall temperatures in excess of 400°C.

Observations in a glass mockup of the bypass indicate that the tube wall was continuously wet when in the vertical position; whereas in the horizontal position a vapor space formed in the upper part of the tube which prevented its being wetted by the solution. Thus deposited solids or liquids were washed away in the vertical arrangement but could build up on the heated, unwetted part of the pipe in the horizontal arrangement.

Additional out-of-pile tests were carried out in an in-pile loop in which the metal wall of the core section was heated. This loop is approximately 1 liter in volume and contains a 5-gpm canned-rotor pump. For conditions of fluid flow and core wall temperature at which boiling occurred at the core wall, loss of salts from solution by deposition on the core wall was observed. It was noted that increasing the excess sulfuric acid concentration of the solution appeared to inhibit the salt deposition. However, deposition of salts occurred at the higher acid concentrations when the core wall heat flux was increased to obtain more vigorous boiling.

Two different hydroclone mountings on a 100A loop have been tested to determine the effectiveness of each mounting in removing corrosion products from the loop. In one case the inlet line to the hydroclone was joined to the main loop piping by a perpendicular tee near the pump discharge. In the second case the inlet line to the hydroclone was attached to the bottom of the pressurizer so that particles could "fall" into the hydroclone. In each case only about 10% of the corrosion products originating from the corrosion in the loop were collected in the hydroclone underflow pot. Most of the corrosion products collected as a tightly adhering film on all interior surfaces of the loop.

Chemical stability tests were run at 300°C on a solution containing 0.025 m UO_2SO_4, 0.2 m Li_2SO_4, 0.1 m D_2SO_4, and 0.02 m $CuSO_4$ and on one identical to the first except diluted by a factor of 3. Both solutions were unstable during 200-hr loop runs; the concentrated solution lost 80% of its copper and none of its uranium, whereas the dilute solution lost 90% of its copper and 60% of its uranium. In a third run 0.2 m $MgSO_4$ was substituted for the 0.2 m Li_2SO_4 of the first solution. The resulting solution lost 20% of its copper and 6% of its uranium during circulation at 300°C. Increasing the acid concentration would result in greater solution stability, but tests showed that the increased acid made the solution very corrosive, particularly in crevice areas.

The addition of fluoride ions to oxygen- and chloride-containing phosphate-treated boiler water did not suppress stress-corrosion cracking of type 347 stainless steel.

The pretreatment of U-bend specimens of type 347 stainless steel in a solution containing 0.04 m UO_2SO_4, 0.02 m H_2SO_4, and 0.005 m $CuSO_4$ at temperatures ranging from 100 to 300°C inhibited stress-corrosion cracking of the specimens when they were subsequently exposed to solution containing chloride ions. Specimens from one heat of an alloy which cracked 50% of the time without pretreatment were completely resistant to cracking after pretreatment; specimens from a different heat of an alloy which cracked 100% of the time in the absence of pretreatment cracked only 15% of the time after pretreatment.

Stressed specimens of cast type 347 stainless steel have shown a high resistance to stress-corrosion cracking in chloride environments. To date, only one small crack (4 mils deep) has been found, and it

resulted from a 1500-hr exposure to a solution containing 100 ppm chloride and oxygen at 300°C for 1500 hr. Under the same conditions wrought type 347 stainless steel specimens develop many, much deeper cracks during tests of 500 hr or less.

Zircaloy-2 was practically unaffected by the heavy phase of a high-temperature uranyl sulfate solution. The presence of copper in the heavy phase did not make it more corrosive.

In 100-hr tests at 250°C, titanium was not corroded significantly by oxygen-free uranyl sulfate solutions, and no definite evidence of solution instability was observed.

The corrosion rate of Incoloy 804 was found to be tolerable but greater than that of type 347 stainless steel in uranyl sulfate solutions in the temperature range of 100 to 300°C. Tests with Electrolyzed coatings on type 304 stainless steel (a proprietary process for depositing hard, chromium-rich deposits on metal surfaces) have shown that the deposited layer dissolves from the surface in high-temperature, oxygenated, aqueous environments and hence is of little value in high-temperature fuel systems. However, at 100°C in the absence of chloride ions, the Electrolyzed coating is stable and could conceivably be useful where a hard surface is necessary.

12. Slurry Corrosion

Dynamic corrosion and slurry-property data are reported for four tests in 100A pump loops; two were carried out to evaluate slurries of two thoria preparations proposed for an in-pile slurry-loop program.

The first of these tests, of 1298-hr duration, was divided into three phases: an initial phase of 485 hr in an oxygen atmosphere; a second phase of 478 hr in a deuterium atmosphere; and a final phase of 335 hr in an oxygen atmosphere. A slurry of 2.4-μ, 1600°C-calcined thoria, ~0.005 m in MoO_3, was circulated at 280°C at an average concentration of 446 g of Th per kg of D_2O. The mean 1298-hr attack rate of the stainless steel loop piping was < 0.3 mpy. The room-temperature yield stress and modulus of rigidity were increased and the high-temperature settling rates of the slurry were diminished after pumping in the deuterium atmosphere.

In the second loop test, which is still in progress, a slurry of 650°C-calcined, 0.8-μ thoria to which UO_3 and palladium metal catalyst were added was circulated for 508 hr in an argon atmosphere. The average thoria concentration was 427 g of Th per kg of D_2O. An increase in the amount of deuterium, resulting from corrosion, was noted. Dropout of slurry was observed at 2.5 fps, with satisfactory resuspension at 4.6 fps. The mean attack rate of the stainless steel loop components was 0.9 mpy.

In addition, two loop runs were made at 200°C to compare the attack rates of a group of selected alloys in a slurry of 1600°C-calcined thoria with and without the addition of $UO_3 \cdot H_2O$. The tests, made at a slurry concentration of approximately 500 g of Th per kg of H_2O, in an oxygen atmosphere, indicated higher attack rates for the ThO_2-UO_3 slurry. The increase may be associated with degradation of the $UO_3 \cdot H_2O$ rods.

The inclusion of substantial proportions of uranium oxide in thoria calcined at 650°C reduced the corrosion of various metals under an oxygen and a deuterium atmosphere in 300-hr toroid tests at 280°C and 26 fps. The slurries consisted of 500 g of Th-U per kg of D_2O, with and without 0.008 m MoO_3. The normalized reference-corrosion-rate for type 347 stainless steel pins was 4 mpy for thoria containing no urania, and under an oxygen atmosphere. The corrosion rates of Ti-75A and Zircaloy-2 were averaged factors of 0.5 and 0.15, relative to this rate of 4 mpy. The effect of the deuterium atmosphere on these materials was to increase corrosion by an average factor of 2. The MoO_3 effect was trivial. With increasing uranium content, the corrosion of these metals was reduced in proportion to the following average factors:

0% U, 1.0; 5% U, 0.7; 9% U, 0.3; 11% U, 0.2; and 33% U, 0.08.

The normalized corrosion rate of Inconel under an oxygen atmosphere and with thoria containing no urania was 12 mpy. Under a deuterium atmosphere, the corrosion rate was 5 mpy. There was no particular effect of urania content on the corrosion of Inconel under an oxygen atmosphere; while under deuterium, the effect of increasing the urania content roughly paralleled the effect given for other metals above. The attack on Inconel under an oxygen atmosphere appeared to be dominated by water corrosion rather than by erosion.

Toroid runs were made to evaluate oxygenated slurries of thoria prepared by the Davison Chemical Company in which two experimental preparations, each calcined at 650, 1000 and 1200°C, were tested. There were normal differences in the response of the various metals. The normalized reference-corrosion-rate for type 347 stainless steel pins was 5 mpy at a concentration of 500 g of Th per kg of H_2O, using the oxalate preparation. The large particle, hydroxide precipitated thoria was much less aggressive than the oxalate preparation. Deposition of thoria on specimen surfaces was observed for all but the 650°C-calcined thoria obtained by oxalate precipitation.

A description is given of a device which was developed to enable a known pressure of a desired gas to be charged into a toroid.

Two HB-6 type rocking-autoclave experiments were prepared and operated in beam hole HB-6 of the LITR in order to obtain radiation-corrosion data for thorium oxide slurries. One of these is presently in operation. Both experiments contained thorium oxide slurry plus

enriched uranium oxide (5 wt % U based on Th), with D_2O as the dispersant. One experiment was at a concentration of about 400 g of Th per kg of D_2O and utilized MoO_3 as the recombination catalyst. The other was at 1000 g of Th per kg of D_2O and used palladium as the catalyst. Both experiments were pressurized with oxygen and were operated at 280°C.

Irradiation of experiment L6Z-127S has been completed. The autoclave was loaded with thoria-urania containing 5 wt % of enriched uranium, based on a thorium concentration of 400 g of Th per kg of D_2O. The catalyst concentration was 0.01 m MoO_3, and an oxygen atmosphere was used. The experiment operated out of pile for 174 hr and in pile for 948 hr at an average fission power density of 0.5 w/ml. The maximum power density achieved was 1.9 w/ml. Initially, the experiment exhibited a catalytic activity of only 0.034 moles of D_2 per liter-hr at 100 psi deuterium, but after 110 hr the catalytic activity had increased to 0.26 moles per liter-hr at 100 psi deuterium. Subsequent operation indicated some decline and then an upswing in the catalytic activity. The G_{D_2} values, 0.74 to 0.92, were obtained in the early portion of the experiment. Again, later operations gave lower and then higher G_{D_2} values. The corrosion rate for the first week in pile was 1.7 mpy at an average fission power density of 0.4 w/ml. The over-all corrosion rate was 0.7 mpy at an average fission power density of 0.5 w/ml.

A sintered-metal filter unit has effectively separated water from thorium oxide slurries in tests in an in-pile development loop. During test runs in which 900 hr of operating time was accumulated, the filter unit prevented the accumulation of thorium oxide in the loop pressurizer by removing the thorium oxide from the pressurizer feed stream. These tests were at temperatures up to 250°C, with slurry concentrations up to 500 g of Th per kg of H_2O.

13. Radiation Corrosion

In a speculative hypothesis to account for the instability of the HRT solution, metal surfaces in the reactor core are heated above the temperature of the bulk solution by an amount sufficient to cause boiling at the surface. The boiling results in a deposition of UO_2SO_4 and other salts, and the deposited material produces still higher temperatures which accelerate further deposition. The temperature at which boiling occurs is less than the temperature at which the vapor pressure of heavy water equals the total pressure on the solution because part or all of the pressure of dissolved gas is included in the vapor pressure of the solution.

Experiments designed to test this hypothesis were carried out with an in-pile loop. Three different solutions were employed, each with D_2O solvent and 0.036 m UO_2SO_4. The other constituents were:

	$CuSO_4$ (m)	H_2SO_4 (m)	Li_2SO_4 (m)
First solution	0.006	0.016	
Second solution	0.006	0.027	
Third solution	0.0014	0.09	0.18

Normal operating conditions with each solution included main-stream and pressurizer temperatures of 280 and 295°C, respectively, and a pump frequency of 60 cps. For all but one of 13 experiments, the pump frequency was reduced to 20 cps to establish a flow rate of about 0.3 fps in the core annulus. The main-stream temperature was held constant at 280°C for all experiments. Radiation-absorption heating in the loop core wall at the nose was at the rate of about 0.4 w/g and was sufficient to establish the desired test condition of a metal-surface temperature greater than the temperature of the bulk solution.

Scouting type experiments were made with solution 1 to determine whether deposition of uranium in the loop core could be produced at low overpressure with the 0.3-fps flow rate. Deposition of uranium was observed when the pressurizer temperature was reduced. Additional experiments were made to define the pressure conditions at which the deposition effect occurred. Other experiments were made to test the effect of a higher flow rate (about 0.8 fps) in the core and, with solutions 2 and 3, the effect of composition on the deposition.

The general results obtained with solution 1 as the pressurizer temperature was lowered from 295°C were the following: At some reduced overpressure, the temperature indicated by each of the two thermocouples attached to the core nose started to rise. At the same time, the electrical power required by the loop heater to maintain the 280°C main-stream temperature started to drop. When the change was initiated, the nose temperature and loop power continued to change until some corrective action was taken. In many of the experiments, the temperature indicated by the core-nose thermocouples decreased by about 0.5°C prior to the rise in temperature and to the decrease in heater power.

The results obtained with the single experiment with solution 2 were similar to those obtained with solution 1. Deposition of uranium was also observed with the lithium-additive solution, but the reduction in overpressure required to produce the effect was greater than that for solution 1.

No deposition was observed in the experiment which employed a solution velocity in the core of about 0.8 fps.

Reduction in LTTR power was effective in redissolving the deposited material.

Solution samples taken during power excursions with solutions 1 and 2 show a reduction of uranium, sulfate, copper, nickel, and manganese from that normally present. Uranium and nickel only were lower in solution 3 excursion samples, but the data for other constituents showed appreciable scatter.

The results obtained with solutions 1 and 2 are consistent with the hypothesis that boiling in the liquid film covering the core-nose surface resulted in the deposition of solids including uranium on that surface. The results also show that this boiling occurs when the total pressure of the solution, including all of the pressure of dissolved gas, is about the same as the pressure on the solution. The results with the solution 3 (lithium additive) are also consistent with the hypothesis that boiling in the core solution resulted in uranium deposition. However, the greater reduction in overpressure required to produce the deposition and also to produce a reduction in the temperature of the outer wall of the core nose indicates that boiling does not occur so readily in this solution as in solution 1.

An in-pile loop for installation in beam hole HN-1 of the ORR is being assembled. All equipment for loop operation has been installed at the reactor.

Three HB-5 rocking-autoclave experiments were assembled and were operated in the LITR to obtain radiation-corrosion data with fuel solutions of interest to the homogeneous-reactor program. In addition, two HB-5 rocking autoclaves were assembled and were operated in the out-of-pile mockup facility to provide a comparison with two comparable in-pile experiments.

An electrochemical method was used to determine the rate of oxidation of Zircaloy-2 in 0.05 m H_2SO_4 containing 600 ppm O_2 at 167 and 208°C. The rate vs time plots at 208°C were characterized by an initial rapid decrease in rate from about 25 mpy, followed by a gradual leveling off to about 0.1 mpy after six days of exposure. An energy of activation of 15 kcal/mole was determined by means of an Arrhenius-type analysis for the corrosion reaction in the temperature range of 208 to 248°C. The Tafel slope for O_2 reduction on platinum in 0.05 m H_2SO_4 containing 600 ppm O_2 at 208°C was measured. The result suggests a different mechanism for O_2 reduction at 208°C from that which has been observed at 25°C.

14. Metallurgy

Metallurgical specimens cut from the screens of the HRT core tank have been examined macroscopically and microscopically. While considerable "corrosion" of the screens was observed, the major weight loss and damage appeared to be due to exfoliation of layers of metal, parallel to the rolled surfaces of the screens, and probably caused by corrosion occurring in the cracks formed during punching of the holes in the screen. No evidence could be found to indicate that the screen

temperature had ever exceeded 600°C, except for one very small area on the top screen. This one exception appeared to be attributable to the proximity of the end of the titanium holder suspended in the core region. Hydrogen and deuterium analyses of screen specimens indicated that deuterium was not picked up during reactor operation.

The titanium specimen-holder inserted in the reactor core during run 17 was received and examined macroscopically. Three "burned" holes were found in one longitudinal web, one at each of the lower three specimen stations. Several areas of bright pits were found, but there was no apparent association to either the welds or heat-affected zones. Approximately 11/16 in. of the tip section of the holder had either melted or corroded away during reactor operation. Specimens cut from the various areas of the holder are now being examined microscopically.

Three Zircaloy-2 specimens, originally located in the titanium specimen-holder, were recovered from the top screen of the core tank. These specimens have been examined macroscopically, and microscopy is in progress. The T-heads of two specimens were burned, apparently because of the events happening to the titanium specimen-holder. Several areas of bright, shiny pits were found on the specimens, with no correlation to any area or feature of the specimens.

Hydride formation on the surfaces of Zircaloy-2 specimens hydrided in the laboratory has been observed to occur as discrete patches, with no hydride on the surface between patches. The patches caused the formation of lenticular twins in the alpha grains bordering the patches.

Chemical machining and pickling studies on Zircaloy-2 have shown that nitric acid contents below 20 vol % appreciably affect the rate of attack of aqueous solutions of hydrofluoric acid. A minimum rate of attack occurs at 3-4 vol % HNO_3, and a maximum at 40 vol %, for an aqueous solution containing 2 vol % hydrofluoric acid solutions. Additions of flocculating agents decreased the rate of attack, while additions of flotation agents increased the rate. The rate of attack on sand-blasted surfaces was initially rapid, but slowed, after a small amount of surface was removed, to the rate typical for pickled surfaces.

A minor loss of ductility was found in titanium samples exposed in the blanket region of the HRT. No, or very small, changes were found in "as received" Zircaloy-2 exposed in the same region, while beta-quenched and welded samples did show small changes.

Experiments in welding the tube-to-header joints with Inconel-clad type 347 stainless steel components have shown a need for a barrier pass between the Inconel and stainless steel layers. Incoloy, Hastelloy W, and INOR-8 show promise as barrier-pass materials; however, a tendency toward weld-crater cracking still exists.

Sound welds of full penetration have been made between titanium (RC-A40) and Zircaloy-2 parts. A maximum hardness of 265 DPH was found in the zirconium-rich region and a maximum of 335 DPH in the titanium-rich zone of the weld. Hardening is thought to have been due to solid-solution effects of the metals rather than to atmospheric contamination.

Recent examinations revealed that seven type 347 stainless steel nipples from slurry loops failed by stress-corrosion cracking. Several variables were found to be common to each of these failures.

The amenability of Zircaloy-2 to fabrication into hemispheres by power spinning has been demonstrated by a study at Titanium Fabricators, Inc. Twelve 15-in.-dia hemispheres, with thicknesses of 1/8, 1/4, and 5/16 in., were spun at a nominal temperature of 1250°F.

A new rig, permitting positioning accuracy of 1/4 in., has been designed for obtaining resonance-thickness measurements of practically all of the HRT core vessel above the screens. A transducer of the "Z" zirconate-titanate ceramic type has been found to have no unwarranted frequency drift after exposure to 10^6 r of x-irradiation.

Attempts to detect embrittlement in welds of titanium or zirconium by means of ultrasonic velocity measurements have not been successful. Concentrations of gases sufficient to cause embrittlement (ppm amounts) did not affect the velocity enough to be measured by available equipment.

The oxygen pressure required for ignition of titanium samples has been shown to be temperature dependent. Modifications in testing techniques have reduced the experimentally determined values of the critical pressure for zirconium ignition by half, and the indications are that this is still not the minimum.

The hardness of irradiated steels has been measured after post-irradiation annealing between 200 and 500°C. The hardness does not decrease monotonically with increasing annealing temperature. Instead, an increase in hardness may be observed when annealing takes place between 200 and 300°C. The annealing behavior is apparently a function of both irradiation temperature and the magnitude of the integrated flux.

PART V. CHEMICAL ENGINEERING DEVELOPMENT

15. Uranyl Sulfate Fuel Processing

Stainless steel and Zircaloy-2 pins partially immersed in simulated HRT fuel solution in quartz tubes and heated inductively so that violent boiling occurred showed evidence of attack in the

liquid-gas interface region but not in areas conpletely submerged in liquid. At a bulk solution temperature below that at which a second-phase transition would occur but with Zircaloy-2 pins heated inductively to produce mild boiling, both liquid and solid second phases were deposited on the metal surface.

Increasing the free acid or nickel content of simulated HRT fuel solutions favored the transition of the uranium-rich second liquid phase to a solid phase. With higher nickel values, this solid phase, when cooled, produced a fine granular solid which redissolved only slowly.

Analysis of HRT solids indicated that such solids may contain as much as 4% uranium. Decontamination of actual HRT fuel solution samples by the uranyl peroxide precipitation method was demonstrated to be satisfactory.

16. Gaseous-Fission-Product Disposal

In hydrogen-oxygen mixtures the concentration of hydrogen at which an explosion will be propagated through a charcoal bed was determined to be between 30 and 78%. When such explosions were followed by a flow of oxygen, combustion of the charcoal was frequently observed. The number of theoretical plates in a charcoal-filled tube used for adsorbing krypton from a flowing oxygen stream was shown to be approximately inversely proportional to the superficial velocity of the oxygen.

17. Equipment Decontamination

Several reagents were successfully used for removal of radioactive oxide scale from HRT pipe specimens. Chromous sulfate (0.5 M) dissolved the scale in the shortest time, 1 hr. Scale was also dissolved by phosphoric acid, by Deoxidine-170 (an inhibited phosphoric acid), and by zinc-reduced uranium sulfate (0.025 M) in simulated HRT fuel. Reagents that removed scale but did not completely dissolve it were Turco 4501 and 4502, alkaline periodate, Turco 4502--periodate mixtures, and alkaline hypophosphite. As decontaminating reagents for ruthenium and niobium on bare stainless steel, alkaline periodate was the most effective tested. Turco 4501-4502 was also very efficient.

18. Thorium Oxide Slurry Development

Three short-term slurry irradiation tests were carried out in the LITR at 300°C to evaluate Westinghouse low-fired thorium oxide and their palladium oxide catalyst preparations. Two tests were with a pumped ThO_2 slurry containing 3% natural uranium and 0.5% U^{235} (to increase power density) and 122 ppm of palladium. No radiolytic gas pressures were noted in either oxygen or deuterium atmospheres. In the third test, with a slurry of unpumped oxide and 145 ppm of palladium at the same power density, there was a small radiolytic gas pressure under an oxygen atmosphere.

Two devices for small-scale evaluation tests of irradiated slurries are under development: an apparatus for measuring slurry settling rates by an ultrasonic pulse echo technique which will determine the location of the slurry interface and a rolling-ball viscometer which will measure slurry viscosity and yield stress. Preliminary data from settling experiments with quartz, ceramic, and barium titanate transducers showed that the ability to detect the interface depended not only on the power of the transducer but also on the freedom of the supernatant from flocs. A ceramic transducer appeared to be best suited. Initial results with the rolling-ball viscometer with both solutions and slurries indicated that this device could be successfully used with small slurry volumes and probably at elevated temperatures.

In out-of-pile studies, to develop a catalyst for the internal recombination of radiolytic deuterium and oxygen in a reactor slurry, pumping under oxygen impaired the catalytic activity of a slurry of 1600°C-fired oxide containing a MoO_3 catalyst. The catalytic activity of a slurry of solids containing palladium recovered from a slurry of 650°C-fired thorium oxide pumped under argon and containing 3% natural uranium showed maximum catalytic activity around 200°C. With the palladium, oxygen in excess of the stoichiometric amount appeared to enhance catalytic activity, while excess deuterium had relatively little effect.

Laboratory studies to determine the effect of the method used in preparing the mixed oxide and the effect of electrolyte concentration on the leaching of uranium by aqueous solutions at reactor temperature showed negligible uranium dissolution in pure water, but appreciable quantities were solubilized by a few hundred ppm of chromate. The ratio of ppm U to ppm Cr in the supernatant of a slurry of 1050°C-fired "carbonate prepared" thorium-uranium oxide (U/Th = 0.08) autoclaved at 280°C was about 2.6 over the soluble chromium concentration range of 125 to 1330 ppm.

An investigation of the use of boric acid as a soluble poison in fuel slurries to control criticality is under way. With a slurry (270 g of Th per kg of H_2O) of the 650°C-fired mixed oxide and initial boron concentration 33% in excess of the amount required for non-criticality (370 ppm boron in supernatant), the solids/supernatant distribution was minimum around 200°C, the expected reactor operating temperature. At this temperature the ratio, grams of boron per gram of solid to grams of boron per gram of water, was 0.6 and the solids boron content was 17 mg per gram. With the 1100°C-fired oxide and at the same temperature and slurry composition, the solids boron content was negligible and very much less than the 0.029 mg of boron per gram of solids which could be tolerated in reactor operation. While the use of such a method for criticality control appears feasible with a slurry of high-fired oxide, failure of the boron to be desorbed from the low-fired solids during poison removal may prevent its use with slurries of low-fired oxide.

Oxide preparation development studies included further work on particle-size control in the oxide production facility at the Pilot Plant, continued development of flame denitration methods for the production of mixed thorium-uranium oxides, and further work on the production of thoria spheres by the fluidized-bed denitration of thorium nitrate solutions. The present procedure for large-scale oxide production in the Thorium Oxide Facility appears capable of producing 185-lb batches of oxide having a mean particle diameter within ± 0.3 μ for any size between 2 and 3 μ. Mixed-oxide products from flame denitration of alcohol solutions of the nitrate had surface areas of 7 to 8 m^2/g and average particle sizes between 0.8 and 3.1 μ.

Twenty-two hundred pounds of slurry oxides was prepared for engineering slurry studies: 120 lb of pure thorium oxide, both 650- and 1600°C-fired, 100 lb of mixed oxide containing 0.5% natural uranium and 900 lb of mixed oxide containing 8% depleted uranium.

19. In-Pile Slurry Loop

Consequent to the decision of the PAR (Pennsylvania Advanced Reactor) project to discontinue development of the proposed slurry reactor, work at Westinghouse on the in-pile slurry loop was discontinued and work at ORNL on the reactor facilities for accommodating the loop has been suspended. Fabrication and construction are approximately 75% complete. A hydroclone transfer system for charging or unloading an in-pile loop was mocked up; it satisfactorily demonstrated the transfer of more than 99% of the slurry.

PART VI. SUPPORTING CHEMICAL RESEARCH

20. Aqueous Systems at Elevated Temperatures

By means of an approach involving the establishment of key solubility points, sufficient data for the five-component system UO_3-CuO-NiO-SO_3-H_2O (D_2O) at 300°C were obtained that preliminary skeletal phase diagrams could be drawn from 0.04 to 0.2 m total SO_3. With this information, starting solution compositions can be picked so that by increasing nickel concentration to exceed a solubility boundary, nickel or copper compounds (rather than a uranium compound) will saturate the solution and appear as solid phases.

Experiments were performed to show that particular HRT core and blanket compositions in the absence of localized boiling were phase-stable to 500°C with respect to precipitation of solids. Other experiments were performed in a study of the effect of temperature gradients between dilute and concentrated UO_2SO_4 solutions. These experiments, which were performed in a manner permitting transfer of water from the concentrated to the dilute solution, simulating localized boiling that could occur if heavy phase separates in the core of the reactor, demonstrated that concentrated UO_2SO_4 solutions

cannot exist in vapor-pressure equilibrium with water at 270°C if the temperature of the concentrated solution is about 290 or 300°C. If the temperature difference between dilute and concentrated solutions exceeds 25 or 30°C, a solid phase, presumably UO_2SO_4 hydrate, appears in the concentrated solution. This compound is converted at higher temperature to an anhydrous uranyl sulfate which appears to be stable up to 880°C.

Comparative investigations of the UO_3-SO_3-H_2O (D_2O) system at 300°C indicated that there is not much difference in solubility behavior in H_2O and D_2O from 0.01 to 0.1 m SO_3.

The compositions in the liquid-liquid immiscibility region of the system UO_3-SO_3-H_2O were determined at 300, 325, and 350°C for stoichiometric UO_2SO_4. These data show the concentrated phase to be most nearly stoichiometric UO_2SO_4 and the light phase to have a considerable amount of excess free H_2SO_4.

21. Reactions in Aqueous Solutions

The previously obtained chemical evidence, that the HRT analytical method for determining free acid was unsatisfactory, was supported by further studies and confirmed by statistical analysis of the analytical control data for the period of HRT run 17-A. A new method, offering promise of overcoming some of the former difficulties, was devised and submitted for consideration. Interfering copper, uranium, and nickel ions are separated on a cation resin column initially in the lithium form; dilute lithium sulfate elutes the hydrogen ions without removing the interfering ions to produce an eluate in which there is no interference with the acid determination.

Isotopic exchange studies of the mechanism of homogeneous catalysis of reactions between dissolved hydrogen and cupric salts have been initiated.

PART VII. ANALYTICAL CHEMISTRY

22. Analytical Chemistry

A method was devised for the determination of U(IV) in mixtures of thorium oxide and uranium oxide which contain from 3 to 30% uranium. The coefficient of variation of the method for U(IV) within the range of 25 to 50 mg is about 1%. A flame-photometric method was developed for the determination of neodymium in solutions of UO_2SO_4 which contain copper and corrosion products of stainless steel. For samples which contain varying amounts of uranium and neodymium within the range of 20 to 100 μg/ml, the coefficient of variation was found to be about 10%. A fusion-pyrolysis technique was shown to be satisfactory for the separation of chloride from high-fired ThO_2, even at concentrations as low as 1 to 3 ppm.

CONTENTS

SUMMARY iii

PART I. HOMOGENEOUS REACTOR TEST

1. HRT OPERATIONS 3
   1.1 Reactor Operations 3
      1.1.1 Operations Preliminary to Startup 3
      1.1.2 Run 18 4
   1.2 Reactor Analysis 5
      1.2.1 Study of Fuel Stability 5
      1.2.2 Corrosion 7
      1.2.3 Measurements of Concentration Required for Criticality at Various Temperatures 7
      1.2.4 Steam System 7

2. HRT PROCESSING PLANT 12
   2.1 Hydroclone System 12
      2.1.1 Circulating-Pump Failure and Replacement 12
      2.1.2 Corrosion-Product Solids Collected 13
      2.1.3 Concentrations of Uranium, Copper, and Nickel 15
      2.1.4 Fission-Product Activity Distribution 15
   2.2 Activity Released from Waste Pond 16

3. HRT REACTOR ANALYSIS 18
   3.1 Hole Formation in the HRT Core Tank 18
   3.2 Calculations of HRT Power Response Following Reactivity Additions 19
   3.3 Critical Mass in HRT-Type Reactors Utilizing D_2O-H_2O Mixtures 19
   3.4 Effect of Core and Reflector Temperatures on Critical Concentrations in HRT-Type Reactors 20

4. HRT DESIGN 23
   4.1 Cost Estimates for Replacement Pressure Vessel 23
   4.2 Heat Generation in the HRT Core Wall Due to the Presence of 0.01% Thorium and 0.001% Natural Uranium in the Metal 23
   4.3 Projected-Light Viewer 23

5. DEVELOPMENT OF HRT COMPONENTS AND REMOTE OPERATIONS 26
5.1 Feed-Pump Endurance Testing 26
5.2 HRT Core Studies 26
5.2.1 Modifications to Present Core 26
5.2.2 HRT Replacement Core 27
5.2.3 HRT Replacement Blanket 27
5.3 Thermal Shock of HRT Flanges 28
5.4 Remote Operations and Development 28
5.4.1 Core-Wall Thickness Gauge 28
5.4.2 Remote Impression Device 28
5.4.3 Removal of Diffuser Screens from the HRT Core 28
5.4.4 Patching of the Defect in the HRT Core Tank 29
5.5 HRT Mockup 29
5.5.1 Operation 29

6. HRT CONTROLS AND INSTRUMENTATION 33
6.1 Component Development 33
6.1.1 Letdown Valves 33
6.1.2 End-Seals for Mineral-Insulated Cable 33
6.1.3 Remote-Area Gamma-Monitoring System 33
6.2 Maintenance and Modifications 34
6.2.1 Control Valves 34
6.2.2 Electric Power Distribution System 34
6.2.3 Revisions of the Controls and Instruments System 34

PART II. REACTOR ANALYSIS AND RESEARCH

7. RESEARCH AND ANALYSIS 39
7.1 Effect of Core-Vessel Thickness on the Nuclear Characteristics of Reflected and Bare Slurry Reactors 39
7.1.1 Effect of Core-Vessel Thickness on Critical-Mass Ratios 39
7.1.2 Effect of Dumping the Reflector 40
7.2 Reactivity Compensation by Addition of Neutron Poisons to Slurry Reactors 40
7.3 Thoria-Slurry Rheology 42
7.3.1 High-Temperature Viscometer 42
7.3.2 Pseudo High-Temperature Slurries 43
7.4 Nucleate-Boiling Heat Transfer in Aqueous-Thoria Slurries 43
7.5 Thoria Caking Studies 45
7.5.1 Effect of Temperature on ThO_2 Cake Formation 45
7.5.2 Circulation of Oxide Previously Autoclaved with HNO_3 47
7.5.3 Circulation of ThO_2 at Low Concentrations 47
7.6 Diaphragm -Pump Stress Studies 48

PART III. ENGINEERING DEVELOPMENT

8. DEVELOPMENT OF FUEL- AND SLURRY-SYSTEM COMPONENTS 55
- 8.1 High-Pressure Recombiner Loop 55
- 8.2 Centrifugal Pumps 55
  - 8.2.1 20-cfm Allis-Chalmers Blower 55
  - 8.2.2 Reliance 6000-gpm Pump 55
  - 8.2.3 300A Slurry Pump and Loop 56
  - 8.2.4 200Z Slurry Pump and Loop 56
  - 8.2.5 Hydraulic Design of Slurry Pump 56
  - 8.2.6 Test Program for Bearings Operating in Slurry Pumps 56
  - 8.2.7 Shaft Seals 56
- 8.3 Feed Pumps 57
  - 8.3.1 Oxygen Compressors 57
  - 8.3.2 Increased-Capacity Solution Pump 57
  - 8.3.3 Slurry Feed Pumps 57
- 8.4 Valve Trim 58
  - 8.4.1 Dump-Valve Trim for Solutions 58
  - 8.4.2 Slurry Valves 58
  - 8.4.3 Slurry Letdown Chokes 58
- 8.5 Heat Exchangers 58
  - 8.5.1 Flow Tests of Slurry Heat Exchanger 58
- 8.6 Hydrodynamics of Slurry Core Vessel 59
- 8.7 Properties of Slurry Settled-Beds 59

9. DEVELOPMENT OF REACTOR SLURRY SYSTEMS 60
- 9.1 Circulating-Slurry Behavior 60
  - 9.1.1 200A-Loop Operation 60
  - 9.1.2 200B Loop, Description and Operation 61
- 9.2 Blanket-System Development 62
  - 9.2.1 Conversion of 300-SM Loop to High-Pressure Operation 62
  - 9.2.2 Pressure-Vessel-Model Studies 64
  - 9.2.3 Development of Gamma-Transmission Densitometer Equipment 65
- 9.3 Study of a Circulating-Slurry Criticality System 66

10. INSTRUMENT AND VALVE DEVELOPMENT 69
- 10.1 Instrument Development 69
  - 10.1.1 High-Temperature Radiation-Resistant Differential Transformers 69
  - 10.1.2 Evaluation of Pressure Transmitters 70
- 10.2 Valve Development 71
  - 10.2.1 Valve Actuators 71
  - 10.2.2 Valve Stem-Sealing Bellows 72
  - 10.2.3 Slurry-Service Valves 72
  - 10.2.4 Slurry-Service Valve Trim 72

PART IV. REACTOR MATERIALS RESEARCH

11. SOLUTION CORROSION 81
- 11.1 Dynamic Solution Corrosion 81
  - 11.1.1 Deposition of Salts from Dilute Fuel Solutions on Heated Surfaces 81
  - 11.1.2 Hydroclone Tests 86
  - 11.1.3 Instability of Uranyl Sulfate - Lithium Sulfate and Uranyl Sulfate - Magnesium Sulfate Solutions 87
  - 11.1.4 Inhibition of Stress-Corrosion Cracking with Fluoride and Phosphate 88
- 11.2 Laboratory Corrosion Studies 89
  - 11.2.1 Stress-Corrosion Cracking in Uranyl Sulfate Solutions 89
  - 11.2.2 Stress-Corrosion Cracking in Chloride-Containing Water 90
  - 11.2.3 Corrosion of Titanium by Oxygen-Free Uranyl Sulfate Solution 92
  - 11.2.4 Corrosion of Zircaloy-2 in the Heavy Phase of a 1.33 m UO_2SO_4 Solution at 300°C 93
  - 11.2.5 Corrosion of Incoloy 804 and Electrolyzed Stainless Steel 93

12. SLURRY CORROSION 101
- 12.1 Pump Loops 101
  - 12.1.1 Introduction to Pump-Loop Tests 101
  - 12.1.2 Circulation of ThO_2-D_2O Slurries in Oxygen and in Deuterium Atmospheres 101
  - 12.1.3 Materials Evaluation Tests 111
- 12.2 Toroids 113
  - 12.2.1 Introduction 113
  - 12.2.2 Tests with Slurries of Thorium-Uranium Oxides 113
  - 12.2.3 Tests with Slurries of Thoria Prepared by Davison Chemical Company 117
  - 12.2.4 Toroid Gas-Addition Device 119
- 12.3 In-Pile Autoclave Slurry-Corrosion Tests 120
  - 12.3.1 Development, Construction, and Operation 120
  - 12.3.2 Introduction to Autoclave Experiments 120
  - 12.3.3 Recombination of Radiolytic Gases 121
  - 12.3.4 Effects of Time and Radiation on Generalized Corrosion Rate 123
- 12.4 In-Pile Slurry Loop 124
  - 12.4.1 Loop Development 124

13. RADIATION CORROSION 133
- 13.1 In-Pile Loops 133
  - 13.1.1 Development and Construction 133
  - 13.1.2 Effect of Overpressure and Other Variables on Deposition of Uranium in In-Pile Loop Core 133

13.2 In-Pile Rocking-Autoclave Tests--LITR 143
13.3 Supporting Research 144

14. METALLURGY 152
14.1 Physical Metallurgy 152
14.1.1 Examination of Specimens Cut from the HRT Core-Tank Screens 152
14.1.2 Examination of the Titanium Specimen-Holder from the HRT Core 155
14.1.3 Zirconium-Hydrogen System 156
14.1.4 Chemical Machining and Pickling Study on Zirconium-Base Alloys 156
14.2 Mechanical Metallurgy 157
14.2.1 Mechanical Properties of Zirconium and Titanium Alloys Exposed in the HRT 157
14.3 Welding Development 158
14.3.1 Stainless Steel 158
14.3.2 Zirconium 159
14.4 Metallurgical Services 159
14.4.1 Examination of Loop Failures 159
14.4.2 Fabrication of Zircaloy-2 Hemispheres 160
14.5 Development of Nondestructive Testing Methods 160
14.5.1 Thickness Measurements of HRT Core Vessel 160
14.5.2 Measurement of Ultrasonic Velocity in Metals 161
14.6 Reactions of Active Metals 161
14.6.1 Combustion of Titanium and Zirconium 161
14.7 Effects of Radiation on Structural Metals and Alloys 162
14.7.1 Equipment and Facilities 162
14.7.2 Tensile Tests 162

PART V. CHEMICAL ENGINEERING DEVELOPMENT

15. URANYL SULFATE FUEL PROCESSING 169
15.1 Fuel-Solution Behavior 169
15.2 Solids Behavior 171
15.3 HRT Solids and Fuel Solution 171

16. GASEOUS-FISSION-PRODUCT DISPOSAL 173

17. EQUIPMENT DECONTAMINATION 176

18. THORIUM OXIDE SLURRY DEVELOPMENT 177
18.1 Slurry Irradiation Studies 177
18.1.1 Slurry Irradiations in the LITR 177
18.1.2 Postirradiation Examinations 178
18.1.3 Equipment Development 179

18.2 Gas Recombination Studies 181
18.2.1 MoO_3 Catalysis 182
18.2.2 Palladium Catalysis 184
18.3 Uranium Leaching Studies 186
18.4 Boron Adsorption Studies 187
18.5 Oxide Preparation Development 188
18.5.1 Particle Size Control 188
18.5.2 Flame Denitration 189
18.5.3 Fluidized-Bed Denitration 192
18.6 Thorium Oxide Production 194

19. IN-PILE SLURRY LOOP 199
19.1 Status of Loop and Auxiliaries 199
19.2 Loop Filling and Discharging Systems 199

PART VI. SUPPORTING CHEMICAL RESEARCH

20. AQUEOUS SYSTEMS AT ELEVATED TEMPERATURES 205
20.1 The System UO_3-NiO-SO_3-H_2O (D_2O) at 300°C 205
20.2 Investigations of Problems Pertinent to HRT Operations 208
20.3 Comparative Solubilities in D_2O and H_2O Systems; System UO_3-SO_3-H_2O (D_2O) 210
20.4 The Two-Liquid Phase Regions of the System UO_3-SO_3-H_2O 210

21. REACTIONS IN AQUEOUS SOLUTIONS 215
21.1 Chemical Studies Related to HRT Analytical Problems 215
21.2 The Mechanism of Homogeneous Catalysis 216

PART VII. ANALYTICAL CHEMISTRY

22. ANALYTICAL CHEMISTRY 223
22.1 Determination of U(IV) in Thorium Oxide - Uranium Oxide Mixtures 223
22.2 Determination of Neodymium by Flame Photometry 223
22.3 Separation of Chloride by Fusion Pyrolysis 224

ORGANIZATION CHART 227

PART I

HOMOGENEOUS REACTOR TEST

S. E. Beall

1. HRT OPERATIONS

S. E. Beall
P. N. Haubenreich
J. W. Hill, Jr.

H. F. Bauman
N. C. Bradley
J. R. Buchanan
S. R. Buxton
J. R. Engel
J. D. Flynn
D. F. Frech
R. H. Guymon
R. J. Harvey
J. Hirota[1]
J. O. Kolb
D. M. Richardson
J. A. Russell
D, Scott
J. E. Sutherland
W. Terry
K. W. West

Reactor operations were resumed upon completion of the remote inspection and maintenance activities which followed run 17. Run 18 was planned to systematically study the fuel instabilities that were seen in runs 16 and 17 as power disturbances and discrepancies between the analyzed uranium inventory and that known to be in the reactor.

1.1 REACTOR OPERATIONS

1.1.1 Operations Preliminary to Startup

At the end of the last quarter, work was in progress to recover the corrosion specimens which had become detached from the specimen holder and had fallen into the core during run 17. Twelve of the twenty-two specimens were recovered; the other ten could not be reached. A new corrosion-specimen holder was installed in the blanket region, but none was inserted in the core.

As was reported last quarter,[2] the major portions of the first, second, and fifth diffuser screens from the top were found detached from the core tank. The screens were replaced in their normal positions, but no attempt was made to attach them.

Maintenance and viewing operations were completed on November 22, with the installation of a new chemical-plant inlet pipe through the access flange of the reactor core tank. The intake of this line is near the junction of the top diffuser plate and the core-tank wall, due east of the center of the core.[3]

During the remote-maintenance operations, about 600 lb of shield flooding water spilled into the reactor piping through the open core access flange. The reactor fuel solution was isolated in the fuel storage tanks at the time and was not contaminated by the light water. The light water was transferred to the waste system, and the reactor equipment was rinsed first with light water and then with 30 kg of heavy-water condensate. The final rinse contained 98% D_2O, showing satisfactory light-water removal. After operation began, analyses of the fuel solution showed 98.7% D_2O, a decrease of only 1% in the first year of use.

As part of the preliminary startup operations, the reactor shield and all its penetrations were leak-tested and several small leaks were repaired. At 30 psia the shield leak rate was established at approximately 4.1 liters/min, which agrees very closely with earlier leak-rate determinations.[4]

The integrity of the high-pressure system was established by hydrostatically testing the piping and equipment at 2965 psig.

A review of the reactor safety was made during the shutdown, and, as a result, two changes in instrumentation were made before operation resumed. To ensure that the required expansion volume in the fuel pressurizer is available at all times, an additional fuel-pressurizer high-level alarm was installed. The loading pressures on the dump valves were lowered to values that allow the blanket and fuel valves to act as relief valves, opening automatically at system pressures of 2400 and 2600 psig, respectively.

1.1.2 Run 18

Run 18 was planned as a continuation of the study of the fuel instability problems, the goal being to establish the relationship between loss of uranium inventory with power under several operating conditions. The first requirement, therefore, was that the fuel inventory be determined accurately at zero power.

Circulation began with D_2O condensate at 150°C and 1500 psig; the chemical plant was connected to permit continuous solids separation. After 29 hr the D_2O temperature was increased to 260°C. Operation continued in this manner until data from 31 fuel dump-tank samples indicated a uranium inventory of approximately 8.5 kg. As an independent determination, 1 kg of U^{238} as UO_2SO_4 was added to the dump-tank fuel solution, so that isotopic dilution could be used to establish the inventory. Results of this test indicated an inventory of 8.4 kg of uranium prior to the U^{238} addition.

After the fuel solution was pumped to the high-pressure system, the reactor was operated at power levels up to 100 kw with the remainder of the heat losses being supplied by the package boiler. Critical concentrations were confirmed at 275, 255, 235, and 220°C. For the first

three weeks of critical operation, the blanket concentrations were consistently 0.23 of the core concentrations. Then the observed ratios abruptly increased to about 0.32, the same as observed in run 17. The change in mixing between the core and blanket is believed to have resulted from movement of the unattached diffuser screen near the core hole.

After the uranium-inventory data were obtained at zero power (see Sec. 1.2.1), the reactor power was increased to 350 kw and held steady for three days. Since there was no indication of fuel instability, the power was raised to 750 kw, 1200 kw, and later to 1600 kw, where the reactor was operating at the end of the quarter. Over 350 Mwhr were accumulated in 1200 hr of operation.

Equipment performance throughout the quarter was good. There were only two brief (a few hours) interruptions because of malfunctioning of reactor equipment. One interruption resulted from the failure of one head of the fuel feed pump. The full load was transferred to the other head of the pump, which easily sustained the required feed rate. The other malfunction was caused by failure of an electronic tube in the control circuit for the fuel-pressurizer level. Early in the run, light-water condensate began collecting in the shield sumps at a rapid rate, about 1500 lb/hr. The leak was determined to be from a feed-water flange near the fuel heat exchanger. Although there is no operational difficulty, water must be jetted frequently from the sumps to the pond; the flange will be repaired during the next scheduled shutdown. On January 23, the purge pump which feeds condensate to the fuel circulating pump was found to have stopped pumping. The pump suction line was frozen to prevent the backflow of fuel solution and thus to avoid contamination of the condensate supply. There was no interruption in reactor operation. The pump will be replaced during the next scheduled shutdown.

1.2 REACTOR ANALYSIS

1.2.1 Study of Fuel Stability

Fuel instabilities may be detected in three ways: (1) a decrease in the quantity of uranium circulating, (2) brief power excursions, and (3) changes in ionic ratios of the fuel-solution components.

(a) Uranium Inventory.--Physical inventory determinations for uranium were made daily throughout run 18 in an effort to detect inventory changes. All inventory values were based on simultaneous samples from the core and blanket, with fuel dump-tank concentrations estimated from the core concentrations and the relative flow rates between the high- and low-pressure systems. Samples taken at varying times after the blanket dump tanks were emptied indicated a steady leakage to those tanks, and the leakage introduced a variable error in the inventory calculations. (This condition existed for several days until the leakage was stopped by successfully freezing the blanket letdown line.)

Figure 1.1 shows the physical inventories of uranium and sulfate after adjustment for the material in the blanket dump tanks. The book inventory at the time of these samples was 10.0 kg of uranium. This quantity, which is the balance of known additions and removals, includes 0.9 kg of uranium presumably left in the reactor when the initial fuel charge was removed at the end of the first power run. Including this 0.9-kg "permanent" loss, the zero-power inventory of uranium is approximately 1.2 kg below the book inventory, although the scatter indicates that these zero-power data may be no better than ±0.6 kg.

There appears to be a decrease in the amount of material in circulation at the 1.5-Mw level, i.e., a power-dependent loss of as much as 0.6 kg. Part of this loss is the result of a gradual decrease in purge flow to the blanket pressurizer during the period in which the power was being raised. The decreased purge flow probably allowed fuel solution to diffuse into the condensate-filled pressurizer, where it would not be included in the calculated inventory. The maximum amount of uranium or sulfate in the pressurizer, if the concentration there were equal to that in the blanket, would be about 0.2 kg, making the apparent loss with power 0.4 kg, maximum.

(b) Power Excursions.--As in run 17, the reactor power was monitored by a sensitive high-speed recorder. No excursions were detected above the background variation of 1-2%.

(c) Fuel-Solution Chemistry.--Molar ratios of core and blanket solution samples removed during critical operation (run 18-B) are plotted against nuclear power in Fig. 1.2. The usual large variation of these ratios is evident. The slight drop in the U/SO_4 and Cu/SO_4 ratios and the slight rise in the H_2SO_4/SO_4 ratio at 1.5 Mw are in the direction expected on the basis of earlier runs. These changes suggest a small loss of uranium and copper, not inconsistent with the physical-inventory data, but not sufficient to be conclusive.

During the critical operation a total of 50 core and blanket solution samples were taken in pairs. These pairs were taken with the reactor system near equilibrium, within 1 hr of each other, and the pairs were analyzed with the same standards and titrated with approximately equal equivalents of reagent. The U/Cu ratios of the pairs are plotted in Fig. 1.3. The U/Cu ratio is consistently high in the blanket and, in the absence of other explanation, is evidence for a significant concentration of solids (in the core or blanket solutions) which are of different composition than the solutions, and which can move through the hole in the core.

During the first part of run 18, when all the fuel solution was in the dump tanks, considerable quantities of Ag, Cr, Fe, and Mn appeared in the solution. At the end of 29 days of boiling at 100°C, the fuel solution contained 0.7 mole Ag, 9.4 moles Cr, 1.7 moles Fe, and 0.9 mole Mn. After the solution had been pumped to the high-pressure system and

the reactor had operated 29 days at 200-280°C and powers below 0.25 Mw, the solution contained 0.8 mole Ag, 0.3 mole Cr, 0.5 mole Fe, and 0.9 mole Mn. In subsequent operation at higher powers, Ag, Cr, and Fe disappeared except for small traces, but the apparent inventory of Mn in solution remained at 0.9 mole.

1.2.2 Corrosion

The corrosion rate of type 347 stainless steel in the core and blanket high-pressure systems during the 1000 hr of critical operation in run 18 is estimated to be 0.08 mpy. This estimate assumes that the Ni/SO_4 ratio of samples at 1.5 Mw should have decreased proportionately, in the absence of corrosion, to the decrease shown by U/SO_4 and Cu/SO_4. These ratios decreased 2.6 and 2.1%, respectively, at 1.5 Mw.

1.2.3 Measurements of Concentration Required for Criticality at Various Temperatures

Figure 1.4 compares critical core concentrations measured when the reactor was at low power during runs 16, 17, and 18. The points for runs 16 and 18 are for blanket-to-core concentration ratios between 0.28 and 0.35. No blanket samples were obtained at the times of the run 17 points, but earlier in the run the blanket-to-core ratio averaged about 0.32. It is remarkable that the points for all three runs seem to lie along a common line, because in run 17, and not in the other two runs, a corrosion-specimen assembly was present in the core. Neutron poisoning by the assembly should have caused an increase of about 7% in the critical concentration.[5] Uranium deposited on the assembly would tend to counterbalance the poisoning effect, which is perhaps the reason why the run 17 data do not show higher critical concentrations than runs 16 and 18.

1.2.4 Steam System

The first blowdown samples from the fuel heat exchanger in run 18 were taken after the nuclear power was raised to "heat loss," or approximately 350 kw. The blowdown lines, which had not been used because the heat exchangers contained no water until this time, were found to be plugged with solids and required purging. The solids contained 10-100% Fe, 1-10% Ca, and 1-10% Cu by spectrographic analysis. Copper and α Fe_2O_3 were identified by x-ray diffraction. The solids were radioactive, primarily due to 12.8-hr Cu^{64}.

During the next five days of heat-loss operation, with continuous injection of feed-water, the chloride concentration in the blowdown samples ranged from 0 to 12 ppm, phosphate and hydrazine were seldom detectable, and the pH ranged from 10 to 11. Since chloride or caustic cracking is likely under these conditions, the heat exchangers were emptied several times while a search was made for the source of contamination. After four days of searching, the contamination was traced

to a leak of potable water at the turbine condenser, which provides feed-water makeup for the reactor steam system. The inleakage of potable water containing a high solids concentration had caused precipitation of phosphates by Ca and Mg, the oxidation of hydrazine, and the high residual chlorides. A new source of feed-water makeup corrected the difficulty immediately.

REFERENCES

1. Japanese Research Institute.

2. S. E. Beall et al., HRP Quar. Prog. Rep. Oct. 31, 1958, ORNL-2654, p 8.

3. W. R. Gall et al., HRP Quar. Prog. Rep. Oct. 31, 1958, ORNL-2654, p 31.

4. S. E. Beall et al., HRP Quar. Prog. Rep. Jan. 31, 1958, ORNL-2493, p 4.

5. P. R. Kasten et al., HRP Quar. Prog. Rep. April 30 and July 31, 1958, ORNL-2561, p 31.

6. S. E. Beall et al., HRP Quar. Prog. Rep. Oct. 31, 1958, ORNL-2654, p 5.

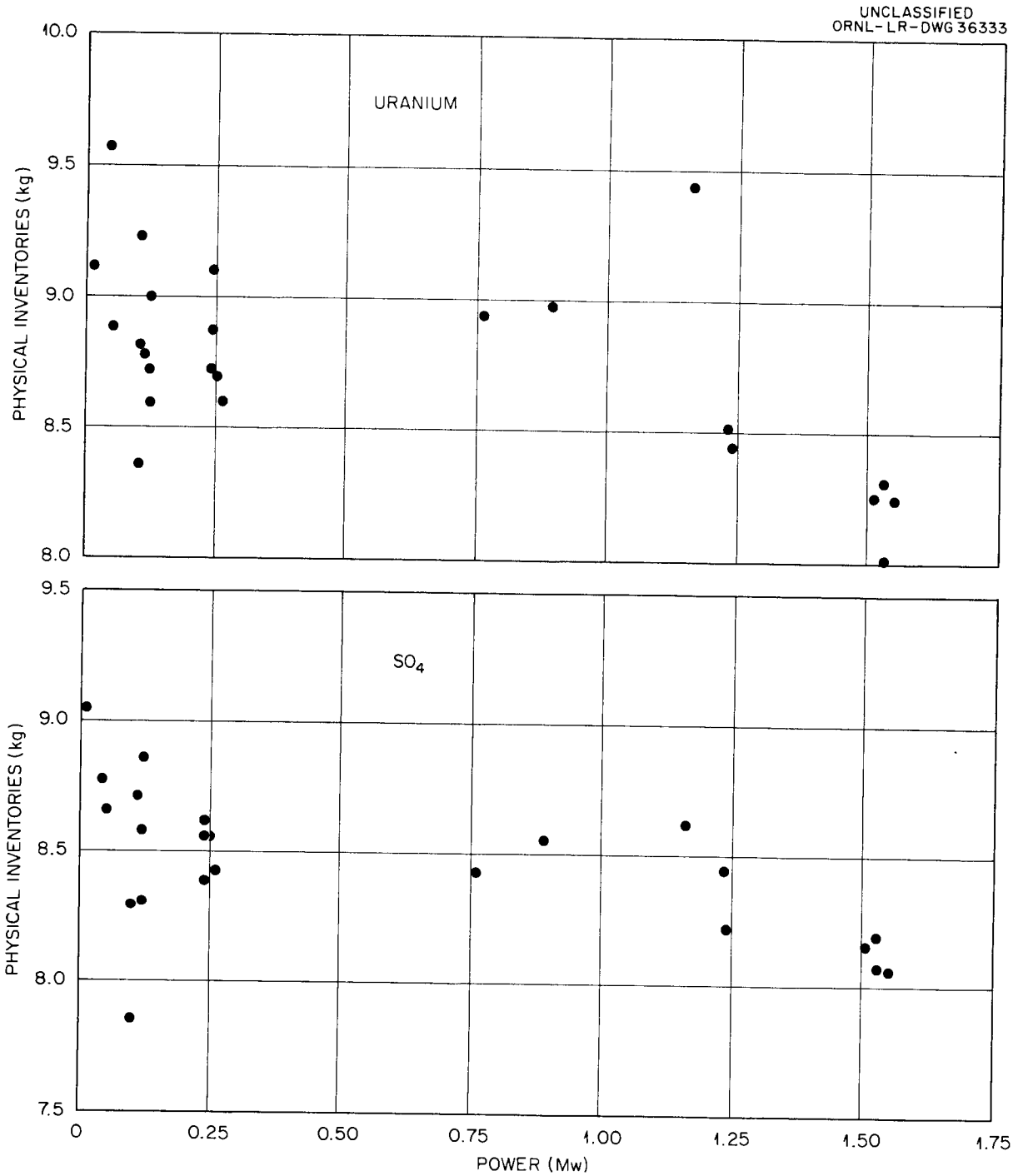

Fig. 1.1. Physical Inventories During Run 18 with Fuel in the High-Pressure System. Compensated for fuel in blanket dump tanks. Book inventories: U, 10.0 kg; SO_4, 9.4 kg.

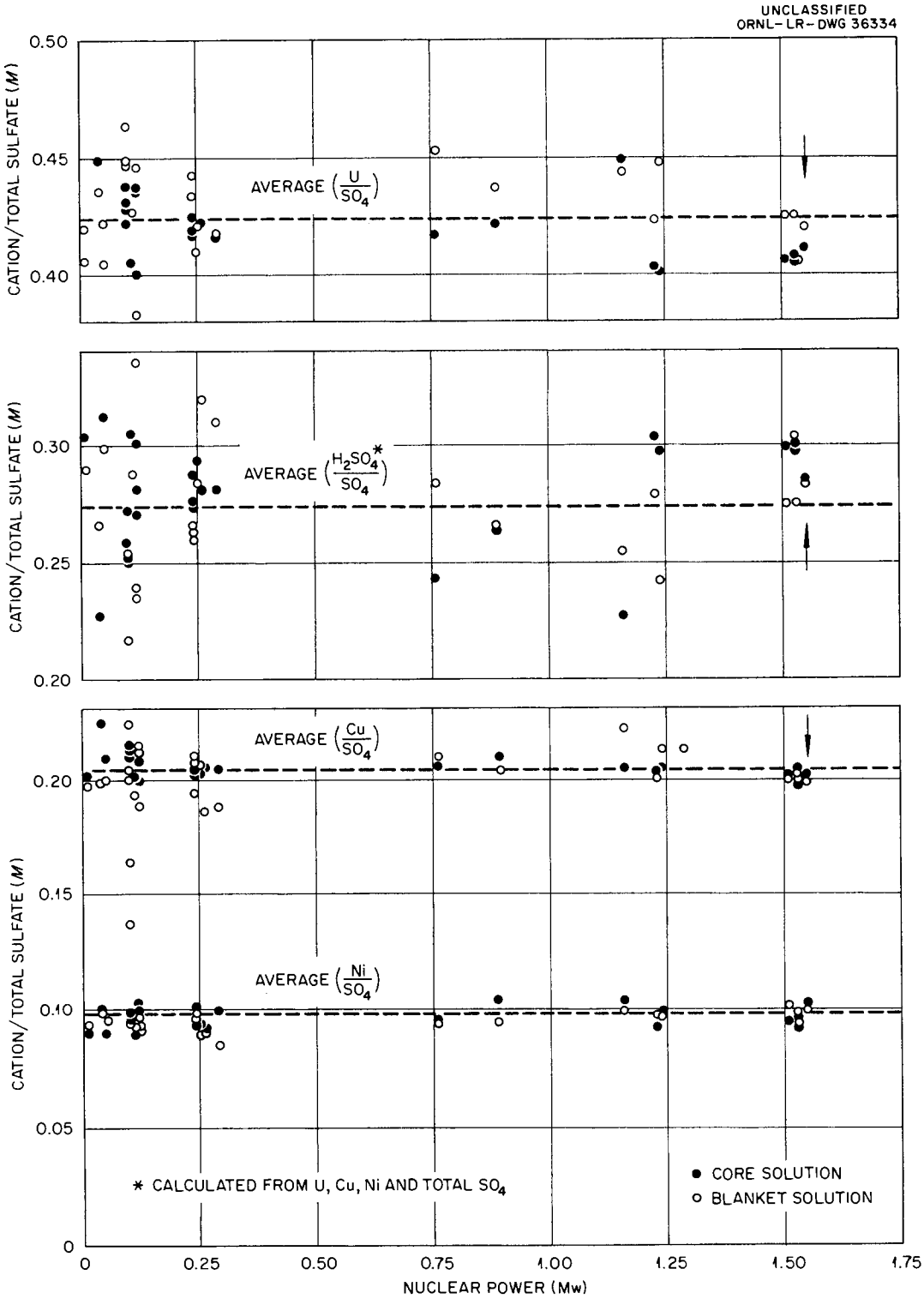

Fig. 1.2. Molar Ratios vs Nuclear Power, HRT Run 18-B.

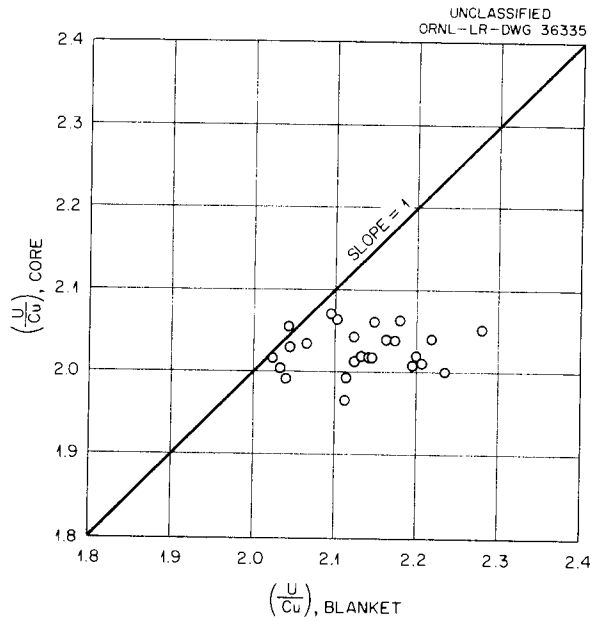

Fig. 1.3. U/Cu Ratios of Core and Blanket Sample Pairs, HRT Run 18-B.

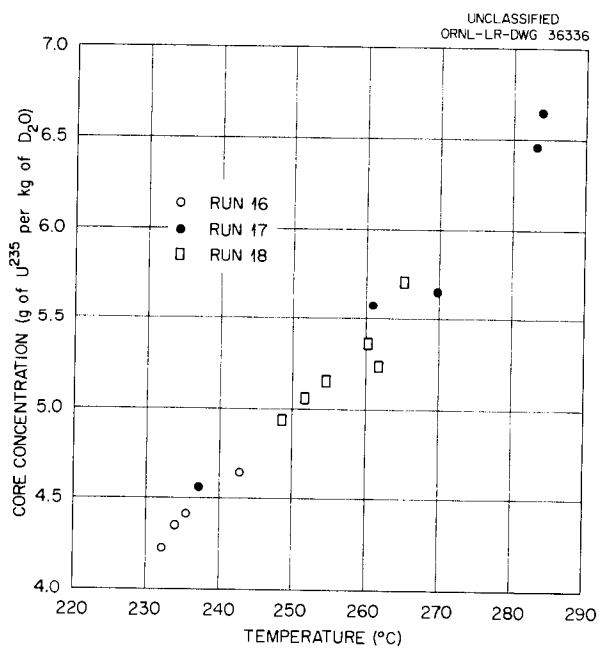

Fig. 1.4. Comparison of Critical Core Concentrations in Runs 16, 17, and 18.

2. HRT PROCESSING PLANT

W. D. Burch R. H. Winget O. O. Yarbro

2.1 HYDROCLONE SYSTEM

The hydroclone system in the HRT chemical plant has been operated for more than 750 hr during HRT run 18. The three chemical plant runs correspond to significant reactor operating periods. Run 18-7 (106 hr) covered the period at the beginning of HRT run 18 in which only D_2O was circulated in the high-pressure system. A two-week shutdown followed while the chemical plant circulating pump, which had failed, was replaced. In run 18-8 (335 hr) the reactor was critical at power levels to 200 kw. The solids from runs 18-7 and -8 were dissolved, and the analytical data are reported here. Run 18-9 (341 hr), with the reactor at power levels from 300 to 750 kw, has just been completed; results will be reported next quarter.

Minor difficulties with a restriction in the take-off line from the reactor were evident throughout run 18-7 and at the beginning of run 18-9. On two occasions, it became necessary to pressurize the hydroclone system above reactor pressure to blow out the line. The restriction was thought to be in the port of the isolation valve rather than in the newly installed core dip pipe, because repeated operation of the valve tended to reduce the restriction and the port diameter is less than half that of any other opening in the line.

2.1.1 Circulating-Pump Failure and Replacement

During attempts to circulate the contents of the underflow receiver to obtain a sample after run 18-7, the circulating-pump breaker tripped. From the current drawn it was evident that the rotor was locked, but after several attempts the pump was started and appeared to operate satisfactorily. However, the difficulty recurred several times while the system was being rinsed, and the pump could not be started when the system was reconnected to the reactor.

The pump was removed with the cell flooded, and a spare was installed in 28 hr; 8 additional hours were required to cut and reweld the seal pans. While the pan seal welds were being checked, the instrument

cubicle, located just below the pan removed, was flooded accidentally. The cell was re-entered, and the pressure cells were dried out and checked thoroughly. These difficulties extended the shutdown period to two weeks. Cell leakage has averaged 6 liters/min since this maintenance, compared with approximately 10 liters/min for the prior period.

Efforts are being made to decontaminate and inspect the pump to ascertain the cause of the failure.

2.1.2 Corrosion-Product Solids Collected

The quantities and compositions of corrosion products collected in run 18 are listed in Table 2.1, with comparable average numbers from previous runs.

Table 2.1. Corrosion-Product Solids Removed

	Chemical Plant Run			
	16*	17*	18-7	18-8
Operating time, hr	769	829	106	335
Total corrosion products removed, g	364	709	273**	613
Average removal rate, g/hr	0.47	0.86	2.6	1.8
Per cent				
Fe	51	22	21	24
Cr	5	5	3	9
Ni	1	0.1	0.5	-
Zr	7	49	49	38
Ti	-	0.5	0.6	0.7
Ag	-	0.2	0.1	0.2

*Average of three chemical plant runs.

**Includes 40 g of solids flushed from the high-pressure system following the pump replacement, and added to the total already found in the run 18-7 dissolution.

The composition of the solids continues to be remarkably constant, suggesting that the hydroclone is removing a representative portion of the total corrosion-product solids formed to date rather than a certain fraction of those formed during each specific run. This leads to the conclusion that the bulk of the corrosion on the zirconium core tank occurred very early in run 17. (The zirconium content of the solids

removed in the first 290 hr of run 17 was 45%.)

The history of zirconium corrosion in the reactor to date has been estimated, with the following assumptions used as bases:

1. The composition of solids removed by the hydroclone is identical to the composition of the sum total of all corrosion products remaining in the reactor.

2. Stainless steel corrosion rates are uniform on all stainless steel surfaces in both core and blanket systems and are calculated from nickel buildup in solution.

3. There is no transfer of solids between core and blanket systems.

While the first assumption cannot be completely verified at this time, the uniform chemical composition since run 17 suggests that it is true.

The corrosion-product buildup calculated in this manner is plotted in Fig. 2.1, along with figures showing accumulated percentages of the solids which formed in the core system only and which have been removed by the hydroclone. It can be shown from estimated solids concentrations and blanket-to-core transfer rates that the quantity of solids formed in the blanket and transferred to the core is insignificant.

This method was also checked by determining the fraction of fission-product zirconium (Zr^{95}) removed in the chemical plant and comparing it with the fraction of corrosion products removed according to the above calculations. These data are listed in Table 2.2, and the agreement is seen to be fairly good. The numbers are percentages of the total corrosion products formed up to the end of a run and removed in that run. Zirconium-95 from adsorption in the core tank has been ignored, but amounts to only a few per cent of the fission product Zr^{95}.

Table 2.2. Calculated Percentages of Zirconium Removed

Run No.	Corrosion Products	Fission Products
16-2	0.41	0.53
16-3	0.47	0.26
17-4	1.06	3.41
17-5	0.33	0.65
17-6	0.11	0.22
18-7	0.67	0.65
18-8	1.5	2.8

These calculations also agree well with the 40-mil total decrease in the core wall thickness measured at the end of run 17. Assuming a uniform 20-mil loss from all surfaces, 29.4 kg of ZrO_2 was formed in the reactor, compared with the above calculated value of 29.9 kg.

2.1.3 Concentrations of Uranium, Copper, and Nickel

In run 18, as in earlier runs, a significant quantity of uranium and copper was associated with the corrosion-product solids. This information is given in Table 2.3, along with average values from previous runs.

Table 2.3. Uranium, Copper, and Nickel Removed by the Chemical Plant

	Chemical Plant Run No.			
	16*	17*	18-1	18-8
Total U, g	133.7	395	24.2	78.4
Insoluble U, g	21.3	200	24.2	27.3
U solids/corrosion-product solids	0.06	0.28	0.09**	0.044
Total Cu, g	19.4	32.7	4.4	16.1
Insoluble Cu, g	2.4	8.3	4.4	9.1
Cu solids/CP solids	0.007	0.012	0.016	0.015
Total Ni, g	7.3	8.9	1.0	2.9
Insoluble Ni, g	2.6	0.8	1.0	0.3
Ni solids/CP solids	0.007	0.001	0.004	<0.001

*Total of three runs.

**A 140-mg sample of solids removed from the underflow pot prior to dissolution contained only 2.8% U; the cause for the large discrepancy is unknown.

2.1.4 Fission-Product Activity Distribution

Reactor power levels were not high enough in runs 18-7 and 18-8 to increase significantly the activity levels of the long-lived fission products. However, the residual activities from previous runs were measured for several of these isotopes, and the distribution between reactor and chemical plant was calculated. These data, in Table 2.4, confirm results of previous runs. Less than 0.1% of the very insoluble Zr^{95} and Ru^{103} are circulating in the reactor; the quantities removed by

Table 2.4. Fission-Product Activity Distributions

Isotope	Run No.	Total Activity in System from Power History (curies)	Removed by Chemical Plant (curies)	Circulating in Reactor (curies)
Zr-95	18-7	2.7×10^4	174	13
	18-8	1.9×10^4	540	2.5
Ru-103	18-7	1.2×10^4	11	1.0
	18-8	6.7×10^3	23	0.25
Sr-89	18-7	2.8×10^4	16	9.6×10^3
	18-8	1.2×10^4	29	5.1×10^3
Cs-137	18-7	492	0.5	748*
	18-8	492	1.8	555*
Y-91	18-7	2.3×10^4	122	1.1×10^4
	18-8	1.6×10^4		

*Reason for discrepancy unknown.

the hydroclone are in proportion to the quantity of corrosion products collected. Cesium is completely soluble, and 30-50% of the Sr^{89} and Y^{91} remain in circulation.

2.2 ACTIVITY RELEASED FROM WASTE POND

A total of 656,000 gal of waste containing 1.89 curies of beta activity was released from the 7500 area waste pond in this quarter. Not more than 0.5 curies was released during any 24-hr period.

After the reactor cell was drained following the maintenance period before run 18, the pond was treated with trisodium phosphate and $CaCl_2$, which reduced the total pond activity from 6.2 to 0.9 curies. The primary activity remaining was ruthenium.

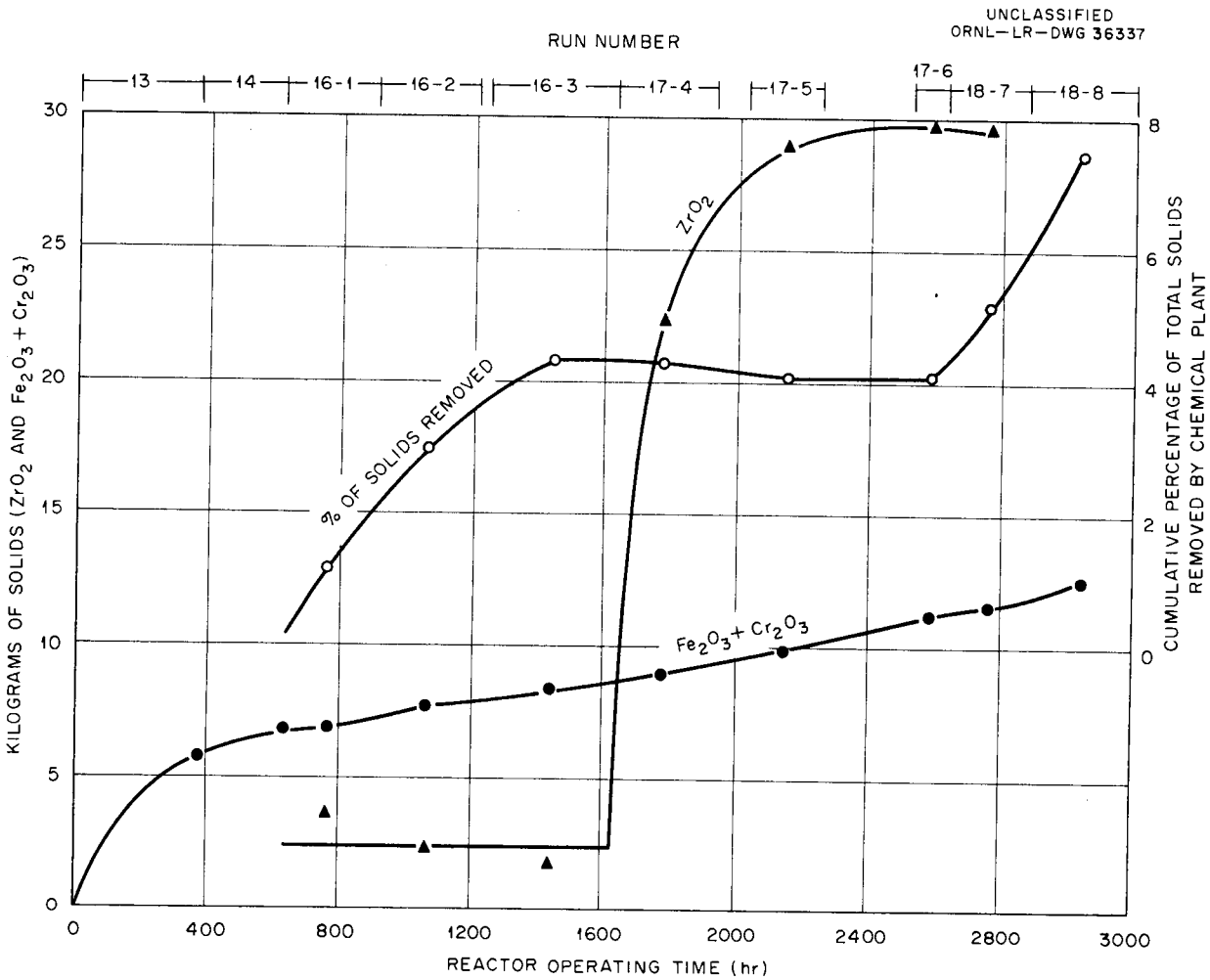

Fig. 2.1. Calculated Buildup of Corrosion Products.

3. HRT REACTOR ANALYSIS

P. R. Kasten

R. Chalkley S. Jaye M. P. Lietzke
H. C. Claiborne M. Tobias

3.1 HOLE FORMATION IN THE HRT CORE TANK

The holes in the HRT core tank and sample holder appear to have been caused by metal temperatures above the melting point; the possibility that the holes resulted from corrosion or chemical reaction appears inconsistent with the available information. Simple heat transfer considerations alone indicate that the melting point could not be attained without uranium deposition. The purpose of this study was to estimate the magnitude of uranium deposition required to cause melting of the core tank.

For the physical model considered, it was assumed that a uranium-bearing scale was deposited on the core-side surface of the core tank. Fissioning of this uranium generated heat which was transferred by conduction through the scale into the core fluid, and through the core-tank wall into the blanket fluid. The conditions under which melting of the zirconium core tank could take place were obtained by mathematically solving the appropriate heat conduction problem.[1] In estimating the surface temperatures of the scale and wall (blanket side), it was assumed that nucleate boiling took place.

The maximum temperature of the core tank would occur at the wall-scale interface. It was assumed that when the interface temperature reached the melting point, the condition existed for formation of a hole in the wall. The thickness of uranium-bearing scale required to raise the wall-scale interface to the melting point is shown in Fig. 3.1 as a function of U^{235} density and effective diameter of the deposit.

The results indicate that uranium deposits of relatively small area and thickness could result in melting of the tank wall. For example, a 1-in.-dia deposit containing 1 g of U^{235} per cubic centimeter of scale need be only 100 mils thick to cause a spot on the wall to reach the melting point. With higher uranium concentrations, the required scale thicknesses were from 30 to 60 mils.

In arriving at these figures, subcooled nucleate boiling was assumed to exist on both surfaces. Whenever the heat flux to be removed exceeds that removable by nucleate boiling, the surface temperature would rise and film boiling would occur. Under these circumstances rapid burnout (melting of the core tank) would also be quite probable.

The above analysis considered the situation at the core wall. The same reasoning, however, applies to the sample holder and screens, and similar results are to be expected.

3.2 CALCULATIONS OF HRT POWER RESPONSE FOLLOWING REACTIVITY ADDITIONS

An instantaneous addition of reactivity in the HRT would cause the reactor power to rise, go through a maximum, and return to near its initial value. The quantity of reactivity associated with a power excursion has been calculated on the IBM-704 computer, by use of five groups of delayed neutrons and separate heat balances over the core and blanket (with constant heat removal).[2] Figure 3.2 shows the ratio of maximum to initial power versus the quantity of reactivity added for various initial power levels, when 40% of the power is generated in the blanket. Since the reactor fuel circulates, the effective heat capacity of the system depends on the time associated with the excursion. For small reactivity additions and low initial power levels, the time required to reach the maximum power is of the same order as the residence time, indicating that the heat capacity of the fluid in the core circulating system (~500 liters) should be used. As the reactivity addition or the initial power level is increased, the time required to reach the maximum power is reduced to 1 sec or less, indicating that the heat capacity of the core itself (~290 liters) should be used. In all cases the heat capacity used for the blanket region was that of the blanket fluid which is within the reactor vessel (~1550 liters).

3.3 CRITICAL MASS IN HRT-TYPE REACTORS UTILIZING D_2O-H_2O MIXTURES

Studies were made concerning the smallest core diameter and the most appropriate D_2O-H_2O composition ratio which would permit criticality in an HRT-type reactor containing no more than 10 g of total uranium per liter at 280°C. The usual two-region spherical reactor was assumed in which the core contained the fuel material (U^{235}) and the reflector region, between the core and the outer pressure vessel, contained only moderator (a mixture of D_2O and H_2O).

With the pressure-vessel diameter fixed at 5 ft and with the same moderator composition in both the core and blanket regions, the core diameter and the percentage of D_2O in the D_2O-H_2O moderator were permitted to vary. The corresponding critical concentrations of total uranium in the core (based upon uranium of 93.4% enrichment) were computed by using an

IBM-704-programed version of the "harmonics" method.[3] In this calculation the criticality condition is based upon the vanishing of a seventh-order determinant. The core tank was included by regarding it as a poison distributed uniformly throughout the core region.

Figure 3.3 shows, for various core diameters, the dependence of critical concentration upon the percentage of D_2O in the moderator. For the present core diameter of 32 in., it was found that an addition of 10% light water to the moderator would reduce the critical concentration from 9.2 to about 7.8 g of uranium per liter at 280°C. The smallest core diameter for which the reactor would remain critical with less than 10 g of uranium per liter was about 29 in. This occurred with a moderator composition of about 85% D_2O.

3.4 EFFECT OF CORE AND REFLECTOR TEMPERATURES ON CRITICAL CONCENTRATIONS IN HRT-TYPE REACTORS

Critical concentrations have been estimated for 30- and 28-in.-dia reactor cores at 300°C for several values of the blanket temperature and pressure-vessel diameter. The "harmonics" method[3] requires that the slowing-down properties in all regions be the same, so that it cannot be used directly to treat cases where the moderator is at different temperatures in different regions. The percentage change in critical concentration due to different reflector temperatures was first calculated by the two-group procedure and applied as a correction to the harmonics calculation result for a uniform reactor temperature of 300°C. The results of these computations are presented in Table 3.1.

It is evident that lowering the blanket temperature causes the critical concentration to be decreased. In fact, the critical concentrations with the core at 300°C and the blanket at 250°C appear to be less than the corresponding critical concentrations when both the core and blanket are at 280°C (see Sec. 3.3).

The addition of some light water lowered the critical concentration; the percentage reduction increased with increasing reflector temperature. Increased reflector thickness likewise produced a noticeable reduction in critical concentration.

Table 3.1. Critical Concentration as a Function of Moderator Composition, Reflector Thickness, and Reflector Temperature for Two Core Diameters*

Core Diameter (in.)	Reflector Thickness (in.)	% D_2O	Core Concentration (g total U/liter) Blanket Temperature		
			300°C	280°C	250°C
30	15	100	14.80	12.12	9.84
		90	10.58	9.40	8.38
		80	10.32	9.65	8.98
	12	100	21.16	16.90	13.38
		90	11.89	10.42	9.15
		80	10.82	10.00	9.25
28	16	100	18.69	15.14	12.18
		90	12.70	11.22	9.92
		80	12.08	11.20	10.32
	13	100	26.92	21.25	16.70
		90	14.19	12.38	10.78
		80	12.58	11.53	10.62

*Core temperature, 300°C in all cases; no fuel in reflector; enrichment of uranium is 93.4%.

REFERENCES

1. H. C. Claiborne, Hole Formation in the HRT Core Tank, ORNL CF-58-11-49 (Nov. 18, 1958).

2. S. Jaye and M. P. Lietzke, Power Response Following Reactivity Addition in HRT, ORNL CF-58-12-106 (Dec. 30, 1958).

3. M. C. Edlund and L. C. Noderer, An Harmonics Method Applied to D_2O-Moderated Reactors, ORNL CF-54-3-120 (Mar. 18, 1954).

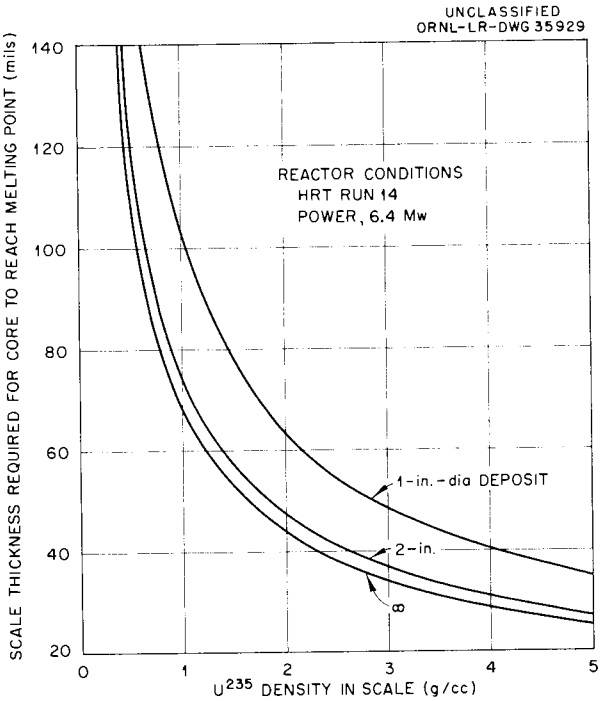

Fig. 3.1. Thickness of Uranium-Bearing Deposit Required for HRT Core Tank to Reach Melting Point.

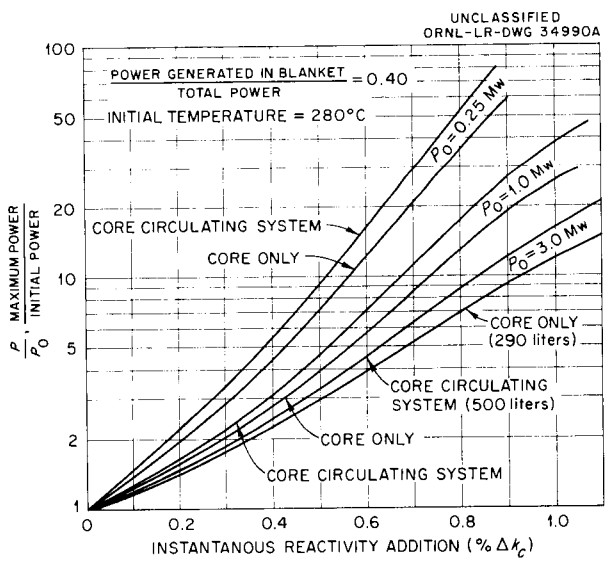

Fig. 3.2. Relative Peak Power in HRT as a Function of Instantaneous Reactivity Addition.

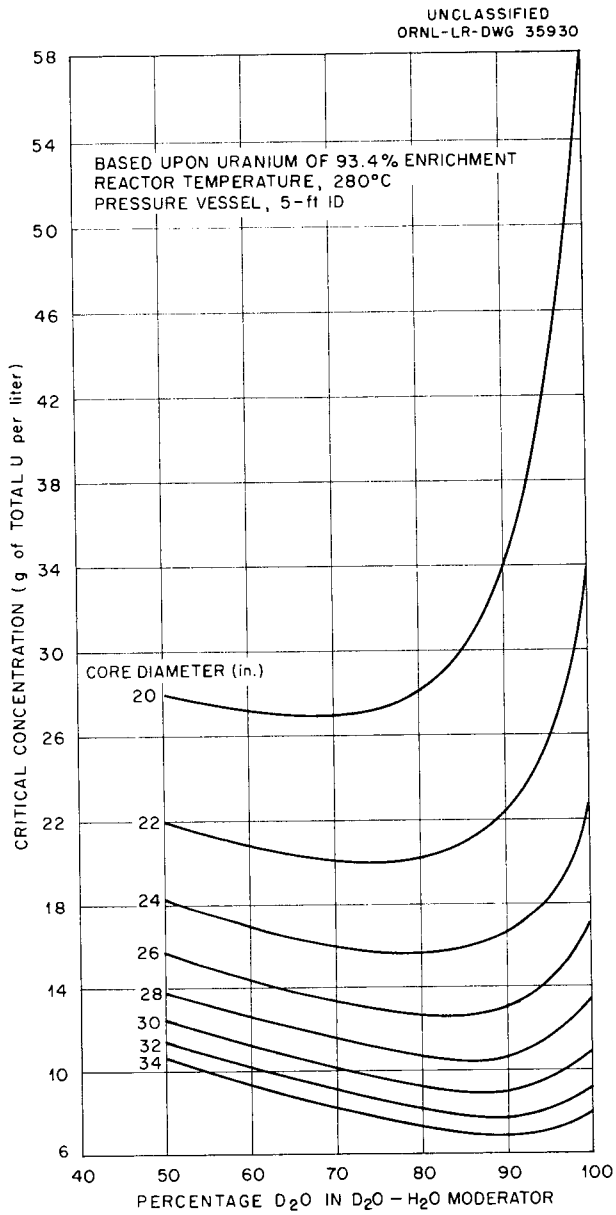

Fig. 3.3. Critical Concentration vs Moderator Composition in HRT-Type Reactors.

4. HRT DESIGN

W. R. Gall
M. I. Lundin
J. R. McWherter

C. A. Burchsted
R. H. Chapman
C. J. Claffey
C. W. Collins
E. H. Gift
L. A. Haack
J. E. Jones
H. A. McLain
R. C. Robertson
D. L. Snyder
F. C. Zapp

4.1 COST ESTIMATES FOR REPLACEMENT PRESSURE VESSEL

Preliminary cost estimates of two concepts[1,2] of the proposed HRT replacement reactor-vessel assembly (core and pressure vessel) were obtained from Newport News Shipbuilding & Dry Dock Company.[3] Concept I, an all-welded vessel, would cost an estimated $500,000. Concept II, a vessel with a closure to permit removal of the core, would cost an estimated $575,000, assuming no closure-development cost.

The detailed cost breakdown[3] was used for estimating the cost of replacement in each case. For concept I, a second vessel assembly was estimated at $326,000; an extra core and head for concept II would cost $186,000.

4.2 HEAT GENERATION IN THE HRT CORE WALL DUE TO THE PRESENCE OF 0.01% THORIUM AND 0.001% NATURAL URANIUM IN THE METAL

Analysis of Zircaloy-2 indicates that it contains 0.01% or less of thorium and 0.001% or less of uranium.[4] Their contribution to the core wall heating is less than 5×10^{-3} w/cc, which is negligible, compared with the 3 w/cc of gamma-heat generation in the wall of the core vessel.

4.3 PROJECTED-LIGHT VIEWER

The design of a projected-light viewer for use in future remote operations at the HRT was completed. This device (Fig. 4.1) is capable of accommodating tools for remote maintenance and has a mounting that can be adjusted as required.

REFERENCES

1. W. R. Gall, et al., HRP Quar. Prog. Rep., April 30 and July 31, 1958, ORNL-2561, p 43-44.

2. W. R. Gall, et al., HRP Quar. Prog. Rep., Oct. 31, 1958, ORNL-2654, p 31.

3. R. H. Chapman and M. I. Lundin, memorandum to W. R. Gall, Nov. 11, 1958.

4. M. C. Wittels to H. A. McLain, personal communication.

UNCLASSIFIED
ORNL-LR-DWG 35931

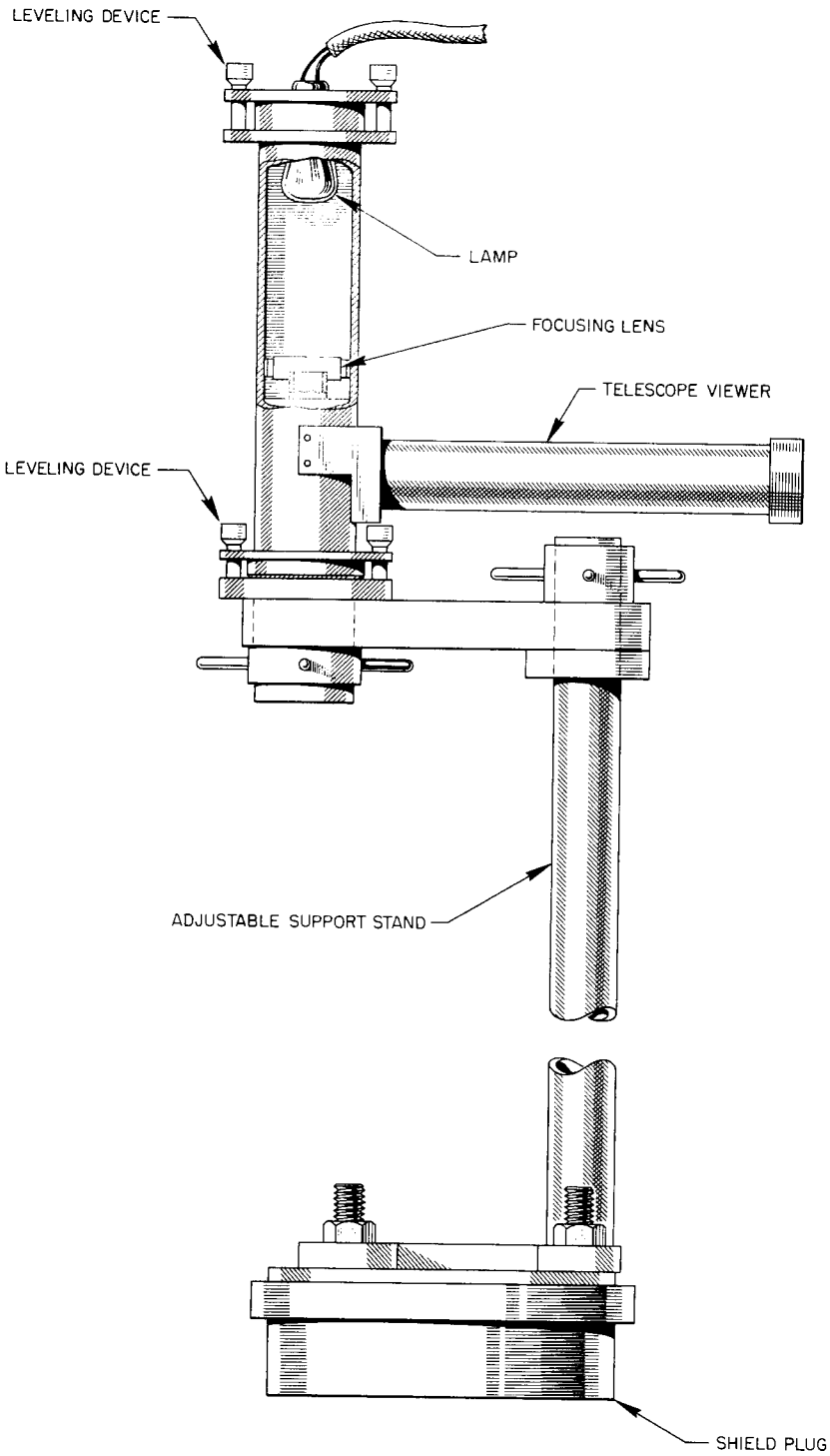

Fig. 4.1. Projected-Light Viewer Assembly.

5. DEVELOPMENT OF HRT COMPONENTS AND REMOTE OPERATIONS

I. Spiewak

R. Blumberg
C. W. Collins
J. S. Culver
B. D. Draper[1]
D. M. Eissenberg
E. C. Hise
P. P. Holz
J. E. Jones, Jr.
C. G. Lawson
M. I. Lundin
R. P. Wichner
F. C. Zapp

5.1 FEED-PUMP ENDURANCE TESTING

Two prototype HRT fuel feed-pump heads have now operated for 14,000 hr in a test loop. Testing of two purge-pump heads was terminated after each had operated the equivalent of 16,000 hr; a third head has operated in the HRT mockup for 7172 hr.

An experimental diaphragm, 1/4 hard and 0.021 in. thick, failed on the HRT mockup feed pump after 13,000 hr of operation.

5.2 HRT CORE STUDIES

5.2.1 Modifications to Present Core

The full-scale flow model of the HRT core was operated to investigate possible changes in flow distribution which would lead to improved core-wall cooling and the removal of sedimentary solids. Visual observations were made of the general flow patterns by use of injected dye; the behavior of injected solids was also studied. Surface heat transfer coefficients were measured in the northern and the southern hemispheres.

Several configurations, with some or all of the screens removed, were tested with flow in the upward direction. In all these tests, there was a tendency for solids to deposit on the 90-deg conical portion of the model. In most cases, the deposition was caused by unsymmetrical flow distribution in the vessel, leading to local semistagnant areas. Further variations are planned in an attempt to find a satisfactory configuration for forward flow.

Reversal of the direction of flow, with screens left in or removed from the model, gave symmetrical flow distributions. Solids injected into the core were removed from the visible regions when flow rates were greater than 150 gpm. Velocities near the spherical wall, inferred from heat transfer measurements, were 4 to 5 fps at 450 gpm. More detailed investigation of the conical portion of the model is planned, particularly with the screens left in the cone.

5.2.2 HRT Replacement Core

Water studies continued on the top-annular-inlet, top-polar-outlet core vessel.[2] At the time an order is placed for a replacement vessel, final selection of a core configuration will be made between this system and the polar-inlet system tested previously.

Several types of flow distributors were installed at the bottom polar outlet (the secondary outlet) in an attempt to stabilize the flow in the bottom hemisphere, to extend the boundary stream formed by the inlet flow to the bottom hemisphere, and to improve solids removal. The most satisfactory distributor tested is illustrated in Fig. 5.1. The 2-in.-dia bottom outlet was covered by a 4-in. disk, with a clearance of 0.2 in. between the disk and the core wall. The inlet distributor vanes imparted a 20-deg rotation to the incoming fluid. At a flow of 300 gpm, with 30-50 gpm removed at the bottom pole, a boundary current covered the surface of the core wall. The fluid movement in the boundary was in a direction 20 deg from the longitude meridians throughout most of its path; however, the tangential component increased as the bottom pole was approached. The remainder of the fluid spiralled upward and out as illustrated in Fig. 5.1. The flow pattern was stable. The pressure drop across the core with the bottom outlet closed was 35 ft of fluid at 300 gpm.

Most of the solids (sand and small pebbles) added to the core were quickly removed via the bottom outlet under the influence of the sweeping action of the boundary layer; however, about 2% attained stable orbits, rotating with the fluid in the region shown dotted in the figure. This phenomenon, predicted though not actually observed by Kelsall,[3] occurs when the centrifugal force on the particle is balanced by the drag caused by the radial, inward component of the fluid velocity and the gravity force, by the upward velocity component. Shutting off the flow, momentarily, removes almost all of these solids.

5.2.3 HRT Replacement Blanket

Because of the desirability of providing high rates of cooling to the core tank of the HRT replacement vessel, a test system containing a 60-in.-ID blanket vessel and a 33-in.-OD core tank was set up. Thermocouples spaced radially through the 1-in.-thick brass core tank will permit calculation of heat fluxes and local blanket-side heat transfer coefficients for various blanket configurations. Steam will be condensed inside the tank. Construction of this system is about 90% complete.

5.3 THERMAL SHOCK OF HRT FLANGES

In operations such as venting or dumping, some of the HRT flanges are subject to rapid temperature changes, which are believed more likely to cause leaks than slow temperature changes. By using an existing high-pressure steam system, 1/2- and 1-in. ring-joint flanges were thermally shocked from 50 to 200°C, and from 200 to 50°C. No leaks were caused under these conditions. Bolt loadings after the test were about the same in flanges having standard HRT carbon steel bolt-ferrules and in flanges having A-110AT titanium ferrules, which have greater resilience.

5.4 REMOTE OPERATIONS AND DEVELOPMENT

5.4.1 Core-Wall Thickness Gauge

A device for measuring core wall thickness was designed, and its construction is in progress. The unit (Fig. 5.2) consists of a crystal transducer mounted in a lower arm pivoted from a 1 1/2-in.-dia pipe sleeve extending from the top of the cell shield to the center of the core tank. The lower arm is raised and lowered by a shaft which is concentrically located within the 1 1/2-in.-dia pipe; the entire assembly can be rotated to scan any part of the core wall from the top diffuser screen to the circumferential weld at the top of the core vessel. An air-driven piston is utilized to position the transducer against the wall. The core tank will be flooded with D_2O when this device is being used.

5.4.2 Remote Impression Device

The design of a device to make an impression of an eroded or corroded section of radioactive pipe in the HRT was started. The tool will place a piece of material, which can be softened by heat, over the suspected area of pipe, and, after heating and cooling, retrieve the impression for examination. Several plastic materials have been tested; the most promising appears to be "Dip Seal" compound.

5.4.3 Removal of Diffuser Screens from the HRT Core

Preliminary studies have been made for determining one or more satisfactory methods for removing the diffuser screens from the HRT core vessel. Preliminary tests indicate[4] that attack rates as high as 1 mm/hr can be attained by anodic dissolution of Zircaloy in HNO_3. Further work will be required to evaluate possible damage to the HRT if such a method is used. Alternatives being considered for further development include machining, punching, and arc cutting. At least one of these methods will be selected for full-scale testing in the maintenance mockup.

5.4.4 Patching of the Defect in the HRT Core Tank

Possible methods of patching the hole formed in the core tank during HRT run 14 are being evaluated before selecting one or two schemes for intensive development. Study of photographs of the defect indicates that a patch would have to be curved to conform to the surfaces of the intersection of the 30- and 90-deg cones, and would have an area of about 1.5 in^2.

The two most promising schemes considered to date are: a remote fusion weld of a patch to the core wall, and a mechanically sealed patch which would be purged continuously with D_2O from the blanket side.

5.5 HRT MOCKUP

R. B. Korsmeyer P. H. Harley

5.5.1 Operation

The HRT mockup was operated for 1663 hr during the past quarter in a continuation of run CS-23. The main objective of the run was to evaluate the use of boiling fuel solution in a titanium heat exchanger as a steam supply for pressurizing the system. Operation was at 1400 to 2000 psi and 280 to 300°C with 0.045 m UO_2SO_4, 0.036 m $CuSO_4$, and 0.025 m H_2SO_4. The two-phase transition temperature for this fuel is 330°C.

Prior to the present test, the loop had been run for 1900 hr at 280°C and 1500 psi with no change occurring in the fuel composition. During the first 1000 hr of this test, on two occasions the pressurizer temperature was increased stepwise from 313°C to 336°C and then reduced, in similar steps, to 313°C. At each temperature the amount of heavy phase formed in the heat exchanger was inferred from the reduction in uranium concentration in the light phase circulating through the rest of the system. The equilibrium analyses of the circulating stream for operation at the various pressurizer temperatures are shown in Table 5.1, along with calculated volumes of the heavy phase that formed, assuming a concentration of 800 g of U per liter in the heavy phase. After each temperature change, except one, equilibrium was reached in about 6 hr. When the operating temperature was set at about 325°C, several days were required for the uranium concentration in the circulating stream to reach steady state, presumably because of the hottest part of the heat exchanger wall was barely at the two-phase temperature. When equilibrium was reached, the uranium concentration indicated a slight amount of heavy-phase formation. Fuel flow through the heat exchanger and pressurizer was 0.4 gpm during the run.

Table 5.1. Circulating-Fuel Composition in HRT Mockup at Several Pressurizer Temperatures

Pressurizer Temp. (°C)	Molal Composition				Heavy-Phase Volume*	
	U	Cu	SO_4	$2H^+$	Liters	% of H.P. System
320	0.0445	0.0358	0.1053	0.025	0	0
325	0.0422	0.0348	0.1030	0.0265	0.09	0.14
330	0.0348	0.0305	0.0930	0.0265	0.38	0.60
336	0.0290	0.0270	0.0832	0.0270	0.66	1.05

*Based on an assumed uranium concentration of 800 g/liter.

Because the fuel velocity through the heat exchanger might affect the fuel stability, the flow was lowered to 0.2 gpm and the system restarted. During the startup the solution was inadvertently boiled in the heat exchanger without liquid flow to the pressurizer, resulting in the formation of a partial plug due to precipitation of salts. The plug was not removed by resumption of flow with steam pressurization, and finally it had to be removed by dropping the pressurizer temperature and operating under gas pressurization at 200°C (i.e., no evaporation in the heat exchanger). The fuel composition and heat transfer returned to normal, and the system is operating in routine manner with the pressurizer temperature at 300°C.

During operation near or above the heavy-phase temperature, the nickel analyses were erratic. The over-all system corrosion rate has been estimated as about 2.6 mpy, which is double the rate reported last quarter for operation at 280°C and 1500 psi.

The only major system component to cause trouble during the quarter was the feed pump. Three rubber pulsators were ruptured, and one stainless steel diaphragm failed. The diaphragm, which had operated for 12,153 hr was 1/4 hard, type 347 stainless steel 0.021 in. thick. Two of the three pulsators were broken during attempts to balance the oil flow to the two feed-pump heads at a time when the oil flow was hampered by a plugged filter in the oil pump suction. The reason for the third pulsator failure was not determined. Each of the three pulsators had operated for less than 2000 hr.

All other system components have operated exceptionally well. The titanium letdown heat exchanger and three titanium-to-stainless-steel transition flanges have operated for 6092 hr. The titanium pressurizer and three other transition flanges have operated for 3468 hr without leakage or other indication of equipment deterioration. Two of these transition flanges have been unbolted and rebolted six times without leaking after reassembly.

The present letdown valve, an HRT type with a 1/8-in. port, appears to be leak-tight after 3468 hr of operation, and the Pressure Products oxygen compressor has operated for 600 hr at 2200 psi without maintenance. The compressor runs intermittently, and this time corresponds to about 3468 hr of system operation.

REFERENCES

1. Tennessee Valley Authority.

2. I. Spiewak et al., HRP Quar. Prog. Rep. Oct. 31, 1958, ORNL-2654, p 36.

3. D. F. Kelsall, "A Study of the Motion of Solid Particles in a Hydraulic Cyclone," Trans. Instn. Chem. Engrs. 30, 87 (1952).

4. W. E. Clark, "The Anodic Decomposition of Zircaloy-2," January 6, 1959, memo to R. Blumberg.

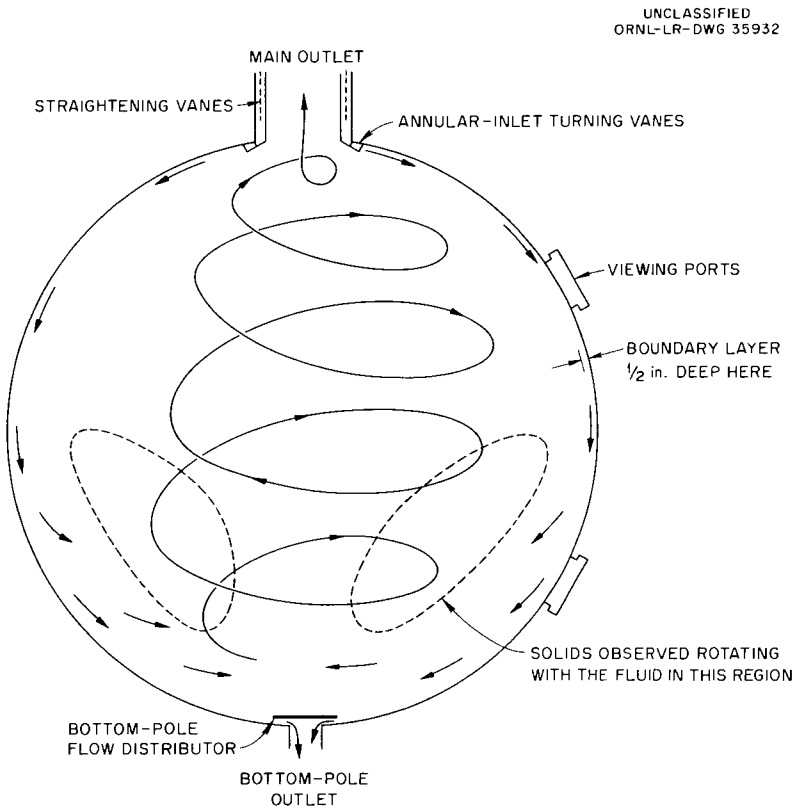

Fig. 5.1. Flow Distribution and Movement of Solids in the Annular-Inlet Core Model.

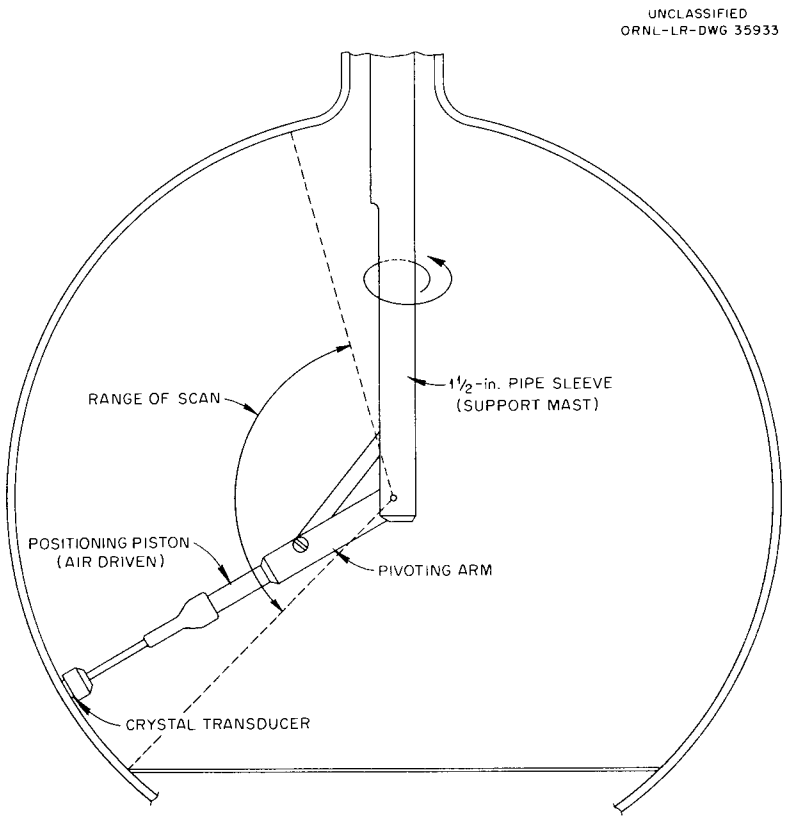

Fig. 5.2. Core-Thickness Measuring Device.

6. HRT CONTROLS AND INSTRUMENTATION

D. S. Toomb

A. M. Billings
J. R. Brown
J. A. Russell
K. W. West

6.1 COMPONENT DEVELOPMENT

6.1.1 Letdown Valves

The HRT letdown valve which throttles about 2 gpm of fuel solution from the reactor high-pressure system to the low-pressure dump tank has now operated satisfactorily for 3000 hr. However, this valve, which has a 1/4-in.-dia port and a 17-4 PH stainless steel plug, is oversized, and a 1/8-in.-dia-port valve was constructed[1] and installed on the HRT mock-up loop for test operation. This valve, which also has a 17-4 PH plug, has now operated satisfactorily for over 3400 hr. After 2600 hr of operation, the valve was leak-tested in the loop and held against system pressure for 50 min without any observable decrease in pressurizer level. An identical valve was made and assembled as a spare for the HRT.

6.1.2 End-Seals for Mineral-Insulated Cable

An improved design, mineral-insulated cable end-seal was specified, and a sample quantity purchased from the Joy Manufacturing Company. These new ceramic-to-metal seals are sturdier and are designed for easier silver-solder sealing than those utilized on the magnesium oxide-insulated copper-sheathed cables now installed in the HRT.[2] The new seals, pictured in Fig. 6.1, are rated for 440-v a-c service and will operate at 700°F with an external pressure of 200 psi. These seals are drilled for a 4-conductor No. 12 AWG cable, but other cable configurations can be accommodated by changing the ID of the end-bell and the bore of the conductor capillary.

6.1.3 Remote-Area Gamma-Monitoring System

An improved experimental solenoid mechanism was built for the sensing head of the Victoreen remote-area radiation-monitoring system.[3] The system is used in the HRT to detect radiation leaks into such reactor auxiliaries as the steam, cooling water, and off-gas systems. The solenoid mechanism provides a calibrating signal for the instrument by positioning

an aluminum beta-particle shield between a built-in strontium-90 source and the radiation sensing chamber. The shield-shutter mechanism presently in use has failed frequently. The new mechanism pictured in Fig. 6.2 utilizes the components of the old head plus an inline shutter slide rack; a new waterproof housing was also made. The new unit will be evaluated before the reworking of the units now in service is considered.

6.2 MAINTENANCE AND MODIFICATIONS

6.2.1 Control Valves

Minor maintenance to plant valves in the last quarter included the replacement of the seats in the solenoid valves (Skinner Electric Valve Division) which pilot air to the actuating cylinder of the 4-in. plug-cock valves (Cameron Iron Works, Inc.). Two of these large valves are installed to isolate the steam generators from the external steam system in case radioactivity is detected in the reactor steam.

A few of the model UP-2-375 valves (Airmatic Valve, Inc.) installed on air lines penetrating the reactor shield-face were found to have flattened O-ring seats; this flattening is attributed to overheating when the 3/8-in. air lines were silver-solder-sealed into the valve bodies.

Only one primary system valve has had to be discarded so far because of being too badly contaminated for maintenance. Two letdown valves and a blanket-system dump valve have been rebuilt after extensive decontamination. When removed from the reactor, the radiation levels of the valves were about 10 r/hr at contact; this was reduced to about 30 mr/hr by electrolytic decontamination procedures.

6.2.2 Electric Power Distribution System

A survey of the operating electrical loads at the reactor site was made and compared with the installed load center and local generating capacity.[4] Particular attention was given to the electrical power requirements necessary to maintain reactor operation in the event of a failure of the TVA supply. The survey indicated that the 312-kva-rated generator (bought for HRE operation) can supply the plant from reactor-produced steam if nonessential loads are disconnected in the event of a TVA supply outage.

6.2.3 Revisions of the Controls and Instruments System

The safety of the reactor was reviewed on the basis of mixed-region operation, and several modifications were made to provide additional protection against unsafe conditions.

The dump-control test-panel was revised to permit the separate air loading of the two reactor emergency drain valves. The loading

pressures which keep the valves closed were also reduced to permit them to function as self-actuating relief valves in case of an uncontrolled pressure rise in the reactor. The lower loading pressures decrease the available sealing force and thereby increase the possibilities of leakage but were considered necessary to increase the inherent safety of the system. With the present settings, the valves will relieve automatically at 2500 psig ± 100 psig.

The temperature of the new core purge-line installed for removing circulating solids from the reactor system is monitored by three thermocouples, and the flow rate is determined by measuring the differential pressure across the chemical plant hydroclone. A low flow condition which might result in insufficient cooling of the line is annunciated so that the operator can reduce the power if it is above 1 mw.

Two thermocouples located relatively low and high in the fuel pressurizer vapor space were connected differentially to provide an independent alarm signal in case of high liquid level in the pressurizer. Such a situation could arise if the pressurizer liquid-level transmitter were to fail.

A patch panel was designed and will be installed to permit individual units in the station battery to be replaced during operation. It will also facilitate the connection of an auxiliary battery-charging generator. This 48-v d-c system supplies power to all critical circuits in the reactor control system.

A small dynamotor was purchased and will be connected to power the public-address system from the station battery in case of failure of the a-c power system.

REFERENCES

1. D. S. Toomb et al, HRP Quar. Prog. Rep. for Quars. ending April 30 and July 31, 1958, ORNL-2561, p 50.

2. Ibid., p 52.

3. W. P. Walker et al, HRP Quar. Prog. Rep., Jan. 31, 1955, ORNL-1853, p 37.

4. J. A. Russell, HRT Electrical Load Survey, CF-59-1-69 (to be issued).

UNCLASSIFIED
PHOTO 33385

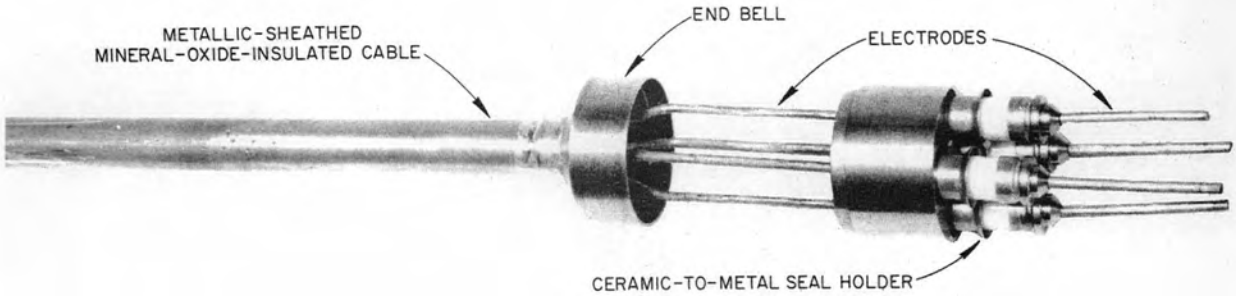

Fig. 6.1. Improved Mineral-Insulated Cable End-Seal.

UNCLASSIFIED
PHOTO 33316

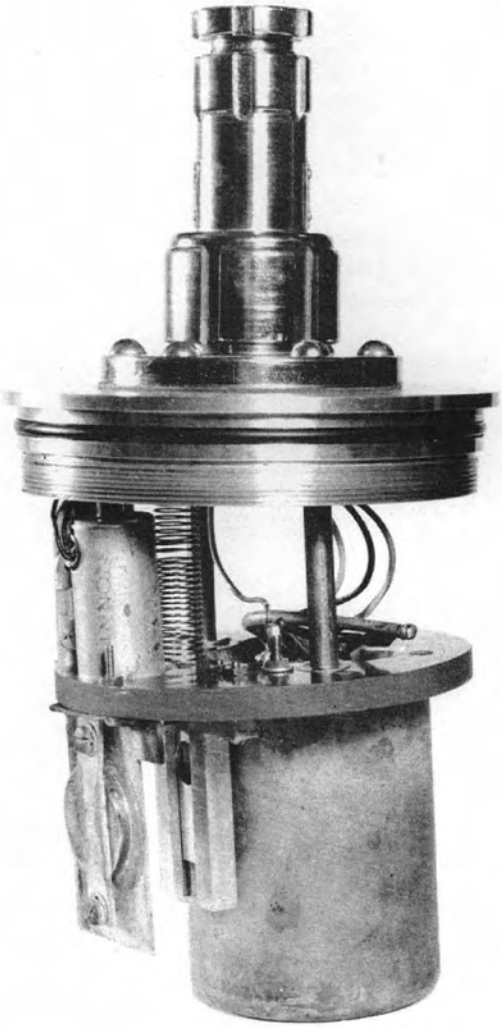

Fig. 6.2. Experimental Solenoid Mechanism for Source-Shutter Positioning.

PART II

REACTOR ANALYSIS AND RESEARCH

R. N. Lyon

7. RESEARCH AND ANALYSIS

P. R. Kasten

R. D. Cheverton
T. B. Fowler
T. H. Mauney
C. S. Morgan
B. E. Prince
M. W. Rosenthal
D. G. Thomas

7.1 EFFECT OF CORE-VESSEL THICKNESS ON THE NUCLEAR CHARACTERISTICS OF REFLECTED AND BARE SLURRY REACTORS

The nuclear characteristics of small slurry reactors reported previously[1] were examined further. The ratio of U^{235} to thorium required for criticality (critical-mass ratio) was computed for some bare and reflected reactors, with the thickness of the stainless steel core vessel treated as a parameter. The critical-mass ratios of the reflected systems at 200°C were obtained; then, with the same cores and core-vessel thicknesses, the critical ratios of unreflected systems at various temperatures were computed, in order to examine the effect on criticality of "dumping" the reflectors. The calculations for the reflected systems were performed on the IBM-704 computer with a two-group, multiregion calculation which treats the core vessel as a separate region. The bare reactors were computed with a two-group, two-region Oracle code, the core vessel being the second region. The core-vessel thickness was assumed to be 3/16, 1/4, and 1 in.; core diameters treated were 2 and 2-1/2 ft; slurry concentration ranged from 200 to 800 g of Th per liter. The core and reflector moderators were either 95% D_2O - 5% H_2O, or 90% D_2O - 10% H_2O. All the reflected reactors had a 5-ft-dia pressure vessel and were assumed to be operating at an average temperature of 200°C, while the temperature of the bare-core systems ranged from 200 to 20°C.

7.1.1 Effect of Core-Vessel Thickness on Critical-Mass Ratios

The effect of the stainless steel core-vessel thickness on critical-mass ratio for the reflected reactors at 200°C is shown in Fig. 7.1 as a function of core size and thorium concentration for a moderator containing 90% D_2O. For a core diameter of 2-1/2 ft, the critical-mass ratio of U^{235} to thorium increased by about 38% in going from a 3/16- to a 1-in.-thick core vessel. The increase was about 50% for a moderator composition of 95% D_2O - 5% H_2O. Since stainless steel acts as a neutron reflector as well as absorber, the effect on critical-mass ratio diminished as the core-vessel thickness increased.

The effect of the core-vessel thickness on the critical-mass ratio was calculated for the bare-reactor systems with the two moderator compositions and various reactor temperatures. Since the stainless steel core vessel was the reflector in this case, increasing the thickness had the effect of decreasing the critical ratio for a particular core thorium concentration. Table 7.1 gives the critical-mass ratio as a function of wall thickness for reactors having a 2-1/2-ft dia core, a moderator composition of 90% D_2O - 10% H_2O, thorium concentration of 200 and 400 g of Th per liter, and temperatures of 200, 100, and 20°C.

7.1.2 Effect of Dumping the Reflector

The results given in Fig. 7.1 and Table 7.1 can be used to determine whether a reflected reactor which is critical at 200°C will be subcritical as a bare reactor (water reflector removed) at 20°C. Only for a core-vessel thickness of 1 in. does the critical-mass ratio of the dumped reactor (at 20°C) fall below that of the corresponding reflected reactor (at 200°C). Figure 7.2 gives some specific results; Fig. 7.2a indicates that for a core-vessel thickness of 1/2 in. the bare reactor would always be subcritical if the critical-mass ratio were less than 0.09; also, this latter value would permit the reflected reactor to become critical at 200°C. As shown in Fig. 7.2b, if the core-wall thickness were 1 in., the bare reactor at 20°C would become critical at a critical-mass ratio less than that required for the reflected reactor at 200°C; however, by utilizing a moderator composition of about 95% D_2O, or by reducing the core diameter, this situation can be avoided. If the core-wall thickness were less than 1/2 in., the reactivity worth of the reflector would be greater than indicated in Fig. 7.2a.

7.2 REACTIVITY COMPENSATION BY ADDITION OF NEUTRON POISONS TO SLURRY REACTORS

Under adverse temperature conditions during startup and shutdown of slurry reactors, large reactivity additions could result from changes in slurry concentration. These problems might be simplified if it were possible to add to the slurry fuel a homogeneous poison which also could be readily removed. The amount of poison to be added would be the amount required to reduce the maximum critical temperature in the reactor from the operating temperature to some permissible level. An estimate was made of the homogeneous thermal-poison levels required for: (1) a large single-region breeder, (2) a bare reactor equivalent in size to the core of a large two-region breeder, and (3) a small single-region slurry reactor.

The large one-region reactor had a 12-ft-dia core, and heavy water was the moderator; at 280°C it had a thorium concentration of about 150 g/liter and a critical-mass ratio of about 0.02 g of U^{235} per g of Th. The reactor equivalent in size to the core of a large two-region breeder had a 4-1/2-ft-dia core and was moderated with heavy water; at 280°C it had a thorium concentration of 200 g/liter and a critical-mass ratio of about 0.08 g of U^{235} per g of Th. The small one-region slurry

Table 7.1. Effect of Core-Vessel Thickness on Critical-Mass Ratio for Bare Reactors Having a 2-1/2-ft ID and a Moderator Composition of 90% D_2O - 10% H_2O

Reactor Temp. (°C)	Th Conc. (g/liter)	Vessel Thickness (in.)	Critical-Mass Ratio (g U^{235}/g Th)
200	200	3/16	0.32
		1/2	0.24
		1	0.18
	400	3/16	0.46
		1/2	0.28
		1	0.18
100	200	3/16	0.15
		1/2	0.13
		1	0.11
	400	3/16	0.14
		1/2	0.12
		1	0.096
20	200	3/16	0.12
		1/2	0.10
		1	0.088
	400	3/16	0.11
		1/2	0.093
		1	0.078

reactor had a 2-1/2-ft-dia core, and the moderator was composed of 20% H_2O - 80% D_2O; the maximum critical temperature was 200°C; at this temperature it had a thorium concentration of about 400 g/liter and a critical-mass ratio of about 0.10 g of U^{235} per g of Th.

The initial poison level in the above reactors was assumed to be zero, and the neutron poisons required to maintain criticality was calculated as a function of reactor temperature. Figure 7.3 summarizes the results of the computations in terms of the poison fraction required for criticality as a function of reactor temperature (the poison fraction is the ratio of thermal neutrons absorbed in poison to thermal neutrons absorbed in U^{235}). The bases for the calculations are discussed in reference 2.

To illustrate the use of Fig. 7.3, consider that the maximum critical temperature in the 12-ft-dia reactor is to be reduced from 280 to 20°C. The poison will be assumed to be a form of natural boron which remains associated with the thoria. From Fig. 7.3 the poison fraction required is about 0.20. Since the thermal-absorption cross section of natural boron is about the same as that for U^{235}, about 50 ppm of natural boron is required to keep the reactor subcritical at temperatures above 20°C. The corresponding boron concentrations for the 4-1/2- and 2-1/2-ft-dia reactors would be about 550 and 700 ppm, respectively. The above values correspond to 0.03 g of boron per kg of water for the large reactor and to about 0.43 g/kg for the small slurry reactor.

7.3 THORIA-SLURRY RHEOLOGY

7.3.1 High-Temperature Viscometer

The high-temperature (200°C) vertical-tube viscometer[3] has been calibrated; dynamic tests were made at room temperature with water (viscosity of 0.9 centipoise) and sugar-water solution (viscosity of 12.3 centipoise). Static calibration tests were made by weighing the amount of mercury required to fill the viscometer tube. The tube diameters obtained by means of the calibration tests are given in Table 7.2. As can be seen, the agreement is quite satisfactory.

Table 7.2. Tube Diameter of High-Temperature Vertical-Tube Viscometer as Determined by Calibration Tests

Method		Tube Diameter (in.)
Dynamic		
Water	(0.9 cp)	0.099 ± 0.002
Sugar-water	(12.3 cp)	0.101 ± 0.001
Static (weight of mercury)		0.100
Nominal tube diameter		0.100

Dynamic tests have also been made with water at 75 and 180°C. The agreement of the data with the smooth-tube relations was within 2%; temperature control was within ±2°C.

7.3.2 Pseudo High-Temperature Slurries

Since it would be desirable to conduct drop-out velocity studies at room temperature with a slurry having essentially the same properties as aqueous ThO_2 slurries at elevated temperatures, a program was initiated to study the characteristics of various organic-ThO_2 systems. The first organic material chosen was methanol. Two oxides were selected: (1) thoria (designated as DT-10 and originally calcined at 1225°C) which had been refired at 650°C after an addition of 0.5 wt % U; and (2) thoria (designated as DT-14) which had been calcined at 1600°C. The mean particle size of thoria DT-10 was 0.7 micron, while that of thoria DT-14 was 2.8 microns.

Previous experimental results[4] have shown that the yield stress of different aqueous thorium oxide slurries at room temperature is given by the relation

$$\tau_y = K \frac{\phi^3}{D_p^{\,2}} , \qquad (1)$$

where τ_y = yield stress, lbf/ft^2,

ϕ = volume fraction solids,

D_p = mean particle diameter, microns,

$K = (2.2 \pm 1.3) \times 10^2$.

The value of K in aqueous suspensions for the particular oxides considered here (DT-10 and DT-14) was $(2.3 \pm 1.0) \times 10^2$ for values of ϕ from 0.07 to 0.15. When suspended in methanol, these oxides had effective K values of $(0.6 \pm 0.1) \times 10^2$ for values of ϕ from 0.09 to 0.18.

7.4 NUCLEATE-BOILING HEAT TRANSFER IN AQUEOUS THORIA SLURRIES

Boiling at the core-blanket interface of large-scale (440 thermal megawatt) two-region homogeneous reactors has been predicted[5] on the basis of calculated heat generation rates in the core-vessel wall. Also, boiling may be partially responsible for slurry caking in high-temperature loops.[6] Although much is known about nucleate-boiling heat transfer in homogeneous-liquid systems, information is meager concerning this phenomenon in slurry systems. Experiments[7] reported here concerned nucleate-boiling heat transfer in ThO_2-H_2O slurries having thorium concentrations ranging from 0 to about 1000 g/liter; the thoria particles were primarily 1-3 microns in diameter.

The equipment was similar to that used by Rosenthal.[8] It consisted basically of a resistance-heated platinum tube (1/8 or 1/16 in. diameter) immersed in ThO_2-H_2O slurry. A thermocouple was used to measure the wall temperature of the platinum tube, while measurement of the current through the tube indicated the rate of energy generation. A 1-gpm centifugal pump was used to recirculate the slurry and maintain it in suspension in a 3-gal tank; heaters were used to keep the slurry at its boiling temperature; vapor condensers maintained the desired slurry concentration. The tank containing the slurry had a glass window; the platinum tube could be placed adjacent to the window, and this permitted visual determination of whether boiling took place.

In initial tests with water, the data obtained were in good agreement with results of other investigations.[8-10] Tests were then made with slurries having 0.02, 0.06, and 0.1 volume-fraction solids; runs were made with the tube adjacent to the glass window and with the tube separated from the window by at least 5/8 in. A typical set of data obtained with a volume-fraction solids of 0.1 is shown in Fig. 7.4. As shown, the reproducibility of the data on repeated heating and cooling cycles was good.

The results were interpreted in terms of the equation

$$\frac{q}{A} = K(\Delta T)^n , \qquad (2)$$

where q/A = heat flux, Btu/hr-ft^2,

K = dimensional constant,

ΔT = temperature difference between platinum-tube wall and bulk-slurry temperature, °F.

For the slurries studied, the heat flux at a ΔT of 10°F was about 10^4 Btu/hr-ft^2, regardless of the slurry concentration. However, the value of the exponent n in Eq. 2 decreased with increasing volume fraction solids, as illustrated in Fig. 7.5 (the value of n was obtained by taking the average slope of the log q/A versus log ΔT curve for ΔT's between 10 and 50°F). The value of n approached unity at a volume fraction solids of 0.1; this value is normally associated with convection rather than nucleate-boiling heat transfer.

Another feature considered was the occurrence of "burnout." Conditions of burnout exist when the heat flux becomes so large that nucleate boiling cannot be sustained and there is a rapid transition to film boiling with a 10- or 20-fold increase in ΔT. If the melting point of the tube from which boiling takes place is exceeded, then true burnout is observed. If the tube has a high melting point, then stable film boiling may be achieved instead of actual burnout.

Maximum heat fluxes that have been observed with water[9] are between 300,000 and 400,000 Btu/hr-ft^2, and the critical ΔT (associated with maximum heat flux under nucleate-boiling conditions) is often between

45 and 50°F. Good correlations of heat flux at the critical ΔT have been achieved with the relation:

$$\frac{(q/A)_{max}}{\lambda\rho_v} = 143\left(\frac{\rho_L - \rho_v}{\rho_v}\right)^{0.6}, \qquad (3)$$

where λ = latent heat of vaporization, Btu/lb,

ρ_L = density of liquid, lb/ft^3,

ρ_v = density of vapor, lb/ft^3,

$(q/A)_{max}$ = maximum heat flux under nucleate boiling conditions, Btu/hr-ft^2.

The value for $(q/A)_{max}$ and the associated conditions are given in Table 7.3; the occurrence of burnout or film boiling is also designated. The value of 490,000 Btu/hr-ft^2 obtained experimentally for maximum heat flux for water is in satisfactory agreement with the value of 420,000 Btu/hr-ft^2 obtained from Eq. 3. The maximum heat flux obtained for the concentrated slurries averaged 210,000 Btu/hr-ft^2, or about half the value observed with water. This difference in $(q/A)_{max}$ corresponds to a reduction in the maximum heat transfer coefficient from 10,000 to 2,000 Btu/hr-ft^2-°F.

Although no data on burnout were obtained for the more dilute slurries, some information can be obtained from the data obtained with a slurry having 0.023 volume fraction solids (about 200 g of Th per kg of H_2O). It was possible to achieve heat fluxes of at least 400,000 Btu/hr-ft^2 with no evidence of transition from nucleate to film boiling. This was not true at a volume fraction solids of 0.059 (about 580 g of Th per kg of H_2O). Thus appreciable concentrations of slurry (greater than 200 but less than 600 g of Th per kg of H_2O) are apparently required before burnout heat fluxes are significantly reduced.

The physical properties of the slurries were measured in conjunction with other studies;[11] these are given in Table 7.4.

7.5 THORIA CAKING STUDIES

7.5.1 Effect of Temperature on ThO_2 Cake Formation

Cake formation during circulation of ThO_2-H_2O slurries has usually been studied in the temperature range of 200 to 300°C. To study the effect of temperature on cake formation, a slurry which normally formed cakes and spheres at above 200°C (made from thoria batch LO-20) was circulated at 45°C in the 30-gpm loop; the initial thorium concentration was about 400 g per kg of H_2O. Cake formation did not occur, and only a few small spheres (5 to 10 microns in diameter) developed. Since surface-active agents appear to be more effective in dispersing slurries at low

Table 7.3. Burnout Data for Pool Boiling of Water and Aqueous ThO_2 Slurries

Tube Dia. (in.)	Placement of Tube*	Slurry Conc. (g Th/kg H_2O)	Phenomena Observed	$(q/A)_{max}$ (Btu/hr-ft^2)
1/16	B	0	Burnout	490,000
1/8	A	740	Film boiling	223,500
1/8	B	986	Film boiling	214,000
1/8	A	1015	Film boiling	160,000
1/16	B	1000	Burnout	240,000

* Designation A refers to placement adjacent to glass window; B refers to placement 5/8 in. from window.

Table 7.4. Physical Properties of ThO_2-H_2O Slurries at 95°C

Slurry Concentration		Yield Stress, (lb/ft^2)	Coeff. of Rigidity, η (cp)	Prandtl Number (using η for viscosity)
g Th / kg H_2O	Volume Fraction Solids			
220*	0.024	0.002	0.6	2.5
710	0.074	0.066	1.7	4.7
1100	0.110	0.49	3.2	8.0

* Estimated value.

temperatures than at elevated temperatures,[12] their presence (small amounts were present) may have prevented cake formation, either by retarding primary-particle degradation or by preventing reagglomeration of fine particles. During this low-temperature run corrosion was extremely low.

After 270 hr of circulation at 45°C the temperature was increased to 275°C and circulation continued an additional 170 hr. Growth of the small spheres was evident in the first 20 hr at the elevated temperature, but the bulk of the oxide was not converted to spheres; the larger spheres subsequently disappeared from the circulating stream. At the end of this run there was an oxide film (0.0069 in. thick) covering most of the surface

which was exposed to a fluid velocity of about 5 fps. This film, which probably formed during the last part of the run at 275°C, occurred only in the 5-fps section; there were no cake deposits in the impeller. The film did not wash away in a water stream but was easily removed with a sponge. An electronmicrograph of the thoria from this film indicated that the smallest particles were less than 0.02 micron. Films formed in the 10- and 5-fps sections during previous runs[13] with LO-20 thoria were also examined with the electron microscope; a large number of the thoria particles in these films were also less than 0.02 micron. No definite variation was noted in the size of particles deposited in sections having different flow velocities.

7.5.2 Circulation of Oxide Previously Autoclaved with HNO_3

Slurry composed of thoria batch LO-20 was autoclaved at 300°C for 36 hr in the presence of 3200 ppm HNO_3 (based on thoria present); it was then circulated in the 30-gpm loop at 275°C. Cake and sphere formation similar to that expected in the absence of autoclaving or other treatment was observed, indicating that the pretreatment caused no appreciable change in thoria structure. The zeta potential of the slurry charged to the loop was +94 mv (as determined by electrophoretic measurements at room temperature); samples drawn during subsequent slurry circulation and cooled to room temperature had approximately the same value.

During circulation of the autoclaved oxide, films or thin cakes formed on surfaces exposed to fluid velocities of 5 and 10 fps, but not on the surface exposed to a 20-fps velocity. Film exposed to the 10-fps velocity was harder than that exposed to the 5-fps velocity, in agreement with results obtained in an earlier run.[13]

The cake resuspension index (CRI) of the slurry studied was measured before nitric acid addition and autoclaving, and was found to be 7 (this value corresponds to a caking slurry). After the acid addition and autoclaving, the CRI was zero, indicating that the slurry should be non-caking, although it actually caked. However, it was also found that the CRI of unautoclaved oxide containing 3200 ppm HNO_3 was only 0.8. Thus it appears that the nitric acid acted as a surface-active agent, reducing the CRI by preventing particle comminution during the Waring Blendor treatment associated with CRI determination. Autoclaving by itself appears to increase particle-structure strength through a process of thoria dissolution and redeposition.

7.5.3 Circulation of ThO_2 at Low Concentrations

To study the effect that thorium concentration may have on slurry caking tendency, slurries made from batch LO-20 thoria were circulated[1] in the 30-gpm loop at concentrations of 75 and 100-200 g of Th per kg of H_2O. The low-concentration slurry did not cake, but the one containing between 100 and 200 g of Th per kg of H_2O formed cakes and spheres.

7.6 DIAPHRAGM-PUMP STRESS STUDIES

It is desirable to obtain the largest possible displacement volume from a given size (diameter) pump for a specified value of the diaphragm stress. A recent study[14] indicates that in the case of a two-radii contour diaphragm pump, shown diagrammatically in Fig. 7.6, an optimum ratio of the two radii exists for which the volume-to-stress ratio is a maximum, with the optimum radii ratio depending only on the ratio of diaphragm thickness to maximum deflection at the center. Figure 7.7 gives the results obtained.

Diaphragms usually fail as a result of fatigue if the stress level is excessive. Therefore, in calculating the volume-stress ratio, a method of calculating the stresses which would consider the fatigue properties of a biaxially stressed object was desired. For this purpose the Mises-Hencky criterion of fatigue failure was used, which states that for an endurance limit σ_e, failure will occur at less than 10^7 cycles (for complete reversal of stresses), when

$$\sigma_e = \sqrt{\sigma_1^{\,2} + \sigma_2^{\,2} - \sigma_1 \sigma_2}\,, \tag{4}$$

where σ_1 and σ_2 are the principal stresses.

The diaphragm stresses include both membrane and bending stresses. As the diaphragm is deflected from one contoured head to the other, the membrane stresses go through zero but do not change sign, while the bending stresses do change sign. To account for this nonreversal of total stress, the modified Goodman diagram was used to obtain the relation:

$$\sigma_a = \frac{2\,\sigma_e\,\sigma_{ult}}{K(\sigma_e + \sigma_{ult})} = \sqrt{\sigma_1^{\,2} + \sigma_2^{\,2} - \sigma_1 \sigma_2}\,, \tag{5}$$

where σ_a = maximum permissible combined stress,

σ_e = endurance limit,

σ_{ult} = ultimate strength of material,

K = factor that reflects the accuracy with which σ_e and σ_{ult} are known.

Equation 5 is to be used in conjunction with the results given in Fig. 7.7.

REFERENCES

1. P. R. Kasten et al., HRP Quar. Prog. Rep. Oct. 31, 1958, ORNL-2654, p 53-62.

2. B. E. Prince and M. P. Lietzke, Survey of the Static Nuclear Characteristics of Small One-Region Slurry Reactors, Part III, ORNL CF-58-12-15 (Dec. 8, 1958).

3. R. B. Korsmeyer et al., HRP Quar. Prog. Rep. April 30, 1957, ORNL-2331, p 66-70.

4. D. G. Thomas, P. H. Hayes, and R. M. Summers, Laminar and Turbulent Flow Characteristics of Aqueous ThO_2 Slurries (ORNL report to be published).

5. R. B. Korsmeyer et al., HRP Quar. Prog. Rep. Jan. 31, 1955, ORNL-1853, p 52.

6. See, for example, A. S. Kitzes and P. R. Crowley in Discussion p 25-26, ORNL CF-56-4-120. Further Information on the Cake Formed During Slurry Test 200A-3, (April 30, 1956).

7. D. G. Thomas, L. D. Felten, and R. M. Summers, Nucleate Boiling Studies with Aqueous ThO_2 Slurries, (ORNL CF report to be published).

8. M. W. Rosenthal and R. L. Miller, Effect of Oil Contamination on the Boiling Heat Transfer Characteristics of Heat Exchangers and Solid Fuel Plate Reactors, ORNL CF-54-5-159 (May 19, 1954).

9. J. W. Westwater, "Boiling of Liquid" in Advances in Chemical Engineering, Ed. by T. B. Drew and J. W. Hoopes, Jr., Vol. 1, Academic Press, New York (1956).

10. C. F. Bonilla, Editor, Nuclear Engineering, McGraw-Hill, New York (1957).

11. D. G. Thomas and P. H. Hayes, Heat Transfer and Fluid Flow Characteristics of Aqueous ThO_2 Slurries, ORNL-2540 (to be published).

12. C. S. Morgan, Influence of Surface Active Agents on ThO_2 Slurries, ORNL CF-58-7-56 (July 15, 1958).

13. P. R. Kasten et al., HRP Quar. Prog. Rep. for Periods Ending April 30 and July 31, 1958, ORNL-2561, p 87-88.

14. R. D. Cheverton, Maximizing Volume to Stress Ratio for a Two-Radii Contour Diaphragm Pump, ORNL CF-59-2-2 (Feb. 2, 1959).

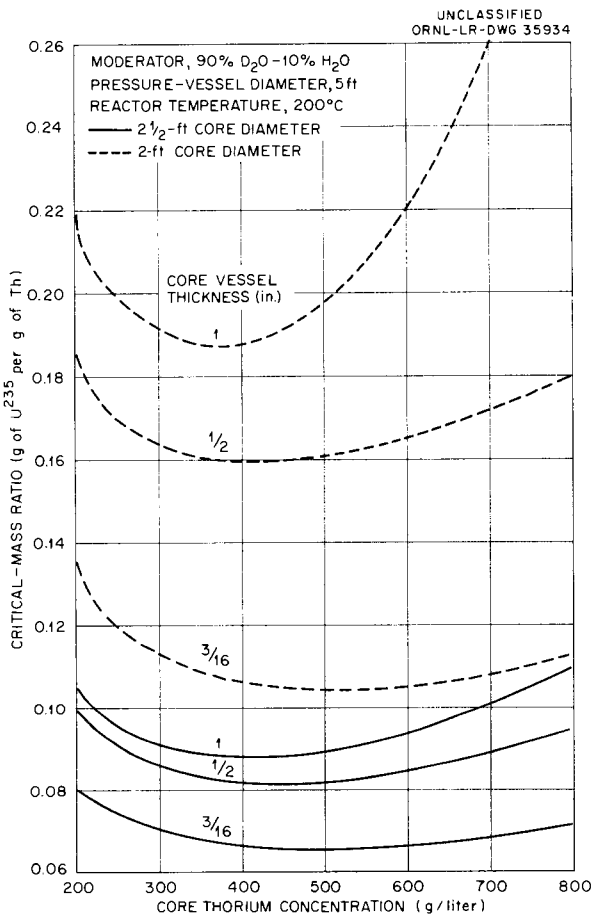

Fig. 7.1. Critical Ratio of U^{235} to Thorium vs Core Thorium Concentration for Reflected Reactors.

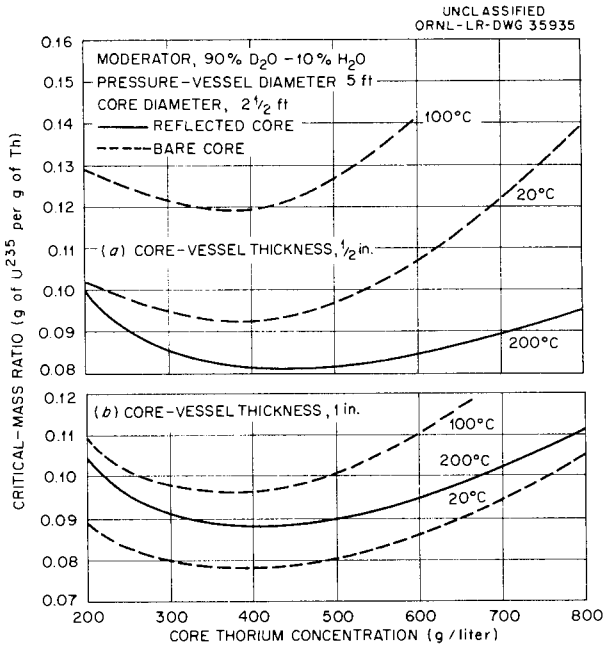

Fig. 7.2. Critical Ratio of U^{235} to Thorium vs Core Thorium Concentration for Reflected and Bare Reactors at Different Temperatures.

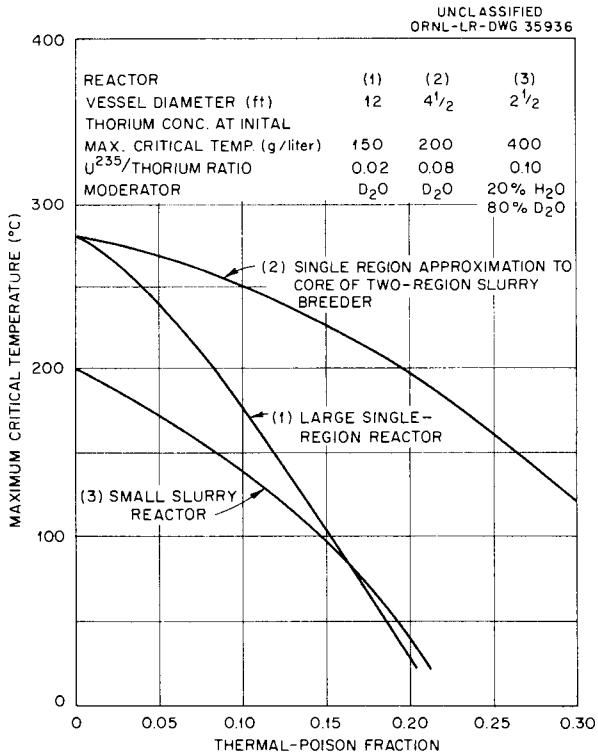

Fig. 7.3. Maximum Critical Temperature in Slurry Reactors vs Neutron-Poison Level.

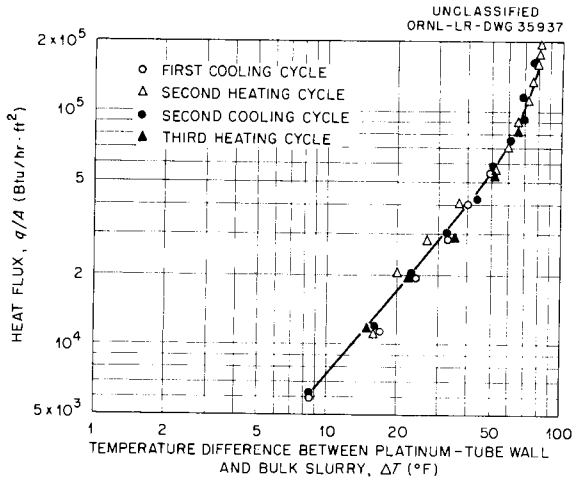

Fig. 7.4. Relation Between Heat Flux and Temperature Driving Force Under Nucleate Boiling Conditions in a ThO_2-H_2O Slurry Containing 0.10 Volume Fraction Solids ($\frac{1}{8}$-in.-dia Platinum Tube at Least $\frac{5}{8}$ in. from Nearest Surface; Forced Convection Rate ~1 gpm in a Tank Containing ~3 gal of Slurry).

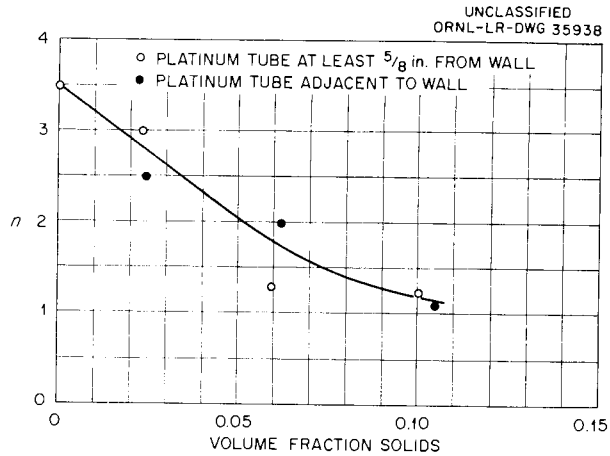

Fig. 7.5. Effect of Volume Fraction Solids on Value of n in Equation $q/A = K(\Delta T)^n$.

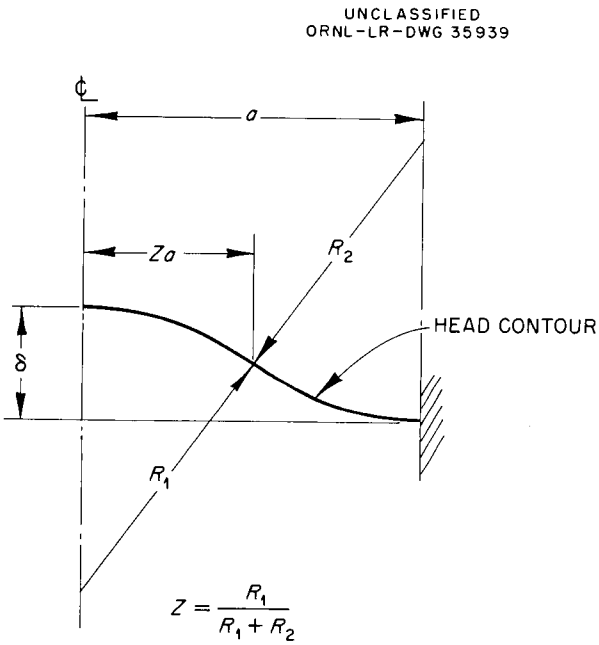

Fig. 7.6. Diagrammatic Representation of Two-Radii Head Contour for Diaphragm Pump.

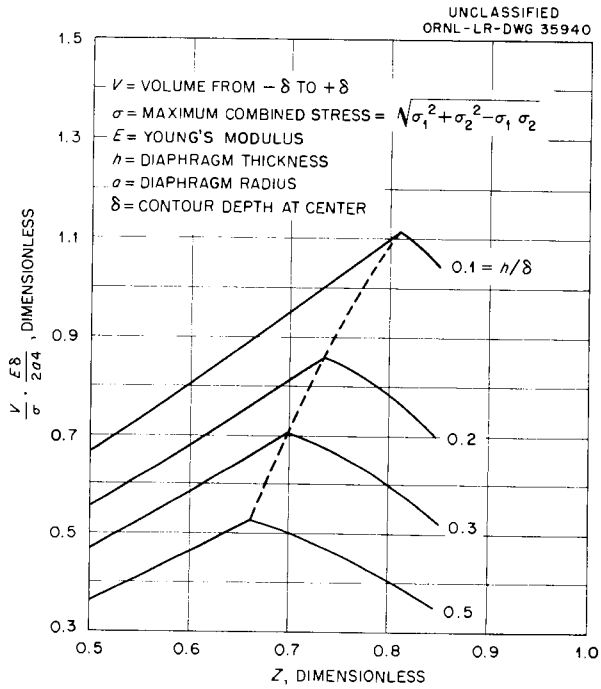

Fig. 7.7. Volume-Stress Ratio vs Z for Various Values of h/δ.

PART III

ENGINEERING DEVELOPMENT

R. N. Lyon

8. DEVELOPMENT OF FUEL- AND SLURRY-SYSTEM COMPONENTS

I. Spiewak

T. G. Chapman
D. M. Eissenberg
C. H. Gabbard
B. A. Hannaford
E. C. Hise
C. G. Lawson
J. C. Moyers
I. K. Namba
H. R. Payne
H. C. Roller
R. P. Wichner

8.1 HIGH-PRESSURE RECOMBINER LOOP

The natural-circulation recombiner was operated for 435 hr at 1500 psi and at an average electrolytic gas input of 0.60 scfm. Operation was routine, although a small leak in a Bourdon tube prevented operation in December, pending arrival of a replacement. Minor piping changes appear to have been effective in controlling caustic transfer from the electrolytic cells to the recombiner.

8.2 CENTRIFUGAL PUMPS

8.2.1 20-cfm Allis-Chalmers Blower

The 20-cfm canned-motor blower continued circulating a steam-nitrogen mixture at 170°C and 1400 psi (4.8 lb/ft^3 density); the blower has operated for approximately 7000 hr with no difficulty.

8.2.2 Reliance 6000-gpm Pump

Work on the Reliance 6000-gpm pump was stopped at the request of the vendor, who has decided tentatively to withdraw from the canned-motor pump field. Possible courses of action for the completion of the prototype unit or for the orderly termination of the contract are being considered.

The insulation-test stator being irradiated in a Co^{60} source has received approximately 2.8×10^9 rad thus far. Although this exposure is greater than would be expected within the service life of a large fuel pump, no significant changes in leakage current or breakdown voltage have been observed.

8.2.3 300A Slurry Pump and Loop

The main closure of the 300A pump was seal welded after a second major leak occurred at the pump flange during a loop startup. Since being seal welded, the loop has operated at 280°C and 1500 psi for approximately 1200 hr, circulating 1600°C-fired thoria at a concentration of 460 g of Th per kg of H_2O. The purpose of the present run, scheduled for 2000 hr, is to evaluate various impeller-vane shapes and to evaluate mechanically-mounted aluminum oxide bearings.

8.2.4 200Z Slurry Pump and Loop

An electrical failure of unknown origin occurred in the 200Z pump stator during performance and thrust testing. A helium-leak test of the stator cavity did not indicate a leak. Start-up of the 200Z loop, construction of which was completed during the quarter, will be delayed pending the repair of the stator.

8.2.5 Hydraulic Design of Slurry Pump

Design of a 350-gpm, 80-ft-head hydraulic end for the 300A pump was completed. This design incorporates a three-dimensionally curved impeller, top and bottom radial shroud ribs intended to reduce the pressure drop across the suction wear ring, and a volute splitter to decrease the radial bearing load. The design will be evaluated in the 300A pump when the necessary parts become available.

The design and fabrication of a vaneless diffuser for use in the 200Z pump was completed.

8.2.6 Test Program for Bearings Operating in Slurry Pumps

The Franklin Institute completed the construction and modification of their test room and bearing-test machines. Test-loading of aluminum oxide bearings is scheduled to start in February.

The aluminum oxide bearings mounted mechanically in the 300A pump have operated satisfactorily for 1200 hr to date. Bearings flame plated with aluminum oxide, and a "solid shoe" thrust bearing are being procured for evaluation.

8.2.7 Shaft Seals

Floating bushing seals were made for testing in the 300A and 200Z pumps, with the objective of reducing motor-hydraulic end fluid mixing to a negligible level. The 300A seal, designed to run at loop temperature, uses mating surfaces of nitrided titanium. The 200A seal, designed for motor temperature, uses aluminum oxide parts.

8.3 FEED PUMPS

8.3.1 Oxygen Compressors

The Pressure Products Industries single-stage diaphragm compressor has operated satisfactorily for 3429 hr in the HRT mockup.

The Pressure Products Industries three-stage contaminated-service oxygen compressor passed a 250,000-cycle test at the factory, compressing 2.9 scfm of atmospheric air to 2500 psi. The unit is now being set up at ORNL for endurance testing.

8.3.2 Increased-Capacity Solution Pump

The double-diaphragm 10-in. head has continued in operation for 5600 hr, delivering about 2 gpm of fuel solution from atmospheric pressure to 1500 psi. Testing of a more conventional, 12-in. single-diaphragm head of similar output was started, and has proceeded for 1000 hr without incident.

8.3.3 Slurry Feed Pumps

Diaphragm heads as high-pressure slurry feed pumps have continued to operate satisfactorily for 2900 hr, circulating 1600°C-fired thoria slurry to 1500 psi.

Aluminum oxide check-valve trim operated for 1330 hr, with the pump output decreasing rapidly during the last few hours. The seats contained radial cracks believed to be evidence of improper mounting and/or loading. They were lightly and uniformly worn except at the cracks, which were sharply eroded. The balls suffered a uniform weight loss averaging 2% and a diametral loss averaging 45 mils/yr. The seat insert mounting will be redesigned and further tests of aluminum oxide trim made.

Particle size degradation and deflocculation of a fresh charge of 1600°C-fired slurry were again observed. The slurry was returned to a flocculated condition by the addition of chromic acid.

Oxygen pressurization in the high-pressure portion of the feed-pump test loop was attempted, leading to immediate and voluminous formation of stable foam in the letdown line because of the release of dissolved gas. Sufficient heat was then added to the low-pressure system to create mild boiling in the dump tank. Foam accumulation was greatly reduced, though not eliminated. It is planned to repeat this test with sufficient heat to create violent boiling. In another test, the addition of phosphoric acid to the dump tank caused the foam to break up into large flocs, completely eliminating all foam formation. The released gas rose through the supernatant water, with no attached thoria particles.

After the phosphoric acid had become thoroughly mixed, the loop was shut down and allowed to settle for 16 hr. It was restarted without incident.

The Vanton "Flexiliner" low-pressure circulating pump has operated without maintenance for 2400 hr, pressurizing the feed-pump suction line.

8.4 VALVE TRIM

8.4.1 Dump-Valve Trim for Solutions

The solution dump-valve test loop was shut down during the quarter for maintenance.

8.4.2 Slurry Valves

The severe-throttling test station for hand valves on the feed-pump test loop was used to test a tungsten carbide-trimmed valve with a ΔP of 1500 psi for delivery of two hundred sixty 100-ml samples. It appeared to be leak-tight up to about 200 samples, and after 260, it leaked about 10 drops/min. At the conclusion of the test, the trim showed evidence of erosive wear. A valve trimmed with a sapphire ball and seat was similarly tested. Although it was operated with extreme care, it would not shut off after seven operations. Upon disassembly it was found that the seat insert had disappeared and the ball had been crushed.

Check-valve trims of beryllia, thoria, and zirconia are on hand for testing. Of the materials tested to date, only alumina and boron carbide show promise of extended service.

8.4.3 Slurry Letdown Chokes

Two chokes were operated at 100°F during the quarter, letting thoria slurry down from 1300-1500 psi to atmospheric pressure. A portion of 0.063-in.-ID, type 309 stainless steel tubing used at 42 ft/sec for 3600 hr was examined metallographically and found to be undamaged. A portion of 0.125-in.-ID type 347 stainless steel tubing showed no weight loss after 1800 hr of operation at 26 ft/sec.

8.5 HEAT EXCHANGERS

8.5.1 Flow Tests of Slurry Heat Exchanger

A plastic, 7-tube, inverted-L tube-bundle was operated at slurry concentrations varying from 180 to 975 g of Th per kg of H_2O. Test results were quite similar to those reported for the horizontal

model[1]; for 180- to 560-g slurries, dropout was observed in the horizontal portion of the tubes at velocities of 1.8 to 2.0 ft/sec. No dropout was observed for 765-g slurries and above, which are in the compaction-settling range.

All plugs formed in these tests of a well-flocculated slurry were readily resuspended by a slight increase in pressure drop.

8.6 HYDRODYNAMICS OF SLURRY CORE VESSEL

Water flow studies were continued on the 30-in.-dia slurry core vessel having the conical bottom, bottom polar inlet, and concentric outlet. A series of runs was made to provide specific design information for the high-pressure model of this core now being installed in the 300 SM loop.[2]

Maximum wall shear was obtained in the conical portion of the core vessel when the inlet nozzle was inserted into the core up to the imaginary extension of the spherical surface. The boundary layer flow observed in the spherical hemisphere did not extend into the conical section, where the flow was characterized by large turbulent eddies extending to the wall. Transfer of the core model to a slurry loop is now in progress.

8.7 PROPERTIES OF SLURRY SETTLED BEDS

The effect of a 100-v dc potential applied at electrodes 1 cm apart, immersed in settled beds of flocculated, unpumped thoria slurry at room temperature, was that the water in the bed flowed to the negative electrode and was repelled from the positive one (electroendosmosis). There was no visual evidence of slurry flow (electrophoresis) or plating out on either electrode. The electrode which attracted the water tended to dry the slurry nearby, whereas the electrode which repelled the water tended to soften the adjacent slurry and cause it to flow.

REFERENCES

1. I. Spiewak, et al., HRP Quar. Prog. Rep. Oct. 31, 1958, ORNL-2654, p 86, 10/29/58.

2. R. P. Wichner, Water Studies on a Conical Bottom Slurry Core Vessel, ORNL CF-59-1-56.

9. DEVELOPMENT OF REACTOR SLURRY SYSTEMS

R. B. Korsmeyer F. N. Peebles

D. G. Davis L. F. Parsly A. N. Smith
R. J. Kedl H. B. Piper R. Van Winkle
M. Richardson

9.1 CIRCULATING-SLURRY BEHAVIOR

9.1.1 200A-Loop Operation

Run 200A-18 was started on October 29, 1958, and, except for one shutdown for the purpose of installing a densitometer, operated continuously for 1026 hr at 224°C and 750 psi. The run was terminated on December 18, 1958. The purpose of the run was to determine handling characteristics, rheological properties, attack rate, and stability (physical and chemical) of the mixed urania-thoria slurry being pumped at temperatures in the range of those expected to be encountered in the proposed experimental slurry reactor (see Sec. 9.3).

The oxide for the run was prepared in the Chemical Technology Division by boiling thorium oxide (fired at 650°C) in ammonium uranyl carbonate in order to adsorb uranium on the thoria. The material was then refired at 1050°C for 4 hr to drive off the carbon dioxide and ammonia, leaving a thoria particle which contained approximately 8.5% uranium (based on the thorium). The final firing temperature was set to give a surface area of approximately 2 m^2/g.

The weight of mixed oxide charged into the loop was 14.94 kg, and the initial mean particle diameter was 1.5 μ. Early in the run, the total oxide concentration was about 235 g of Th per kg of H_2O, but this value gradually decreased, as sampling depleted the loop inventory, to 160 g of Th per kg of H_2O shortly before the end of the run (about 4.8 kg was removed by sampling).

There was no apparent loss of uranium from the mixed oxide, the U:Th ratio remaining at 0.089 ± 0.002; and there was no measurable particle degradation. The concentration of dissolved uranium and chromium in the slurry filtrate remained less than 2 ppm and 7 ppm, respectively, for the pH range of 4.0 to 6.5.

The attack rate on the stainless steel piping, as indicated by iron accumulation in the slurry, was less than 0.1 mpy; the pump parts were free of visible damage by slurry abrasion. The titanium-impeller weight loss was only 1.2 g, and there was no measurable change in bearing dimensions. At the end of the run, about 1.5 kg of oxide was not recovered and was unaccounted for. The loop pipe walls were clean, and the pressurizer surfaces were coated with a very thin layer of oxide which was brushed and washed off, thereby recovering only about 20 g of oxide. Some of the recovered oxide from the pressurizer was white (believed to have remained from earlier runs). The baffles in the pressurizer were coated fairly uniformly with about 1 mg of oxide per square centimeter.

9.1.2 200B Loop, Description and Operation

During the quarter, construction and preoperational testing of the 200B slurry-loop was completed. The flow diagram is shown in Fig. 9.1. It differs from the 200A loop in two respects:

1. Instead of a single, horizontal pipe flow circuit, three parallel, vertical flow paths are provided from a horizontal discharge header. These lines are 1-in. sched-80, 1-1/2-in. sched-80, and 2-in. sched-160 pipes, approximately 12 ft long, and are equipped with valves.

2. The pressurizer is equipped to operate as either a gas or a steam pressurizer.

The presence of three lines in which the flow rate may be controlled permits flexibility in the installation of special test apparatus in the loop. One such special test device, installed in the 1-1/2-in. pipe, is a heat transfer meter which was designed for detecting the deposition of thorium oxide scales or films on the pipe wall. It consists of a 0.95-in.-thick, nickel-plated copper disc, bored to the same inside diameter as the pipe and clamped between a pair of flanges in the 1-1/2-in. pipe (see Fig. 9.2). A coolant channel is located in the outer rim. Heat is transferred from the flowing stream through the stagnant film at the inner surface of the disc and into the copper, and then by conduction through the copper to the outer coolant channel. Heat is removed from the channel by the boiling of water, the steam from which is condensed. Conduction from the stainless steel flanges to the copper is reduced by use of asbestos gaskets. Nine thermocouples are located at various depths in the copper to permit estimation of the heat flux and inner surface temperature from the temperature gradient in the copper. The amount of heat removed from the coolant is also determined from observing the flow and temperature rise of cooling water to the condenser. Agreement between the values of total heat dissipation determined from the cooling-water heat balance and those calculated from the temperature gradient in the copper supports the validity of the estimate of the inner surface temperatures, and of the experimentally determined liquid-film heat-transfer coefficients. Although the L/D of the inner-liquid

channel is less than one, and thermal end effects may be expected to give higher experimental coefficients than calculated from an accepted empirical correlation for high L/D channels, it is believed that useful apparent heat transfer coefficients for slurry may be obtained and compared with values for water. The formation of scale as much as 5 mils thick will certainly be detectable.

Table 9.1 presents typical results of experiments in which the flow rate of water circulating in the loop past the copper disc was varied from 57.6 to 95 gpm. It can be seen that the experimental values of h are higher than the calculated values (based on the Colburn equation), as was expected, because of heat conduction from the stainless steel pipe to the copper disc and the short length of cooled surface.

The loop was loaded to a concentration of 210 g of Th per kg of H_2O with oxide containing 78.0% and 8.6% uranium, prepared as described above, on January 14, 1959, and will be operated at this concentration to duplicate in this loop the same conditions that were used in run 200A-18. Slurry-performance data from the run are not available at this time.

9.2 BLANKET-SYSTEM DEVELOPMENT

9.2.1 Conversion of 300-SM Loop to High-Pressure Operation

The 30-in.-dia experimental pressure vessel[1] was received on schedule and is being installed in the existing test loop. The vessel installation and changes to the loop will be completed early in the next quarter. After pressure tests, cleanout runs, and water shakedown runs, a slurry run will be started at the tentative design conditions for the proposed experimental slurry reactor.

Fig. 9.3 shows the flowsheet of the high-pressure circulating loop. Slurry circulates from the canned-motor pump through the bottom of the pressurizer to the vessel inlet. Approximately 95% of the flow leaves the vessel at the bottom, the balance leaving through the bypass line at the top. A bypass across the vessel is provided to permit complete drainage of the system. Six sample points are provided on the vessel; three flush with the vessel wall, two projecting 3 in. into the vessel, and one projecting 6 in. into the vessel. Facilities for connecting 16 additional samplers to the vessel, if needed, are provided. Samplers are also provided on the bypass line, the main loop, and at two points on the pressurizer. Provision is also being made to monitor the loop and bypass slurry concentrations by means of continuous gamma absorption densitometers.

A low-pressure system (Fig. 9.4) is also being fabricated, and should be in service approximately one month after completion of the high-pressure system. The dump tank is a 30-in.-dia, vertical, cylindrical tank with a 90-deg included-angle conical bottom. The

Table 9.1. 200B-Loop Typical Water Heat Transfer Measurements

Test	Flow (lb/hr)	Reynolds Number Dg/μ	Loop Temp. (°C)	Heat Flux (Btu/hr) According to Temperature Gradient	Heat Flux (Btu/hr) According to Condensate Measurement	Heat Transfer Coefficient, h (Btu/hr-ft^2-°F) Calc. from Temp. Gradient	Heat Transfer Coefficient, h (Btu/hr-ft^2-°F) Calc. from Colburn Equation
3	40,300	1.20×10^6	218	11,500	11,700	6230	5100
4	37,600	1.12×10^6	218	10,700	11,300	5520	4820
8	24,300	0.72×10^6	219	10,600	9,700	4870	3390

bottom quarter of the tank is jacketed for steam heating (the jacket is divided into four sections so that all or any part can be used). Cooling during a dump is provided by means of a condenser rated at 1316 lb/hr, which is adequate to limit the dump-tank pressure to 135 psig at a dump rate of 100 lb/min from a loop operating at 280°C. The dump flow-rate is limited by a choke section in the dump line. An auxiliary steam generator is provided to furnish open steam for agitation, and the tank is arranged so that internal flow guides or baffles can readily be installed or altered to simulate nuclear-poison arrays in the tank. Two rows of sample openings spaced at 6-in. intervals provide facilities for determining the uniformity of the slurry in the tank, and the tank is mounted on weigh cells for inventory determination.

The low-pressure system also contains a centrifugal transfer pump for filling the loop with water or slurry, for circulating slurry to the feed pump suction, or for making other material transfers; a diaphragm feed pump for charging slurry to the pressurized loop; and a water storage tank.

9.2.2 Pressure-Vessel-Model Studies

In order to obtain some guidance as to the best initial flow pattern for the 300-SM pressure vessel, a series of slurry flow and distribution tests was made by using a 6-in.-dia model of identical shape.[2] The tests were run with 1600°C-fired thoria having a settling velocity of 0.125 cm/sec. Hypodermic-tube samplers were installed in order to traverse the vessel horizontally at four levels. In addition, visual observations were made of the boundary layer flow during the runs.

The runs to date have covered upward straight-through flow over a range of 0.37 to 3.14 gpm, downward straight-through flow over a range of 0.53 to 2.0 gpm, and bottom re-entrant flow over a range of 0.85 to 8.0 gpm, the flow rate being limited by the outlet line size. In the case of re-entrant flow, three top-head closures were tested: a simple flat top, a cusp-shaped filler to serve as a flow guide directing the impinging inlet jet toward the bottom outlet, and a filler shaped to continue the spherical contour of the vessel body. The latter two seem superior, and of these two, the spherical contour is preferable because trapped gas can be vented from the vessel more easily. Tests with and without a small vent stream from the top of the vessel indicated that the vent stream is desirable because of better gas removal and a stabilizing effect on the re-entrant flow pattern.

In upward straight-through flow there was no significant variation in density in the flowing stream from top to bottom for flow rates greater than approximately 1 gpm. At lower flow rates, a marked density gradient developed within the vessel, giving high densities near the bottom of the vessel and at the conical walls; the mean density in the vessel became greater than the density in the vessel outlet line. For downward flow, a concentration gradient within the

vessel persisted up to a flow rate of 2 gpm, the maximum tested. The diameter of the inlet nozzle was 0.305 in. for these tests.

The re-entrant flow tests were made with an inlet nozzle of 0.555-in. dia, and a measurable concentration gradient within the vessel was found only for flow rates less than approximately 2.5 gpm. At a very low flow rate, a slurry-water interface formed near the top of the vessel.

Visual observations of the flow behavior at the vessel wall indicated:

1. For upward straight-through flow, there appeared to be stagnant slurry on the bottom conical wall at all flows.

2. For downward straight-through flow, there was stagnant slurry on the bottom conical wall and the wall flow in the upper hemisphere was in a random direction for all flows.

3. For re-entrant flow with the preferred top head contours and the inlet nozzle placed at the sphere radius below the sphere center, active wall-layer flow was observed over the entire vessel surface.

Three runs were made with a 0.7-in.-dia standpipe connected to the top of the vessel in order to simulate a pressurizer mounted directly on the vessel. At flow rates of 5 to 7 gpm, the slurry-water interface formed approximately 2 in. above the top flange of the vessel.

9.2.3 Development of Gamma-Transmission Densitometer Equipment

Tests were continued on the measurement of slurry density by means of gamma-ray transmission, using modifications of commercial equipment.[2] Room-temperature measurements on a 1600°C-fired slurry of high settling rate (0.125 cm/sec) were highly reproducible and of satisfactory accuracy.

The densitometer was placed in service on the 200A loop with a bypass slurry stream flowing through the test cell at approximately 2 gpm at 224°C, 750 psig. The slurry density, on the basis of circulating-loop samples, was 1.00 g/cc; the densitometer readout was 1.05 g/cc, which slowly increased to 1.085 g/cc. The 1.05-g/cc value could be restored by vibrating the test cell. Examination of the test cell revealed a weld burnthrough at the 45-deg bends, and it is believed that the slurry accumulated at these flow obstructions. A new test section is being fabricated for further flow tests at elevated temperature.

At the completion of the slurry run in the 200A loop, the densitometer was used to monitor the density of water being circulated in the loop over the range of 20 to 200°C. The readings agreed with the known density of water at the temperatures of measurement.

9.3 STUDY OF A CIRCULATING-SLURRY CRITICALITY SYSTEM

During this quarter, the possibility has been investigated of building a circulating thorium-uranium oxide slurry system in order to study the reactivity fluctuations which may occur in the core of a circulating-slurry reactor. The system under consideration has a maximum thermal output of 100 kw and operates at about 200°C. Analysis shows that a core of 2 or 2-1/2 ft diameter, with a 90% D_2O - 10% H_2O moderator, permits adequate shutdown control by a pure water blanket of the same isotopic concentration, even with a 1-in.-thick stainless steel core wall.

A 24-ft-dia steel containment vessel, now located in an unused building (7503), appears adequate for containing the circulating and storage tank portions of the system, if the height is increased by about 12 ft.

In addition to the reactivity information, equipment reliability, maintenance, concentration control, and fuel accountability methods can be developed with the system.

REFERENCES

1. R. B. Korsmeyer et al., HRP Quar. Prog. Rep., July 31, 1958, ORNL-2561, p 126-127.

2. R. B. Korsmeyer et al., HRP Quar. Prog. Rep., October 31, 1958, ORNL-2654, p 99-100.

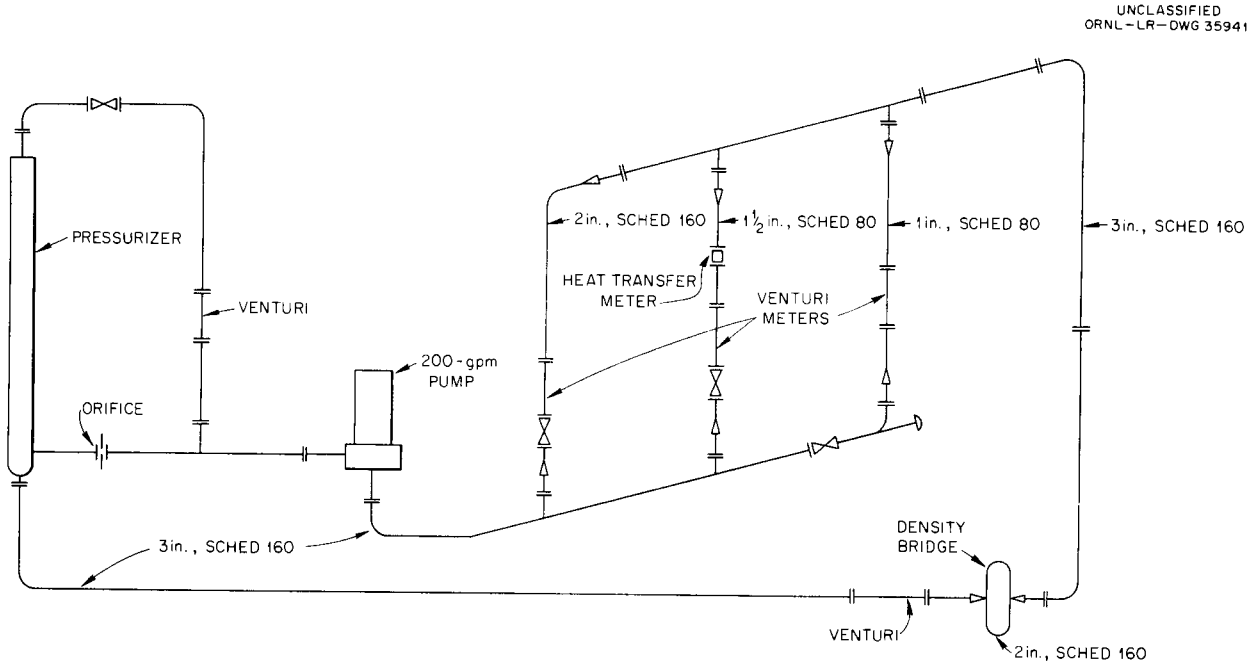

Fig. 9.1. Schematic Flowsheet of the 200B Loop.

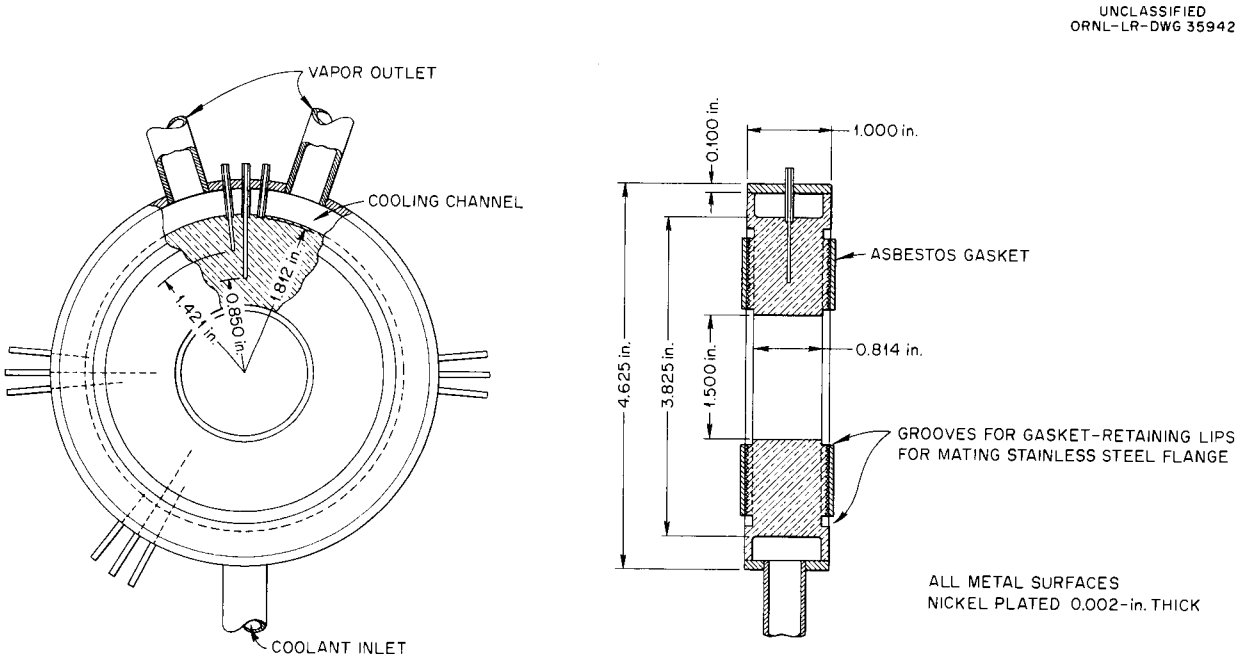

Fig. 9.2. Copper-Disc Heat Transfer Meter, 200B Loop.

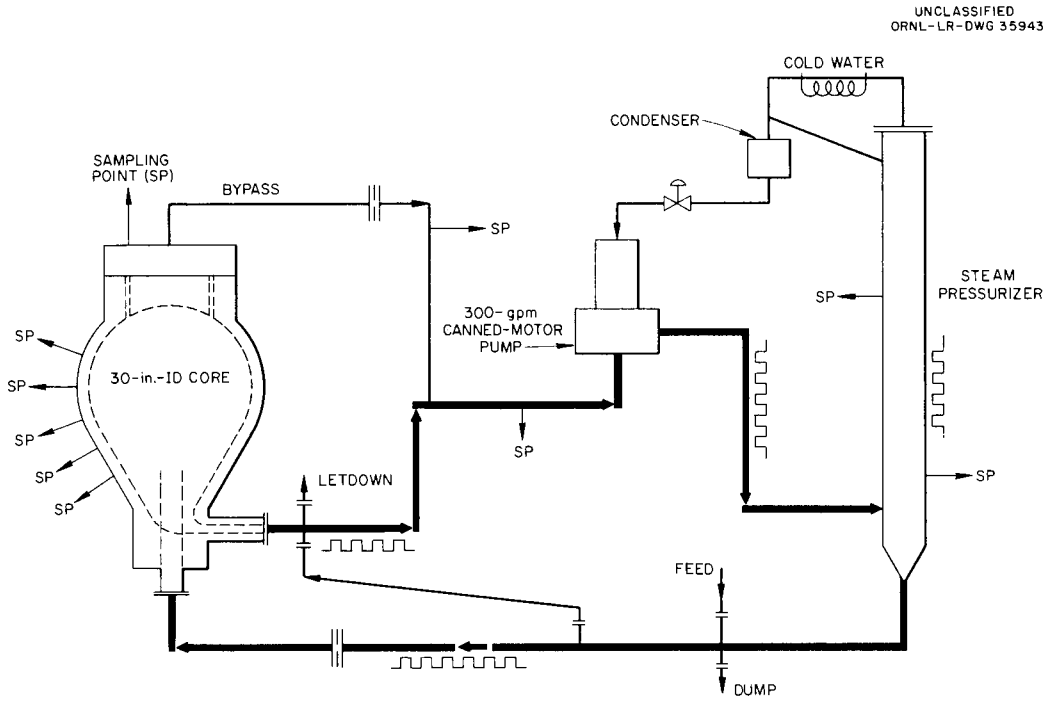

Fig. 9.3. 300-SM High-Pressure Slurry-Circulating System.

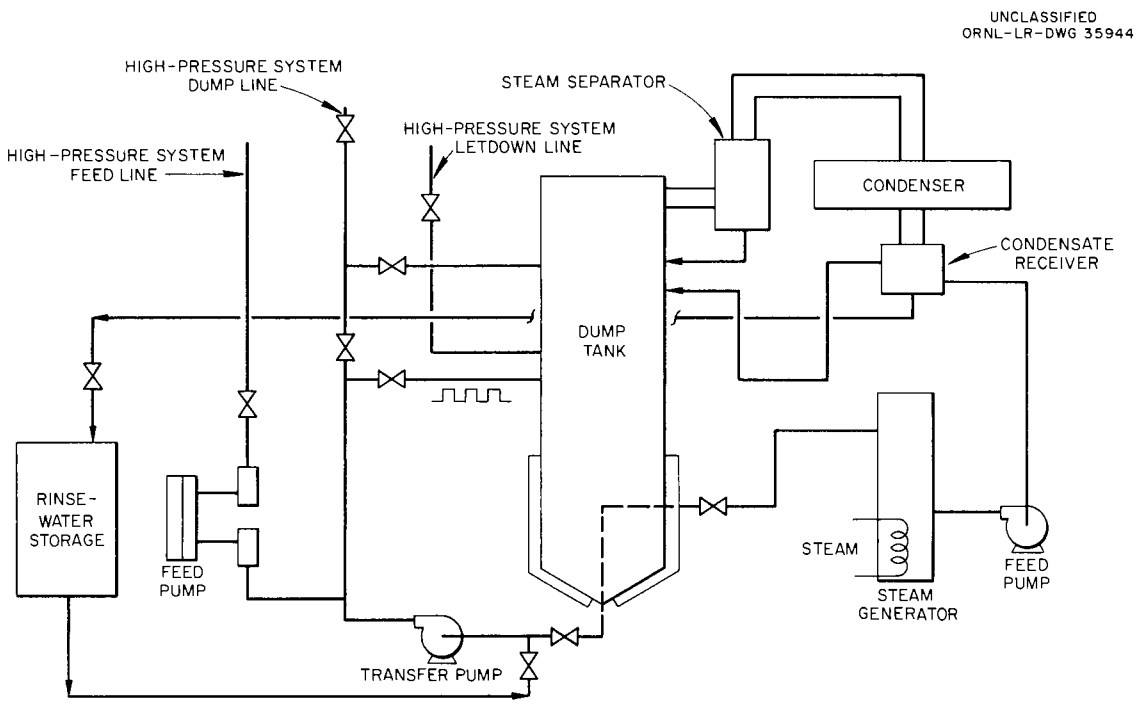

Fig. 9.4. 300-SM Low-Pressure System.

10. INSTRUMENT AND VALVE DEVELOPMENT

D. S. Toomb

A. M. Billings
E. H. Bell
R. L. Moore
J. L. Redford

10.1 INSTRUMENT DEVELOPMENT

10.1.1 High-Temperature Radiation-Resistant Differential Transformers

The development of differential transformers for sensing the primary-element motions of instruments and capable of operating for long periods at high temperatures and in radiation fields was continued.

The transformer wound with anodized aluminum wire on an aluminum form, described in an earlier report,[1] did not test satisfactorily. The poor performance of this transformer was traced to the temperature-induced change in the resistance of the aluminum coil-bobbin and of the ceramic cement with which the coil was impregnated.

The resistivity of the coil form was a significant factor because the coil form acts as a shorted secondary turn on the transformer and results in a phase shift and a reduction in amplitude of the output signal. For this reason, materials of low resistivity and high temperature coefficient of resistivity, such as aluminum, were found undersirable. Inconel, which has a high resistivity and a very low temperature coefficient of resistivity, now appears to be the best choice. Inconel is much better than the 300-series stainless steels in this respect since its temperature coefficient is about 1/10 that of stainless steel.

A high primary-to-secondary resistance is required in order to avoid resistive primary-to-secondary winding coupling. Although the resulting residual voltage can be balanced out, a change in the primary-to-secondary resistance will upset the balance and result in a residual component in the output signal. Controlled measurements of the resistivity of Allen PBX cement showed that its resistivity decreases by a factor of 10^4 as the temperature was increased from 50 to 300°C. Similarily, the resistivity of Sauereisen No. 1 and No. 32 ceramic cements was found to decrease by a factor of 10^5 over the same temperature range.

In order to reduce these effects to an acceptable level, the transformer was redesigned as follows:

1. The number of primary turns was reduced from 1000 to 250.

2. The number of turns per secondary was reduced from 500 to 125.

3. The wire size was increased from No. 30 AWG to No. 24 AWG.

4. The coil-form material was changed to Inconel.

These changes result in a new differential transformer of the same dimensions, span, and linearity, but with a large reduction in primary-to-secondary resistive and capacitive coupling. It is considered to be more reliable, and winding is facilitated by the use of the larger wire. The reduction in primary impedance due to the reduced number of turns is compensated by appropriate matching and a 4-to-1 stepup transformer is used to offset the decreased sensitivity resulting from the reduced number of secondary turns.

A differential transformer of this type, but wound on a type 347 stainless steel form, operated for about six weeks at temperatures varying from 25 to 350°C, without failure. However, a 10% increase in sensitivity as the temperature was increased from 25 to 350°C was noted, and the zero drift due to temperature change from 25 to 300°C was about 10 to 15% when the instrument was set for a 0.020-in. total core movement. Part or all of the zero shift may be due to differential expansion and inductive coupling between the transformer and the test jig, rather than being due to changes within the transformer.

10.1.2 Evaluation of Pressure Transmitters

Two pressure transmitters which are now commercially available were evaluated as to suitability for HRP applications and found to be quite satisfactory.[2,3]

The Swartwout Company model 1-H-130, illustrated in Fig. 10.1, has a nominal range of 0 to 2800 psi. The transmitter consists of a dual Bourdon-tube pressure element which positions the core of a linear variable differential transformer. The transducer is enclosed by a safety housing which will withstand full system pressure in the event of a Bourdon-tube rupture. The Bourdon tubes, safety housing, and pipe connection are all made from type 347 stainless steel.

The Norwood Controls Division pressure transmitter was tested in conjunction with their magnetic amplifier and indicating receiver. The transmitter, illustrated in Fig. 10.2, consists of a rotary differential transformer, a twisted Bourdon-type pressure tube and a safety housing. The range of the transmitter tested was 0 to 2500 psi; the Bourdon tube, safety housing, and pressure connection were fabricated from type 347 stainless steel. This transmitter has an

exceptionally high pressure rating of 5000 psi.

10.2 VALVE DEVELOPMENT

10.2.1 Valve Actuators

Life testing was completed for the all-metal control-valve actuator having a 40-in.^{2} effective area (described in an earlier report[4]). Results from a test stand similar to that illustrated earlier[5] were as follows:

Test	Failed Component	Stroke	Cycles to Failure
1	Stem-sealing bellows	1 in.	12,000
2	Stem-sealing bellows	1 in.	26,000
3	Stem-sealing bellows	3/4 in.	42,116
4	No failure	1 in.	42,000
4	No failure	3/4 in.	42,116

It is concluded that a longer stem-sealing bellows is advisable for strokes exceeding 3/4 in. However, as the actuator was specified to withstand 20,000 cycles at a 3/4-in. stroke, it is considered to be very satisfactory.

Testing of the stacked-bellows actuator for large valves, shown in Fig. 10.3 and previously described,[6,7] was also concluded, with the following results:

Test	Failed Component	Stroke	Cycles to Failure
1	Stem-sealing bellows	1-1/4 in.	18,083
2	Actuating bellows (seam weld)	1-1/4 in.	68,584
3	No failure	1-1/4 in.	46,815

Performance of this actuator is considered more than adequate.

10.2.2 Valve Stem-Sealing Bellows

Life testing of a larger bellows than those now used for control valve stem-sealing in the HRT was begun because a larger bellows may be required for future HRP systems. The bellows now in use in the HRT has an ID of 0.875 in. The new bellows being tested is a seamless, dual-stacked assembly with an ID of 1-1/16 in. and constructed of three 0.0085-in. plies of type 347 stainless steel. In cycling the bellows 1/4 in. in uranyl sulfate at 1000 psi and 250°C, the first failed at 17,553 strokes and the second at 18,994. (The larger bellows is Fulton Sylphon Division No. FS-C01509-A01.)

10.2.3 Slurry-Service Valves

A prototype Y-body design valve for 500-psi service was designed for slurry applications and made in the ORNL shops. The valve, shown in Fig. 10.4, has a 1-in.-dia port and a bellows stem-seal which can be butt-weld sealed. Integral ring-gasket faces permit straddle bolting of the mating flanges, and a recessed indicator ring is provided to aid realigning the valve body in a lathe, facilitating repair. Provision is made to flush the bellows compartment with a flow which enters through the bonnet and leaves via the lower stem guide. However, it is possible that this may not be necessary in slurry service if the lower guide is ported to permit free flow in and out of the bellows chamber.

Although this prototype was machined from type 347 stainless steel bar stock, contour forgings would be specified if the valve should be required in quantity.

10.2.4 Slurry-Service Valve Trim

The Hammel-Dahl control valve[8] installed in the 30-gpm slurry loop was fitted with a Zircaloy-2 plug and seat after tungsten and chromium carbides proved unsatisfactory as trim materials. The valve has now operated satisfactorily for 1360 hr, including 125 hr in a 65%-closed position. During this time, loop pressure and temperature were about 1650 psi and 275°C; slurry concentration has varied from 400 to 500 g of Th per kg of H_2O.

In slurry loop 200B, another Hammel-Dahl valve, utilizing a long-radius pipe-bend body design[9] and fitted with tungsten carbide trim, was exposed to a 3-hr nitric acid loop-rinse. Figure 10.5 shows the etched condition of the Colmonoy-faced stem following this operation. This stem was reinstalled in the loop and has performed satisfactorily for a total of 597 hr to date, including 43 hr in a slurry of 200 g of the per kg of H_2O at 750 psi and 220°C during shakedown operation of the loop. Two sets of Zircaloy-2 replacement trim was fabricated for this valve, and it is hoped that a hardening procedure for this material can be developed to provide a more satisfactory valve trim for slurry service.

REFERENCES

1. D. S. Toomb et al, HRP Prog. Rep. for Quarters ending April 30 and July 31, 1958, ORNL-2561, p 130.

2. R. L. Moore and T. M. Cate, Performance Test of a Swartwout Model 1-H-130 Pressure Transmitter, ORNL CF-58-11-104, Nov. 3, 1958.

3. R. L. Moore and T. M. Cate, Performance Test of a Norwood Electrosyn Pressure Measuring System, ORNL CF-58-11-105, Nov. 11, 1958.

4. D. S. Toomb et al, HRP Prog. Rep. for Quarters ending April 30 and July 31, 1958, ORNL-2561, p 134.

5. Ibid. p 139.

6. D. S. Toomb et al, HRP Quar. Prog. Rep., Jan. 31, 1958, ORNL-2493, p 83.

7. D. S. Toomb et al, HRP Prog. Rep. for Quarters ending April 30 and July 31, 1958, ORNL-2561, p 135.

8. Ibid. p 138.

9. D. S. Toomb et al, HRP Quar. Prog. Rep., Jan. 31, 1958, ORNL-2493, p 83.

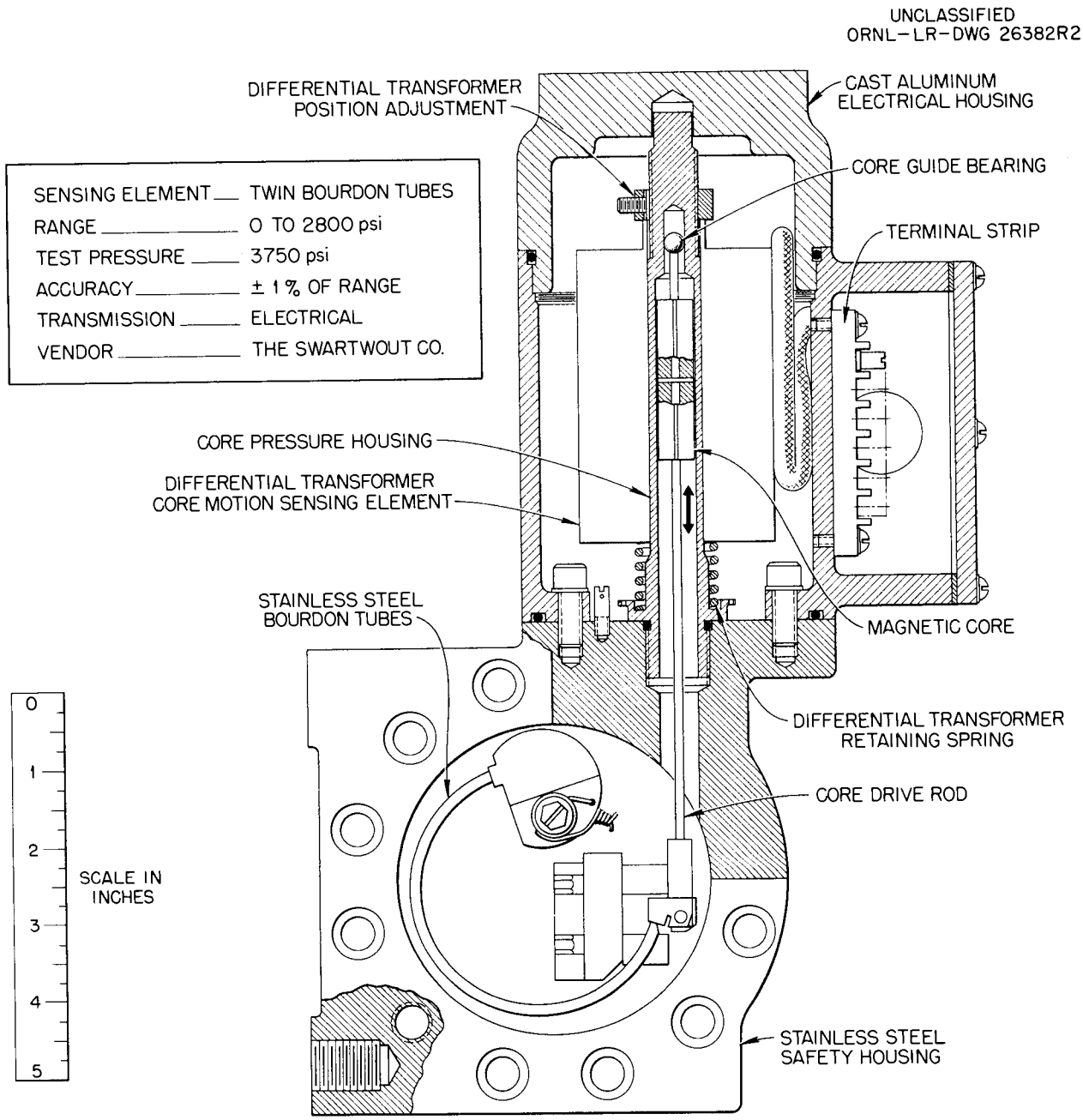

Fig. 10.1. Pressure Transmitter with Safety Housing.

UNCLASSIFIED
ORNL-LR-DWG 32332

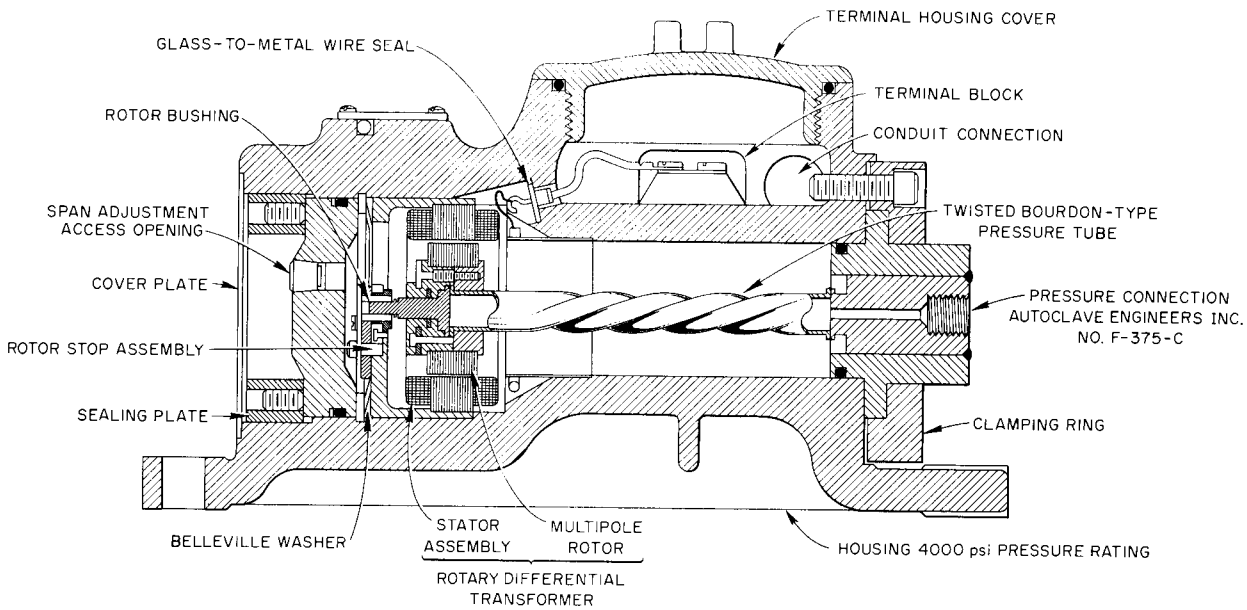

NOTES:
PROCESS CONTAINING PARTS—347 SS
RANGE—0-2500 psig
OUTPUT SIGNAL—0 TO 8.5 volts, 60 cps OPEN CIRCUIT
ERROR—±1%
TEST PRESSURE—5000 psig
PRESSURE RATING WITHOUT RUPTURE—12,500 psig
MAX.—ENVIRONMENTAL TEMP.-200°F
VENDOR—NORWOOD CONTROLS DIV.

Fig. 10.2. Twisted Bourdon-Tube Type of Pressure Transmitter.

UNCLASSIFIED
ORNL-LR-DWG 34776

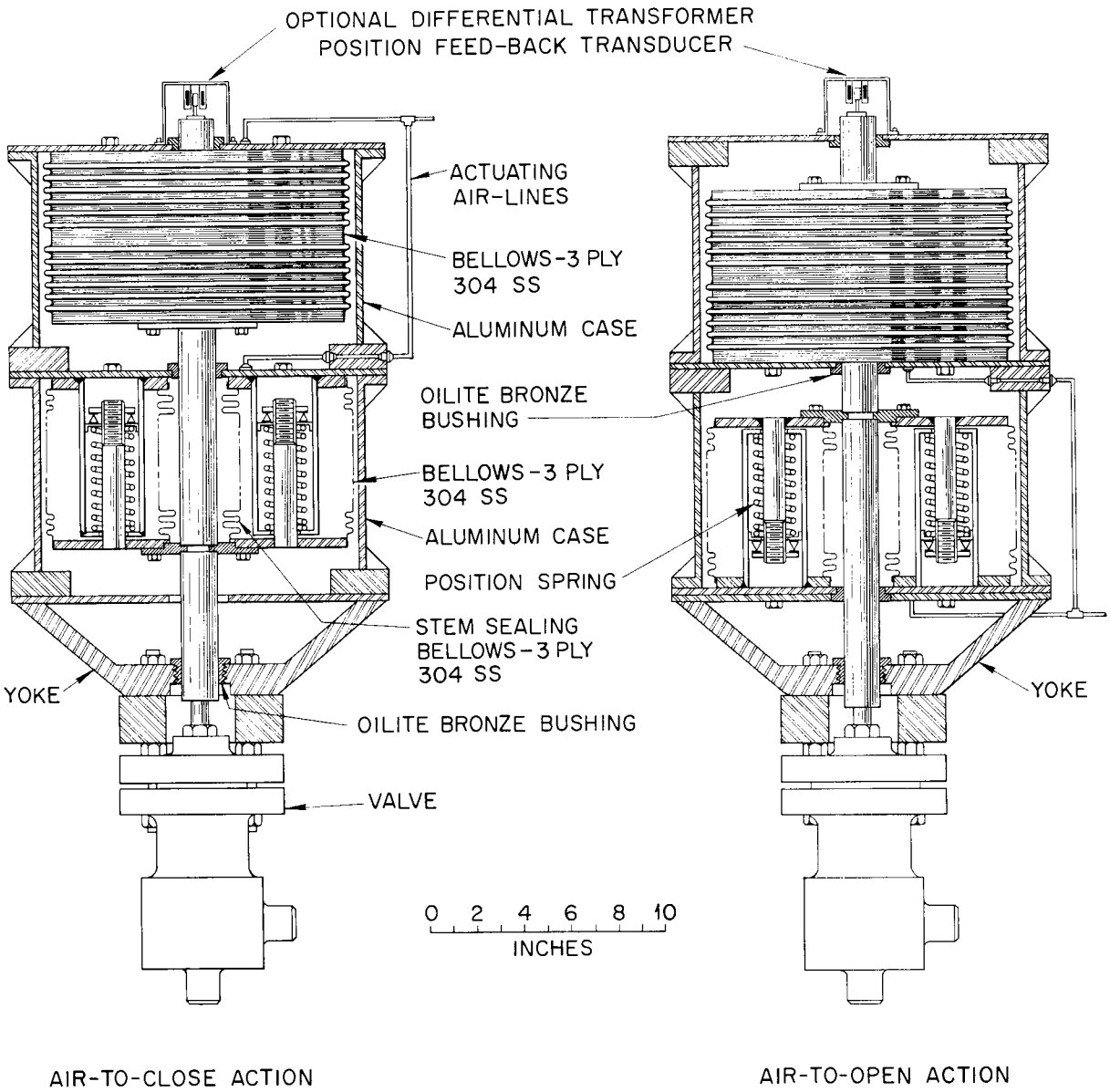

Fig. 10.3. Stacked-Bellows Actuator.

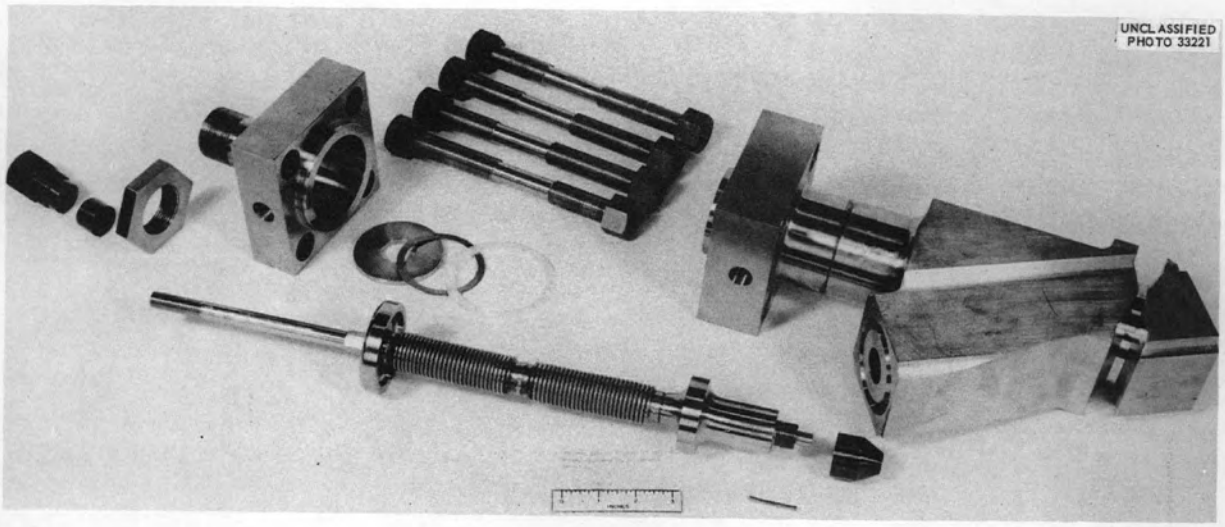

Fig. 10.4. Y-Body Slurry Valve.

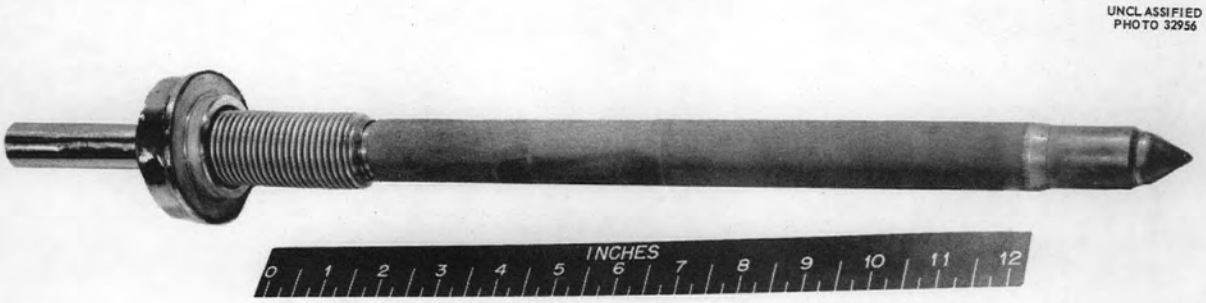

Fig. 10.5. Colmonoy-Faced Valve Stem Following Nitric Acid Rinse.

PART IV

REACTOR MATERIALS RESEARCH

E. G. Bohlmann

11. SOLUTION CORROSION[1]

J. C. Griess
H. C. Savage

S. E. Bolt
J. L. English
R. S. Greeley
D. N. Hess
P. D. Neumann
A. J. Shor
E. S. Snavely
W. C. Ulrich

11.1 DYNAMIC SOLUTION CORROSION

11.1.1 Deposition of Salts from Dilute Fuel Solutions on Heated Surfaces

(a) 100A Loop H.--Experimentation has continued in an effort to understand the loss of salts from simulated HRT fuel solutions circulated in a loop containing a heated Zircaloy-2 bypass. As noted previously,[2] uranium, copper, and nickel sulfates collected in the heated bypass either as a second liquid phase or as salt crystals when the temperature of the solution emerging from the bypass was 20°C or more above the loop temperature of 280°C and when the solution flow rate through the bypass was 0.2 fps. In these tests the bypass was mounted on a 10-deg decline to the horizontal (inlet about 4 in. above outlet), and the loop was pressurized with oxygen.

In order to determine the effect of gas concentration, the loop was fitted with a letdown system and a diaphragm-type fuel feed pump so that it could be operated with hydraulic pressurization. An oxygen concentration of 20 ppm was maintained by saturating the feed solution with oxygen at room temperature and atmospheric pressure. With this system, sulfates were not deposited when the loop was at 280°C and the solution emerging from the bypass was at 290, 300, or 312°C. Heat to the bypass was increased until the temperature of the emerging solution was equal to the saturated vapor point at the loop pressure of 1570 psia. Boiling and flashing of solution in the bypass were apparent, since a thermocouple on the bypass inlet occasionally indicated a temperature higher than the loop temperature. Under these conditions about 20% of the salts deposited, an amount less than had been observed with gas pressurization.

When deposition was at a maximum, the loop pressure was increased from 1570 to 1775 psia to prevent boiling. The deposited uranium, copper,

and nickel quickly dissolved and reappeared in the main circulating solution. Therefore it appeared that boiling was the cause of the salt deposition.

At the end of the test the Zircaloy-2 bypass was sectioned for microscopic and metallographic examination. It was found[3] that the interior surface in approximately the top half of the bypass pipe had suffered a pitting-type attack resulting in a porous appearance. The lower half was covered with a thick scale, which was mainly zirconium dioxide but contained 11% uranium and 0.3% copper.

A new bypass was constructed, and further tests were made in run H-124. The basic configuration of the original bypass[4] was maintained, but certain changes were made to obtain more accurate information from the system:

(1) A calibrated metering orifice connected to a differential-pressure-measuring cell was installed upstream of the heated section of the bypass to determine flow rates at operating conditions. In the previous run, H-123, flow rates measured at room temperature with water were used as bases for estimates of flow rates at operating conditions.

(2) Thermocouple wells of 1/4-in. Zircaloy-2 tubing were welded on the 3/8-in. Zircaloy-2 pipe (see Fig. 11.1). Thermocouples were then discharge-welded directly onto the outside of the pipe wall. Ceramic insulation was packed around the thermocouples to reduce the effects of the heating elements on the thermocouples. The number and location of thermocouples were the same on the original and new bypass assemblies. However, on the original assembly the thermocouples were not welded to the pipe wall but were simply pushed against the pipe through holes drilled in the aluminum-heater jacket. As a result, paired-thermocouple readings did not agree closely and were undoubtedly indicating the temperature of the aluminum-heater jacket rather than the wall temperature of the Zircaloy-2 pipe.

(3) The orientation of the heated section of the bypass was changed from an inclined position to a vertical position with the flow from top to bottom. This change allowed an investigation of the effect of a different geometry and different flow pattern on solution stability and heat transfer properties.

For the initial tests in run H-124 the temperatures of the main loop and pressurizer were controlled at 280°C, and a total loop pressure of 1150 psia was maintained by oxygen and steam pressure. Flow rates ranging from 0.08 gpm (about 0.13 fps) to 0.39 gpm (about 0.65 fps) in the bypass were obtained by operating the main loop circulating pump at various frequencies from 20 to 70 cps. The maximum heat flux, determined from heater-power measurements, reached about 58,000 Btu/hr·ft^2.

The solution temperature rise through the heated section of the bypass was obtained by taking the difference between inlet and outlet

thermocouples 12 and 11 (Fig. 11.1). The temperature gradient along the length of pipe was found to be approximately linear for nonboiling conditions; when boiling occurred, however, the gradient was nonlinear and erratic. By calculating the inside pipe wall temperatures from measured outside wall temperatures and comparing them with the solution saturation temperature, it was found that wall temperatures were high enough to produce boiling at low heat fluxes--about 7500 Btu/hr·ft^2. Therefore most of the data were obtained in the boiling region. The maximum inside Zircaloy-2 pipe wall temperature during the initial tests in run H-124 was 824°F (430°C) at a heat flux of about 58,000 Btu/hr·ft^2, with a flow of 0.12 gpm (0.2 fps) through the Zircaloy-2 pipe.

It is difficult to determine the type of boiling that occurred in the bypass. The transition from convection to nucleate boiling to film boiling should cause changes in the value of the fluid-film heat transfer coefficient, h, as the heat flux is increased. No such change was observed, and the average value of h over the entire range of heat fluxes was ~400 Btu/hr·ft^2·°F. This value is lower than would be expected for nucleate boiling conditions. A possible explanation is intermittent interruption of flow in the bypass caused by vapor and gas and the formation of relatively stable large bubbles in the pipe such as those which were observed in a glass mockup of the system described below. These bubbles of steam and gas could prevent nucleate-type boiling. During the periods of boiling, the flowmeter indicated rather large and rapid flow fluctuations. The calculated h ranged between 300 and 400 Btu/hr·ft^2·°F at flow rates varying from 0.13 to 0.65 fps and at heat fluxes up to 56,000 Btu/hr·ft^2. Figure 11.2 is a log-log plot of q/A (Btu/hr·ft^2) versus Δt_{sat} (Δt_{sat} is $t_{wall} - t_{sat}$), where t_{wall} is the calculated inside pipe wall temperature and t_{sat} is the solution saturation temperature at the total system pressure of water vapor plus gas pressure. This plot gives a straight line with a slope of 0.5. A slope of 3 to 4 would be expected in the nucleate boiling region at low velocities.[5] Thus only some type of film boiling was observed in the heated bypass.

Even under the conditions of highest heat flux (58,000 Btu/hr·ft^2) and lowest flow rate (0.13 fps), there was no evidence of loss of uranium from the solution although vigorous boiling was indicated. The reason for the difference between this test, in which no deposition occurred, and previous tests with the heated pipe in a position slightly inclined from the horizontal, in which deposition did occur, might be explained from observations of a glass mockup of the bypass through which water and air mixtures were passed. In the horizontal or near-horizontal position at low liquid flow rates, a vapor space formed in the upper part of the tube which prevented its being wetted by the solution. In the vertical position, however, the solution continuously wet the tube walls; and air, injected to simulate vapor in the heated bypass, either was swept out of the tube at the higher velocities or formed bubbles which collected to form a gas space at the top of the tube. However, the liquid flowed around the gas space along the tube. Hence deposited solids or liquids would be washed away in the vertical arrangement but could build up on the heated, unwetted part of the pipe in the horizontal arrangement.

(b) Loop L-2-23.--Following construction of in-pile loop L-2-23, insertion in the LITR was delayed so that additional out-of-pile tests could be performed for the purpose of studying the stability of uranyl sulfate solutions in contact with heated metal surfaces. The loop was modified by the addition of a heater on the core for simulating gamma heating in the core wall.

Figure 11.3 is a schematic drawing of the core and core heater, which supplies up to approximately 1 kw over a core area of about 0.1 ft^2. Three thermocouples are located on the core and heater to measure metal temperatures. Power to the heater is manually controlled by means of a variable transformer. The core material is titanium, and the core contains a number of corrosion specimens as previously described.[6] The remaining components of the loop are of stainless steel and have been described previously.[7]

A number of solutions have been circulated in this apparatus under various conditions of core heat, total loop pressure, and flow rate through the core. Table 11.1 is a summary of the runs that have been made to date. Uranyl sulfate concentrations of 0.04 and 0.025 *m* containing 0.08 and 0.011 *m* $CuSO_4$ with D_2SO_4 concentrations ranging between 0.008 and 0.025 *m* have been studied. All solutions were made up in D_2O.

The loop main-stream temperature was maintained at about 280°C, and the pressurizer temperature was varied from about 286 down to 280°C to reduce the system pressure and thereby produce boiling in the heated core section. The total pressure of the loop was the saturated D_2O vapor pressure plus the oxygen pressure. Heat fluxes ranging from 8,000 to 20,000 $Btu/hr \cdot ft^2$ were applied to the core. Most runs were made at a flow rate of 0.3 fps through the annular region of the core. Loss of salts from solution is noted qualitatively in Table 11.1. Core nose temperatures and loop main-stream temperatures are also reported. The difference between these two temperatures is noted for each run. Radiographs of the loop core section taken when loss of salts from solution was essentially complete revealed a deposit of material on the top section of the inside core wall under the heated area. No such deposit was seen when there was no loss of salts from the solution.

Although the data are preliminary and the parameters have been studied only in an exploratory fashion, a number of observations may be made. Estimates of inside wall temperatures in the core and observations of the core nose temperature, total system pressure, and pressurizer temperature indicate that boiling at the inside surface of the core occurred in all the runs described in Table 11.1. In runs 1 to 4, 9, 12, and 14, loss of salts from solution was observed. Concurrently, the excess acid concentration of the solution decreased slightly, as has been observed previously under similar conditions.[2] During such deposition, the temperature difference between the core nose and the loop main-stream was higher, at equivalent heat fluxes, by a factor of ~2 than in runs in which no loss of salts was observed. This increase in core temperature is as yet unexplained.

Table 11.1. Summary of Operating Conditions, Loop L-2-23 (D_2O System)

Run No.	UO_2SO_4 Conc. (*m*)	D_2SO_4 Conc. (*m*)	$CuSO_4$ Conc. (*m*)	Est. Flow Rate (fps)	O_2 (psi)	Total Press. (psia)	Net Core Heat Flux (Btu/hr·ft^2)	Press. Temp. (°C)	Loop Temp. (°C)	Core Nose Temp. (°C)[a]	Core Nose Temp. Minus Loop Temp. (°C)	Deposit
1	0.04	0.006	0.0067	0.3	126	1142	8,000	286.4	280.0	286	6[b]	Yes
2	0.04	0.006	0.0067	0.3	141	1118	8,000	282.5	279.5	292	12[b]	Yes
3	0.04	0.006	0.0067	0.5	94	1070	8,000	282.5	279.8	290	10[b]	Yes
4	0.04	0.006	0.0067	0.6	101	1079	8,000	282.6	280.0	289	9[b]	Yes
5	0.04	0.025	0.0067	0.3	133	1124	8,000	283.5	280.0	286	6	No
6	0.04	0.025	0.0067	0.3	158	1134	8,000	282.5	280.0	283	3	No
7	0.04	0.025	0.0067	0.3	137	1096	8,000	281.3	280.2	284	4	No
8	0.04	0.025	0.0067	0.3	145	1090	8,000	280.3	280.3	284	3	No
9	0.04	0.025	0.0067	0.3	148	1073	20,000	278.8	280.4	294	14[b]	Yes
10	0.04	0.010	0.0067	0.3	151	1124	8,000	282.3	280.1	284	3	No
11[c]	0.025	0.015	0.011	0.3	203	1175	10,500	282.2	279.9	284	4	No
12[c]	0.025	0.015	0.011	0.3	138	1085	8,000	280.5	280.0	291	11[b]	Yes
13[c]	0.025	0.025	0.011	0.3	138	1094	10,500	281.1	280.0	283	3	No
14[c]	0.025	0.014	0.011	0.3	199	795	8,000	251.6	249.4	257	7[b]	Yes

a. Core nose thermocouple on outside metal surface.
b. Note rise in core nose temperature difference when loss of salts occurred.
c. 230 ppm Ni added.

When runs 1 to 4, containing 0.006 *m* D_2SO_4, are compared with runs 5 to 8, containing 0.025 *m* D_2SO_4, it is noted that under comparable conditions of flow rate and core heat flux, deposition did not occur in the solution containing 0.025 *m* D_2SO_4. In run 9, containing 0.025 *m* D_2SO_4, with higher heat flux and lower pressurizer temperature (and thus loop pressure), deposition occurred at a rapid rate. It appeared that the higher acid concentration inhibited the deposition, which, however, could still be forced to occur at higher heat fluxes and at a lower system pressure. Run 10 was an attempt to reproduce the results of run 2; however, deposition did not occur in run 10. As a result of a change in emphasis to a 0.025 *m* uranium solution, which was in use in the HRT and in H loop (see above), this anomaly was not investigated. However, it may be significant that the acid concentration in run 10 was slightly higher than in run 2 (0.01 *m* versus 0.006 *m*).

In runs 11, 12, and 13, with solutions of 0.025 *m* UO_2SO_4, the tendency for the higher acid concentration to prevent deposition is still apparent. In these runs about 200 ppm nickel as nickel sulfate was added to the solution to test its effect. The nickel addition, together with the small number of runs at the lower uranium concentrations, makes questionable any comparisons between the two solutions with different uranium concentrations.

A single run, No. 14, at a main-stream temperature of 249°C is shown in Table 11.1. Results of this run, particularly the fact that loss of salts occurred at temperatures well below the two-liquid-phase temperature of the solution, indicate that salts were lost from solution by salt deposition rather than by formation of a second liquid phase.

11.1.2 Hydroclone Tests

During several loop tests in which a hydroclone was attached to the loop, the amount of solids that collected in the hydroclone underflow pot was only about 10% of the amount of solids formed by corrosion during the run. In an attempt to improve the effectiveness of the hydroclone, the inlet line to the hydroclone was redesigned by the Chemical Technology Division and two tests were made to determine whether the change of inlet-line location and orientation increased the fraction of solids collected.

Before redesign the inlet line was a 1/4-in. tube which was joined to the main loop piping in a perpendicular tee near the pump outlet. After redesign the inlet line was a 1/2-in. pipe welded to the bottom of the pressurizer so that solids could "fall" into the inlet line. In each test, 0.04 *m* UO_2SO_4 containing 0.025 *m* H_2SO_4 and 0.01 *m* $CuSO_4$ was circulated at 250°C for 200 hr. Carbon steel pins were exposed to the solution at high velocity, and these pins corroded heavily, introducing about 40 g of ferric oxide into circulation. The hydroclone underflow pot was drained of the solids collected each day and the solids were separated, dried, and weighed.

In each run the total amount of solids collected was only about 10% of the amount formed in the loop by corrosion. Therefore, no effect of hydroclone inlet-line location and orientation was evident.

Platinum pins were also exposed in each run, and these gained weight, primarily by deposition of a tenacious oxide scale and, to a lesser extent, by deposition of a loose, "fine" oxide film. Very roughly, the fraction of the solids produced which was not collected in the hydroclone underflow pot could be accounted for by extrapolating to the entire loop interior surface the weight gain per square centimeter of the platinum pins. Therefore, it appeared that 90% of the solids formed by corrosion circulated only briefly, perhaps as colloidal-size particles, and deposited on all surfaces. The tenacious scale on the platinum pins contained about 4% uranium by weight.

In previous runs when a loop was thermal-cycled repeatedly, the proportion of solids collected in the underflow pot of the hydroclone was greater than in a similar, but isothermal, run.[8] The oxide which is removed from the surface of the loop as a result of the thermal cycling has a much larger average particle size than does the initially formed corrosion products, and hence the hydroclone separates it from solution much more efficiently.

11.1.3 Instability of Uranyl Sulfate - Lithium Sulfate and Uranyl Sulfate - Magnesium Sulfate Solutions

Several recent in-pile loop experiments have indicated that the presence of a relatively high concentration of sulfate ions have a beneficial effect on the corrosion of Zircaloy-2.[9] Solutions similar to the one used in-pile, except containing a lower concentration of uranium and higher concentrations of copper believed necessary for HRT use, were circulated out-of-pile at 300°C to investigate solution stability. In one test the solution was 0.025 *m* UO_2SO_4 containing 0.13 *m* Li_2SO_4, 0.063 *m* D_2SO_4, and 0.02 *m* $CuSO_4$ in D_2O, corresponding to the uranium concentration in the core of the HRT; in another test the solution was 0.01 *m* UO_2SO_4 containing 0.045 *m* Li_2SO_4, 0.027 *m* D_2SO_4, and 0.005 *m* $CuSO_4$ in D_2O, corresponding to the blanket solution.

Both solutions were unstable; the more concentrated solution lost 80% of its copper but none of its uranium, whereas the more dilute solution lost 90% of its copper and 60% of its uranium. When the temperature of the dilute solution was lowered from 300 to 250°C, all the uranium, but only half the copper, reappeared in solution.

Since magnesium sulfate is generally more soluble in these solutions than lithium sulfate,[2] the first test was repeated with 0.025 *m* UO_2SO_4 containing 0.2 *m* $MgSO_4$, 0.1 *m* D_2SO_4, and 0.02 *m* $CuSO_4$ in D_2O at 300°C. This solution also was unstable, losing 20% of its copper and 6% of its uranium during the 430-hr run.

It was realized that the addition of sulfuric acid would stabilize these solutions but would also increase their corrosiveness, particularly in crevices. In order to determine the effect of acid on corrosion, two runs were made with 0.025 *m* UO_2SO_4 containing H_2SO_4, 0.2 *m* Li_2SO_4, and 0.02 *m* $CuSO_4$ at 225°C. In the first run the sulfuric acid concentration was 0.1 *m*, and in the second it was 0.2 *m*. Corrosion of stainless steel was slight in the first run. The type 347 stainless steel coupons and pins were filmed over up to the critical velocity of 20 to 25 fps. Type 347 stainless steel specimens bolted together to form a crevice and exposed in the pressurizer to the solution flowing at about 0.1 fps showed no significant crevice attack. In the second run with 0.2 *m* D_2SO_4, however, a type 347 stainless steel ring gasket corroded drastically at a crevice between it and a type 347 stainless steel sample barrel, causing a leak within 143 hr. Cast type 347 stainless steel pins were severely attacked during the run, as were the stainless steel clamping bands, which were in a stagnant area. Therefore it was demonstrated that the addition of relatively large concentrations of acid to these solutions can lead to severe attack, particularly in crevices and on cast type 347 stainless steel.

11.1.4 Inhibition of Stress-Corrosion Cracking with Fluoride and Phosphate

Previous experiments showed that either fluoride or phosphate ions were partially effective in reducing stress-corrosion cracking of type 347 stainless steel in chloride- and oxygen-containing water at 200°C.[2] Recently a 1000-hr loop run was made to determine the combined effect of fluoride and phosphate ions. The water contained 50 ppm chloride as potassium chloride, 190 ppm fluoride as potassium fluoride, 60 ppm phosphate as trisodium phosphate, and about 14 ppm oxygen and was circulated at 200°C. Type 347 stainless steel stress specimens, stressed beyond their elastic limit, were immersed in the solution, at a flow rate of about 3 fps.

Under the above conditions in the absence of fluoride and phosphate ions, many stress-corrosion cracks developed in less than 200 hr; whereas in the presence of either fluoride or phosphate, cracking was much less prevalent.[2]

After 1000 hr in the present test, one small stress-corrosion crack was found by metallographic examination of seven specimens. Therefore, since the combination of fluoride and phosphate did not completely prevent stress-corrosion cracking and since phosphate is already present in HRT boiler water, there appears to be no advantage to adding fluoride ions.

11.2 LABORATORY CORROSION STUDIES

11.2.1 Stress-Corrosion Cracking in Uranyl Sulfate Solution

(a) Effect of Preformed Film.--Studies have been continued to determine the effectiveness of a preformed film on type 347 stainless steel in preventing stress-corrosion cracking of the alloy in a chloride-containing, simulated reactor fuel solution. In particular, the effectiveness of the film as a function of the prefilming temperature has been studied, and preliminary results have been reported.[10] Prefilming was conducted for 100-hr periods in chloride-free, oxygenated 0.04 *m* UO_2SO_4-0.02 *m* H_2SO_4-0.005 *m* $CuSO_4$ solution at 25°C intervals between 100 and 300°C. Test specimens were elastically stressed U-bends prepared from annealed and sheared 0.025-in.-thick type 347 stainless steel strip. Previous studies had shown that 50% of similar untreated specimens of this material developed cracks during the first 500 hr of exposure in boiling, aerated 0.04 *m* UO_2SO_4-0.02 *m* H_2SO_4-0.005 *m* $CuSO_4$ solution containing 50 ppm of chloride as potassium chloride.[2] A similar environment was used for the studies with prefilmed specimens. Table 11.2 summarizes the results of the tests.

Table 11.2. Effect of Prefilming Temperature[(a)] on Stress-Corrosion Cracking Behavior of Type 347 Stainless Steel in Boiling, Chloride-Containing HRT Fuel Solution[(b)]

Prefilming Temperature (°C)	Number of Specimens	Total Test Time (hr)	Observations
100	6	3500	No cracking
125	9	2500	No cracking
150	9	2500	No cracking
175	9	2500	No cracking
200	9	2500	No cracking
225	9	2500	No cracking
250	9	2000	No cracking
275	9	1500	No cracking
300	9	500	No cracking
300[(c)]	6	500	No cracking

(a) Prefilming treatments conducted for 100 hr in chloride-free 0.04 *m* UO_2SO_4-0.02 *m* H_2SO_4-0.005 *m* $CuSO_4$ solution.
(b) 0.04 *m* UO_2SO_4-0.02 *m* H_2SO_4-0.005 *m* $CuSO_4$ solution containing 50 ppm of chloride.
(c) Specimens prefilmed prior to stressing.

In all cases except one, the specimens were stressed prior to the filming treatment. One set of six specimens, prefilmed at 300°C, was stressed after the 100-hr prefilming treatment. Not a single crack was observed on any of the specimens, during exposure periods from 500 to 3500 hr. It has been the experience in control tests with untreated specimens that when cracking occurs it invariably takes place during the first 500 hr of exposure in the chloride-containing environment.

In view of the complete success obtained with the above prefilming technique, several similar experiments were conducted with a different heat of type 347 stainless steel. Untreated, elastically stressed U-bend specimens that were prepared from annealed 1/16-in.-thick sheet had been found previously to crack 100% of the time in the boiling, chloride-containing, simulated HRT fuel solution.[4] Of nine specimens, all cracked during the first 200 hr of test. The present tests consisted of prefilming 12 of the 1/16-in.-thick specimens for 100 hr in boiling, chloride-free 0.04 *m* UO_2SO_4-0.02 *m* H_2SO_4-0.005 *m* $CuSO_4$ solution. Six of the specimens were prefilmed after stressing, and six, before stressing. All specimens were exposed in the boiling solution containing 50 ppm of chloride. After 1500 hr of exposure, the following results were obtained: (1) one of the six specimens that were prefilmed after stressing cracked, during the interval between 500 and 1000 hr of test, and (2) three of the six specimens that were prefilmed before stressing cracked, during the exposure interval between 200 and 500 hr. The high percentage of failures observed on the latter specimens may have been related to film rupture during the stressing. No explanation is apparent for the single case of cracking on the specimen that was prefilmed after stressing.

Thus the experimental data clearly show that preformed films effectively reduce the susceptibility of type 347 stainless steel to stress-corrosion cracking in a boiling, chloride-containing, simulated homogeneous reactor fuel solution. Prefilming before stressing afforded complete protection on specimens from a heat of the alloy that in the absence of the preformed film exhibited a 50% susceptibility to cracking, and approximately 85% protection on a heat that was 100% subject to cracking in the absence of a preformed film. Why the two alloys behaved differently remains unanswered at this time.

11.2.2 Stress-Corrosion Cracking in Chloride-Containing Water

(a) Cast Type 347 Stainless Steel.--Previous tests with cast type 347 stainless steel showed it to be highly resistant to chloride-induced stress-corrosion cracking.[2] Of particular note was the fact that no cracking occurred during a 100-hr exposure of the alloy in a stressed condition in boiling 42% $MgCl_2$ solution, an environment which normally produces cracking of wrought type 347 stainless steel in 5 hr or less. Further tests with the same heat of the cast alloy were made with simple-beam stress assemblies exposed at 300°C in water saturated with air at room temperature and containing 100 ppm of chloride. Initial

solution pH values of 2.8, 6.5, and 10.5 were obtained by the use of either hydrochloric acid or sodium hydroxide. Unstressed control specimens of the alloy were also exposed in pH 6 chloride-free water at 300°C.

One crack occurred on a specimen in the pH 6.5 environment, although this crack may have been the result of an imperfection in the casting which opened up on stressing. A photomicrograph of the defect appears in Fig. 11.4. As shown, the crack extended to a depth of 4 mils. Since metallographic polishing and etching did not disclose any grain boundaries in the immediate vicinity of the affected area, it was assumed that the defect was confined to a single crystal of the alloy. Grain boundaries were disclosed by the etching procedure in the remaining portion of the specimen.

The general corrosion resistance of cast type 347 stainless steel, as determined from the present tests, appeared to be at least comparable to the corrosion resistance of the wrought alloy observed in other similar tests. Actually, the cast material was more resistant to the formation of heavy scales and edge pitting, which are commonly found on wrought specimens in the same environments.

Additional stress-corrosion cracking tests with cast type 347 stainless steel will be conducted in chloride-containing environments. A number of different heats of the alloy as well as several heats of other cast, austenitic stainless steels will be tested in an effort to determine whether the cast structure is responsible for the high degree of immunity to stress-corrosion cracking or whether the resistance to cracking is peculiar to the one heat of cast steel tested to date.

(b) CD4MCu Stainless Steel.--Stress-corrosion cracking tests with both cast and wrought forms of CD4MCu stainless steel are being continued; preliminary results have been reported.[2] The environments for the present tests are oxygenated water, at 300°C, containing 100 ppm of chloride at initial pH values of 2.8 and 10.5. The initial solution pH values were obtained by the use of hydrochloric acid and sodium hydroxide, respectively. Unstressed control specimens of the alloy are being exposed in chloride-free, pH 6 oxygenated, distilled water at 300°C. A summary of the test results is given in Table 11.3.

One crack was observed on one of the stressed wrought specimens after 500 hr in pH 2.8 chloride-containing water; the crack is shown in Fig. 11.5. From all indications, it was transgranular and approximately 7 mils deep. No other evidence of cracking was observed. The appearance of specimens was characterized by thin, light tan-colored films; the corrosion attack was very mild. The tests will be continued.

Table 11.3. Stress-Corrosion Cracking Behavior of CD4MCu Stainless Steel in Oxygenated[a] Water at 300°C

Chloride Content (ppm)	Alloy Form	Initial Solution pH	Total Time (hr)	Specimen Appearance
0[b]	Wrought	6.0	1000	No significant attack
100	Wrought	2.8	1000	Crack in one specimen after 500 hr; light general corrosion
100	Cast	2.8	300	No crack; light general corrosion
100	Wrought	10.5	1000	No cracks; light general corrosion
100	Cast	10.5	300	No cracks; light general corrosion

(a) Air-saturated at room temperature.
(b) Unstressed control specimens.

11.2.3 Corrosion of Titanium by Oxygen-Free Uranyl Sulfate Solution

A number of tests were run at 250°C to determine the corrosion resistance of titanium-75A in oxygen-free heavy-water solutions containing uranyl sulfate and deuterium sulfate and to determine the chemical stability of the solutions in such a system. Uranyl sulfate concentrations ranged from 0.04 to 1.0 *m*; two deuterium sulfate concentrations were used, 0.02 and 0.1 *m*.

The tests were conducted in quartz tubes with coils of thin titanium sheet as specimens. The ratio of titanium surface area to solution volume was 17 cm^2/ml in each test. The oxygen was removed by sparging with helium. The solutions were then frozen, evacuated, and sealed under vacuum.

The corrosion specimens, three in each of four different solutions, exhibited weight gains between 0.1 and 0.3 mg/cm^2 after a 100-hr exposure. Corrosion rates, calculated from the observed weight gains, assuming no loss of titanium dioxide, varied between 0.6 and 1.0 mpy. There was no significant difference in the corrosivity of the four test solutions. The appearance of all specimens was characterized by thin, uniform, golden-tan films, similar to those usually observed on specimens exposed in oxygenated uranyl sulfate solutions at elevated temperatures.

Initial and final solution compositions and average corrosion rates are shown in Table 11.4. Although the solution analyses showed slightly lower concentrations of uranium and sulfate in the final solutions than in the original solutions, there was no visible evidence that the solutions had undergone any reduction. Part of the difference between reported initial and final concentrations may have been due to the fact that relatively large aliquots of solution were used in the initial determinations but a 5-ml solution volume from each test was used in the final determinations. Also, the fact that both sulfate and uranium were lost from solution indicates that reduction and hydrolytic precipitation to uranium oxides did not occur.

These tests indicate that titanium and oxygen-free uranyl sulfate solutions are relatively stable for limited periods of time under certain conditions. However, the results should not be construed to mean that the tests could have been run indefinitely without evidence of chemical instability. Indeed, it has been reported that nearly complete reduction of a 0.17 *m* UO_2SO_4 solution occurred during a 1000-hr run at 315°C in a titanium thermal loop.[11]

11.2.4 Corrosion of Zircaloy-2 in the Heavy Phase of a 1.33 *m* UO_2SO_4 Solution at 300°C

In a reactor fuel solution, it is possible that the temperature will get high enough to cause separation of a second liquid phase containing very high concentrations of uranium and appreciable concentrations of copper. Since this possibility exists, tests were carried out to determine the corrosion rate of Zircaloy-2 in such a heavy phase (out-of-pile) as a function of copper concentration. The test solutions were 1.33 *m* UO_2SO_4 containing 0, 0.01, 0.04, and 0.10 *m* $CuSO_4$. The solutions and specimens were placed in quartz liners and tested at 300°C, a temperature at which two distinct liquid phases are present. The four tests were made with an oxygen overpressure of approximately 150 psi. At various intervals during a 980-hr test, solutions and specimens were examined. New solution was used for each run.

Zircaloy-2 specimens immersed in the second phase acquired dark-colored films with small, numerous striations of white oxide deposits. All specimens exhibited weight gains, not exceeding 0.3 mg/cm^2. Analyses on the mixed light and heavy solution phases after the second run, which lasted 400 hr, showed the zirconium content to be less than 5 ppm in all cases. Thus it must be assumed that Zircaloy-2 corrosion in second-liquid-phase uranyl sulfate solution is negligible and that copper concentrations up to 0.1 *m* as copper sulfate in the room-temperature solution have no effect on the corrosion behavior of the alloy in the second phase at 300°C.

11.2.5 Corrosion of Incoloy 804 and Electrolyzed Stainless Steel

The corrosion behavior of Incoloy 804 and Electrolyzed stainless steel was examined in a number of reactor-related environments. Results of the tests are presented as follows:

Table 11.4. Corrosion Rates and Solution Compositions for 100-hr Tests with Titanium-75A in Oxygen-Free Uranyl Sulfate Solutions at 250°C

Test Solution		Composition	pH	U (mg/ml)	SO_4 (mg/ml)	$\frac{SO_4}{U}$	Excess Acid (*m*)	Average Corrosion Rate (mpy)[a]
UO_2SO_4 (*m*)	D_2SO_4 (*m*)							
0.04	0.02	Initial	1.4	10.8	6.5	1.511	0.021	0.7
		Final	1.3	8.5	5.4	1.574	0.020	
0.04	0.1	Initial	0.8	11.1	14.2	3.149	0.099	0.6
		Final	0.8	9.2	13.9	3.751	0.115	
0.2	0.02	Initial	1.3	51.3	23.4	1.135	0.022	1.0
		Final	1.1	48.6	21.4	1.092	0.018	
1.0	0.02	Initial	1.0	251	106	1.046	0.024	0.7
		Final	1.0	248	100	1.000	ND[b]	

(a) Determined from average weight gains observed on three specimens per test.
(b) No excess acid detected.

(a) Incoloy 804.--A new nickel-base alloy, Incoloy 804 (developed by the International Nickel Company), was corrosion tested in an oxygenated, simulated HRT fuel solution at 100, 200, and 300°C. The composition of the alloy is 29% Cr, 25% Ni, 1% Mn, 0.4% Cu, 0.06% C, and balance iron; the hardness of the test material was 90 Rockwell B.

Corrosion tests were run for 1000 hr at each temperature in 0.04 *m* UO_2SO_4-0.025 *m* H_2SO_4-0.01 *m* $CuSO_4$ solution. The average rates of attack were 0.01, 1.3, and 3.8 mpy, respectively, at 100, 200, and 300°C. Specimens exposed at 100°C showed no change in physical appearance, whereas those exposed at 200 and 300°C exhibited thin, lustrous-black films and a shallow pitting attack. At 200°C the corrosion rate was relatively constant with accumulated exposure time, but at 300°C the rate decreased slightly with increased exposure time.

Although the corrosion behavior of Incoloy 804 was tolerable, it was inferior to that of type 347 stainless steel. Unless the alloy possesses mechanical properties or resistance to stress-corrosion cracking superior to that of type 347 stainless steel, its use in homogeneous reactor systems cannot be recommended.

(b) Electrolyzed Stainless Steel.--Electrolyzing (a proprietary process developed by The Electrolyzing Corporation of Chicago, Illinois) is used to coat metallic parts with a high-chromium-content coating for wear and corrosion protection. The hardness of the applied coating varies between 70 and 72 Rockwell C. Since materials with such surface hardness would be useful in many homogeneous reactor applications, a number of corrosion tests were performed with coated specimens.

In the initial tests, duplicate coupons of type 347 stainless steel which had an Electrolyzed coating 0.0002 in. thick (0.2 mil) were exposed for 1000 hr in oxygenated 0.04 *m* UO_2SO_4-0.02 *m* H_2SO_4-0.005 *m* $CuSO_4$ solution at 100 and at 300°C. At 100°C neither visual nor weight changes were observed. A red-brown film was found on the 300°C specimen, which corroded at a slightly increasing rate of 1.1 mpy during the 1000-hr test. Metallographic examination disclosed no evidence that Electrolyzed coating remained on the 300°C specimen; the coating thickness on the 100°C specimen was unchanged by the exposure.

The behavior of the Electrolyzed coating was examined also in oxygenated, deionized water at 300°C in a titanium autoclave. A coated cylindrical pin of type 304 stainless steel was used; the Electrolyzed coating was somewhat less than 0.2 mil thick. At the end of a 300-hr test substantial quantities of hexavalent chromium were present in the water, and metallographic examination showed that the chromium-rich layer had been completely removed.

In other tests an Electrolyzed type 304 stainless steel cap screw, of the type used for bolting the thermal barrier in centrifugal pumps, was stressed at approximately 11,000 psi and exposed in boiling (100°C) 0.04 *m* UO_2SO_4-0.025 *m* H_2SO_4-0.01 *m* $CuSO_4$ solution containing 50 ppm of

chloride as potassium chloride. Upon completion of the test, an apparent crack was found on the head of the bolt. Since megallographic examination of various areas on the cap screw revealed that little if any of the original Electrolyzed layer was present after the exposure, the observed "crack" on the head could not be attributed to stress-corrosion cracking of the Electrolyzed layer itself. Grinding to determine the depth of the "crack" disclosed massive areas of subsurface attack, as shown in Fig. 11.6, rather than a conventional stress-corrosion crack. No other localized attack was found on the cap screw.

Other tests run specifically to determine qualitatively the galling and seizing properties of the coating indicated it to be essentially free from such difficulties. The torque required to release the stress applied to a nut and bolt assembly never varied appreciably from the initial torque.

Since the Electrolyzed layer was gradually removed at 300°C in both oxygenated, deionized water and simulated HRT reactor fuel solution and at 100°C in chloride-containing fuel solution, its use in such environments could not be considered. Its corrosion resistance was excellent, however, in boiling, chloride-free simulated reactor fuel solution, and presumably it could be used for hard-facing applications at this temperature or lower.

REFERENCES

1. Reported in greater detail by J. C. Griess et al., Quar. Rep. of the Solution Corrosion Section for the Period Ending January 31, 1959, ORNL CF-59-1-79.

2. J. C. Griess et al., HRP Quar. Prog. Rep. Oct. 31, 1958, ORNL-2654, p 115.

3. E. S. Bomar, Metallographical Examination of Zircaloy-2 Bypass from H Loop, memorandum no. HRP-MET-77 (Jan. 5, 1959).

4. J. C. Griess et al., Quar. Rep. of the Solution Corrosion Group for the Period Ending Oct. 31, 1958, ORNL CF-58-10-95, p 9.

5. W. H. McAdams, Heat Transmission, p 378, McGraw-Hill, New York, 1954.

6. H. C. Savage et al., HRP Quar. Prog. Rep. Oct. 31, 1956, ORNL-2222, p 100.

7. G. H. Jenks et al., HRP Quar. Prog. Rep. Oct. 31, 1953, ORNL-1658, p 71.

8. J. C. Griess et al., Quar. Rep. of the Solution Corrosion Group for the Period Ending April 30, 1958, ORNL CF-58-4-131, p 21.

9. G. H. Jenks et al., HRP Quar. Prog. Rep. for Periods Ending April 30 and July 31, 1958, ORNL-2561, pp 214 and 223.

10. J. C. Griess et al., Quar. Rep. of the Solution Corrosion Group for the Period Ending July 31, 1958, ORNL CF-58-7-132, pp 24-27.

11. F. W. Cooke, Metallurgical Examination of Titanium Thermal Loop and Corrosion Specimens from Second-Liquid-Phase Study, memorandum no. HRP-MET-44 (Nov. 21, 1958).

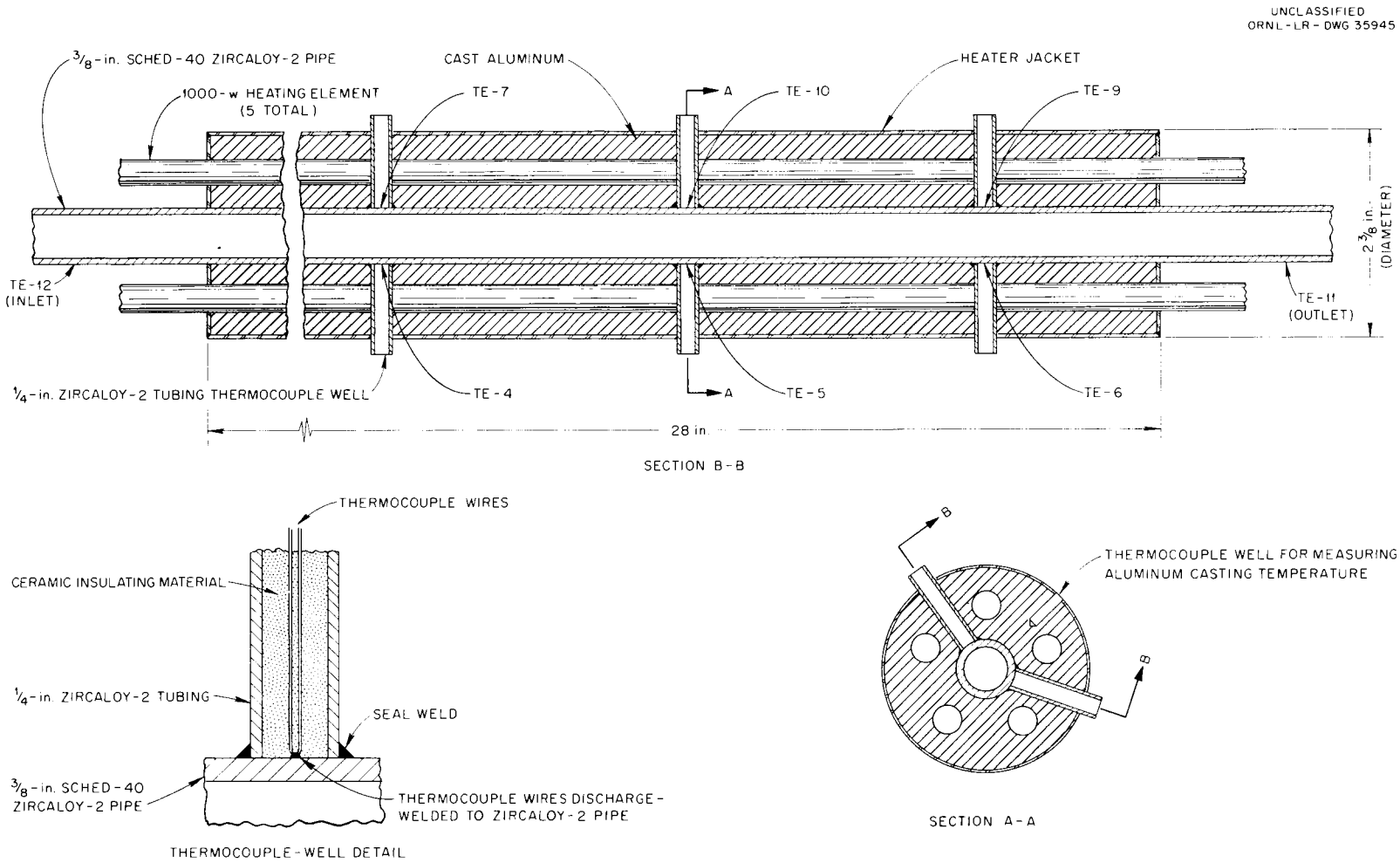

Fig. 11.1. Heated Zircaloy-2 Bypass, 100A Loop H.

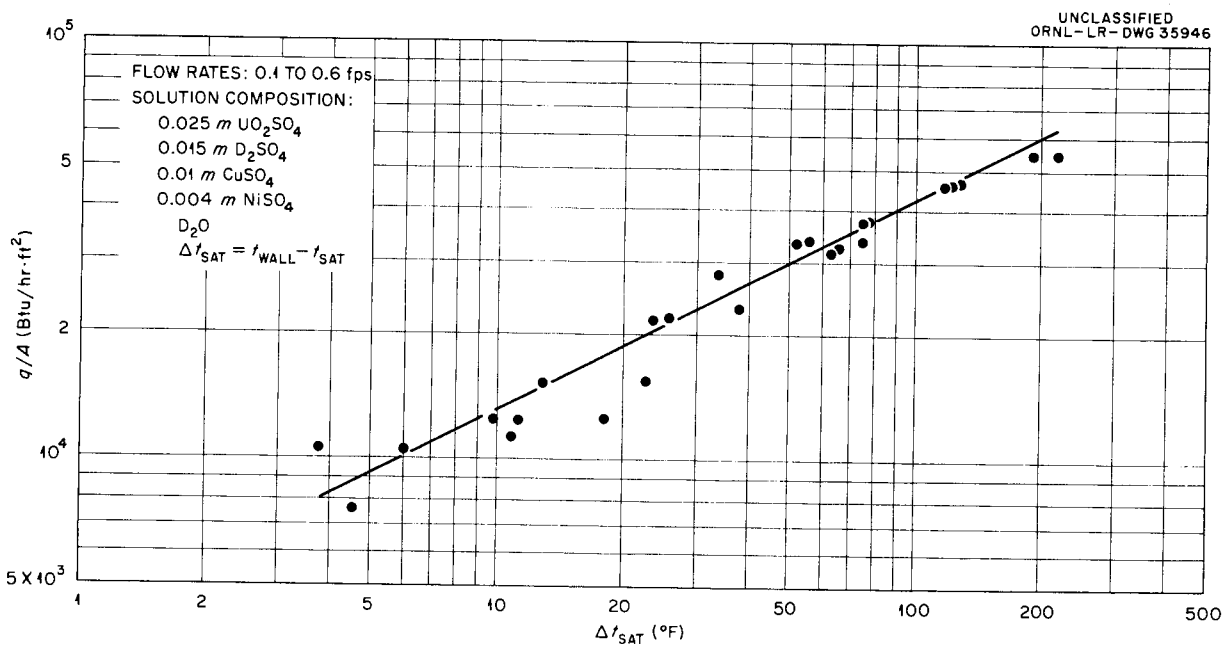

Fig. 11.2. Plot of Heat Flux vs Δt_{sat} in the Heated Zircaloy-2 Bypass, Run H-124.

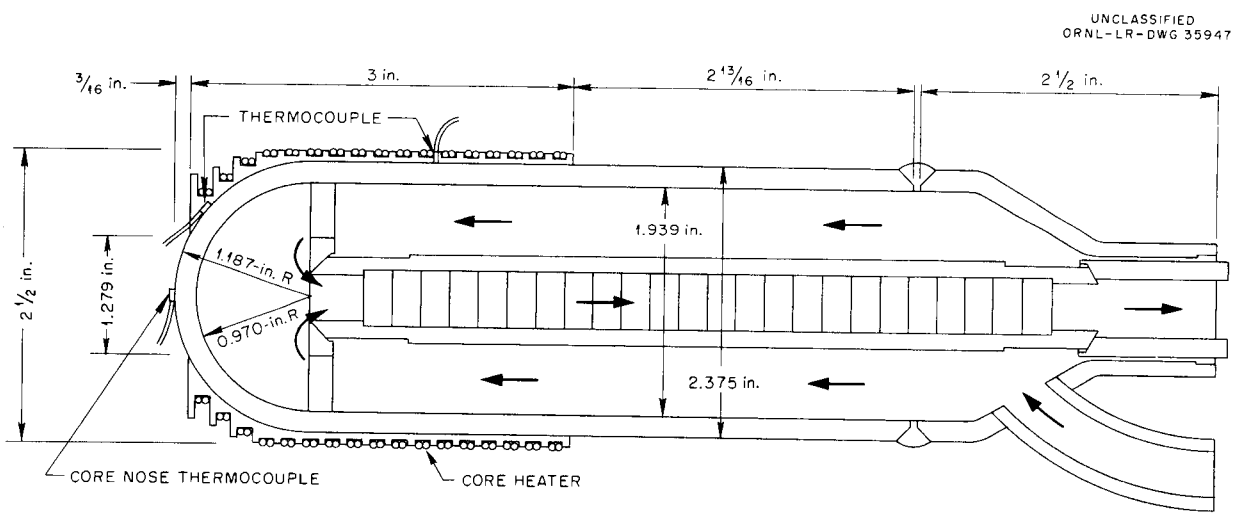

Fig. 11.3. Core Heater Used During Solution Stability Studies in Loop L-2-23.

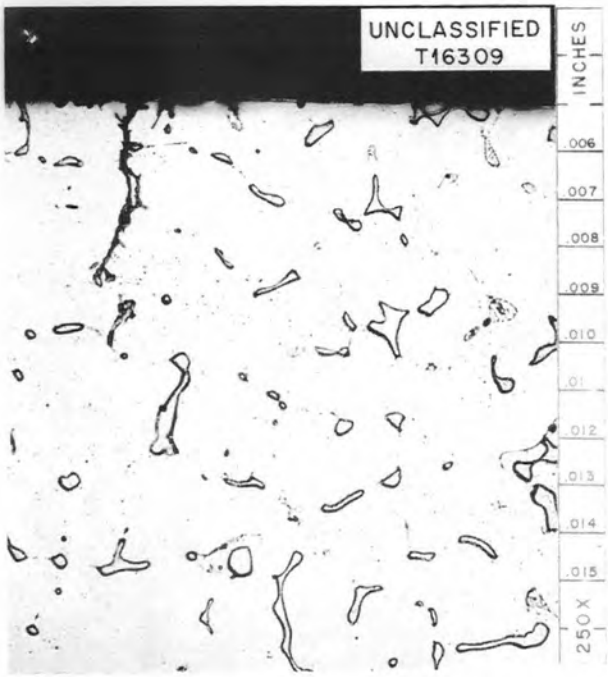

Fig. 11.4. Defect or Crack Found in Stressed Cast Type 347 Stainless Steel After 1500 hr at 300°C in Chloride-Containing Water.

Fig. 11.5. Crack in Wrought CD4MCu Stainless Steel After 1000 hr at 300°C in Chloride-Containing Water.

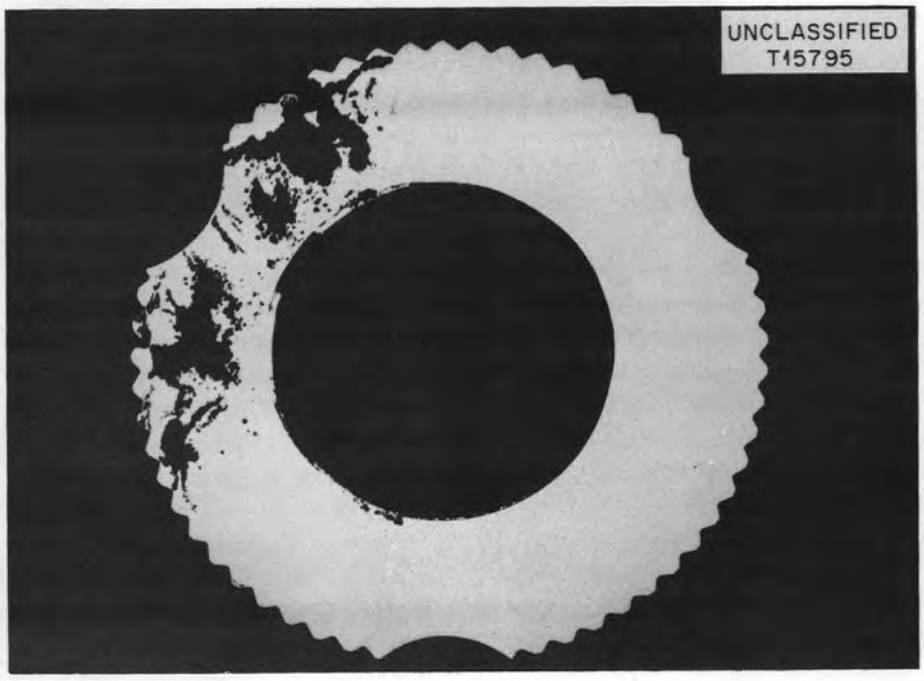

Fig. 11.6. Subsurface Corrosion Attack in Electrolyzed Type 304 Stainless Steel Cap Screw After 1000 hr in Boiling, Chloride-Containing Simulated HRT Fuel Solution.

12. SLURRY CORROSION

E. L. Compere H. C. Savage

J. M. Baker
S. E. Bolt
V. A. DeCarlo
R. B. Gallaher
D. T. Jones
R. A. Lorenz
A. R. Olsen
S. A. Reed
L. Rice
W. C. Ulrich
L. F. Woo

12.1 PUMP LOOPS

12.1.1 Introduction to Pump-Loop Tests

Two 100A-loop tests were in progress during the quarter to evaluate D_2O slurries of two thoria preparations proposed for use in the in-pile slurry-loop program. In one test already completed, the slurry consisted of a 2.4-μ, 1600°C-calcined thoria to which MoO_3, a proposed recombination catalyst, was added. The second run, for testing a slurry of 0.8-μ, 650°C-calcined thoria with additions of UO_3 and palladium metal catalyst, is still in progress.

Two additional tests were made at 200°C by use of oxygenated slurries of ThO_2 and mixed ThO_2-$UO_3 \cdot H_2O$ to determine the corrosion-erosion attack of a group of selected alloys for possible application in a mixed Th-U oxide slurry reactor.

12.1.2 Circulation of ThO_2-D_2O Slurries in Oxygen and in Deuterium Atmospheres

Two 100A-loop runs, BS-24 and BS-25, were carried out during the quarter to evaluate slurries of two different thoria preparations which were proposed for use in the in-pile slurry loop program. The tests were designed to provide corrosion-erosion data and slurry property data with heavy water slurries of the two thoria preparations during circulation at 280°C at approximately 450 g of Th per kg of D_2O concentration using both oxygen and deuterium atmospheres. The latter test is still in progress.

One preparation, batch DT-15, was prepared at ORNL by calcining 10°C-precipitated $Th(C_2O_4)_2$ at 1600°C for 4 hr. The material was then sized by sedimentation classification to provide an average particle

size of 2.4 μ (σ= 1.25). Molybdenum trioxide (~0.005 *m*), a recombination catalyst, was added to the slurry.

The second preparation, batch LCC-29108, furnished by the Westinghouse PAR Project, had been prepared by calcining "long-digested" (16 hr at 85°C) $Th(C_2O_4)_2$ at 650°C for 4 hr. The thoria, which was not classified, had a mean particle size of 0.8 μ (σ= 1.42). Sufficient $UO_3 \cdot H_2O$ (rods) to provide a 0.009 *m* uranium concentration, and a palladium metal catalyst (7×10^{-4} *m*) specially prepared by the PAR Project, were mixed with the slurry.

Catalyst activities of samples withdrawn from the test loop during the runs were measured in the Chemical Technology Division laboratory. The results are reported in Section 18.2.1.

(a) Run BS-24.--Data have been reported for the first two phases of run BS-24 which consisted first of a circulation period of 485 hr, using an oxygen atmosphere (460 std cc O_2 per liter of slurry), and then a period of 478 hr, in a deuterium atmosphere (650 std cc of D_2 per liter of slurry).[1] The final phase of the test, completed without incident during the current quarter, consisted of an additional 335 hr of circulation under an oxygen atmosphere (820 std cc of O_2 per liter of slurry). To determine its effect on the catalytic activity of the MoO_3 and on corrosion-erosion, the oxygen concentration during this phase of the run was maintained at approximately twice that used in the first phase of the run.

Conditions and results of the entire test are summarized in Table 12.1.

(b) System Material Balance, Run BS-24.--The run was concluded by removing the slurry solids from the system at operating temperature and pressure by means of a 0.4-in. hydroclone using induced underflow.[2] When solids removal was initiated by using the hydroclone, the system inventory was 7.75 kg of ThO_2 and 43.7 g of MoO_3. Hydrocloning was stopped after 45 min, at which time, based on chemical analysis of samples withdrawn from the loop, 36 g of ThO_2 was circulating. Based on inventory, 85.3% of the solids were recovered by the hydroclone. The solids (0.9 kg) which remained in the system were recovered during the rinsing operations described below. The total recovery of thoria was 99.5%.

Based on chemical analysis of samples, the molybdenum concentration of the slurry dropped from 0.020 to 0.014 *m* during the last 137 hr of operation in the second phase of the run having a deuterium atmosphere. Prior to that time, no loss had been noted. The downtrend continued during the final phase of the run. On the basis of the analysis of a sample taken immediately before hydrocloning was started, 11 g of MoO_3 was unaccounted for in the circulating slurry.

Table 12.1. Synopsis of Run BS-24

Test temperature: 280°C
Slurry prepared from Batch DT-15 ThO_2, 1600°C-calcined
Average particle size, 2.4 μ

	First Phase		Second Phase	Third Phase	Total Run	
Time (hr)	485		478	335	1298	
Average concentration (g of Th per kg of D_2O)						
Inventory	490		475	449	474	
Circulating	449		444	444	446	
Atmosphere (std cc/liter of slurry)	O_2 (460)		D_2, Ar (D_2-650)	O_2 (820)	O_2, D_2-Ar, O_2	
Additives (average concentration)	0.003 *m* MoO_3		0.007 *m* MoO_3	0.008 *m* MoO_3	0.006 *m* MoO_3	
pH of slurry	5.7 - <u>2.3</u>[a]		3.6 - <u>8.6</u>[a]	2.8 - <u>4.2</u>[a]	2.8 - 8.6	
System attack rate, mpy	0.9		5.6	0.6	<u>Loop Piping <0.3</u>[b]	
Pin attack rates, mpy	<u>20 fps</u>	<u>40 fps</u>			<u>20 fps</u>	<u>40 fps</u>
Austenitic stainless steels	0.3	4			0.3 - 0.5	18 - 33
Inconel	4	11			3.1	9
Incoloy	0.8	7			0.6	12
Croloy 2 1/4, 5	0.3, 0.3	0.6, 0.6			2.7, 2.4	4, 4
Zircaloy-2	None detected	0.4			None detected	1

(a) Underlined values predominated during the period.

(b) Pipeline velocity, 4.7 fps; corrected for system components attack as follows.
Slurry contained 62 g of corrosion products;
Type 347 SS impeller lost 36 g;
Type 347 SS specimen holder lost 15.5 g.

Therefore, after hydrocloning, the loop was rinsed with a 3% solution of trisodium phosphate, circulated at 100°C for 48 hr. Eight-tenths of a kilogram of ThO_2 and 10.8 g of MoO_3 were recovered from the system.

(c) Slurry Properties, Run BS-24.--During the three phases of the run (total of 1298 hr of circulation), no thoria particle-size degradation was noted. However, the room-temperature yield stress and modulus of rigidity and the settling rates of the slurry were changed as a result of circulation under the different atmospheres.

Values of yield stress and modulus of rigidity at room temperature for the original slurry charge and of material removed from the system after each phase of operation are shown in Table 12.2. Settling rates of the slurries plotted as a function of temperature are presented in Fig. 12.1. The rheological data were computed from measurements made at room temperature by the Analytical Chemistry Division, using a capillary-tube viscometer. It should be noted that no MoO_3 was included with the charge material.[1]

Table 12.2. Yield Stress and Modulus of Rigidity at Room Temperature of ThO_2-D_2O Slurry Circulated in Loop Test BS-24

Batch DT-15 thoria, 1600°C-calcined
Average particle size, 2.4 μ
Slurry concentration, 500 g of Th per kg of D_2O

	Yield Stress* (lb/ft^2)	Modulus of Rigidity* (centipoises)
Charge to loop	0.02	1.4
After first phase (O_2 atmosphere)	0.03	1.3
After second phase (D_2 atmosphere)	0.58	3.3
After third phase (O_2 atmosphere)	0.12	1.5

*Determined at room temperature with a capillary-tube viscometer.

Other than a shift in the settling-rate curves, no significant changes in slurry properties occurred as a result of the first circulation period, during which there was an oxygen atmosphere in the loop. After the slurry had been circulated in a deuterium atmosphere, the yield stress and modulus of rigidity of the slurry increased markedly, and a general decrease in settling rates was observed. After the third phase of the test, in which an oxygen atmosphere was used, the values for yield stress and modulus of rigidity dropped, and settling

rates of the slurry increased. However, the rates were lower than those observed for the original slurry charge.

Before terminating the last phase of the test, the flow rate in the loop was gradually lowered by means of a variable-frequency power supply in order to determine at what flow velocity the slurry solids segregated in the loop piping. Concentration changes in the system were determined from samples withdrawn from the loop at 30-min intervals.

A computed minimum pipeline velocity of 4.7 fps was maintained in the loop during the three phases of the test. No segregation was observed. As the flow rate in the loop was changed, no observable dropout of solids was noted until a flow velocity of approximately 2 fps was reached, at which time about 38% of the solids was lost immediately from the flowing stream. Over the next 22 hr of circulation, no further dropout occurred.

The solids were completely resuspended 30 min after the velocity was increased to 4 fps.

(d) Corrosion-Erosion, Run BS-24.--Attack data for run BS-24 are shown in Table 12.1.

Attack rates of the type 347 stainless steel test loop and impeller and of the titanium pump scroll and thermal barrier were computed during the three portions of the test, according to the quantity of corrosion products detected by chemical analysis of slurry samples withdrawn from the system. No titanium was detected in the samples throughout the run, which indicated negligible attack of the pump scroll and thermal barrier. During the first 485-hr portion of the run (oxygenated slurry; pH 5.7 to 2.3), the mean attack rate of the stainless steel components of the system was 0.9 mpy. The mean rate increased to 5.6 mpy during the 478-hr circulation period (deuterium-argon atmosphere). The average pH of the slurry during that phase of the test was 8. An attack rate of 0.6 mpy was computed for the final 335-hr circulation period (oxygenated slurry). Slurry pH values ranged from 2.8 to 4.2 during that period of operation.

Based on total corrosion products in the slurry, 62 g of stainless steel was removed from the loop system during the 1298 hr of slurry circulation. The stainless steel impeller lost 36 g and the corrosion-specimen holders lost 15.5 g. Therefore, an estimated 10.5 g of stainless steel was removed from the loop piping, flow restrictors, and pump sealing rings. The calculated mean attack rate of the loop piping was <0.3 mpy.

Attack rates of the defilmed pin corrosion specimens exposed during the 1298 hr to velocities of 20 and 40 fps were, respectively (in mpy): type 347 stainless steel, 0.4 and 26; type 430 stainless steel, 0.4 and 4; Croloys 2 1/4 and 5, 2.5 and 4; Inconel, 3 and 9;

Incoloy, 0.6 and 12; titanium RC-55, <0.1 and 0.6; Zircaloy-2, 0 and 1; platinum, 0.3 and 7; and gold, 0.1 and 6.

(e) Run BS-25.--Run BS-25, which is still in progress, is programmed to provide practically the same information as that sought in run BS-24. However, the sequence of atmosphere studies has been changed. For the first phase of the test, the loop was pressurized with argon in order to simulate conditions under consideration for an in-pile slurry-loop experiment. The deuterium concentration (as a result of corrosion) was allowed to increase gradually during the run to 35 std cc per liter of slurry. An oxygen atmosphere (approximately 400 std cc per liter of slurry) is being maintained in the current phase of the test.

Conditions and results of the first phase of the test are summarized in Tables 12.3 and 12.4.

(f) Slurry Loading, Run BS-25.--The preparation of the slurry charge followed, as closely as possible, the procedure used for charging a similar slurry to an in-pile slurry-loop mockup at the PAR site. The charge consisted of 9.3 kg of batch LCC-29108 ThO_2, 54 g of $UO_3 \cdot H_2O$ (rods), and 323 g of the palladium-containing catalyst. The material was to be injected into the test loop in two equal portions.

First, the dry solids were mixed and blended by rolling in a plastic bottle. Four liters of D_2O were added, and the mixture was shaken vigorously for 15 min. It was then attempted to transfer the contents of the bottle to the loop addition tank in the usual manner by evacuating the charge tank and drawing the slurry through a 3/8-in. tubing, but a plug formed in the tubing. Therefore, the mixture was transferred to a baffled container and mixed with a mechanical stirrer for 30 min. As stirring was continued, a second transfer was attempted. Two liters of D_2O were used to rinse the solids from the container as the transfer was being made. In this manner all but 5 g of lumpy solids was transferred to the loop addition system. The residue was composed essentially of UO_3 and palladium metal catalyst.

(g) Slurry Properties, Run BS-25.--The slurry circulated satisfactorily in the argon-deuterium atmosphere for 508 hr, which comprised the first phase of the test. No thoria particle-size degradation was noted during that period. The pH of the slurry, which ranged from 4.5 to 8.3, increased gradually during the course of the run. The calculated slurry-charge concentration in the loop was 454 g of Th per kg of D_2O, and the ratios of the additions were 5.15 mg of U per g of Th and 0.158 mg of Pd per g of Th. Based on chemical analysis of samples withdrawn from the loop during the test, the average circulating concentration was 427 g of Th per kg of D_2O; uranium and palladium ratios were 5.25 mg of U per g of Th and 0.185 mg of Pd per g of Th. The concentration of uranium and palladium in the supernatant liquid was less than 2 ppm.

Table 12.3. Operating Characteristics of Slurry-Loop Tests

	First Phase BS-25	ES-5	ES-6	ES-7	ES-8
Time, hr	508	223	510	334	306
Temperature, °C	280	280	280	200	200
Concentration, g Th/kg H_2O					
Charged	454[a]	308	430	561	524
Average	427[a]	277	432	505	522
Calcination temperature, °C	650	1600	1600	1600	1600
Thoria batch number	LCC-29108	LO-39	DT-9	DT-9[b]	DT-9[b]
Additives	UO_3, Pd	None	None	None	$UO_3 \cdot H_2O$
Concentration, *m*	0.009, 7×10^{-4}				0.15
Atmosphere	Ar	O_2	O_2	O_2	O_2
pH of slurry (room temp.)	8	5-6	5-6	5-6	5-6
Average particle size, μ					
Prerun	0.8	0.9	1.8	1.7	1.8
Postrun	0.8	0.9	1.8	1.8	1.9
Impeller weight loss, g	-	0	0	0	1.0

(a) g Th/kg D_2O
(b) Prepumped

Table 12.4. Corrosion by Circulating Thoria Slurries in Loop Tests

	BS-25	ES-5	ES-6	ES-7	ES-8
Loop corrosion rate, mpy	0.9	0.4	1.1	0.7	0.8
Range of pin attack rates at given velocity, mpy					
Velocity, fps		Austenitic Stainless Steels			
16-21	0.8	0.1		<0.1	0.1
24-26				<0.1	0.1
37-44	4.4		1.3-3.7	<0.1	0.4
51-54			1.1-2.8	0.4-1	0.6
		Ferritic Stainless Steels			
16-21				<0.1-0.2	<0.1-0.5
24-26				<0.1-0.2	0.3-0.8
37-44				0.1-0.5	0.4-0.9
51				0.3-2	0.6-2.9
		Zirconium Alloys			
18-22	0.4			None detected	None detected
37-40	2.5		0.1-0.2		
54			0.1-0.2		
		Noble Metals			
16-21				Au <0.1, Pt <0.1	Au <0.1, Pt <0.1
24				Au <0.1, Pt <0.1	Au 0.2, Pt 0.2
37-40			Au 2.1, Pt (5%, Ir), 5.1	Au 0.1, Pt 0.1	Au 2.9, Pt 0.8
51-54			Au 1.4, Pt (5%, Ir), 4.0	Au 0.7, Pt 1.8	Au 18.8, Pt 8.2

Table 12.4. (continued)

Velocity, fps	BS-25		ES-5	ES-6	ES-7	ES-8
				Nickel Alloys		
16-21					0.1-11	0.2-1.1
24-26					0.1-8	0.2-1.3
37-44				14-17	0.4-8	0.9-1.5
51				13-15	1.9-10	5.5-7.1
				Hastelloys		
16					5-13	1.9-13
24					0.3-9	2.0-16
37					6-7	3.2-160
51					15-30	11-600
				Alloy Steels		
	ASTM-A7	(0% Cr)	4.2		1.7	3.4
	Croloy 1/2	(1/2% Cr)	2.6		0.7	2.7
	Croloy 1	(1% Cr)	2.0		0.6	2.2
	Croloy 2 1/4	(2 1/4% Cr)	1.4		0.4	1.5
20-22	Croloy 3	(3% Cr)	1.3		0.3	1.5
	Croloy 5	(5% Cr)	0.5		0.2	0.7
	Croloy 7	(7% Cr)	0.4		0.1	0.5
	Croloy 9M	(9% Cr)	0.2		0.1	0.4

(h) Dropout, Run BS-25.--Near the end of the first part of the run, dropout tests were performed according to the same procedure used in run BS-24 in order to determine the minimum flow velocity required to keep the solids in suspension. At a pipeline velocity of 4.6 fps, no segregation of solids was observed during 500 hr of circulation. As the flow rate in the loop was reduced, no observable dropout occurred until a velocity of 2.5 fps was reached. At that velocity, 15% of the slurry solids was not in circulation. In 1 hr after the velocity was again increased to 4.6 fps, the solids were resuspended.

The first portion of the test was concluded by removing the slurry solids from the loop by means of a 0.4-in. hydroclone employing induced underflow while the system was operated at 280°C and ~1100 psig pressure. In this manner 90% of the solids was removed from the system in 45 min.

(i) Palladium Deposition, Run BS-25.--Based on chemical analyses of slurry samples withdrawn from the test loop during the run, the concentration of palladium varied without trend between 7- and 10 x 10^{-4} *m*, which indicated no apparent loss of palladium from the circulating slurry. However, when the specimen arrays were removed from the loop after the run, the two gold pins were coated with thin, dull, metallic films which were found by chemical and electron diffraction analyses to be palladium metal. Traces of Fe_3O_4 and ThO_2 were also present. Because of the tenacity of the deposits, the film thicknesses could not be determined. By microscopic examination, the metallic palladium particles appeared to be imbedded in the surfaces of the gold specimens.

(j) Corrosion-Erosion, Run BS-25.--Attack rates of the type 347 stainless steel loop components and of the titanium pump scroll and thermal barrier were calculated during the test from the corrosion products detected by chemical analysis of slurry samples withdrawn from the system. The mean stainless steel corrosion rate for the 508-hr period using the argon-deuterium atmosphere was 0.9 mpy. Titanium was not detected in any of the samples, indicating negligible attack on the pump scroll and thermal barrier.

Two type 347 stainless steel and two Zircaloy-2 pin-type corrosion specimens were removed from the specimen arrays at the end of the first test period. Attack rates, calculated from weight losses of the defilmed specimens, at velocities of 20 and 40 fps, respectively, were: type 347 stainless steel, 0.8 and 4 mpy; Zircaloy-2, 0.4 and 2.5 mpy.

The remaining pin-type specimens in the arrays which were weighed but not defilmed were returned to the loop for further exposure. Average attack rates, approximated from weight changes of these specimens were, at 20 and 40 ft/sec, respectively: type 430 stainless steel, 2 and 11 mpy; CD4MCu cast stainless steel, 0.5 and 5 mpy; Croloy 2 1/4, 14 and 141 mpy; Croloy 5, 6 and 47 mpy; Incoloy, 0.2 and 2 mpy; Inconel, 0 and 0.6 mpy; and titanium RC-55, 0.3 and 0.3 mpy. The gold and platinum specimens were not detectably attacked at either velocity.

12.1.3 Materials Evaluation Tests

A series of tests was initiated during the report period to determine the corrosion-erosion attack of a group of selected materials of possible interest for application in a Th-U oxide slurry reactor. The test series is being made at 200°C at a slurry concentration of ~500 g of Th per kg of H_2O in order to study the effect of additions of UO_3 (~8% U/Th) to the slurry and the effect of hydrogen and oxygen atmospheres. Operational characteristics of the runs are given in Table 12.3. Tests involving hydrogen atmospheres are in progress.

It was of interest to use the same prepumped slurry throughout the test series. Slurry for the tests was prepumped in run ES-6, which was made at 280°C and used an oxygenated slurry of batch DT-9 thoria. The oxide was prepared at ORNL by calcining $Th(C_2O_4)_2$, precipitated at 20°C and digested at 85°C for 6 hr, at 1600°C for 4 hr. The material was then classified by sedimentation. The mean particle size of the product was 1.3 μ (σ = 1.76).

The test loop was charged with raw thoria to a concentration of ~450 g of Th per kg of H_2O. After 120 hr of circulation, about half of the solids were removed from the system by means of a hydroclone, and an equal quantity of unpumped thoria was added to the loop while the system operating conditions were maintained very nearly constant. Five such removals and additions were made during the 510-hr run. The mean oxygen concentration during the run was 400 (std) cc per liter of slurry; the average circulating slurry concentration was 432 g of Th per kg of H_2O.

The first test in the comparison series, run ES-7, circulated slurry (prepumped in run ES-6) at an average concentration of 505 g of Th per kg of H_2O at 200°C and 1100 psig with 1085 (std) cc of O_2 per liter of slurry for 334 hr. The slurry charge was added to the loop in two increments over a 7-hr period while the loop was operated at 200°C and 1100 psig.

The slurry recovered from run ES-7, along with enough makeup thoria from run ES-6 to replace losses from sampling and from clean-out operations, was reloaded into the system for run ES-8. Before the charge was injected into the loop, a sufficient quantity of $UO_3 \cdot H_2O$ rods was mixed with the thoria to provide 7.8% U/Th. The slurry was charged into the loop in two equal portions over a 6-hr period, with no difficulty. The 306-hr test was made at an average concentration of 522 g of Th per kg of H_2O at 200°C and 1100 psig, with an average of 1638 (std) cc of O_2 per liter of slurry.

(a) Conversion of Uranium Oxide Rods to Platelets.--The rods were slowly converted to platelets during the run. Each sample withdrawn from the test loop was examined by using an optical microscope. Very few platelets were present in the original $UO_3 \cdot H_2O$ charged to the loop.

The rods were 10 to 15 μ long, but after 2.5 hr of circulation, approximately half the rods had broken or degraded to about 5 μ. After an additional 20 hr of pumping, about 85% of the rods were degraded, and some platelets were present. In the 47-hr sample, most of the urania had converted to platelets of ~4 μ diameter. After 150 hr of circulation, few rods could be discerned. The slow transition of rods to platelets was similar to those already reported for $UO_3 \cdot H_2O$ slurries.[3-5]

For both tests, the loop was operated with steam pressurization. With this type of operation, the soluble ions tend to concentrate in the semistagnant water leg of the vertical pressurizer. In run ES-8, 21 ppm of uranium and 32 ppm of Cr^{+6} were detected in the pressurizer liquid after 24 hr of circulation. At the conclusion of the test, the concentration of the respective ions had increased to 152 ppm and 254 ppm. The pH of the pressurizer liquid, measured at room temperature, varied from 4.2 to 3.0 during the test. The average pH of the slurry was 5.6. According to the analytical data, the uranium-to-thorium ratio in the circulating slurry remained constant for the entire run.

The slurry was removed from the system at the end of the test with a 0.4-in. hydroclone. A total of 93% of the solids was recovered from the loop. During the hydrocloning operations, the uranium appeared to be preferentially removed. When half of the thorium had been removed, 75% of the uranium had been removed. Samples taken during the hydrocloning operation are under examination to see if the causes of this phenomenon can be identified.

(b) Pump Performance.--The 7 3/4-in. Zircaloy-2 impeller showed no weight loss during runs ES-6 and ES-7 and lost only 1 g out of 2296 during ES-8. There was no measurable wear on the sintered aluminum oxide bearing and journals which have operated for over 1400 hr with slurry and are still in excellent condition. The stainless steel front seal rings wore approximately 0.025 in., and the rear seal rings wore 0.015 in. per run.

(c) Corrosion-Erosion.--Attack data for runs ES-6, -7 and -8 are given in Table 12.4. During run ES-6, which was charged with five additions of unpumped thoria, the attack rate of the stainless steel system at 280°C was 1 mpy. Prepumped thoria slurry was used in run ES-7 (200°C), and the attack rate was 0.7 mpy. In run ES-8 which was made at 200°C with prepumped slurry containing UO_3, the attack rate of the system was 0.8 mpy.

In one test, run ES-5, made prior to this series,[1] it was observed that the attack of alloy steels by oxygenated ThO_2 slurry at 280°C was strongly dependent upon the chromium content of the alloys. The corrosion rates of steels which contained from 0 to 19% chromium, when normalized to the rate of type 347 stainless steel, were approximated by the expression

$$\log R/R_o = - k\ Cr^{1/2}.$$

To study the phenomenon further, duplicate arrays of the alloys were exposed in runs ES-7 and ES-8 at 200°C at a flow velocity of 20 fps. A comparison of these data is shown in Table 12.4. The rates of the alloys in run ES-7 were approximately one-third the rates in run ES-5, a normal result of the difference in temperature between the two tests and the slightly higher flow velocity (22 fps) in run ES-5. In contrast, when the same slurry was circulated at 200°C in run ES-8 with the addition of $UO_3 \cdot H_2O$, the attack rates of all the materials (see Table 12.4), including the alloy steel series, increased markedly. However, the relationship of relative attack rates and chromium contents of the alloy steels was nearly constant in the three tests.

The enhanced attack by the slurry containing UO_3 increased with increasing flow velocity. As shown in Table 12.4, the attack rates of gold and platinum as well as those of the other materials increased significantly in run ES-8, which indicated that the enhanced attack was primarily due to erosion rather than to chemical corrosion.

Incremental corrosion rates during the first part of run ES-8 were about 2 mpy during the period when many broken or whole $UO_2 \cdot H_2O$ rods could be observed in the slurry. Subsequently, the loop incremental rate fell to 0.2 mpy. This agreed with the final value for thoria, alone, in run ES-7, which became the charge to run ES-8. Thus the breakup of the 15-μ $UO_3 \cdot H_2O$ rods may be associated with the rate increase, and the attack would be of a transient nature. Further tests would be required to establish this firmly.

12.2 TOROIDS

12.2.1 Introduction

Toroid tests during the quarter were concerned with pilot tests of D_2O slurries of 650°C-calcined thorium-uranium oxides prepared by an adsorption technique, with special thoria preparations, and with the development of a device for obtaining known overpressures of a desired gas in the toroid rings.

12.2.2 Tests with Slurries of Thorium-Uranium Oxides

A series of tests was conducted in toroids during the quarter to study the corrosion-erosion characteristics and general properties of aqueous slurries of a group of experimental Th-U oxide preparations produced in the Chemical Technology Division. The oxides, prepared by adsorption of uranium on ThO_2 from alkaline carbonate solutions of uranium, were calcined at 650°C,[6] under ambient atmosphere. The respective batches contained approximately 5, 9, 11 and 33% U/Th.

Slurries of the mixed oxides and of the thorium oxide used as the base for their preparation were circulated at a concentration of 500 g of Th-U per kg of D_2O at 26 fps and 280°C in 300-hr tests. Each preparation was tested in an atmosphere of oxygen and of deuterium, with and without the addition of MoO_3, a proposed recombination catalyst. One additional 300-hr test in which oxygenated slurries of the uranium-containing preparations were circulated at a concentration of 200 g of Th-U per kg of D_2O at 26 fps and 280°C was also included in this series. The data for the series are presented in Table 12.5. The attack data were examined by using a factor analysis method[7] which permitted the separation of the effects of the variables as multiplicative factors. These results are presented in Table 12.6.

The following generalized effects may be noted. There was a substantial difference in the response of the various metals, and with the exception of Inconel, the factors for the metals are generally consistent with those previously reported for oxygen and hydrogen systems.[8] The normalized reference corrosion rate for type 347 stainless steel pins was 4 mpy under an oxygen atmosphere with batch DT-7, the base thoria containing no uranium. The corrosion rates expressed as multiplicative factors for the type 347 stainless steel toroid (different flow), Ti-75A and Zircaloy-2 were respectively 0.15, 0.5 and 0.15 relative to this.

The average effect of the deuterium atmosphere on these metals was to increase corrosion by a factor of 2. The effect of MoO_3 addition was trivial. With increasing uranium content, the corrosion of these metals was reduced by the following average factors:

0% U, 1.0; 5% U, 0.7; 9% U, 0.3; 11% U, 0.2; and 33% U, 0.08.

The normalized corrosion rate of Inconel under an oxygen atmosphere and with batch DT-7 thoria containing no uranium was 12 mpy. Under a deuterium atmosphere, it was reduced to 5 mpy. There was no particular effect produced by the uranium content on the corrosion of Inconel under an oxygen atmosphere, but under deuterium, the effect of increasing the uranium content roughly paralleled the effect given for other metals above. The attack on Inconel under oxygen atmosphere appeared to be dominated by water corrosion rather than by erosion.

According to chemical analysis, uranium was present in the supernatant liquid of most of the postrun slurries that had been circulated in oxygen atmosphere. Factors influencing the solubilization of uranium from thoria-urania are indicated to be worthy of more direct consideration than resulted from these studies because of the effect of uranium mobility on potential reactor operations.

Reduction of uranium by deuterium in the experiments was also suggested, in addition. Because the deuterium atmospheres were obtained by the flushing of the toroid rings with deuterium, one atmosphere or less of deuterium was charged to the toroid ring. Therefore it was possible

Table 12.5. Results of Toroid Tests with Slurries of Thorium-Uranium Oxides

Time, 300 hr
Velocity, 26 fps
Concentration, 500 g of Th-U per kg of D_2O
Temperature, 280°C
Calcination Temperature, 650°C
Base Thoria, DT-7

Per Cent U/Th	Atmosphere	Additive (0.008 *m* MoO_3)	Attack Rate* (mpy)					Slurry pH, Postrun	Concentration of Ions in Supernatant Liquid (ppm)			Average Particle Size (μ)	
			Toroid (347 SS)	347 SS	Ti-75A	Inconel	Zr-2		Cr^{+6}	U	Mo	Prerun	Postrun
None	O_2	No	1.1	5.4	6.0	20	2.7	7.1	<1	-	-	2.1	1.3
	O_2	Yes	1.0	2.6	1.7	7.3	0.9	7.0	10	-	<2	2.1	1.0
	D_2	No	7.6	38	11	5.8	2.6	8.8	1	-	-	2.1	2.5
	D_2	Yes	6.4	52	12	4.9	3.0	8.9	2	-	<2	2.1	2.5
5.3	O_2**	No	0.4	1.5	0.7	14	WG	5.0	1	5	-	1.3	1.3
	O_2	No	0.9	9.8	4.8	27	0.9	5.4	-	5	-	1.3	1.2
	O_2	Yes	2.7	12	3.1	29	0.3	5.6	-	-	-	1.3	1.5
	D_2	No	1.8	40	5.6	5.3	2.6	10.2	-	14	-	1.3	1.9
	D_2	Yes	1.4	25	12	3.2	4.3	10.3	-	7	-	1.3	5.8
8.7	O_2**	No	0.1	0.4	WG	13	WG	5.5	-	4	-	1.4	1.4
	O_2	No	1.6	11	3.7	27	0.2	5.5	-	<5	-	1.4	1.3
	O_2	Yes	0.1	2.0	0.6	34	0.2	6.8	-	<15	14	1.4	0.9
	D_2	No	0.4	3.2	5.0	2.3	1.4	9.4	-	-	-	1.4	0.7
	D_2	Yes	0.9	13	3.3	6.2	1.4	8.9	-	-	-	1.4	1.8
11	O_2**	No	0.1	0.4	WG	29	WG	6.0	7	177	-	1.3	1.4
	O_2	No	0.2	3.2	0.3	47	WG	6.6	-	14	-	1.3	1.0
	O_2	Yes	1.0	7.8	1.8	17	WG	5.1	13	95	-	1.3	1.2
	D_2	No	0.2	2.9	6.5	4.5	4.9	8.5	-	<15	-	1.3	2.4
	D_2	Yes	0.1	1.0	0.8	0.8	0.5	8.4	-	-	-	1.3	1.0
33	O_2**	No	1.5	0	WG	7.4	WG	4.7	8	4	-	1.7	1.0
	O_2	No	0.3	0.5	WG	4.3	WG	6.3	-	-	-	1.7	1.1
	O_2	Yes	0.1	2.3	WG	91	1.5	7.0	-	-	-	1.7	2.7
	D_2	No	0.2	1.1	1.4	0.2	WG	7.2	<1	<5	-	1.7	1.1
	D_2	Yes	0.9	0.2	WG	0.4	WG	6.8	-	-	-	1.7	0.8

*Corrected for slug flow.
**200 g Th-U per kg of D_2O.

Table 12.6. Factors in Attack by Thoria-Urania Slurries

Average effect of major variables expressed as multiplicative factors obtained by statistical analysis of data of Table 12.5.

Metal	Normalized Attack Rate				Average Effect* of Variables for Given Metal						
	O_2 Atmosphere*		D_2 Atmosphere**		Atmosphere (D_2 Relative to O_2)	MoO_3 (Relative to None Added)	Preparation (% U)				
	mpy	Relative to 347 SS	mpy	Relative to 347 SS			None	5.3	8.7	11	33
347 SS	4.3	1.0	6.3	1.0	1.47	1.07	1.0	1.43	0.42	0.22	0.06
Toroid (347 SS)	0.6	0.15	0.9	0.14	1.45	0.95	1.0	0.58	0.20	0.10	0.11
Ti-75A	1.8	0.42	3.8	0.59	2.05	0.71	1.0	0.52	0.41	0.28	0.05
Zircaloy-2	0.4	0.11	1.4	0.22	3.09	1.1	1.0	0.66	0.25	0.24	0.13
Inconel** under D_2 atmosphere:			5.2	0.82	(2.2)	0.98	1.0	0.78	0.63	0.32	0.05
Mean (geometrical) factor					2.0	0.96	1.0	0.74	0.35	0.22	0.07
Separately: Inconel* under O_2:	12	2.7	-	-	-	0.96	1.0	2.3	2.5	2.4	1.6

*Reference condition: O_2; no MoO_3; batch DT-7 - no uranium.

**Reference condition: D_2; no MoO_3; batch DT-7 - no uranium.

that the deuterium atmosphere was depleted in some tests because of the reduction of U^{+6}. In the original preparations, 75 to 90% of the uranium was in the hexavalent state, the lowest values being associated with the greatest total uranium content. The attack rates of specimens could have been affected by such reduction. By using the gas-addition device described in Sec. 12.2.4, atmospheres of known pressures can be charged to the toroid rings, which should enable the effect of atmosphere concentration to be evaluated experimentally.

The above results, generally showing a reduction in attack rate as uranium content is increased, indicate a different effect than was reported for pump-loop tests in Sec. 12.1.3, above. However, in the pump-loop experiments 15 μ rods of $UO_3 \cdot H_2O$ were added to thoria which had been calcined at 1600°C, and loop operation was at 200°C. In the toroid tests, the uranium was adsorbed on low-fired thoria from carbonate solutions, with final calcination at 650°C. The toroid tests were at 280°C. Thus the loops and toroids were operated with different materials at different temperatures.

No particular particle-degradation was noted in the toroid tests. On the other hand, the degradation of the $UO_3 \cdot H_2O$ rods (a transient phenomenon) in the loop tests may account for the increase in corrosion rate in the loops, as indicated in Sec. 12.1.3 above.

The levels of the attack in the respective loop and toroid tests appear to be largely a function of temperature. It has been demonstrated that the attack rates of most materials almost doubles with every 30-60°C increase in operating temperature.[9] When the attack rates from the loop and toroid tests using slurries containing approximately the same uranium concentrations are normalized to compensate for the effects of operating temperature and flow velocity, the data are found to be in good agreement.

12.2.3 Tests with Slurries of Thoria Prepared by Davison Chemical Company

In conjunction with a program of the Chemical Technology Division aimed at producing spheroidized thoria particles, toroid tests were conducted during the quarter with slurries of two experimental preparations of ThO_2 furnished by the Davison Chemical Company. The samples had been prepared by calcining $Th(OH)_4$ and $Th(C_2O_4)_2$, produced by controlled precipitation techniques, at 650°C. Portions of each preparation were recalcined at ORNL for 4 hr at 1000 and 1200°C.

Oxygenated aqueous slurries of each preparation were circulated at 280°C at 26 fps. The original 650°C-calcined preparations were circulated in 300-hr tests at slurry concentrations of 500 and 1000 g of Th per kg of H_2O. Slurries of the recalcined preparations were circulated in 100-hr tests at a concentration of 500 g of Th per kg of H_2O. Test data for the series and the results of the statistical analysis[7] of data for the tests using 650°C-calcined thoria are summarized in Table 12.7. Because negligible attack rates were observed in runs using the recalcined preparations, no statistical analysis of the data was made.

Table 12.7. Summary of Toroid Tests with Slurries of Thoria Prepared by the Davison Chemical Company

Velocity, 26 fps
Temperature, 280°C
Atmosphere, Oxygen

	Thoria Prepared from	Calcination Temperature (°C)	Concentration (g Th/kg H_2O)	Attack Rate[a] (mpy)					Postrun pH	Average Particle Size (μ)	
				Toroid (347 SS)	347 SS	Ti-75A	SA-212-B	Zr-2		Prerun	Postrun
A.	Oxalate	650	500	0.7	4.4	1.6	36	WG	7.2	0.8	0.5
	Oxalate	650	1000	1.6	14	33	37	6.7	-	0.8	0.7
	Hydroxide	650	500	0.7	1.1	WG	15	WG	7.0	11	18
	Hydroxide	650	1000	1.1	2.2	WG	30	0.6	7.6	11	17
B.	Oxalate	1000	500	2.1	WG	WG	60	WG	6.7	0.8	0.6
	Oxalate	1200	500	3.2	4.2	WG	32	WG	5.8	0.9	0.7
	Hydroxide	1000	500	1.6	WG	WG	46	WG	7.0	11	13
	Hydroxide	1200	500	1.1	WG	WG	40	WG	8.5	12	13

Average Effects of Major Variables for Given Metals from Part A, Expressed as Multiplicative Factors Obtained by Statistical Analysis

Metal	Normalized Attack Rate (reference condition)[b]		Effect of Variables for Metal Relative to Reference Condition	
	mpy	Relative to 347 SS	Hydroxide Relative to Oxalate	1000 g Th/kg H_2O Relative to 500 g Th/kg H_2O
347 SS	5	1.0	0.2	3
Toroid (347 SS)	0.8	0.2	0.8	2
Ti-75A	3	0.7	0.0[c]	5
SA-212-B	30	6	0.6	1.5
Zircaloy-2	0.3	0.1	0.3	15[c]

(a) Corrected for slug flow.
(b) Reference condition is oxalate preparation at 500 g of Th per kg of H_2O.
(c) Uncertain due to nil weight loss of some specimens in comparison.

The following generalized effects were noted. There was a substantial difference in the response of the various metals which was consistent with previous experience in the toroids. The attack of SA-212-B mild steel was primarily that of water corrosion and apparently was independent of slurry or slurry concentration. A significant difference between thoria preparations was noted with the oxalate preparation being more aggressive. The normalized rate for type 347 stainless steel of 5 mpy with the oxalate preparation was consistent with previous normalized rates ranging from 4-12 mpy in oxygen for slurries consisting of 500 g of Th per kg of H_2O.

The higher concentrations generally produced attack rates which, when normalized, were consistent with factors previously observed in the toroids.[8]

Prerun and postrun particle-size analyses indicated that the mean particle size of the oxalate preparations decreased during circulation. In contrast, the size of the hydroxide preparation increased during circulation.

Because most of the pin corrosion specimens exposed to slurries of all but the 650°C-oxalate preparation were covered with thin, adherent thoria films, reliable attack rates could not be computed for these pins from weight changes.

(a) Examination for Stress-Corrosion Cracking.--Analysis of the original oxalate and hydroxide preparations before the toroids were loaded indicated high levels of sulfate (~600 and 1000 ppm) and chloride (~15 and 36 ppm) contaminants. Therefore, stressed type 347 stainless steel corrosion pin specimens were used in the tests to determine if stress-corrosion cracking would occur. In a previous toroid test[10] made at 26 fps and 280°C, it was shown that stress-corrosion cracking occurred in about 70 hr with stressed type 347 stainless steel pin specimens exposed to oxygenated water which contained about 50 ppm chloride.

The pin specimens from one run in which 51 ppm chloride was detected in the slurry supernatant were submitted for metallographic examination, but no evidence of stress-corrosion cracking was found.

12.2.4 Toroid Gas-Addition Device

Tests were successfully completed during the report period with a device by which a known overpressure of a desired gas may be charged to a toroid. Heretofore an estimated overpressure of oxygen could be obtained in a toroid by the thermal decomposition of a calculated amount of hydrogen peroxide added to the slurry. However, where other gaseous atmospheres were used, the toroids were merely flushed (at atmospheric pressure) with the desired gas and then sealed.

The device is shown schematically in Fig. 12.2.

No additional opening in the toroid is required for the gas injection. One of the four specimen holders on the ring, which is normally a recessed cap, was replaced by a modified Parker fitting as shown in the sketch. The fitting, which seats in a cone seal, is bored axially and a vent hole bored radially through the threaded region. On the inner, coned end of the fitting a thimble to hold the corrosion pin specimen is welded. To the outer end a gas connection may be made. A Teflon washer provides a semitight shoulder seal between the fitting and the ring when the coned part is almost seated.

12.3 IN-PILE AUTOCLAVE SLURRY-CORROSION TESTS

12.3.1 Development, Construction, and Operation

Two HB-6-type rocking autoclave experiments, L6Z-127S and L6Z-129S, containing thorium oxide slurry were operated in beam hole HB-6 of the LITR to obtain radiation-corrosion data for slurries.

Experiment L6Z-127S[11] was removed from the reactor after operating in-pile for 1122 hr at 280°C. The autoclave was fabricated from Zircaloy-2 and contained six pin-type corrosion specimens: three of Zircaloy-2, two of type 347 stainless steel, and one of Inconel. The autoclave was loaded with dry thorium oxide coprecipitated with 5 wt % of enriched uranium, based on thorium, and D_2O was added to obtain a thorium oxide slurry having a nominal concentration of 400 g of Th per kg of D_2O. Molybdic oxide was added to catalyze the recombination of radiolytic gas. An initial oxygen overpressure of approximately 470 psia at 25°C was obtained by the addition of oxygen to the vapor space of the autoclave. The autoclave was operated in the out-of-pile mockup for approximately 174 hr at 280°C and 1090 psia oxygen partial pressure as a final test before insertion in the LITR.

Autoclave L6Z-129S, which was inserted in beam hole HB-6 of the LITR on January 6, 1959, and is still in operation, was also fabricated from Zircaloy-2 and contained six pin-type corrosion specimens of the following composition: two of Zircaloy-2, two of type 347 stainless steel, one of Inconel, and one of Croloy 2 1/4. The autoclave was loaded with thorium oxide containing 5 wt % enriched uranium, based on thorium, a Pd-ThO_2 catalyst for radiolytic gas recombination (130 ppm Pd based on total solids, or 0.0017 *m*), and D_2O dispersant to give a nominal composition of 1000 g of Th per kg of D_2O. An initial oxygen atmosphere of about 470 psia at 25°C was used. The autoclave was operated in the out-of-pile mockup facility for about 168 hr at 280°C and 940 psia oxygen partial pressure as a final test before insertion in the LITR.

12.3.2 Introduction to Autoclave Experiments

Operating results from L6Z-127S, an in-pile Zircaloy-2 autoclave slurry corrosion experiment at 280°C in the HB-6 facility of the LITR,

are presented below. The experiment contained the same 5 wt % enriched uranium thoria-urania preparation that was used in the previous experiment, L6Z-126S.[12] The autoclave was loaded to a concentration of 400 g of Th per kg of D_2O and 0.01 *m* MoO_3 with an oxygen overpressure. Maximum fission power density which could be achieved in this experiment was at least four times the maximum power density of the last oxygenated experiment, L6Z-122S. Studies of the catalytic recombination of the radiolytic gases and the G values for deuterium production were made during in-pile operation. The experiment operated out of pile for 174 hr and in pile at an average fission power density of 0.5 w/ml for 948 hr.

12.3.3 Recombination of Radiolytic Gases

Table 12.8 and Fig. 12.3 contain the results of 17 recombination experiments which were performed with L6Z-127S. Although potentially the experiment could have operated at a fission power density of 2.6 w/ml, assuming a flux of 0.5×10^{13} neutrons/cm^2-sec, the maximum fission power density achieved was limited by the generation of a safe level of radiolytic gas. Consequently, the distance to which the experiment could be inserted, using the screw mechanism described previously,[13] was varied during the course of the run to obtain the largest amount of irradiation possible without generating a quantity of radiolytic gas which would be in the explosive regions if both the heater to the autoclave failed and/or the rocking stopped.

Figure 12.4 shows the relationship of the relative intensity of the neutron flux and the distance of insertion of the autoclave in the HB-6 facility, based on a flux map reported by G. H. Jenks.[14] By using the relative intensity of the flux from this graph for the various distances of insertion and assuming that the neutron flux in the autoclave in the fully inserted position was 0.5×10^{13} neutrons/cm^2-sec, the fission power density at a particular position of insertion and the G_{D_2} value for a recombination experiment could be calculated. A current recalibration of the flux in beam hole HB-6 will apply to experiment L6Z-127S as well as earlier experiments L6Z-122S, -125S and -126S. However, the effective power density of the experiments is not expected to be substantially different from that used in computing the results given in this report.

Because of the number of unexplained pressure excursions observed in the previous experiment, L6Z-126S, pretreatment of the MoO_3 catalyst, as prescribed by the Chemical Technology Division, was carried out to minimize deactivation of the MoO_3. The pretreatment consisted of operation of the autoclave after it had been loaded with the thoria-urania, MoO_3, and D_2O at 280°C with an oxygen overpressure for 3 hr and then operation at 270°C with a deuterium overpressure for 2 hr. The deuterium was then replaced with oxygen, and the autoclave was operated for 174 hr out of pile.

Table 12.8. In-Pile Recombination of Radiolytic Gas in an Excess Oxygen Atmosphere, Experiment L6Z-127S

Conditions: 400 g of Th per kg of D_2O, 5% enriched uranium, based on thorium, 0.01 *m* MoO_3, 280°C, 850 to 1100 psi Excess O_2
3000 kw LITR, flux at 16-in. inserted = 0.5×10^{13} n/cm^2-sec (HB-6)

Time at Temperature (hr)	Duration of Radiation (hr)	Type of Experiment	Maximum Fission Power (w/ml)	D_2 (Equilibrium Pressure)	D_2 Production Rate (moles/l-hr)	Catalytic Activity (moles/l-hr at 100 psi D_2)	G_{D_2}
180	0	Reactor startup, retracted	0.2			0.034	
		Insertion					
193	1	0 in. ⟶ 4 in.	0.4	137	0.116	0.085	0.74
864	150	0 in. ⟶ 4 in.	0.4	119	0.155	0.130	0.98
		Retraction					
1048	174	4 in. ⟶ 0 in.	0.4	159	0.119	0.075	0.76
1098	182	4 in. ⟶ 0 in.	0.4	105	0.150	0.142	0.95
1106	183	4 in. ⟶ 0 in.	0.4	101	0.170	0.169	1.08
		Insertion					
293	19	0 in. ⟶ 8 in.	0.8	119	0.244	0.204	0.84
1007	169	0 in. ⟶ 8 in.	0.8	216	0.379	0.176	1.31
1057	175	0 in. ⟶ 8 in.	0.8	251	0.419	0.166	1.45
		Retraction					
478	67	10 1/2 in. ⟶ 0 in.	1.1	187	0.226	0.121	0.54
505	76	10 1/2 in. ⟶ 0 in.	1.1	210	0.200	0.096	0.48
598	102	10 1/2 in. ⟶ 0 in.	1.1	269	0.256	0.096	0.61
		Insertion					
289	18	0 in. ⟶ 12 in.	1.4	185	0.484	0.262	0.92
1103	182	0 in. ⟶ 12 in.	1.4	467	0.928	0.199	1.77
		Insertion					
430	48	0 in. ⟶ 14 in.	1.9	191	0.396	0.207	0.56
454	58	8 in. ⟶ 14 in.	1.9	248	0.346	0.140	0.49
		Retraction					
386	44	14 in. ⟶ 0 in.	1.9	204	0.306	0.150	0.43

On the first reactor startup with I6Z-127S, the experiment was operated completely retracted in order to establish a reference point for the generation of radiolytic gas. Thus, it was possible to determine the degree of insertion which could be safely carried out. After 9 hr of irradiation, 130 psi of radiolytic gas was generated, corresponding to a catalytic activity of 0.034 mole D_2/liter-hr at 100 psi D_2. Five hours after equilibrium had been established, which was at 193 hr of high-temperature operation, the autoclave was inserted 4 in. to an estimated fission power density of 0.4 w/ml. The catalytic activity as measured by this insertion had increased to 0.085 mole D_2/liter hr. During this period, the catalyst appeared to be slowly increasing in activity until a maximum of 0.262 mole D_2/liter-hr was reached at an insertion to 1.4 w/ml after 289 hr of operation. The catalytic activity then began to diminish, and after 500 hours had elapsed, the activity had dropped to 0.096 mole D_2/liter-hr as measured by a retraction experiment from 1.1 w/ml. Another 100 hr of operation was accumulated, with no apparent change in the catalytic activity. Thereafter, the catalytic activity appeared to increase, but the values became less consistent.

In this experiment, the G_{D_2} values also appeared to change with time. In the first 100 hr of in-pile operation, insertion experiments to three different power levels gave G_{D_2} values between 0.74 to 0.92. These values may be high because preliminary but unconfirmed results of the neutron flux in an autoclave in the HB-6 facility prior to the I6Z-127S experiment indicated that a flux of greater than the assumed 0.5×10^{13} neutrons/cm^2-sec was present. A higher flux value for a given observed production rate would give a lower G_{D_2} value.

After 386 hr of operation, retraction experiments from two power levels, 1.9 and 1.1 w/ml, and insertion experiments to 1.9 w/ml showed a drop in the G_{D_2} to between 0.43 and 0.61. As in the case with the catalytic activity in this experiment, after 600 hr of operation the G_{D_2} showed an upward trend with considerably less consistency in the values.

12.3.4 Effects of Time and Radiation on Generalized Corrosion Rates

In experiment I6Z-127S, generalized corrosion of the autoclave and contents were followed in the usual way:[15,16] observing the temperature and pressure of the autoclave at suitable times, especially at room temperatures during reactor shutdown.

Figure 12.5 presents the corrosion results for the experiment as estimated from a decrease in the oxygen pressure measured at 25°C during reactor shutdown periods. The solid points represent the experimental data. By use of a graphical-multiple correlation[17] technique, a separation of the time and the radiation effects are made.

The solid line represents the expression:

$$\text{mpy} = \frac{70}{\text{hr}} + \frac{580}{\text{hr}} \times (\text{w/ml}),$$

which appeared to fit the data best. It will be noted that, according to this equation, the radiation effect on corrosion diminishes as time increases. Expressions of similar form were used in evaluating the results of irradiations under a deuterium atmosphere. In the deuterium-atmosphere experiments, the expression was:[17]

$$\text{mpy} = \frac{20}{\text{hr}} + \frac{340}{\text{hr}} \times (\text{w/ml}).$$

Consequently, in the present experiment the effect of radiation appears to be about twice as great as when under deuterium atmosphere.

The dotted line in Fig. 12.5 represents the expression used to fit previous experiments under an oxygen atmosphere,[17]

$$\text{mpy} = \frac{75}{\text{hr}} + 1.2\ (\text{w/ml}),$$

and indicates reasonably good agreement between the present and previous experiments under an oxygen atmosphere.

12.4 IN-PILE SLURRY LOOP

12.4.1 Loop Development

Two test runs, 13 and 14, were made in the 5-gpm in-pile slurry development loop during the past quarter. Both runs were made in order to evaluate the effectiveness of sintered-metal filter units in preventing thorium oxide from entering and accumulating in the horizontal pressurizer, where the bulk fluid flow velocity is <0.01 ft/sec. As reported previously,[18,19] a sintered-metal filter unit, arranged in such a way that the slurry flow from a bypass line was directed into an annular space between the filter and its housing, effectively removed thorium oxide from the pressurizer feed stream. However, a partial loss of thorium oxide from the loop circulating stream resulted from the filter cake of thorium oxide deposited in this annular space.

In an attempt to eliminate this loss of thorium oxide from the circulating stream, the slurry flow through the sintered-metal filter unit, containing a 5-μ mean pore-size filter, was changed in such a way that the main stream slurry flow (~5 gpm) was through the center of the filter, 5/8-in. ID x 12 in. long. The filtrate flow was through the annular space between the filter and its housing and then to the pressurizer. It was felt that the relatively high fluid velocity of ~8 ft/sec past the inside surface of the filter would prevent buildup

and accumulation of a thorium oxide cake. The filter unit is shown in Fig. 12.6.

(a) First Run.--Run 13 in development loop L-4-24S was made with the loop arrangement shown in Fig. 12.7. The loop was charged, while operating, with three increments of thorium oxide from batch LO-40, calcined at 1600°C, resulting in an inventory concentration in the loop main stream of 580 g of Th per kg of H_2O.

The loop concentration from samples removed 20 and 40 hr after the slurry additions was 420 g of Th per kg of H_2O. At a loop operating time of 200 hr at 250°C, the thoria concentration in the loop main stream had decreased to 260 and at 300 hr to 25 g of Th per kg of H_2O. At this point the loop temperature was lowered to 95°C, which resulted in an increase in concentration to 320 g of Th per kg of H_2O. The loop was reheated to 250°C; after 75 hr, the concentration had decreased to <25 g of Th per kg of H_2O. The pressurizer feed-stream (filtrate) flow rate during the run was approximately 10 cc/sec (at a loop temperature of 250°C), as determined from a heat balance.

In order to determine the location of the noncirculating thorium oxide, radiographs were made of all loop components, with the exception of the pump, while the loop continued to operate at 250°C. The radiographs revealed that a substantial quantity of thorium oxide had settled in the pressurizer. Smaller quantities of thorium oxide were also seen in the loop core and in the annular space between the filter and its housing. Thus, slurry had passed through the filter into the pressurizer. The filter was removed and examined for evidence of mechanical failure. The filter appeared to be in good condition.

The essential difference between the filter unit used in runs 11 and 12, which prevented thorium oxide from entering the pressurizer, and the one used in run 13 was that the flow pattern allowed cake formation in the annulus of the unit used in runs 11 and 12. Consequently, the sintered-metal filter used in run 13 was fitted with a stainless steel inner liner containing a number of 0.002-in. perforations to provide an annular space of 0.060-in. width in which a filter cake could form. This filter unit is shown in Fig. 12.8. This unit satisfactorily filtered slurry containing 500 g of Th per kg of H_2O in tests at 25°C. The unit was then installed in loop L-4-24S for operation at 250°C without disturbing the filter cake formed in the annulus during the 25°C tests.

(b) Second Run.--Run 14, which followed, was charged with sufficient batch LO-40 thorium oxide slurry to produce a loop main-stream concentration of 600 g of Th per kg of H_2O. The loop main-stream temperature was 250°C with the pressurizer at 260°C. An oxygen overpressure of 150 psi in excess of pressurizer steam pressure was used.

During the first 190 hr of operation, the concentration of slurry in the loop main stream ranged between 200 and 450 g of Th per kg of H_2O, with no definite trend. Radiographs of the pressurizer after 190 hr of operation at 250°C showed it to be free of thorium oxide. The pressurizer feed-stream (filtrate) flow during the run was ~3 cc/sec, as determined from a heat balance. After 250 hr of operation at 250°C, at which time a loop slurry sample gave a concentration of 360 g of Th per kg of H_2O, the circulating-pump speed was increased by increasing the electrical frequency of the pump power supply from 60 to 80 cps in an attempt to pick up any thoria settled out in the loop components. This resulted in an estimated increase in the main-stream slurry flow velocity from 8 to 10 ft/sec. However, a sample taken 60 hr after increasing the pump speed gave a loop concentration of <25 g of Th per kg of H_2O. Radiographs of the loop showed that there was still no slurry in the pressurizer. Although a small quantity of thorium oxide had settled in the core region, it did not appear at all sufficient to account for the noncirculating amount. No increase in circulating concentration was noted when the pump speed was returned to 60 cps with the loop remaining at 250°C. One region of the loop which has not been checked for thorium oxide as yet is the rotor cavity of the canned motor pump.

(c) Conclusions.--Based on test runs 11, 12, 13, and 14, the following conclusions are drawn:

1. When the filter was arranged in such a way that a filter cake was built up and maintained on the filter surface, a clean separation of water from the slurry during 900 hr of operating time in runs 11, 12 and 14 was accomplished. No incident of thorium oxide of more than trace amounts entering the pressurizer was noted during these runs. There has been no evidence of plugging the filter. Loop operating temperatures ranged from 95 to 250°C with thorium oxide concentrations up to 500 g of Th per kg of H_2O.

2. The 5-μ mean pore-size filter used above did not effectively filter the slurry when operating at a temperature of 250°C and with slurry concentrations up to 500 g of Th per kg of H_2O during run 13 when no filter cake formed on the filter surface.

3. Pump operation during these tests has been satisfactory. The pump[20] is a 5-gpm canned-rotor type fitted with aluminum oxide bearings and journal bushings, as used in the solution in-pile loops. The rotor and bearing region has not been purged to prevent thoria from entering the bearing region.

4. Thoria circulating-inventory losses other than in the pressurizer remain a problem and appear, according to recent evidence, to be associated with the pump cavity and the core region.

REFERENCES

1. E. L. Compere et al., HRP Quar. Prog. Rep. Oct. 31, 1958, ORNL-2654, p 125-126.

2. H. C. Savage et al., HRP Quar. Prog. Rep. Oct. 31, 1958, ORNL-2654, p 124-125.

3. A. S. Kitzes and R. N. Lyon, Aqueous Uranium and Thorium Slurries: Proc. ICPUAE, Vol. 9, Session 20B, P/811, p 414.

4. J. O. Blomeke, The Preparation of γ-$UO_3 \cdot H_2O$ from Uranyl Nitrate, ORNL CF-51-12-67.

5. J. P. McBride and D. G. Thomas, in Fluid Fuel Reactors, p 137-139, ed. by J. A. Lane et al., Addison-Wesley, Reading, Mass., 1958.

6. R. L. Pearson et al., HRP Quar. Prog. Rep. Oct. 31, 1958, ORNL-2654, p 213-214.

7. E. L. Compere, Factor Analysis of Corrosion Data Using Logarithmic Transformation, ORNL CF-58-9-3.

8. E. L. Compere et al., HRP Prog. Rep. for Qtrs. Ending April 30 and July 31, 1958, ORNL-2561, p 180.

9. E. L. Compere, in Fluid Fuel Reactors, p 261, ed. by J. A. Lane et al., Addison-Wesley, Reading, Mass., 1958.

10. L. Rice et al., Summary of Toroid Run 258, ORNL CF-58-10-79.

11. H. C. Savage et al., HRP Quar. Prog. Rep. Oct. 31, 1958, ORNL-2654, p 133-140.

12. E. L. Compere et al., HRP Quar. Prog. Rep. Oct. 31, 1958, ORNL-2654, p 133.

13. E. L. Compere et al., HRP Prog. Rep. for Qtrs. Ending April 30 and July 31, 1958, ORNL-2561, p 193.

14. G. H. Jenks et al., HRP Quar. Prog. Rep. Oct. 31, 1957, ORNL-2432, p 128.

15. E. L. Compere et al., HRP Quar. Prog. Rep. Jan. 31, 1958, ORNL-2493, p 113.

16. K. S. Warren and R. J. Davis, In-Reactor Autoclave Corrosion Studies - LITR I - Outlines of Methods and Procedures, ORNL CF-57-5-110.

17. E. L. Compere et al., HRP Prog. Rep. for Qtrs. Ending April 30 and July 31, 1958, ORNL-2561, p 195.

18. H. C. Savage et al., HRP Quar. Prog. Rep. Oct. 31, 1958, ORNL-2654, p 140-141.

19. D. T. Jones and J. M. Baker, Thorium Oxide Slurry Filtration: Preliminary Tests of a 3-Micron Poroloy Sintered Filter; Runs 11, 12 and 13 in Loop L-4-24S, ORNL CF-59-1-49.

20. H. C. Savage, Sintered Alumina as a Pump Bearing and Journal Material, ORNL CF-57-11-122.

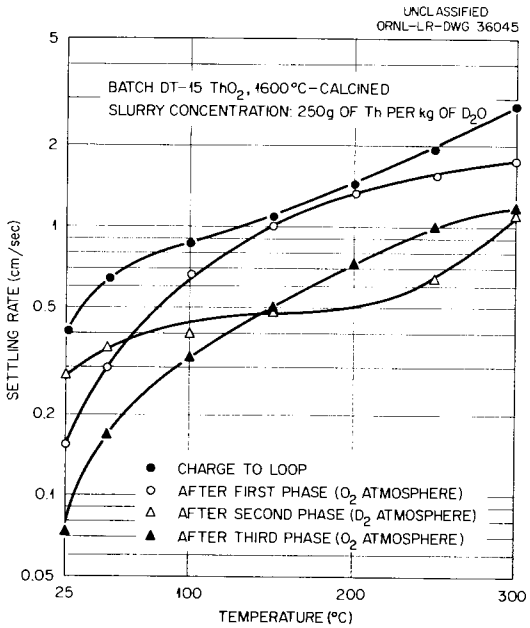

Fig. 12.1. Settling Rates of Slurry Circulated in Loop Test, BS-24.

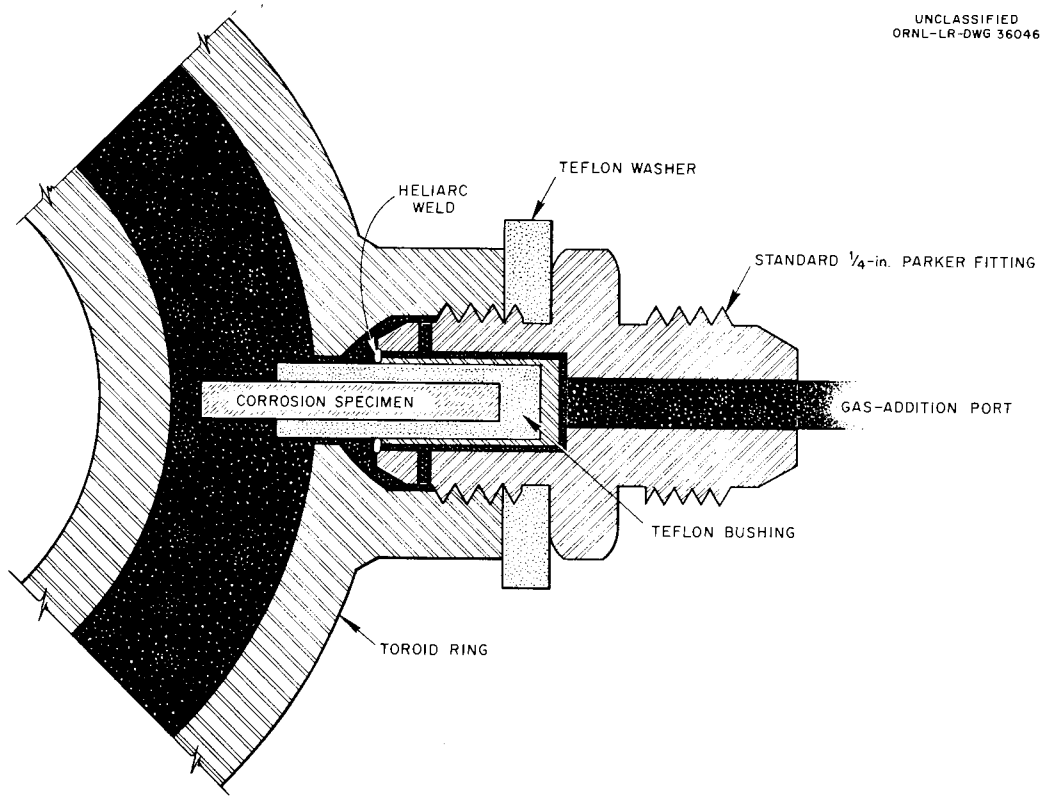

Fig. 12.2. Toroid Gas-Addition Device.

UNCLASSIFIED
ORNL-LR-DWG 36047

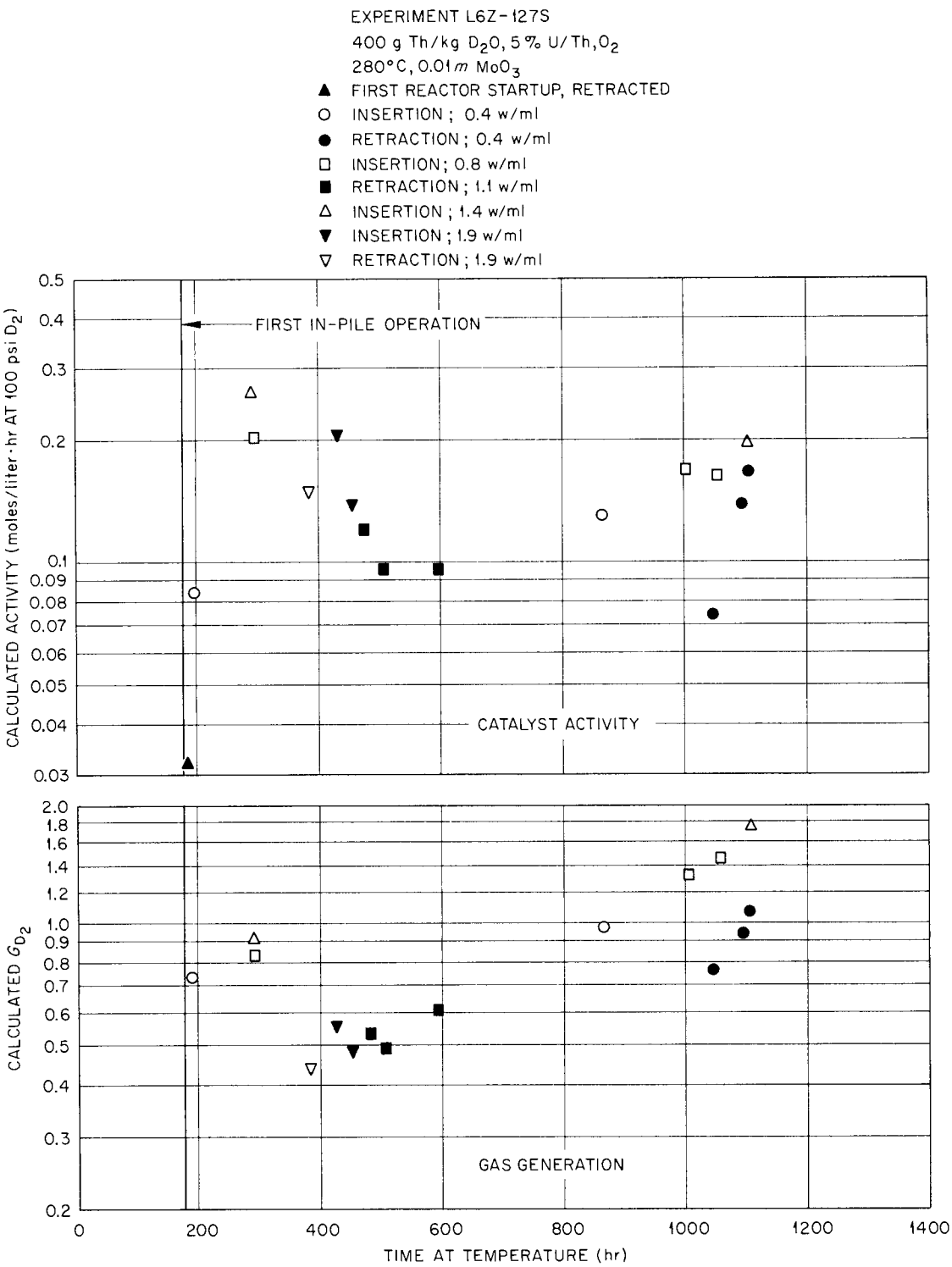

Fig. 12.3. Radiolytic Gas Phenomena During In-Pile Slurry Autoclave Experiment L6Z-127S.

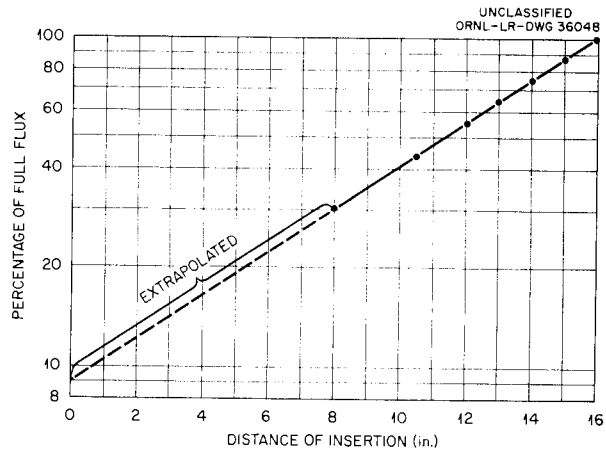

Fig. 12.4. Comparison of Relative Flux and Distance of Insertion, LITR Beam Hole HB-6.

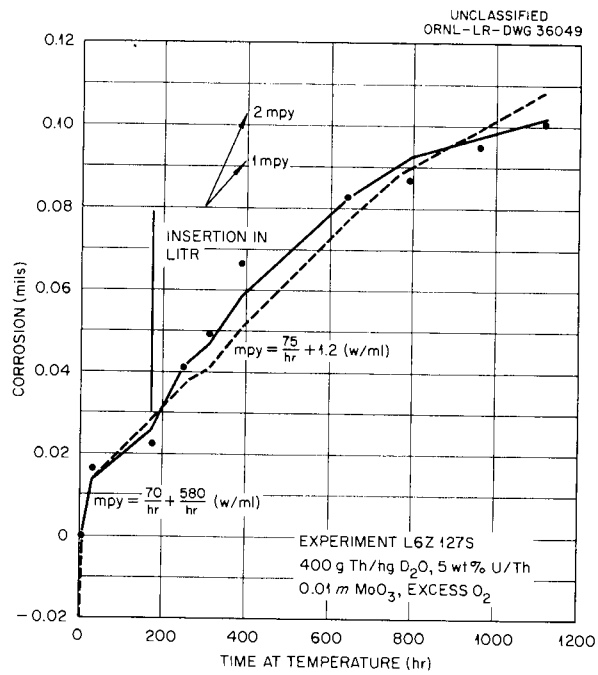

Fig. 12.5. Effect of Time and Radiation on Zircaloy Corrosion Under Oxygen Atmosphere.

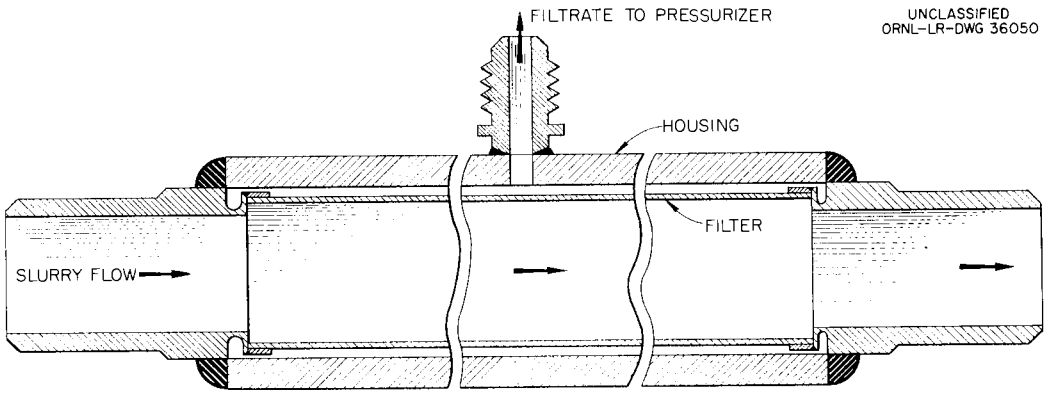

Fig. 12.6. Sintered-Metal Filter Unit Arranged for Slurry Flow Through Center.

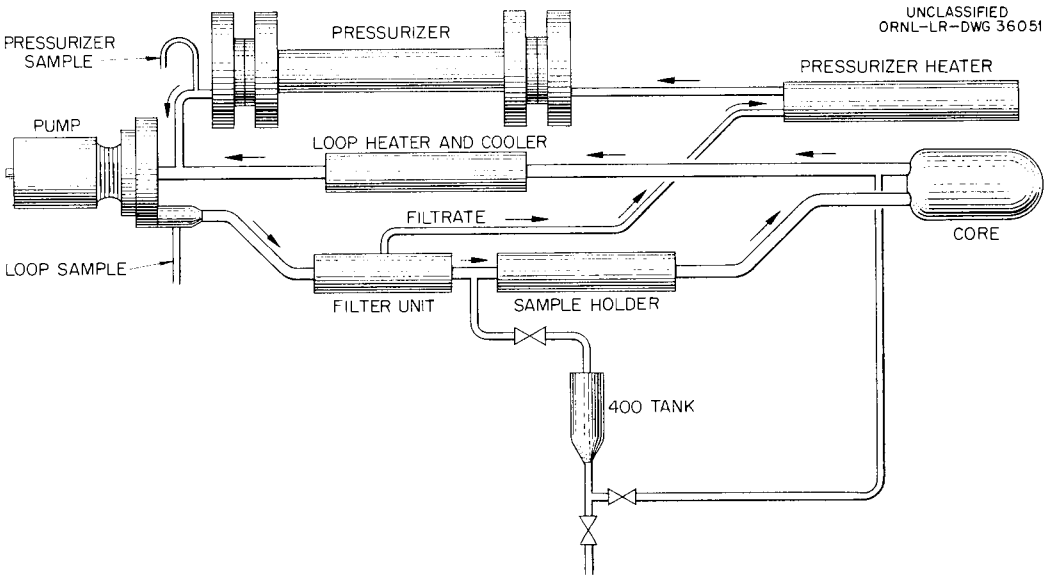

Fig. 12.7. Loop L-4-24S with Filter Unit for Run 13.

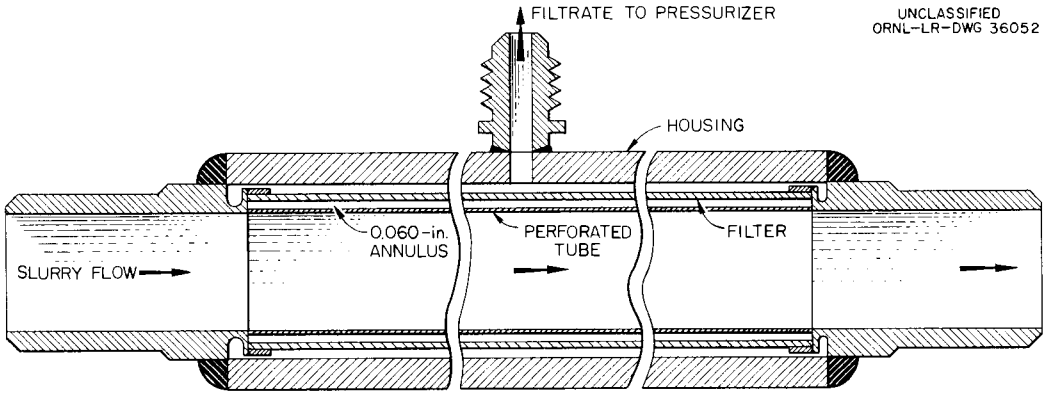

Fig. 12.8. Sintered-Metal Filter Unit Arranged for Slurry Flow Through Center, with Perforated Liner Added.

13. RADIATION CORROSION

G. H. Jenks H. C. Savage

A. L. Bacarella
J. E. Baker
S. J. Ball
J. C. Banter
S. E. Bolt
R. J. Davis
V. A. DeCarlo
D. T. Jones
R. A. Lorenz
A. R. Olsen
A. J. Shor
M. D. Silverman
W. C. Ulrich
K. S. Warren
S. H. Wheeler
W. C. Yee

13.1 IN-PILE LOOPS

13.1.1 Development and Construction

(a) HB-2 Loop Package.--Insertion of loop L-2-23 in the LITR has been delayed pending completion of special out-of-pile tests in which this loop is being used (see Sec. 11.1.1).

(b) ORR Loop Package.--Assembly of the first ORR in-pile loop, designated O-1-25, is continuing. The individual components of the loop, including the corrosion specimens and core, have been completed. As a result of out-of-pile tests on a mockup loop,[1] only minor changes to the loop package were found necessary. The ORR loop package has been described in previous reports.[1,2]

(c) ORR Beam Hole HN-1.--Installation of all equipment and shielding for loop operation in beam hole HN-1 of the ORR has been completed. The instrument panels are being connected. Test operation with a mockup loop is required before installation and operation of the first in-pile loop.

13.1.2 Effect of Overpressure and Other Variables on Deposition of Uranium in In-Pile Loop Core

(a) Introduction.--As reported by Beall and coworkers,[3] the HRT fuel solution has proved unstable toward the loss of uranium and other metal ions from the circulating solution when the reactor is operating at power. The change in the solution is power dependent and reversible since the separated components are redissolved at lowered reactor power. The instability effect is not very sensitive

to operating temperature in the investigated range of 240 to 280°C. Criticality measurements show that some of the noncirculating uranium is in the reactor core.

Griess and coworkers,[4] by use of an out-of-pile loop and a solution similar to that in the HRT, have produced instability effects in the solution which are similar, in some respects at least, to those in the HRT. The metal ions in the solution, uranium, copper, and nickel, were concentrated in a heated section of the circulating system in which the solution flow velocity was 0.2 fps, a velocity near that in the core of the HRT.

Several different mechanisms have been proposed to account for the instability in the reactor and in the loop tests. One hypothesis, speculative in nature, which was investigated in the present work with an in-pile loop, is, in general terms, the following: Metal surfaces in the reactor core are heated above the temperature of bulk solution by an amount sufficient to cause boiling at the surface. The boiling results in a deposition of UO_2SO_4 and other salts on the surface, and the deposited material produces still higher temperatures which accelerate further deposition. The temperature at which boiling occurs is less than the temperature at which the vapor pressure of heavy water equals the total pressure on the system because part or all of the pressure of dissolved gases is included in the vapor pressure of the solution. This condition is included in the hypothesis to account for the small effect of reactor operating temperature on the instability. The pressure of dissolved radiolytic gas at a given reactor power increases with decreasing temperature, and this increase may about offset any decrease in D_2O pressure with decreasing operating temperature.

The investigation reported here included some scouting type experiments carried out to determine whether deposition of UO_2SO_4 in the core of an in-pile loop could be produced at low overpressure under conditions in which the solution flow rate was similar to that in Griess' studies, and in which the temperature of some surface in the core was greater than that of the bulk solution. After deposition was observed in the initial experiments, additional experiments were made to define the pressure conditions at which the effect occurred. One experiment was made to test the effect on the deposition of a higher flow rate in the core. Other experiments were made to test the effect of solution composition on the deposition. The effect of changes in operating variables on the resolution of the deposited uranium was tested in each experiment in which deposition occurred; the variables thus tested included reductions in reactor power, increases in overpressure, and increases in solution flow rate.

(b) Equipment and Solutions.--Loop L-2-22, constructed of stainless steel, was employed for this investigation. Prior to its use for this purpose, the loop had operated in-pile for 1947 hr with a solution 0.036 m UO_2SO_4, 0.002 m $CuSO_4$, 0.18 m Li_2SO_4, and 0.09 m H_2SO_4 in D_2O, at main-stream and pressurizer temperatures of 280 and 295°C, respectively.

Solutions of three different compositions, listed in Table 13.1, were tested for stability. Solution 1 was converted into solution 2 in the loop by the addition of H_2SO_4. All solutions were in D_2O solvent.

Table 13.1. Solutions Employed in Stability Tests

Solution No.	Constituent (m)			
	UO_2SO_4	$CuSO_4$	Li_2SO_4	H_2SO_4
1	0.036	0.006		0.016
2	0.036	0.006		0.027
3	0.036	0.0014	0.18	0.09

Normal operating conditions with each solution included main-stream and pressurizer temperatures of 280 and 295°C, respectively, and a pump frequency of 60 cps. The main-stream temperature was held constant at 280°C at the core inlet for all experiments. Heating in the core wall at the nose end due to absorption of nuclear radiations was at the rate of about 0.4 w/g and was sufficient to establish the specified test condition of a metal-surface temperature greater than the temperature of the bulk solution.

(c) Methods.--The general method of carrying out the tests was as follows: Starting from normal operating conditions, the test flow rate in the core was established, and the overpressure on the system was then reduced. At the low overpressures, evidence was sought for an increase in the amount of fission power in the core. When an increase was detected, the overpressure was held constant for a time to permit measurements of the amount and rate of increase of fission power and, in several experiments, to permit sampling the loop solution while the fission power was high. Tests of methods of redissolving excess uranium in the core completed the experiment.

The average flow rate in the core annulus was about 0.3 fps in all experiments except one. This velocity was obtained by operating the pump at 20 cps. For the one experiment, the pump was operated at the normal 60 cps, and the velocity in the core annulus was about 0.8 fps.

The overpressure was varied by changing the pressurizer temperature.

Changes in fission power in the core were detected and measured by

measuring changes in the power required by the loop heater in maintaining the main-stream temperature at 280°C. The temperature of the outer surface of the core nose, as indicated by thermocouples at that location, was also measured to determine possible changes in temperature at the inner surface with uranium deposition.

Solution samples were withdrawn from a portion of the circulating stream outside the core.

In evaluating the results of the experiments, with respect to their significance to the boiling-deposition hypothesis, it is necessary to have estimates of the vapor pressure of the solution in the core including the pressures of D_2O and of dissolved radiolytic gas and excess oxygen. The D_2O pressure is, of course, determined by the solution temperatures in the core, and the dissolved-gas pressures are also dependent upon the temperatures. The method of obtaining the temperatures is outlined in Fig. 13.1, which includes a sketch of the core. In the sketch, A and B indicate the outer and inner surface of the core nose, respectively. Point C indicates the bulk solution which is about to enter the tapered-channel coupon holder and leave the core. It is assumed that liquid at C is at the highest temperature attained by bulk liquid in the core.

In calculating the vapor pressure of dissolved excess oxygen, it was assumed that the oxygen concentration in the main stream was uniform and equal to the concentration in the pressurizer liquid. The latter was determined from the pressure of excess oxygen obtained, with the reactor down, as the difference between the total pressure and the D_2O pressure at the measured temperature. The vapor pressure of oxygen and the concentration were related through solubility constants estimated from Battelle Memorial Institute[5] data. The estimated constants are listed in Table 13.2.

Table 13.2. Solubility Constants Employed in Relating Dissolved-Gas Pressure and Concentration

Solution No.	Gas	Solubility Constant at the Indicated Temperatures $\left(\frac{\text{psi, liter of solution at } 4^\circ\text{C}}{\text{cc gas (STP)}}\right)$	
		280°C*	295°C*
1 and 2	O_2	0.223	0.185
	H_2	0.214	0.179
3	O_2	0.252	0.209
	H_2	0.282	0.234

* Variation of solubility constant with temperature between 280 and 295°C assumed to be linear.

The method of estimating the radiolytic-gas concentration in the core solution will not be described fully in this report. It may be noted, however, that the concentration is estimated from the pressure of radiolytic gas in the pressurizer, the recombination rate constant in the loop, and flow characteristics of the loop. The recombination rate constant is estimated from the pressure in the pressurizer, the flow characteristics, and the estimated rate of radiolytic-gas generation in the loop solution. Solubility constants employed with the radiolytic-gas estimates are those listed in Table 13.2.

(d) Procedure and Results.--Thirteen "stability" experiments were carried out in which loop operating conditions differed from the normal. In all but two of these, the pressurizer temperature was lowered from the normal 295°C during the experiment. The pump frequency was 20 cps in all experiments but one, in which the frequency was 60 cps. In addition to the stability experiments there were periods of normal operation with each solution. The LITR was at full power for all experiments.

The general procedure followed and the results obtained in the experiments in which the overpressure was lowered were as follows: With the pump at 20 cps, the pressurizer temperature was lowered from the normal 295°C, sometimes several degrees at a time and at other times in one-degree steps, with some given period of operation at each pressurizer temperature. At some reduced overpressure, the temperature indicated by each of the two thermocouples attached to the core nose started to rise. At the same time, the electrical power required by the loop heater to maintain the 280°C main-stream temperature started to drop. When the change was initiated, the nose temperature and loop power continued to change until some corrective action was taken. In many of the experiments the temperature indicated by the core-nose thermocouples decreased by about 0.5°C prior to the rise in temperature and to the decrease in loop heater power. The final corrective action taken in nearly all experiments was a reduction in the LITR power.

No evidence of increased fission power was noted in the experiment at the pump frequency of 60 cps.

In the following discussion, the increase in fission power will be regarded as due to an increase in uranium concentration in the core and will be called the "concentration effect."

Data for each of the stability tests are summarized in Table 13.3. "Hours of circulation before test" signifies the total time during which solution was circulated in-pile in the loop prior to the test. Temperature and pressure conditions at the time the concentration effect was initiated are listed for the pressurizer, the liquid in contact with the inner surface of the core nose, and the bulk liquid in the core at point C (Fig. 13.1). Where no concentration effect

occurred, the temperature and pressure conditions are those for the lowest pressurizer temperature tested in the experiment (the methods of estimating temperature and pressure conditions were described previously). The maximum increase in fission power and the maximum increase in temperature indicated by one core-nose thermocouple, which were observed in a given test prior to the application of corrective action, are shown in the bottom lines. The initial decrease in core-nose temperature, where observed, is also listed.

The results of measurements of loop-heater power during excursions with the first and third solutions are shown in Figs. 13.2 and 13.3, respectively. The estimated fission power in the core under normal conditions was 515 w. As noted in these graphs a test of the effect of raising the pressurizer temperature during the power excursion was made in each experiment. The increase was usually to the normal 295°C, but a temperature of 298°C was tested in one experiment. In experiment No. 9, a 0.5°C change was made. None of these pressurizer changes produced any significant effect upon the increase in fission energy. The flow velocity through the core was increased by increasing the pump frequency during experiments 10B and 11. In each case, the increase in flow rate resulted in a return of the fission power to the normal value, over a period of a few minutes, before any change in corrective action was taken. The reactor power was reduced a few minutes after this occurrence. In all experiments except 10B, 11, and 9, a reduction in reactor power was employed to eliminate the concentration of uranium in the core. After the reactor power was reduced or after the pump frequency was changed, no accurate measurements could be made of the fission power in the core.

The results of analyses of solution samples taken during operation with the first and second solutions are shown graphically in Fig. 13.4; those for the third solution are shown in Fig. 13.5. The pump frequencies and the reactor power levels employed during the experiments are shown in these graphs. Samples 32, 36, 44, and 45 were withdrawn during the power excursions in experiments 2, 7, 10B, and 11, respectively.

Experiment 5 was carried out to determine the effect of increased gas pressure on the concentration effect. Sufficient oxygen was added to increase the oxygen pressure in the pressurizer to 134 psi or a pressure 79 psi greater than that employed in a previous experiment, No. 3. The procedure followed in lowering the pressurizer pressure was the same in experiments 5 and 3. The power excursion in experiment 5 was initiated at a pressurizer pressure 97 psi greater than that in experiment 3. In experiment 6, with the pump frequency at 20 cps and the pressurizer temperature at the normal 295°C, a power excursion gradually developed after 8 hr of operation. The reactor was shut down after the excursion developed, and the pump frequency was raised to 35 cps. Operation of the

Table 13.3. Test Conditions and Results for Uranium-Deposition Experiments

	Solution No. 1							Solution No. 2	Solution No. 3				
	No Concentration, 40 hr of Operation	Pressurizer Temperature Lowered 1°C Every 10 min	Pressurizer Temperature Lowered 4°C, Rapidly	Pressurizer Temperature Lowered 1°C Every 80 min	No Concentration; 60 cps	High Oxygen; Pressurizer Temperature Lowered 1°C Every 80 min	Walk-Away; Concentration After 8 hr at Normal Temperature, 20 cps	High Acid; Pressurizer Temperature Lowered 1°C Every 60 min	No Concentration; Pressurizer Temperature Lowered 1°C Every 30 min; Held at 288.4°C for 70 min	Fission Power Drop; Pressurizer Temperature Lowered 7°C ,Rapidly	No Concentration; 8 hr of Operation	Pressurizer Temperature Lowered Slowly; "Recovery" at 60 cps	Pressurizer Temperature Lowered Rapidly; "Recovery" at 30 cps
Test number	1A	1B	2	3	4	5	6	7	8	9	10A	10B	11
Date	10-24-58	10-27-58	10-28-58	10-29-58	10-30-58	10-31-58	11-2-58	11-4-58	11-6-58	11-7-58	11-10-58	11-13-58	11-14-58
Hours of circulation before test	2080	2170	2190	2210	2240	2260	2320	2355	2395	2415	2495	2560	2580
Pump frequency, cps	20	20	20	20	60	20	20	20	20	20	20	20	20
Pressurizer conditions													
Temperature, °C	295.3	289.3	291.2	292.2	285.5	293.3	295.3	293.3	288.4	288.4	293.3	287.6	288.2
Vapor pressure, psi	1179	1081	1094	1128	1021	1146	1179	1146	1066	1066	1146	1054	1063
Radiolytic gas, psi	13	14	14	14	24	14	14	14	24	24	33	42	33
Oxygen, psi	83	67	60	55	59	134	127	108	57	57	77	74	115
Total pressure, psi	1275	1162	1168	1197	1104	1294	1320	1268	1147	1147	1256	1170	1211
Core-nose conditions													
Temperature, °C	287.6	288.4	288.4	288.4	283.3	288.4	288.4	288.4	288.4	288.4	288.4	288.4	288.4
Vapor pressure, psi	1053	1066	1066	1066	988	1066	1066	1066	1066	1066	1066	1066	1066
Radiolytic gas, psi	72	77	77	77	69	77	77	77	138	138	138	138	138
Oxygen, psi	95	68	61	57	60	143	139	115	57	57	82	73	114
Total pressure, psi	1220	1211	1204	1200	1117	1286	1282	1258	1261	1261	1286	1277	1318
Bulk-solution conditions													
Temperature, °C	282.2	282.4	282.4	282.4	280.8	282.4	282.4	282.4	282.4	282.4	282.4	282.4	282.4
Vapor pressure, psi	972	976	976	976	952	976	976	976	976	976	976	976	976
Radiolytic gas, psi	77	84	84	84	71	84	84	84	150	150	150	157	150
Oxygen, psi	100	73	66	62	62	153	149	123	61	61	88	78	123
Total pressure, psi	1149	1133	1226	1122	1085	1213	1209	1183	1187	1187	1214	1211	1249
Maximum decrease in loop-heater power before corrective action	0	500	700	500	0	400	250	400	0	150	0	200	200
Observed decrease in temperature on core-nose couple No. 2		(−0.5)	(−0.5)	(−0.6)	(−0.5)				(−0.5)	(−0.5)		(−0.4)	
Maximum temperature rise in core-nose couple No. 2	0	3.5	4.0	1.6	0	1.8	1.6	2.9	0	0.9	0	1.3	1.3

reactor was resumed, and no evidence of concentration was observed during the 14 hr of operation at 35 cps.

(e) Discussion of Results.--(1) Deposition of Uranium and Other Solutes in the Core.--The occurrence of power excursions as measured by the loop heater power and core-nose thermocouples demonstrates that the amount of uranium in the core was greater during the excursions than under normal conditions. No other explanation appears likely. The amount of decrease in loop heater power is regarded as approximately equivalent to the amount of increase of fission power. Comparison of values for the core-nose temperature rise and for the decrease in loop heater power in a given experiment show that the increase in core-nose temperature due to the increased fission power is greater than the calculated increase in solution temperature in the core. This result shows that some of the deposited uranium was on the core wall at the nose end.

The results of analyses of solution samples show that uranium and other solutes were lost from the solution circulating outside the core during the power excursions. The uranium concentration in each of the four samples taken during excursions was significantly lower than that of samples taken during periods of normal fission power. The excursion samples of the first and second solution were also low in sulfate, copper, nickel, and manganese. No significant change in free acid was observed in either of these two samples. However, the analytical results for free acid in these solutions showed considerable scatter, and an appreciable change in acid, if present, would be masked by the scatter. The two excursion samples taken with the third solution showed a loss of nickel in addition to uranium, but for the other constituents there was no change which was outside the appreciable scatter of the analytical results for samples taken under normal power conditions.

(2) Calculated Values of Temperature and Pressure in the Core Solution.--The calculated temperature values for solution in contact with the core nose and for the bulk solution are estimated to have a probable error of $\pm$ 1°C. Most of this error is due to estimated uncertainties in the ratio of the film heat transfer coefficient at the pump frequencies of 60 and 20 cps. The estimated probable error in the value of 280°C for t_D (Fig. 13.1) is $\pm$ 0.5°C. The estimated value of 0.5 w/cm^2 for the constant, w, is considered reliable; but, in any case, this constant may differ appreciably from 0.5 and have little effect on the calculated temperatures. The value of -4.9 for (t_A60U-t_A20U) has an estimated probable error of $\pm$ 0.2°C. The estimated probable error of values for total pressure in the core solution is $\pm$ 25 psi for the first and second solutions, and $\pm$ 45 psi for the third solution. These are rough estimates which include the estimated probable errors in the D_2O and radiolytic gas pressures. The values for the pressure of excess oxygen are considered to have negligible error.

(3) General Discussion of Results.--The pressure data for the

first and second solutions show that the power excursions at 20 cps were generally initiated when the calculated total vapor pressure of solution in contact with the surface of the core nose was about the same or greater than the total pressure on the solution. The total vapor pressure of bulk solution in the core was less than that in the pressurizer in each experiment with these solutions. The results show that an appreciable length of time was required for an excursion to develop when the pressure of the core nose solution was about the same as that in the pressurizer. The results of experiment 6 in which the excursion developed after 8 hr of operation are an extreme example of this delay. Actually, in this experiment, the calculated pressure in solution was 38 psi less than that in the pressurizer at the time the excursion developed, and, based on the estimated probable error of the pressure values, these results are an exception to the above generalization. For comparison with the result of experiment 6, no deposition was observed in experiment 1A, which operated for 40 hr with the pressurizer pressure 55 psi greater than the pressure in the core solution.

No deposition was observed in experiment 4, at 60 cps, but the test was not very severe since the pressurizer pressure was only 13 psi less than the calculated vapor pressure at the core nose and was 19 psi greater than the vapor pressure in the bulk solution.

The effect of dissolved oxygen on the deposition in the core is illustrated by the results of experiments 3 and 5, which were similar experiments except that the oxygen pressure in experiment 5 was about 2.5 times greater than that in experiment 3. The pressures at which deposition commenced in the two experiments show that the added oxygen did not effectively increase the overpressure or, conversely, that the additional pressure in the core solution due to the additional dissolved oxygen counterbalanced the increase in pressure in the pressurizer.

The results obtained with the single excursion experiment with solution 2 in comparison with the results of excursion experiments in solution 1 indicate that the addition of acid to solution 1 had no appreciable effect on the deposition phenomenon.

With solution 3, which contained Li_2SO_4 and H_2SO_4 additives, the power excursions occurred when the total pressure in the bulk core solution exceeded that in the pressurizer by about 40 psi. They did not occur when the calculated pressure of the solution in contact with the core nose was greater than that in the pressurizer. The probable error of the calculated pressures is greater for this solution than for solutions 1 and 2. However, it is very unlikely that the calculated values are high by 100 psi or more, that is, by the amount by which the vapor pressure of core-nose solution exceeded the pressurizer pressure when the power excursions developed.

The slight drop in core-nose temperature which was observed in several experiments as the pressurizer pressure was reduced shows that a change occurred in the film heat transfer coefficient due to the reduced pressure. This change is ascribed to boiling in the film. It is instructive that a drop in core-nose temperature was observed in experiment 4 at 60 cps and in experiment 8. No power excursion occurred in these experiments, but the pressure relationships in each were such that the steam-gas bubbles could exist in the core-nose solution.

In general, the results obtained with solutions 1 and 2 are consistent with the hypothesis that boiling in the liquid film covering the core-nose surface resulted in the deposition of solids including uranium on that surface. The results also show that this boiling occurs when the total pressure of the solution including all of the pressure of dissolved gas is about the same as the pressure on the solution. The results with solution 3 (lithium additive) are also consistent with the hypothesis that boiling in the core solution resulted in uranium deposition. However, the greater reduction in overpressure required to produce the deposition and also to produce a reduction in the temperature of the outer wall of the core nose indicates that boiling does not occur so readily in this solution as in solution 1. It is possible that only a fraction of the total pressure of dissolved gas is effective in initiating bubbles in this solution.

13.2 IN-PILE ROCKING-AUTOCLAVE TESTS--LITR

The assembly and operation of HB-5 rocking autoclaves for solution radiation-corrosion studies in beam hole HB-5 of the LITR continued. Three experiments, L53T-138, L51Z-144, and L52T-145, were assembled and were operated in the LITR during the period covered by this report. In addition, two out-of-pile control experiments, L53Z-135B and L52Z-136B, were assembled and operated in the mockup facility.

Autoclave L53T-138 was operated in the HB-5 hole of the LITR for 760 hr without incident, but, upon removal from the reactor, it was found that the capillary tubing connecting the autoclave to the Baldwin pressure-measuring cell had become plugged. A plug in this capillary tubing was also formed during pretreatment operations in the out-of-pile mockup facility. The experiment was disassembled, cleaned, and pretreated again before it was inserted in the LITR. No plugging was observed after the second pretreatment. The autoclave was made of titanium and contained three type 347 stainless steel and three Zircaloy-2 corrosion coupons.

Experiment L51Z-144, which contained a small amount (0.97 g) of hydrous TiO_2 as an additive to the uranyl sulfate fuel solution, operated for 830 hr in the HB-5 beam hole of the LITR without difficulty.

Autoclave L52T-145 contained a special, sealed, pin-type corrosion specimen of Zircaloy-2 which was filled with enriched UO_2 to give a hot metal surface during reactor exposure in order to produce boiling of the fuel solution. The effect of boiling on the corrosion of Zircaloy-2 in the presence of reactor radiation was to be noted. This experiment operated 897 hr in the LITR.

Experiments L53Z-135B and L52Z-136B were out-of-pile controls of experiments L53Z-135 and L52Z-136 which were operated in the HB-5 facility of the LITR.[6] Experiments 135 and 135B were designed to study the type and character of oxide film formed on Zircaloy-2 during the initial period of exposure to uranyl sulfate fuel solution in-pile. For this purpose, experiment 135 was operated at 280°C for only 1 hr in-pile following out-of-pile test and pretreatment. The Zircaloy-2 corrosion specimens are to be examined visually for the comparison of their corrosion films with those of coupons in experiment 135B, which were subjected to out-of-pile test and pretreatment only. Experiments 136 and 136B were designed to study the effect on Zircaloy-2 corrosion produced by a uranyl sulfate solution (0.15 m UO_2SO_4, 0.13 m $CuSO_4$ in D_2O) when operated at a temperature (320°C) above the two liquid-phase temperature.

13.3 SUPPORTING RESEARCH

An electrochemical method has been developed for studying the out-of-pile corrosion behavior of zirconium alloys in high-temperature aqueous environments. In the experiments here reported, the rate vs time behavior for oxide film growth on Zircaloy-2 in 0.05 m H_2SO_4, containing 600 ppm O_2, at 208°C has been determined. The over-all reaction is presumed to be the oxidation of zirconium to zirconium dioxide, the anodic process being the oxidation of zirconium and the cathodic process the reduction of O_2.

Recently, several investigators have demonstrated a correlation between the polarization resistance of a corroding electrode and its corrosion rate.[7-9] The polarization resistance of a corroding electrode is defined as $(dE/dI)_{E \rightarrow E_o}$, where I is the net current flowing through the electrode at the measured potential E, and E_o is the potential at open circuit or zero net current. On the basis of electrochemical kinetics, Posey[10] and Stern[11] have presented theoretical justification for such a correlation.

The expression which finds practical application in the present study is:

$$(1) \quad \left(\frac{d\eta}{dI}\right)_{\eta = o} = \frac{b_a \times b_c}{2.3\, I_{corr}\, (b_a + b_c)} .$$

Here, I_{corr} is the corrosion rate of the electrode; $\eta = E - E_o$; b_a

and b_c are the Tafel slopes ($d\eta/(d \log I)$ for the oxidation and reduction reactions.

All the data required for the use of Eq. 1 can be determined by means of a complete cathodic polarization curve, Fig. 13.6. It is demonstrated that the oxygen reduction kinetics follows an equation of the form:

$$(2) \quad I = I_{o,c} \exp^{-\frac{\alpha_c \lambda_c \eta F}{RT}},$$

where α_c is the symmetry factor, $I_{o,c}$ is the current at $\eta = 0$, and λ_c is the charge number. This equation is the Tafel equation written in exponential form, with $b_c = 2.3\ RT/(\alpha_c \lambda_c F)$. Equation 1 can now be expressed in terms of these variables as:

$$(3) \quad I_{corr} = \frac{RT/F}{(\alpha_c \lambda_c + \alpha_a \lambda_a)(d\eta/dI)_{\eta = 0}}$$

The quantity $d\eta/dI$ is determined from a plot of I vs η on a linear scale and determining the slope at $\eta = 0$. The $\alpha\lambda$ values are determined from Eq. 2. Application of large anodic currents to determine $\alpha_a \lambda_a$ via Eq. 2 has been avoided, since anodic currents can materially affect the surface of a corroding electrode, and therefore affect the subsequent corrosion behavior. It has therefore been the practice to determine the anodic Tafel slope by an indirect method. The points for the anodic curve have been determined by the method demonstrated in Fig. 13.6. Here, the points for the anodic curve are obtained as a difference between the net current and the extrapolated cathodic current.

Numerous experiments have demonstrated that the $\alpha_c \lambda_c$ values have ranged from 0.25 at the beginning of an experiment to 0.38 at the end. The anodic $\alpha_a \lambda_a$ value ranged from 0.25 to 0.10 $\pm$ 0.05. The sum ($\alpha_c \lambda_c + \alpha_a \lambda_a$) remains constant at 0.47 $\pm$ 0.07.

The measurements were carried out in a titanium cell with provisions for solution entry and exit and with three electrodes: A Zircaloy-2 test electrode, a platinum reference electrode, and a titanium polarizing electrode (which also contains a thermocouple for temperature measurements). A Teflon cone was used to insulate the electrodes from the reaction cell. Provisions were made for rapid attainment and for control of operating temperature ($\sim$210°C). Potentials were measured on a modified L & N model 7664 pH meter, and recorded on a 10-mv Brown recorder.

All the experimental data reported in Fig. 13.7 as rate vs time plots have been based on the assumption that ($\alpha_c \lambda_c + \alpha_a \lambda_a$) = 0.47, and have been calculated from experimental η vs I measurements, maintaining $\eta = E - E_o < 20$ mv.

If the data for the first 100 min of the corrosion reaction are presented as a reciprocal rate vs time plot, the slope of the straight line obtained in $cm^2/\mu g$ units (corrosion-rate units, μg of O_2 per cm^2 per min) is B = 0.8 $cm^2/\mu g$. This value agrees with the value, 0.9 $cm^2/\mu g$, obtained by replotting Gulbranson's[12] data for crystal-bar zirconium at 200, 258, and 275°C in an oxygen atmosphere.

Two experiments were performed to determine the effect of temperature on the corrosion rate. These measurements were performed after different exposure times, and consequently at different oxide film thicknesses. It is demonstrated that the slope of the logarithm of the rate vs the reciprocal of the temperature is independent of film thickness for these exposure times. The calculated (Arrhenius) activation energy for the over-all corrosion reaction, $Zr + O_2 \longrightarrow ZrO_2$, is 15-16 kcal/mole. An estimation of the activation energy for the anodic partial process, zirconium oxidation, yields a value of the order of 21 kcal/mole. This calculation is based on an equation developed by Posey[13] of the ORNL Chemistry Division.

Two experiments were performed to determine the Tafel slope for oxygen reduction on platinum in 0.05 m H_2SO_4 at 208°C, 600 ppm O_2. If the value obtained for the Tafel slope is normalized to 25°C, a value, b_c = 0.03, is obtained. This differs greatly from the value, b_c = 0.11-0.12, which is obtained for oxygen reduction on platinum in aqueous acid at 25°C.

Meyer[14] of the ORNL Chemistry Division, has studied the oxide film growth on crystal-bar zirconium in aqueous Na_2SO_4 at 66°C and pH = 3.5, using the same techniques. The rate vs time behavior and the time variation in the α λ constants are similar to those obtained in the present study.

The results presented in this report have not received a complete discussion. A more detailed description of this work is to be reported elsewhere.

REFERENCES

1. H. C. Savage, et al., HRP Quar. Prog. Rep. Oct. 31, 1958, ORNL-2654, pp 164-166.
2. G. H. Jenks, et al., HRP Quar. Prog. Rep. April 30, 1957, ORNL-2331, p 113.
3. S. E. Beall, et al., HRP Quar. Prog. Rep. Oct. 31, 1958, ORNL-2654, pp 3-7.
4. J. C. Griess, et al., HRP Quar. Prog. Rep. Oct. 31, 1958, ORNL-2654, pp 115-116.
5. E. F. Stephen, et al., The Solubility of Gases in Water and in Aqueous Uranyl Salt Solution at Elevated Temperatures and Pressures, BMI-1067, (Jan. 23, 1956).

6. H. C. Savage, et al., HRP Quar. Prog. Rep. Oct. 31, 1958, ORNL-2654, pp 166-173.
7. R. V. Skold and T. E. Larson, Corrosion 13, 139 (1957).
8. E. J. Simmons, Corrosion 11, 255 (1955).
9. K. F. Bonhoeffer and W. Jena, Z. Elektrochem. 55, 151 (1951).
10. F. A. Posey, Kinetic Studies on Corrosion Systems I. Polyelectrodes Under Activation Control (to be published).
11. M. Stern and A. L. Geary, J. Electrochem. Soc. 104, 56 (1957).
12. G. H. Jenks, private communication.
13. F. A. Posey, private communication.
14. R. E. Meyer, Thin Film Formation on Zirconium (to be published).

UNCLASSIFIED
ORNL-LR-DWG 36338

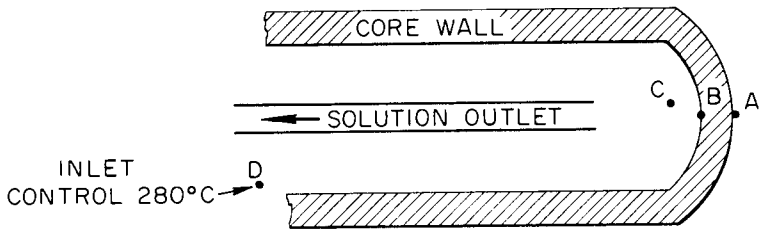

SKETCH OF CORE

Nomenclature

t_A, temperature of outer wall of core nose, location of two thermocouples, °C
t_B, temperature of inner surface of core nose, °C
t_C, bulk solution temperature at core nose, °C
t_D, bulk solution temperature at core inlet, °C
W, heat loss from core walls to surroundings, w/cm^2
F, fission and gamma-ray heat in core, w
$60U$, denote condition of 60 cps with reactor at full power
$20U$, denote condition of 20 cps with reactor at full power
R, ratio of volume flow rate in core at 60 cps to that at 20 cps

Known quantities

$t_D = 280°C$, controlled
$F = 1300w$, measured
$t_A60U - t_A20U = -4.9$ observed average temperature increase upon change from 60 to 20 cps
$R = 3$, measured
Solution volume flow rate = 360 cc/sec at 60 cps and the heatup in core at 280°C is 7.1×10^{-4}°C/w at 60 cps.

Assumed quantities

Heat loss from core surface of 350 cm^2 constant at 0.5 w/cm^2
Heat transfer resistance of liquid film varies with solution velocity to the 0.8 power
Heating in wall at core nose due to absorption of nuclear radiations constant with the reactor at power

Computations

With the above quantities the temperatures of interest are expressed by the following equations and may be calculated as follows:

(1) $$t_B20U = t_D - (t_A60U - t_A20U) + (t_A60U - t_A20U)/(1 - R^{0.8}) + 7.1 \times 10^{-4}(F - 350W)(R^{0.8} - R)/(1 - R^{0.8})$$

(2) $$t_B60U = t_B20U + (t_A60U - t_A20U)$$

(3) $$t_C60U = t_D + 7.1 \times 10^{-4}(F - 350W)$$

(4) $$t_c20U = t_D + 7.1 \times 10^{-4}(F - 350W)R$$

Fig. 13.1. Method of Calculating Temperatures in Loop Core.

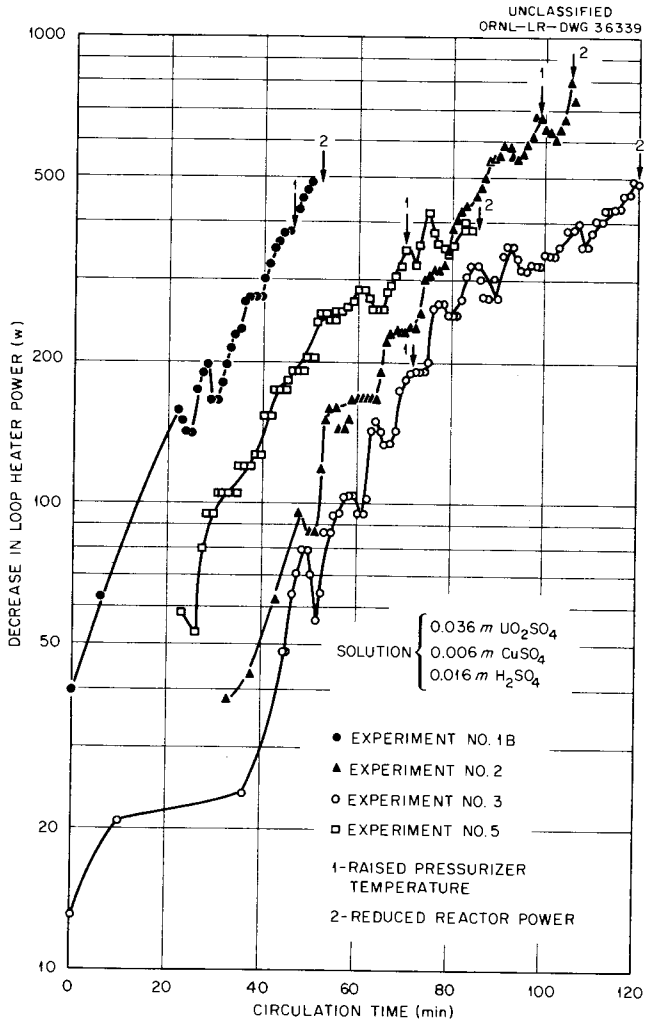

Fig. 13.2. Decrease in Loop Heater Power During Excursions, First Solution.

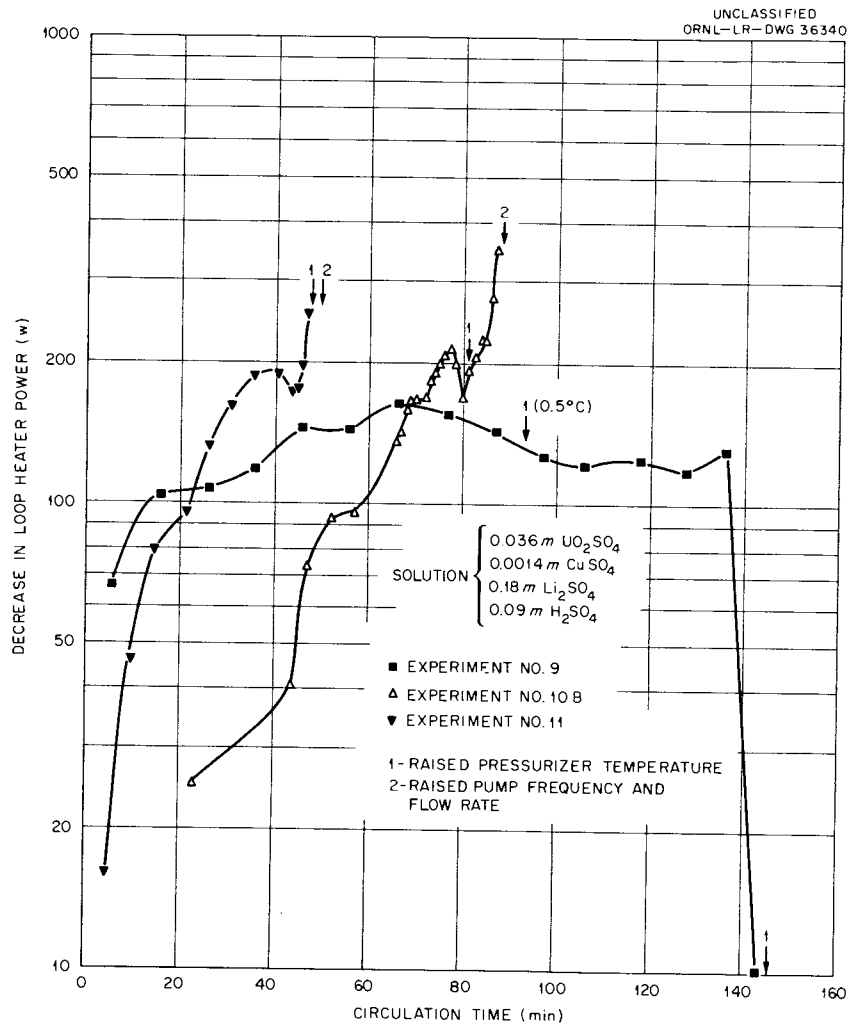

Fig. 13.3. Decrease in Loop Heater Power During Excursions, Third Solution.

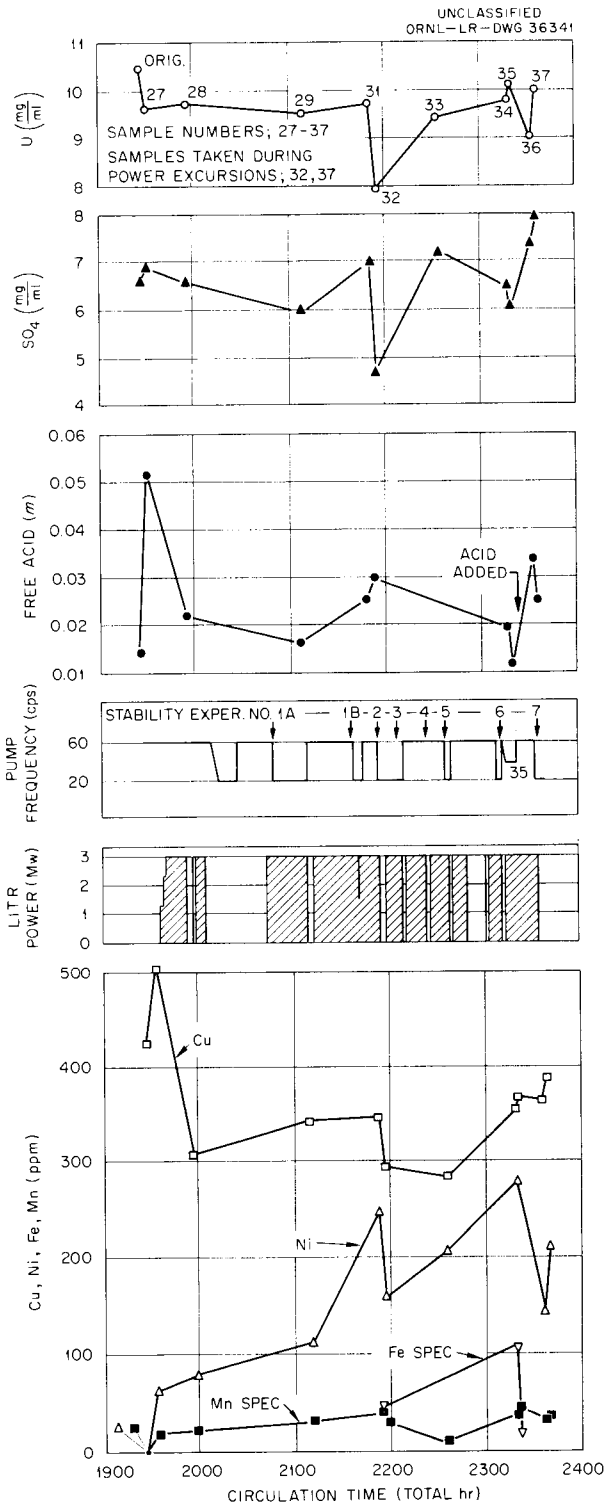

Fig. 13.4. Solution Analyses, Pump Frequencies, and LITR Power Levels for First and Second Solutions.

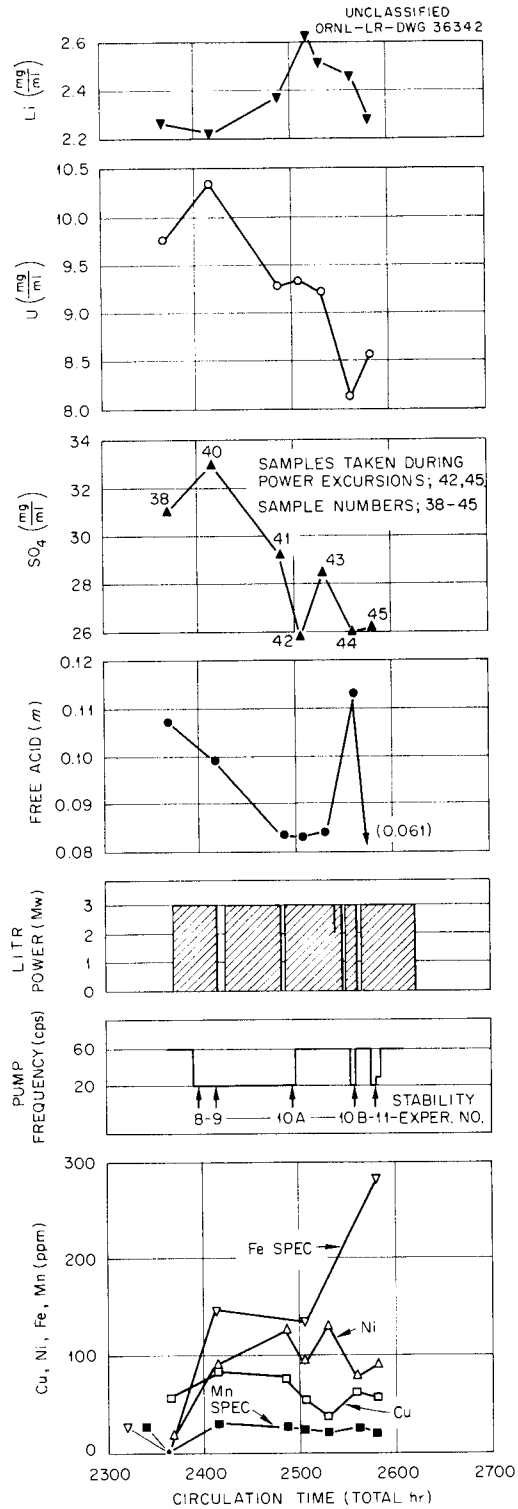

Fig. 13.5. Solution Analyses, Pump Frequencies, and LITR Power Levels, Third Solution.

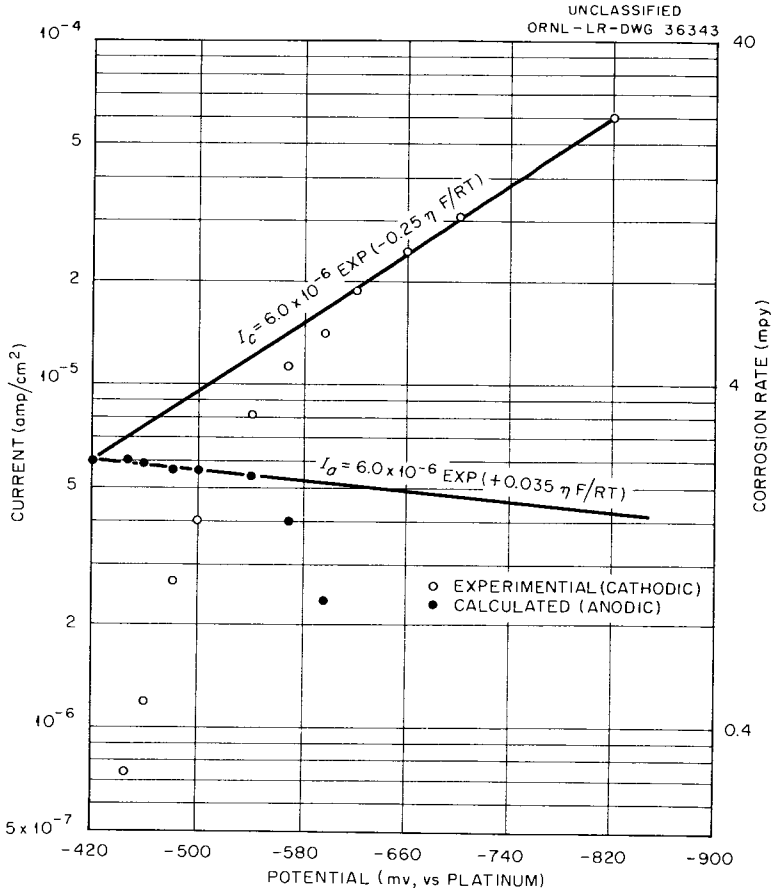

Fig. 13.6. Experimental Current-Potential Plot. Conditions: 0.05 *m* H_2SO_4, 600 ppm O_2, 208°C, 60 min.

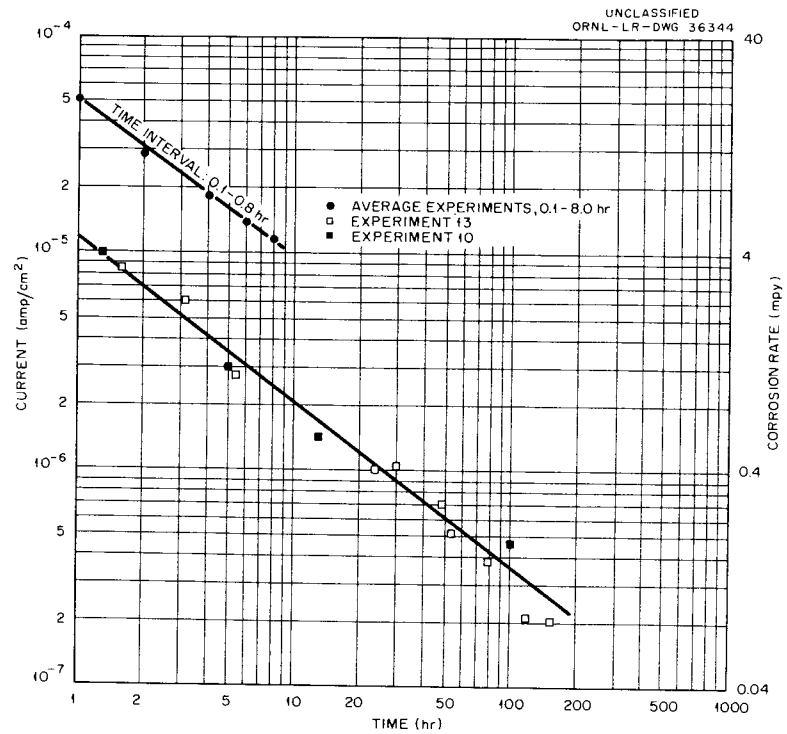

Fig. 13.7. Logarithmic Plot of Rate vs Time. Zircaloy-2 in 0.05 *m* H_2SO_4, 600 ppm O_2, at 208–210°C.

14. METALLURGY

G. M. Adamson

R. G. Berggren
E. S. Bomar
F. W. Cooke
T. M. Kegley, Jr.
W. J. Leonard
M. L. Picklesimer
J. J. Prislinger
P. L. Rittenhouse
R. L. Stephenson
J. K. White
J. C. Wilson
C. H. Wodtke

14.1 PHYSICAL METALLURGY

14.1.1 Examination of Specimens Cut from the HRT Core-Tank Screens

Disks nominally 2 in. in diameter were cut from the top six screens of the HRT core tank after run 17,[1] and five of the six disks were recovered. They were submitted to the HRP Metallurgy Group for examination.

The specimens were macrophotographed on both surfaces; then, metallographic and hydrogen-analysis specimens were cut. The metallographic specimens were mounted in Bakelite, then ground and polished by the Solid State Hot Metallography Group. Hydrogen specimens were submitted to the Analytical Chemistry Group for the determination of hydrogen contents. The evolved gas from each of the specimens was then sent to the Mass Spectrograph Analytical Group, Y-12, for a determination of the H-D ratio to determine the amount of D_2 picked up during reactor operation.

The screens were originally fabricated from 1/8-in.-thick Zircaloy-2 sheet which had been rolled by the commercial fabrication schedule in use in 1954.[2] Holes, approximately 3/8 in. in diameter, were punched through the sheet in a triangular pattern, on 1/2-in. centers, leaving a minimum web width of 1/8 in. between neighboring holes.

Metallographic examination of scrap material from the original fabrication stock for the screens showed many sheet-type intermetallic stringers throughout the structure, with some being 1/16 in. or more in length and width. The material had a very small (less than ASTM 7) grain size, with the grains showing evidence of appreciable cold working and a very considerable amount of preferred orientation. Examination of scraps cut from the sheet stock after the punching of the holes

showed that the punching operation had produced more cold working of the material and had caused many of the intermetallic stringers to open up into actual cracks and voids extending in from the surfaces of the holes. Other cracks were produced by the punching operation and could not be related to intermetallic stringers. Recent punching and shearing tests on Zircaloy-2 material which contained no intermetallic stringers and little preferred orientation have shown that such cracks are almost always produced by these operations, and that the intermetallic stringers in the screen material did not cause the cracks, although the amount of cracking was increased by their presence.

Macroexamination of the screen specimens showed considerable roughening of all surfaces of all specimens; the roughening appeared to be caused by exfoliation of layers parallel to the rolled surface of the screen sheet and to the sheet-type intermetallic stringers existing in the material. All top surfaces showed more exfoliation than the bottom surfaces. The screens, numbered in sequence from the bottom position, showed the following relative amounts of exfoliation: screen No. 9, greatest degree; screen No. 5, next greatest degree; screen No. 4, next greatest; and screens No. 7 and 6 or No. 8 and 6, the least degree. It is believed that the missing screen-specimen is from screen No. 7 or 8; the exact screen cannot be determined at present. Certain areas of screen No. 9 showed exfoliation almost half way through the thickness of the web. The majority of the exposed cracks in the rims of the holes were filled with oxide. On the upper surface of a web, one small area located between two neighboring holes near the center of screen No. 9 showed evidence of having been molten at some time during reactor operation. Later microstructural examination of this area and of the titanium specimen holder (which is believed to have been in contact with this particular web section) showed that the molten area was probably caused by molten, and presumably burning, titanium from the titanium specimen-holder tip.

Metallographic examinations were made of several sections of each of the screen samples received. Examinations were made on a Bausch and Lomb research metallograph, using magnifications from 50X to 750X in bright field, with both flat and oblique illumination, and in polarized light. With the exception of the "molten area" observed on the top screen, no evidence was found which would indicate that a temperature as high as 600-700°C could have been reached in the center area of the screens. The microstructures showed a degree of remaining cold work sufficient to obviate the possibility of temperatures having been in excess of about 600°C. At these temperatures, recrystallization would have occurred to some degree in a matter of a few minutes, at most. Rather extensive metallographic examination of specimens cut from the region of the "molten area" of the top screen showed that the outermost structure of the surface had been molten.

The order of appearance of structures from the surface inward were:

1. oxygen-stabilized alpha Zr mixed with molten Zr at maximum

temperature,

2. a layer of oxygen-stabilized alpha Zr below the molten pool,

3. a layer of oxygen-enriched prior beta phase below that (showing a very coarse needle, basket-weave pattern typical of oxygen contamination),

4. a relatively thick layer of very fine martensitic alpha phase, typical of a prior beta phase which had been very rapidly quenched,

5. an extremely thin layer which was probably alpha-plus-beta phase at temperature,

6. a very thin layer of recrystallized, very fine-grained alpha phase,

7. the cold-worked, fine-grained alpha structure typical of the remainder of the screen.

The entire range of structures occurred within a distance of not more than 1/4 in. from the center of the "molten area." The hydrogen and deuterium analyses of the screens indicated that, at most, only a small pickup of deuterium occurred during reactor operation. It is believed that at least the major portion of the deuterium found was adsorbed or otherwise incorporated in the oxides filling most of the cracks in the webs. The reporting of the data is awaiting control determinations with heavilty pickled screen specimens.

The major conclusions reached were:

1. The screens were never at a temperature greater than 600°C.

2. The maximum temperatures in the screen materials were probably much less than 500°C.

3. The exfoliation of the screens was caused by corrosion in the cracks present in the sheet after the punching of the holes.

4. The cracks present in the screen sheet were accentuated by by the intermetallic stringers but not caused primarily by them.

5. No appreciable pickup of deuterium by the Zircaloy-2 screen occurred.

6. The "molten area" observed on the upper surface of the top screen was caused by contact with the titanium holder tip or by a droplet of molten and burning titanium from the titanium specimen-holder.

14.1.2 Examination of the Titanium Specimen-Holder from the HRT Core

The titanium specimen-holder[3] located in the HRT core during run 17 was sectioned, examined, and macrophotographed. Metallographic specimens were cut from several areas of the holder for microscopic examination, but the metallography is not complete enough to report.

The macroexamination revealed three holes penetrating the same longitudinal web of the holder, one at each of the lower three stations (where the mechanical-property specimens were located). The holes appeared to have been melted or "burned" through the web. The hole at the lowest station, nearest the tip that originally had penetrated the top screen, appeared to have been formed by at least two separate events. The crosswebs of the holder (which supported the mechanical-property specimens) were "burned" and/or corroded away in both of the lower two stations and partially in the third and fourth stations, dropping all but two of the mechanical-property specimens onto the top screen of the core tank.

Several areas of the longitudinal webs of the titanium holder showed rather extensive pitting, but other areas showed only scattered pits or appeared to have the original machined surface still present.

In no case observed to date, in the macro- or microexamination, could the holes or pitting be associated exclusively with either the welded or the heat-affected (by the welding assembly operation) zones of the webs or stations.

Approximately 11/16 in. of the length of the titanium holder tip had disappeared during the exposure in the reactor. The tip was initially used for locating and anchoring the holder in the top diffuser screen and extended through the screen approximately 3/4 in. Metallography is continuing. When this examination has proceeded sufficiently specimens for deuterium analysis will be cut from various areas of the titanium holder. No major conclusions can be presented until the metallographic examination is reasonably complete.

Three Zircaloy-2 mechanical-property specimens,[4] originally located on the titanium specimen-holder for run 17, but which fell off during the run, were received after their recovery from the top screen, at the end of the run. These specimens have been examined macroscopically and are now being examined microscopically. Portions of the T-heads of the specimens were "burned" and/or corroded away, apparently as a result of the events happening to the titanium specimen-holder. Several areas of rather uniform, shiny, pits were observed on the surfaces of the specimens, but there was no apparent relationship between their occurrence and any particular area or feature of the specimens.

While only preliminary results are available from the metallographic and deuterium studies, the results in both cases are consistent. The deuterium values are not available, but the combined hydrogen and

deuterium concentrations are approximately equal to the control hydrogen concentration, indicating at least that there was no large increase in deuterium during operation. As yet, metallographically, no area showing an altered structure has been found that was not also close to the burned titanium. A wide variety of high-temperature structures may, however, be found near the holder. It appears that most of the damage to the Zircaloy specimens was initiated by the nearby holder.

14.1.3 Zirconium-Hydrogen System

In a continuing study of the zirconium-hydrogen system,[5] its phase diagram, morphology, and physical metallurgy, Zircaloy-2 specimens were hydrided at 400°C and below in order to produce a surface layer of hydride. At 400°C and below, the hydride formed in patches on the surface of the specimen, with no detectable hydride on the surface between the patches. Microexamination of polished Zircaloy-2 specimens showed that the patches (1) had discrete boundaries on the surface of the specimen, (2) caused lenticular twins to form in the alpha grains bordering the patch on the surface, and (3) caused the formation of extremely thin "line markings" in the grains below the surface and immediately surrounding the hydride patch. Slant polishing of the hydrided surface showed that the "line markings" were actually the traces of lenticular twins produced by the deformation of the matrix as a result of the formation of the hydride patch on the surface. The patches extend for several thousandths of an inch below the surface of the specimen. A photograph, at approximately 3X magnification, of the patches of hydride on a Zircaloy-2 specimen is shown in Fig. 14.1a. One of the patches was polished off until the surface of the specimen was flat. A photomicrograph of the patch after polishing is presented in Fig. 14.1b. The lenticular twins formed in the surface grains bordering the patch are shown in Fig. 14.2. These lenticular twins may be the so-called anisotropic "intermediate" hydride reported by several investigators.

14.1.4 Chemical Machining and Pickling Study on Zirconium-Base Alloys

Mechanical surface-preparation of Zircaloy-2, such as machining, grinding, sandblasting, gritblasting, etc., has been shown[6] to cause a decrease in the corrosion resistance, compared with acid-pickled surfaces. Pickling after welding has also been shown to produce increased corrosion resistance in both the deposited weld metal and in the heat-affected zone bordering the weld.[7]

Since the zirconium-alloy core tank of a reactor vessel must be welded, it would seem advisable to pickle the entire vessel after final assembly and heat treatment. Because of the size and complexity of a core-tank assembly, the rate of attack of the pickling solution would have to be rather slow. The rinsing of the vessel would have to be complete, and rapid rinsing should not be a requirement. With these requirements in mind, a chemical polishing and pickling study is being

conducted with Zircaloy-2. Other zirconium alloys will be investigated later.

Concentrations of HF vary from 1 to 5 vol %; concentrations of HNO_3 vary from 0.5 to 50 vol %; and additives such as glycerine and lactic acid vary from 0 to 10 vol %. Bath temperatures from room temperature to 60°C, and surface conditions are also being studied as variables.

The rate of metal removal has been found to be a function of all the variables being studied. A concentration of 2% or more of HF has been found to be necessary if sandblasted surfaces are to be smoothed sufficiently in a reasonable time. Nitric acid concentrations have been found to be relatively important, controlling both the rate of metal removal and the smoothing of the surfaces. For a bath having an HF concentration of 2% the rate of attack decreases with increasing HNO_3 content (Fig. 14.3) to a minimum rate when the HNO_3 concentration is between 3 and 4% and then increases as the concentration is increased to about 20%. Above the concentration of 20%, the rate of attack increases slowly until a maximum is reached at 40%. Black films and deep pitting were found on all specimens pickled in baths containing 2% HF and less than 2% HNO_3. Increasing the temperature of the bath increased the rate of attack and improved the smoothing of the surfaces. Almost constant rates of attack were found for previously pickled or hand-abraded surfaces; for sandblasted surfaces, the rate of attack was initially rapid, but, after a small amount of the surface metal was removed, it decreased to the same value found previously for pickled surfaces.

Bath additives (glycerine, lactic acid, and surface wetting agents) decreased the rate of attack for several bath compositions, while additions of flotation agents increased the rate.

Similar studies are being made with baths containing 3 and 5% HF.

14.2 MECHANICAL METALLURGY

14.2.1 Mechanical Properties of Zirconium and Titanium Alloys Exposed in the HRT

Mechanical-property tests have been completed on the samples from the first and second blanket loading from the HRT. The samples exposed in the core exit pipe and those recovered from the core are not yet available for testing. No values are yet available for the neutron dose received by the samples. The slow-neutron dose is being determined by means of activation analyses, and the Research and Analysis Section is calculating the fast dose.

Two types of Zircaloy-2 had been exposed as blanket samples: samples of the actual core-tank plate and material fabricated according to the ORNL schedule now in use.[8] In the as-received condition, neither material showed significant changes when compared with controls. To

learn whether a slight loss of ductility occurred, increased accuracy must be attained in the comparisons both with controls that have received the same thermal history and with the low-flux samples.

Samples of the ORNL-schedule material were exposed in the as-welded condition and as heat treated by beta-quenching. For these two types of samples, there does appear to be a slight decrease in ductility.

Various titanium alloys were also exposed. Titanium A-40 from the first and second loading, and 6 Al-4V Ti from the second loading, showed small increases in the tensile and yield strengths with decreases in ductility. The changes were slightly larger than those found in the beta-quenched Zircaloy-2.

14.3 WELDING DEVELOPMENT

14.3.1 Stainless Steel

Heat exchangers with composite tubing and tube sheets are being considered for homogeneous-reactor application. Aqueous uranyl sulfate solution would circulate through the tubes and be in contact with the tube-sheet surface where the tubes emerge. The secondary liquid, in contact with the outer tube surface and the inner tube sheet, would be boiler water. Because of corrosion resistance considerations, the metal in contact with the primary liquid would be type 347 stainless steel; Inconel or carbon steel would be desirable on the secondary side. Due to the dilution of the base metals and filler wire in welding such a joint, various resultant compositions having varying properties occur in the weld metal.

A welding investigation was made by using 1/2-in.-dia, 1/16-in.-wall stainless steel tubing clad exteriorly with Inconel, having a wall-thickness ratio of 60/40 (Inconel/stainless steel). The tube sheet was also of Inconel-clad stainless steel. Since the root surface is in contact with process water, an Inconel root-pass was used in all cases. Type 347 stainless steel or 308L weld metal, deposited on the Inconel root pass, cracked badly. Three nickel-iron-chromium-base alloys were found which may be deposited over Inconel without cracking: Incoloy, Hastelloy W, and INOR-8 (73% Ni, 15% Mo, 6% Cr, balance Fe). The nickel content of these alloys is too high, however, for adequate corrosion resistance in aqueous uranyl sulfate solutions. Therefore a cover pass of type 347 stainless steel weld metal was deposited, and each of the three above-mentioned metals was used as a barrier pass between the Inconel and the type 347 stainless steel. In each case, minor cracking was detected in the type 347 stainless steel cover pass.

The welding study was continued in order to improve the welding techniques. Welding variables, such as current, speed, amount of filler additions, and dilutions, were varied to obtain optimum welding conditions, with the final result that, with the exception of in the

crater at the weld termination, cracking was eliminated. Current tapering, overfilling with wire or reversal of welding direction at the crater did not completely eliminate crater cracking. The use of Incoloy resulted in the least amount of crater cracking in the type 347 stainless steel cover pass, while the other two alloys gave approximately equal amounts. Since it appears that a barrier alloy of lower nickel content is required for achieving sound cover passes, various stainless steel alloys which may permit welding on Inconel are being investigated.

14.3.2 Zirconium

To determine the results of making a titanium-to-Zircaloy-2 weldment, two 1/4-in. plates, one of Zircaloy-2, and the other of titanium (RC-A40), were welded, using Zircaloy-2 filler wire. A section of the weld was taken for metallographic examination. There were no cracks or porosity in the weld. The weld had full penetration and appeared sound. The weld metal adjacent to the Zircaloy base plate and in the central area of the weld appeared normal, having a hardness in the range of 180-200 DPH. Zircaloy-2 weld metal adjacent to the titanium fusion line gave a maximum DPH reading of 265. A maximum DPH reading of 335 was observed in melted titanium base metal which had been diluted with Zircaloy-2. The hardening is believed to be due to the mutual solid-solution hardening effect of the two metals rather than to any contamination of either metal by nitrogen or oxygen. Tensile properties of the weldment were not evaluated.

14.4 METALLURGICAL SERVICES

14.4.1 Examination of Loop Failures

Recent examinations revealed that seven type 347 stainless steel nipples from ORNL slurry loops have failed by stress-corrosion cracking. In all cases, the following conditions were encountered:

1. The stress in the nipples was low.
2. The chloride content of the bulk slurry was generally 1 ppm or less, although in the initial stages values as high as 5 ppm may have been present.
3. The slurry in the nipples was stagnant.
4. A weld was near by.
5. A temperature differential existed along the nipples.
6. The nipples had been in service in excess of 5000 hr.

Despite the long time required for these failures to occur, it

is significant that they occurred at all in an environment in which the elements that produce stress-corrosion cracking had been reduced to such a low level.

Further investigation has been recommended to evaluate the effect of convection circulation in the nipples, the possibility of chloride buildup and other concentration changes in the stagnant slurry, and the magnitude of the axial temperature differential.

14.4.2 Fabrication of Zircaloy-2 Hemispheres

A study has been conducted by Titanium Fabricators, Inc., of Burbank, California, to determine the feasibility of forming Zircaloy-2 hemispheres by power spinning. Ultimately such hemispheres are intended to be used as components of spherical vessels for the HRP.

The evaluation of the hemispheres has not been completed, but it seems that spinning such hemispheres is feasible. However, for the dimensional control required for welding, it would be necessary to machine the surfaces in the weld area. The problem in this process is to achieve diametral control while avoiding rippling or excessive wall thinning.

After rough polishing and dimpling, disks of 1/8, 1/4, and 5/16 in. thickness were spun, at about 1250°F, into 15-in.-dia (approximately half size) hemispherical shells. The process required two or three passes to form a 30-in.-dia shell on a die of the same size, followed by two or three more passes on a 15-in.-dia die. While some difficulties were encountered with the 1/8-in.-thick shells, the other two thicknesses were handled with surprising ease.

14.5 DEVELOPMENT OF NONDESTRUCTIVE TESTING METHODS

14.5.1 Thickness Measurement of HRT Core Vessel

Recent results from the resonance-thickness measurements made from the blanket side of the HRT core vessel have caused considerable interest in a more extensive corrosion survey of the vessel. Operation of the HRT as a one-region reactor, with the consequent contamination of the blanket area, has brought about a re-evaluation of procedures for thickness monitoring of the core vessel. The high levels of contamination now encountered require disposal of portions of the measurement equipment after a single use from either side, and this new condition removes the largest objection to measuring core thickness from the inside.

Therefore a new positioning system has been designed by REED design personnel and is being fabricated. This rig enters through the center-line flange and pivots from the center of the vessel to allow measurement of almost the entire core above the screens. The system is designed to provide positioning accuracy to within 1/4 in. and to allow for return to the same position with similar accuracy. A pneumatic extension system provides transducer loading against the core surface. Transducers had to

be tested to determine whether they would withstand the radiation expected in the core. To this end, a Branson Instruments type Z zirconate-titanate ceramic transducer was tested by 10^6 r of x-irradiation, and no unwarranted frequency drift was observed nor was the signal amplitude significantly diminished. Branson made special convex transducers to fit the core curvature. Three of the transducers have been received and tested on core stock; signal amplitudes were adequate, and final trials await fabrication of the positioning rig.

14.5.2 Measurement of Ultrasonic Velocity in Metals

Ultrasonic velocity measurements were attempted as a solution to the problem of locating embrittlement of titanium or zirconium welds caused by dissolved oxygen or nitrogen. Large amounts of gases dissolved in titanium have been measured by their retardation of the velocity of ultrasound, but the concentrations of these gases which can cause embrittlement (ppm amounts) were too low to cause any observable change in velocity.

Measurements of ultrasonic velocity allow for a rather simple determination of the elastic constants of a metal. The Lamé constants, Poisson's ratio and Young's modulus, are readily computed if the density of the metal is available as well as the longitudinal and shear sound velocities. This possibility has only recently been exploited by this group, and accurate values cannot be determined until the sources of error in the velocity measurements can be removed. Preliminary determinations are quite promising.

14.6 REACTIONS OF ACTIVE METALS

14.6.1 Combustion of Titanium and Zirconium

The work on the combustion of titanium and zirconium has continued under subcontract at Stanford Research Institute.

For titanium it has been shown that the ignition limits vary inversely with the temperature. Typical values for the oxygen pressure required for combustion are 350 psi at room temperature, 250 at 300°C, 130 at 600°C, 100 at 900°C, and 70 at 1200°C.

For zirconium, a new test has been used in which a larger surface area is present. Strips 0.5 x 3 x 0.020 in. are rolled into cylinders, and the oxygen-free surface is obtained by heating in vacuum. After cooling, oxygen at the desired pressure is admitted to the capsule. With such a method, the critical pressure for ignition has been lowered from about 650 psi to 300 psi and will probably drop more as the method is improved.

14.7 EFFECTS OF RADIATION ON STRUCTURAL METALS AND ALLOYS

14.7.1 Equipment and Facilities

The first ORR irradiation apparatus is being assembled for insertion during the February shutdown. One section contains a set of furnaces for elevated-temperature irradiations, and there are two sections for irradiations at 200°F and below. The first irradiation is expected to give gamma-heating information necessary to the design of more efficient rigs.

14.7.2 Tensile Tests

Several hundred irradiated tensile specimens were tested during the quarter; about 80% of the irradiated steel specimens have been tested. Tensile, impact, and flux data are being organized so that a summary of properties can be prepared for each of the steels tested.

Preliminary annealing data were obtained on irradiated type A-212 grade B steel by measuring the Rockwell hardness after annealing in the range from 200 to 500°C. (This work is being done by K. Tanosaki, of Hitachi Ltd., while assigned to ORNL). The results show that an increase in hardness results from annealing around 300°C, but that at higher annealing temperatures the radiation-induced hardness decreases during annealing. The results are not entirely unexpected, in view of less complete data by others[9,10] on the effects of postirradiation annealing. Annealing studies will be continued in order to locate temperature ranges for more definitive studies by using tensile and notch impact tests. There is some indication that annealing after an elevated temperature irradiation takes place more slowly than in specimens irradiated at a lower temperature. The data imply that the effects of irradiation and temperature are more complicated than annealing of simple point defects.

Studies on the effect of aging after the usual normalizing heat treatment for pressure-vessel steels have started. The purpose of the work was to check a suspicion that the properties of steels were not thermally stable in the range 150 to 300°C. Because irradiation (and service in reactor pressure vessels) may take place in this temperature range, it is necessary to determine what changes are due to thermal effects in order to separate the portion due to radiation effects. The first tests on a simulated steel (high purity iron--0.2% carbon alloy) showed that the yield stress and uniform elongation would change, by amounts comparable to changes induced by low flux irradiations, during thermal aging between 120 and 300°C. The data will be extended to other steels. It is hoped that a stable state can be reached by preirradiation aging so that the irradiation effects at elevated irradiation temperatures will not be complicated by thermal-aging effects.

REFERENCES

1. S. E. Beall et al., HRP Quar. Prog. Rep. Oct. 31, 1958, ORNL-2654, p 9.

2. D. E. Tackett, Fabrication History of HRT Core Tank, ORNL CF-58-12-6, p 68 ff.

3. R. M. Warner, D. T. Jones, and B. W. Scott, HRT Corrosion Specimens and Holder: Core Region of Pressure Vessel (Loading No. 1), ORNL CF-58-7-68, p 1-5.

4. Ibid., p 8 ff.

5. G. M. Adamson et al., HRP Quar. Prog. Rep. July 31, 1958, ORNL-2561, p 246.

6. G. H. Jenks et al., HRP Quar. Prog. Rep. Oct 31, 1958, ORNL-2654, p 166.

7. G. M. Adamson et al., HRP Quar. Prog. Rep. Oct 31, 1958, ORNL-2654, p 189.

8. M. L. Picklesimer and G. M. Adamson, Development of a Fabrication Procedure for Zircaloy-2, ORNL CF-56-11-115.

9. L. P. Trudeau, A/Conf.15/P/190, Second UN Conference on the Peaceful Uses of Atomic Energy (1958).

10. E. E. Baldwin, Welding Journal 36, 342-s (1957).

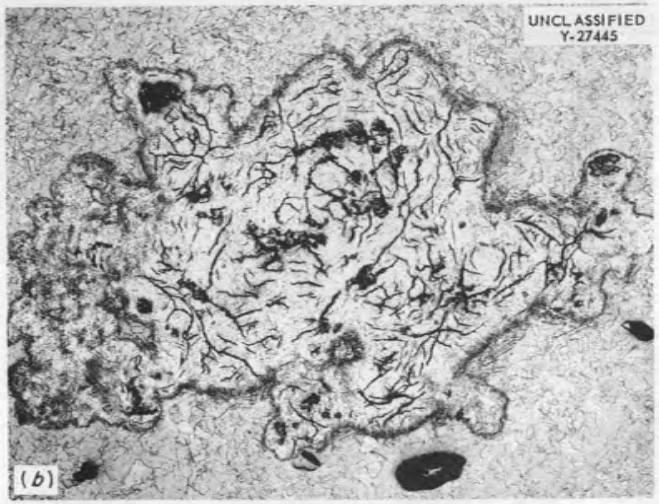

Fig. 14.1. Patches of Hydride Formed on Zircaloy-2 at 400°C. (*a*) As-deposited, macrophotograph, 3X. Reduced 23%. (*b*) Hydride patch polished down to specimen surface; bright field, 50X. Reduced 23%.

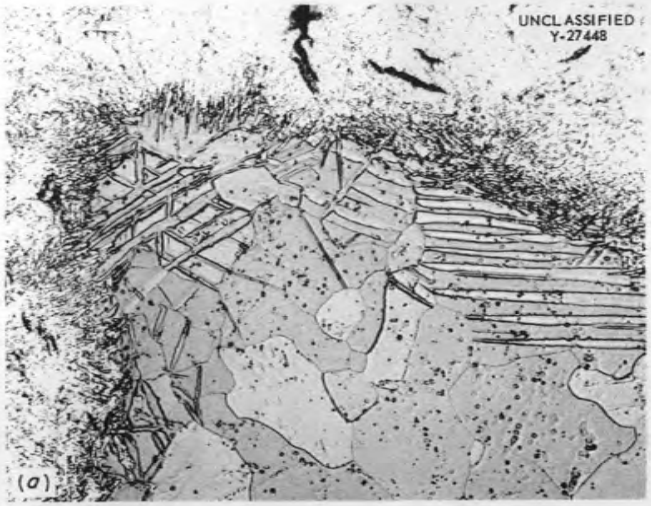

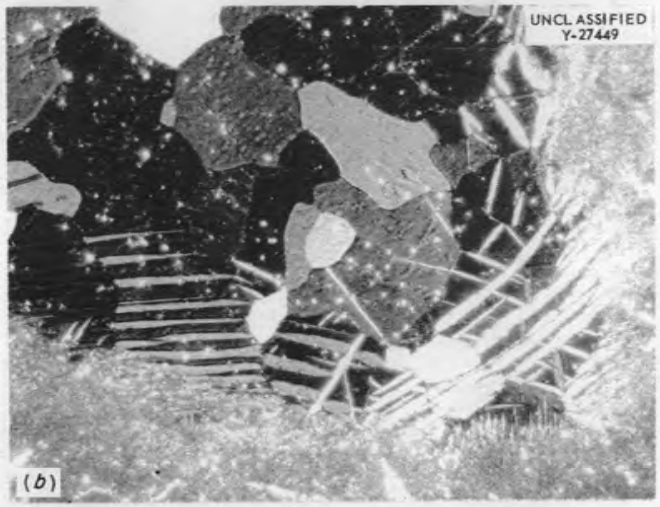

Fig. 14.2. Lenticular Twins Formed in Matrix Zircaloy-2 Grains Surrounding Hydride Patch. 400X. Reduced 23%. (*a*) Bright field. (*b*) Polarized Light.

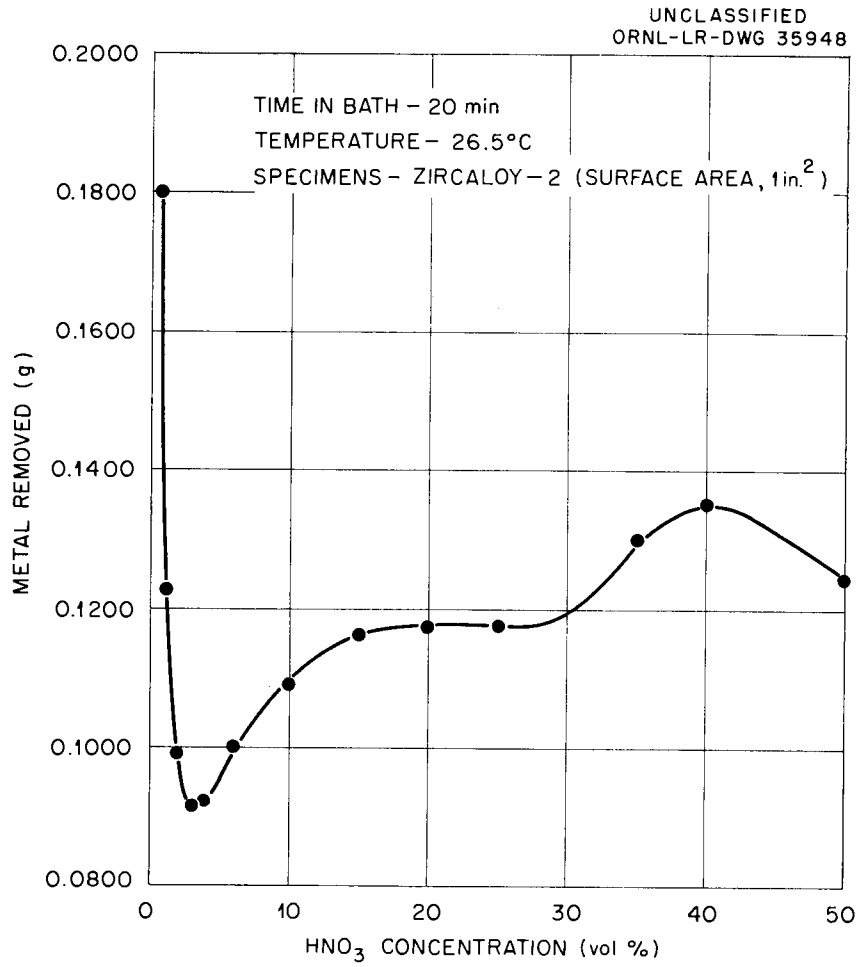

Fig. 14.3. Effect of HNO_3 Content on Removal of Zircaloy-2 in 20 min in a 2 vol % HF-HNO_3-H_2O Solution.

PART V

CHEMICAL ENGINEERING DEVELOPMENT

D. E. Ferguson

15. URANYL SULFATE FUEL PROCESSING

R. A. McNees

M. H. Lloyd S. Peterson

15.1 FUEL-SOLUTION BEHAVIOR

The effects of hot metal surfaces in contact with simulated HRT fuel solution and the effects of variations in the composition of such solutions on temperature-phase relations were studied in quartz-tube experiments. Results showed that deposition of a second liquid or solid phase on a hot Zircaloy-2 surface is possible even when the temperature of the bulk solution is below the phase transition temperature.

In these experiments pins of Zircaloy-2 or type 347 stainless steel were sealed in quartz tubes along with simulated HRT fuel solution (0.025 m UO_2SO_4, 0.011 m $CuSO_4$, 0.0046 m $NiSO_4$ and 0.020 m D_2SO_4 in D_2O) and H_2O_2 to provide an oxygen atmosphere. The quartz tube was surrounded by another tube through which heated air could be passed, and the entire assembly was placed in the coil of an induction heater. The temperature of the solution was estimated by measuring visually the expansion of the liquid.

When all the heat to the system was supplied by the induction heater and the metal pins were long enough to extend into the vapor space above the solution, violent boiling occurred and the metal was attacked at the liquid-vapor interface. In this area Zircaloy-2 pins were coated with a white deposit and stainless steel pins with a rust-colored deposit, while particles of corrosion-product solids were suspended in the liquid. Portions of the pins completely submerged in liquid at all times were not affected in this way. After prolonged heating (2 to 6 hr), small deposits of solids were observed on completely immersed Zircaloy-2 pins, but the deposits were shown to be amorphous silica and not ZrO_2.

When similar tubes were heated to 300 to 320°C by a combination of a hot air stream and induction, boiling occurred and yellow-green crystals or liquid formed on the surface of the Zircaloy-2 pins. When the induction heating was stopped, boiling also stopped and the crystals or liquid gradually dissolved. No second-phase material was seen anywhere else in the system. These results clearly show that, where boiling

occurs at a hot metal surface, a high-temperature second phase can separate even though the solution from which the second phase is being formed is below the temperature at which such a phase is stable. Experimental equipment is being designed for study of this behavior under more closely controlled conditions.

The effect of the presence of corrosion-product solids, buildup of nickel, and wide variations in free sulfuric acid concentration on the phase behavior of simulated HRT fuel solution in the absence of hot metal surfaces was also studied. With corrosion-product solids at a concentration of 50 g per liter of fuel solution, the temperature at which a second liquid phase appeared in simulated HRT fuel solution (0.021 m UO_2SO_4, 0.011 m $CuSO_4$, 0.0046 m $NiSO_4$ and 0.022 m D_2SO_4 in D_2O) was lower, at most, by 2 or 3°C.

When the concentrations of the constituents of the simulated fuel solution were held constant, except for the sulfuric acid, the temperature at which a second liquid phase appeared was lowered as the concentration of acid was lowered (Fig. 15.1). With acid concentrations of 0.006 m or greater, only a second liquid phase formed, but at lower acid concentrations, solids also appeared at temperatures significantly below the second-liquid-phase temperature. At zero acidity, yellow-brown crystals formed at 258°C; at 0.0019 m D_2SO_4, both yellow-brown and dark-green crystals formed at 245°C. At an acid concentration of 0.0038 m, both types of crystals appeared at 289°C and remained as solids after cooling. The composition of these solids has not been determined.

In a slightly different solution (0.023 m UO_2SO_4, 0.023 m D_2SO_4, 0.011 m $CuSO_4$, 0.0046 m $NiSO_4$) the second liquid phase formed at 333°C and crystallized after a short time with no apparent increase in temperature. This transformation of the second liquid phase into a solid phase was retarded by decreasing the acid concentration; at 0.008 m D_2SO_4, the second phase crystallized only after 24 hr at 353°C. Furthermore, crystallization of the second liquid plase was retarded by increasing copper concentration. Thus at 0.017 m $CuSO_4$, the second liquid phase only partially crystallized after 72 hr at 353°C, while at 0.022 m $CuSO_4$ no crystallization was observed after identical treatment.

Increasing the nickel concentration of the simulated fuel solution from 0.0046 m to 0.031 m decreased the temperature of second-liquid-phase formation from 333 to 329°C, and enhanced crystallization of the second phase. At 0.014 m $NiSO_4$, transformation of the second liquid phase into a solid phase occurred after 16 hr at 343°C; but at 0.025 m $NiSO_4$, solids were obtained directly at 310°C; at a nickel concentration of 0.031 m, crystals were obtained at 300°C. Upon cooling to room temperature, all solids obtained from solutions which were 0.018 m or greater in $NiSO_4$ concentration underwent a transformation to produce a powdery light-yellow-green material which slowly redissolved over a period of four days at 27°C. These solids appear to be $NiSO_4 \cdot H_2O$.

15.2 SOLIDS BEHAVIOR

When the feed point for a hydroclone operating on a REED corrosion test loop at 250°C was changed to a presumably more favorable position, no increase was observed in the amount of solids collected. The original geometry of the system was such that the hydroclone feed takeoff flow was perpendicular to the flow of the circulating stream; in the new location, the loop stream is turned 90 deg, and the feed line to the hydroclone is a continuation of the original flow direction. Of the approximately 42 g of solids produced in each of two runs, the hydroclone separated 3.9 g when in the original position and 2.2 g after the change in position.

15.3 HRT SOLIDS AND FUEL SOLUTION

Two separate batches of solids that had been isolated from the HRT were analyzed for particle size by using the activity of the solids to measure the rate of sedimentation. The particle size distribution is shown in Fig. 15.2.

Another portion of reactor solids was subjected to a single cycle of the sulfuric acid dissolving procedure used in the HRT chemical processing plant, and 95% solids dissolution was obtained. The solids were 14% iron, 5% chromium, and 0.4% nickel; valid uranium and zirconium determinations were not obtained. When another portion of HRT solids was treated with 16 m nitric acid for 4 hr, only 20% of the solids was dissolved. The solids dissolved contained 3.6% U, 3.4% sulfate, 0.9% Cu, and 0.3% Ni. Treatment of the residue by a single cycle of the sulfuric acid treatment gave >99% dissolution of the solids remaining from the nitric acid treatment.

A sample of the HRT fuel solution, diluted with an unirradiated solution of uranyl sulfate to provide a sufficient volume of solution, was decontaminated by UO_4 precipitation. The decontamination factors obtained for various elements were: Cu, 86; Ni, 14; gross β, 5; Sr, 151, Ba, 72; Ce, 2.2; total rare earths, 11; Cs, 7; Ru, 6. The uranium material balance was 110%, with measured losses to waste solutions being less than 0.1%.

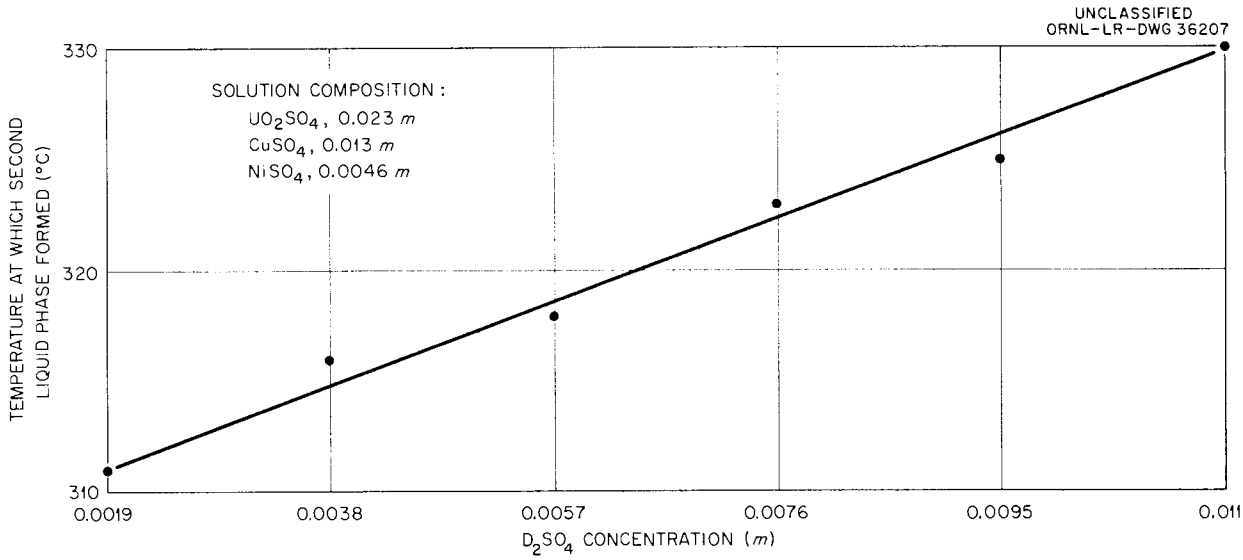

Fig. 15.1. Effect of D_2SO_4 Concentration on Second-Liquid-Phase Formation in Simulated HRT Fuel Solution.

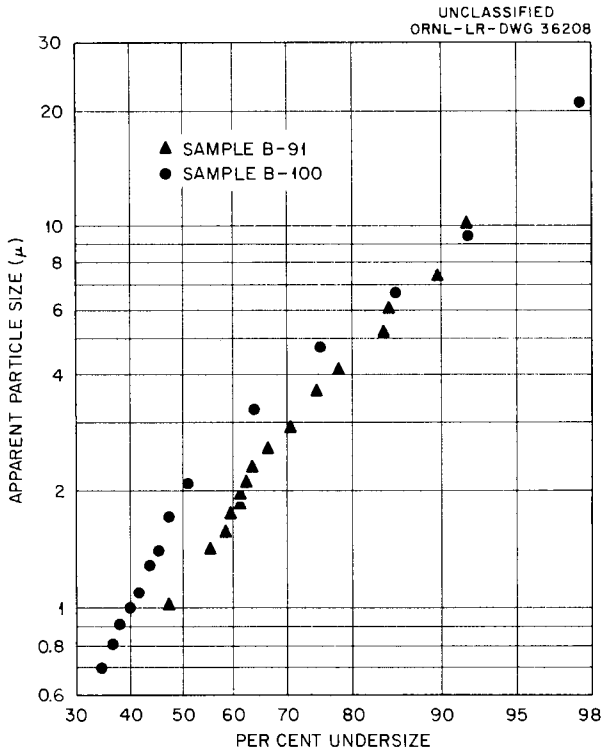

Fig. 15.2. Size Distribution of Solids from HRT.

16. GASEOUS-FISSION-PRODUCT DISPOSAL

R. D. Ackley R. E. Adams W. E. Browning

Studies of the behavior of fission-product gases have been primarily concerned with propagation of hydrogen-oxygen explosions through charcoal beds and with the heating of small quantities of charcoal above the ignition temperature as a result of the heat liberated by such explosions. Results of the studies indicate that the combustion of the charcoal in HRT bed A could have been initiated by deuterium-oxygen flame propagation from the recombiner to the point of ignition of the charcoal.

With a stoichiometric mixture of hydrogen and oxygen, propagation of the explosion could be obtained through the length of a 28-ft trap filled with Columbia G charcoal. Bed temperature rises were as great as 15°C after an explosion. This is about the same as the value obtained by calculation from the heat of reaction and the heat capacity of charcoal.

In other experiments, hydrogen-oxygen explosions in charcoal were initiated and oxygen, the HRT sweep gas, was allowed to flow through the charcoal immediately thereafter. In a number of cases the charcoal burned. Concentration limits of hydrogen in hydrogen-oxygen mixtures that will permit the propagation of an explosion front through an 8-ft glass pipe, 1-in. ID, filled with Columbia G charcoal, 8-14 mesh, were 30 and 70% for upward, downward, and horizontal propagation. Quenching distances for hydrogen-oxygen mixtures corresponding to these limits are in agreement with the estimated average distance between the charcoal granules in the pipe. With the glass pipe in a horizontal position, a tendency toward a wider range of limits during the time that the pipe was used in this work was observed, probably resulting from settling of the charcoal. Most of these data were obtained with the tubing at the explosion end of the glass pipe plugged and the tubing at the other end open to the atmosphere; with both ends open a slightly wider range of limits was indicated. Propagation was indicated by a temperature change in the bed and by visual observation. On the basis of available information on deuterium, it is not anticipated that the analogous limits for deuterium-oxygen would be appreciably different. High-speed motion pictures of explosions corresponding to various hydrogen-oxygen mixtures were obtained.

Work to determine the effect of the linear velocity of the sweep or carrier gas on holdup time and on N, the number of theoretical chambers or plates, was substantially completed. Seven traps were used, each 7 ft long, with an ID of 0.80 in., and filled with approximately 340 g of Columbia G charcoal. Krypton-85 elution curves were obtained for various flow rates of the carrier gas (oxygen), and approximate values of N were calculated by a method similar to that customarily used in gas chromatography. Results are shown in Fig. 16.1. The first two points were obtained with only one trap, the third with two traps (in series), the fourth with four traps, and the last four with all seven traps. The observed variation of N with linear velocity is, at least superficially, in accordance with theory. However, mathematical analysis of the data is preliminary and incomplete.

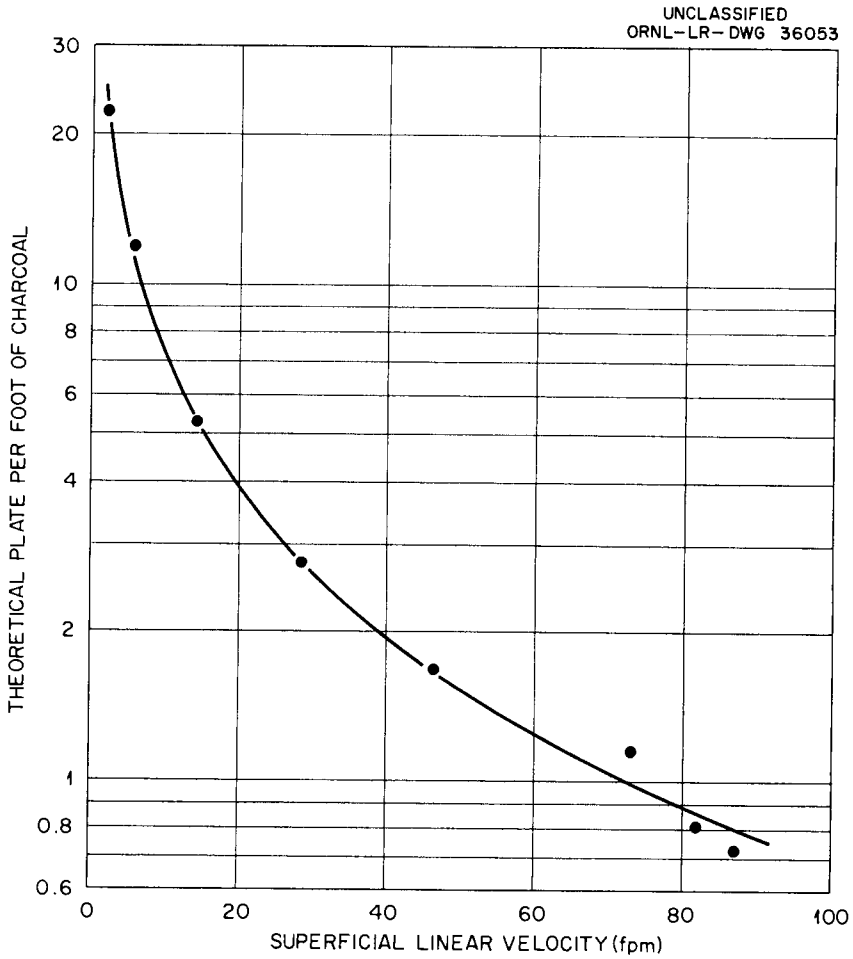

Fig. 16.1. Effect of Linear Velocity of the Sweep Gas on the Number of Theoretical Plates in a Charcoal-Filled Adsorption Trap. Sweep gas, O_2; tracer, Kr^{85}; adsorbent, Columbia G charcoal (at 24°C).

17. EQUIPMENT DECONTAMINATION

R. E. Leuze

J. F. Manneschmidt A. B. Meservey

Radioactive oxide scale on specimens of stainless steel HRT pipe, cut from a valve which had been serviced in the HRT chemical plant, was dissolved in 1 hr by 0.5 M $CrSO_4$ in 0.5 M H_2SO_4. This reagent, developed several years ago,[1] had not previously been tested on HRT scale. The gamma decontamination factor in descaling was 40 to 70 in the present study, and the corrosion rate was 20 to 40 mils/month. Most of the remaining activity, largely ruthenium and niobium, was removed by oxidizing reagents, e.g., acidic hydrogen peroxide or alkaline periodate.

Other descaling reagents also were found. Two treatments with Turco 4501 removed HRT scale in flakes, giving a gamma decontamination factor of 5×10^3, with surface corrosion of 1 to 4 mils/month. Deoxidine 170, an inhibited phosphoric acid, in preliminary trials completely dissolved a similar scale from stainless steel pipe in about 10 hr at 85 to 120°C. The corrosion rate at 93°C was 1 to 2 mils/month. Other phosphoric acid preparations have also shown promise in simultaneous scale dissolution and metal decontamination, with little corrosion. Alkaline periodate[2] (1 M KIO_4 in 2 M KOH) mixed with Turco 4502 (an alkaline permanganate) removed HRT scale in small flakes in 2 hr at 100°C with the best decontamination yet achieved ($> 5 \times 10^3$), but surface corrosion was about 75 mils/month. Alkaline periodate alone was the most effective decontaminating agent for ruthenium and niobium on bare metal yet tried in this laboratory, but it was not so efficient for descaling as was the mixture; the corrosion rate was 10 mils/month at 90°C. Alkaline hypophosphite, after the scale had been oxidized, converted the scale to a form soluble in acidic peroxide, resulting in a gamma decontamination factor of 10^3. The lower valence forms of uranium in simulated HRT fuel itself successfully dissolved HRT scale in 10 hr at 75 to 90°C when the fuel was circulated through mossy zinc, and small amounts of sulfuric acid were periodically added to compensate for acid losses to the zinc. The decontamination factor was 10^3 after ruthenium and niobium had been removed by brief warming with dilute acidic hydrogen peroxide.

REFERENCE

1. R. D. Baybarz, Decontamination of a Homogeneous Reactor, ORNL-CF-57-9-59 (Sept. 9, 1957).

18. THORIUM OXIDE SLURRY DEVELOPMENT

J. P. McBride P. A. Haas W. H. Lewis

S. D. Clinton K. O. Johnsson L. E. Morse
C. V. Ellison N. A. Krohn R. L. Pearson
C. C. Haws K. H. McCorkle C. E. Schilling

18.1 SLURRY IRRADIATION STUDIES

18.1.1 Slurry Irradiations in the LITR

Three short-term slurry irradiations were made in the C-44 vertical tube facility to evaluate Westinghouse low-fired oxide and their palladium oxide catalyst preparations. The first two tests (LITR-50 and 51) were on slurries containing 500 g of Th per kg of D_2O of a loop-drain sample containing 122 ppm of palladium (based on slurry solids) and 3% natural uranium. Uranium-235 was added (0.5 wt %) to increase the power density during irradiation, and the two tests were made at 300°C, one under an overpressure of oxygen and one under deuterium (250 psi at room temperature). In the third experiment (LITR-52) the slurry was unpumped Westinghouse 650°C-fired ThO_2, 500 g of Th per kg of D_2O, and 200 ppm palladium, based on total solids and the Westinghouse palladium analysis. Analysis at ORNL indicated only 145 ppm palladium. Uranium-235 was added (0.5%) as in the previous experiment, and the slurry was irradiated at 300°C under an oxygen overpressure (250 psi at room temperature).

The slurry of loop-drain oxide under oxygen was stirred with difficulty, and only for a few hours, when stirring stopped and could not be restarted. No gas pressure increase was noted during 6 days' irradiation, and upon termination and cooling to room temperature, 250 psi of gas, presumably the original oxygen, was found. The test under deuterium was stirred in-pile for six days. A leak forced its removal. No gas pressure increase was noted during the run.

In LITR-52 the total pressure at 300°C prior to reactor startup was normal, 1100 psi. When the reactor power was raised to 2000 kw and held there for 3.43 hr, the pressure increased at a rate of ~55 psi/hr and reached apparent equilibrium at ~1175 psi. When the reactor power was raised to 3000 kw, the pressure increased further at

a rate of ~80 psi/hr, reaching equilibrium at a total pressure of 1385 psi. After ~14.5 hr at 3000 kw, the reactor was shut down for 78 min, during which time the radiolytic gases recombined, lowering the pressure to 1275 psi. When the reactor again reached 3000 kw, the pressure increased to 1385 psi and leveled out. After 23 hr of operation, the stirrer stopped. When the experiment was cooled for removal, the residual gas pressure was 350 psi. During the irradiation, the net radiolytic gas production rates were proportional to reactor power, and hence to the fission power density in the slurry. The equilibrium gas pressures, however, were not in the ratio expected from first-order gas-recombination kinetics.

It may be concluded that either catalytic recombination activity decreased during the first few hours of operation (at 2000 kw) or the recombination rate was not first order with respect to radiolytic gas pressure. Attempts out-of-pile to measure gas recombination rates above 150°C in a control experiment were unsuccessful because of the high catalytic activity of the slurry. Gas added to the slurry autoclave at room temperature recombined before temperatures in excess of 150°C could be attained.

18.1.2 Postirradiation Examinations

Two previously irradiated slurries (LITR-48 and 49)[1] of 1000°C-fired thorium - 5% natural uranium oxide prepared from the coprecipitated oxalates were recovered. The first had been irradiated 310 hr under an initial atmosphere of air (15 psi), and the second, 354 hr under a pressure of 200 psi of deuterium. Both slurries were dark brown and did not settle in 24 hr. Radiochemical analyses showed most of the fission product activity to be associated with the slurry solids, as usual (Table 18.1), and corrosion product analyses (Table 18.2) showed the high pickup rate characteristic of slurries of thorium-uranium oxide prepared as above and stirred in the dash-pot-stirred slurry irradiation autoclave.

Table 18.1. Distribution of Fission Products in Irradiated Slurries
250 g of Th per kg of D_2O
1000°C-fired ThO_2--5% natural U

	Amount in Supernatant (%)									
Experiment	Gross β	Gross γ	Sr	Zr	Cs	Ru	RE	Nb	I	Pa
LITR-48	0.4	0.1	1.8	0.2	23.0	0.7	0.4	0.4	---	0.1
LITR-49	0.1	0.1	2.4	2.2	1.1	0.1	11.5	5.0	1.9	8.0

Table 18.2. Corrosion Products in Irradiated Slurries
250 g of Th per kg of D_2O
1000°C-fired ThO_2--5% natural U

Experiment	Atmosphere	Time Stirred (hr)	Time Irradiated (hr)	Corrosion Products (g/kg of Th)		
				Fe	Ni	Cr
LITR-48	O_2	384	310	197	23	4
LITR-49	D_2	408	354	327	54	1

18.1.3 Equipment Development

Two devices for small-scale evaluation of irradiated slurries are under development: an apparatus using an ultrasonic pulse-echo technique to determine the slurry interface for use in measuring slurry settling rates, and a rolling-ball viscometer to measure slurry viscosity and yield stress. Both apparatus will utilize only a few milliliters of slurry and will be able to operate at elevated temperatures.

(a) Slurry-Settling-Rate Apparatus.--Several transducers were used in conjunction with a Sperry UR Reflectoscope to determine the possibility of detecting a settling slurry interface by the reflection of ultrasonic vibrations. These included a quartz transducer manufactured by Sperry Products Corporation,[2] a Branson type Z ceramic transducer, and several barium titanate transducers. While none of the devices were completely satisfactory, results with the ceramic transducer were sufficiently promising to justify continued development. The bottom of a container could be readily detected through plain water, but reflection from the settling slurry interface showed considerable hash. The ability to detect the settling interface appeared to depend not only on the power of the transducer but also on the freedom of the supernatant from stray flocs and the sharpness and density of the settling interface. It is believed that reflection from individual flocs remaining in the supernatant was the most serious source of the reflection that garbled the signal from the interface, but it is also possible that the slurry interface itself attenuated and spread out the reflection.

The quartz transducer was designed by the Sperry Company to fit the slurry irradiation autoclave for use at 300°C and pressures up to 2000 psi. Two transducers were received but one was completely inoperable and the other was received with its protective coating of gold chipped, eliminating tests at elevated temperatures and pressures. At room temperature, the quartz transducer produced a sharp, easily detected reflection from the bottom of the bomb through plain water, but the reflection with a slurry containing 100 g of ThO_2 per liter was too faint and too garbled to be useful.

With a Branson type Z ceramic transducer it was possible to estimate within about 0.5 in. the location of the settling slurry interface. The signal appeared to be much more powerful than that produced by quartz. A transducer of this type, mounted for use with the slurry irradiation autoclave at elevated temperatures and pressures, is being ordered. With this transducer, the temperature will be limited to 230°C, however.

For barium titanate transducers with frequencies of 2.5, 5, and 10 Mc there was no significant change in the quality of the reflected signal as a function of frequency, although theoretically the individual flocs in the slurry supernatant should be invisible at a sufficiently low frequency.

(b) Rolling-Ball Slurry Viscometer.--The necessity of determining the effect of radiation on the rheological properties of slurries prompted the development of a slurry viscometer that could use a small volume of slurry. Effort was directed toward a falling-rolling-sphere viscometer even though literature on the application of this type of viscometer to non-Newtonian fluids is scant, and the theoretical treatment is much less developed than that of the capillary viscometer. A reasonably extensive semitheoretical development of the rolling-sphere viscometer is given by Hubbard and Brown[3] for Newtonian fluids, and a short, predominantly empirical, treatment of the falling-sphere viscometer is presented by Williams and Fulmer[4] for non-Newtonian fluids. It is believed that the limitations of the falling-sphere viscometer will be offset, however, by the simplicity and rapidity of the operating procedure, the adaptability of the equipment to remote operation, and the small size of the slurry sample required (less than 10 ml). Preliminary results with slurry have been encouraging.

The equipment consists of a precision-bore stainless steel tube (Fig. 18.1) which is filled with the fluid to be tested and through which a magnetic steel sphere rolls or falls. The sphere is held at one end of the tube by a d-c electromagnet during positioning of the tube after stirring. Inductance coils are wrapped around the tube at several spacings along its length. When the ball passes through the coils during its fall, the change in inductance is detected and recorded as a function of time by a Sanborn recorder with a limit of resolution of about 0.05 sec.

The viscometer tube is pivoted on a rotating shaft which permits the tube to be rocked by hand for stirring and which can be stopped quickly at one of a set of predetermined angles. Stirring inside the tube is enhanced by allowing the ball to roll freely during rocking of the viscometer through 180° from the vertical.

The effective shear rate at which a viscosity determination is made can be varied by changing the size of the sphere and the angle of fall. Since the detection and holding systems for the sphere are

magnetic, the composition, and hence density, of the sphere is restricted to that of the iron alloys.

The viscometer has been calibrated with ethyl ether, chloroform, water, and water-glycerol mixtures for chrome steel spheres of 0.1885, 0.208, and 0.225 in. diameter in a tube of 0.2425 in. ID at angles from 5 to 90° from horizontal (Fig. 18.2). The reproducibility of the terminal velocity measurements on Newtonian liquids is approximately ±5%. Under conditions of highly turbulent flow (i.e., tests at high angles of inclination with chloroform) with the larger spheres, the viscometer behaves in an anomalous but reproducible manner. It seems possible to circumvent this difficulty by using a smaller sphere or a lower angle of inclination.

Terminal velocities through slurries of DT-7-650 thoria at concentrations of approximately 100 and 200 g per liter of H_2O were reproducible within ±10%, and empirical comparison with the Newtonian-fluids calibrations gave effective viscosities of 1.3 and 2.5 centipoises. No yield stress was detected.

Determination of terminal ball velocities at low angles of inclination is hindered since the short settling path allows the slurry to settle in several seconds. The effect of elapsed time on the region of usefulness of the viscometer is shown in Fig. 18.3. At very low angles (5°) the settled slurry bed will often stop the sphere from rolling because the bed distributes along the tube instead of collecting at the bottom.

It is planned to investigate further the influence of slurry concentration, temperature, and thoria calcination temperature on the operability of the viscometer and the interpretability of the measurements. Equipment for rocking the viscometer mechanically, setting the angle very rapidly (within 1 sec), and heating the viscometer has been designed and is being constructed.

18.2 GAS RECOMBINATION STUDIES

Effort to develop a catalyst for the internal recombination of radiolytic gas in thorium oxide slurries continued with further studies on the effect of pumping at elevated temperature on the catalytic activity of slurries containing MoO_3 and palladium. The results with MoO_3 indicated that reducing conditions were more favorable for high catalytic activity and that pumping under oxygen impairs catalytic activity to some extent. Catalytic activity of a slurry of solids containing palladium recovered from a pumped slurry showed a maximum catalytic activity around 200°C. Oxygen in excess of the stoichiometric amount appeared to enhance catalytic activity while excess deuterium had relatively little effect. The work on the MoO_3 was carried out as a joint effort between the Chemical Technology and Reactor Experimental Engineering Divisions; the palladium work was in cooperation with the Westinghouse PAR group.[5]

18.2.1 MoO_3 Catalysis

The high-temperature loop study (BS-24) being carried out[6] at 200°C under both oxygen and deuterium atmospheres to determine the effect of loop conditions on the handling characteristics and catalytic activity of a slurry containing a MoO_3 catalyst was completed. The slurry (450 g of Th per kg of D_2O) was prepared from 1600°C-fired oxide and pumped for 200 hr under an oxygen atmosphere before the addition of 0.008 m MoO_3. Subsequently, the slurry containing MoO_3 was pumped an additional 300 hr under oxygen, some 500 hr under deuterium, and finally 300 hr again under an oxygen atmosphere. Samples of the slurry were withdrawn from time to time and used in gas recombination experiments in small stainless steel autoclaves. Fresh materials were added during the course of the run as the slurry became depleted because of sampling. At about 800 hr of total pumping time, the MoO_3 concentration was increased to 0.012 m.

The principal effect noted during the initial pumping of the slurry under an oxygen atmosphere was the development of an "induction period" before maximum catalytic activity was achieved.[6] The slurry was apparently deactivated on pumping under oxygen and reactivated when placed in a $D_2 + 1/2\ O_2$ atmosphere in the recombination tests. Substitution of deuterium for oxygen in the loop eliminated the induction period. The second pumping under oxygen appeared to have little effect on recombination activity, the induction period, if present at all, being only a few seconds in duration. All rates observed, after maximum catalytic activities were achieved in the out-of-pile tests, were in excess of the 2 moles of D_2 per hour per liter of slurry at 100 psi D_2 partial pressure and temperatures of 280°C or less, which is a satisfactory rate for an internal recombination catalyst (Table 18.3).

Recombination experiments were performed in groups of three for each slurry sample. Deuterium and oxygen were added at room temperature for each experiment, the reaction autoclaves were brought to temperature, and the recombination rate was followed by the decrease in total pressure. In the first experiments with the samples from the initial pumping under oxygen, the reaction rate was relatively slow and decreased with increasing pumping time. In the third experiments with the same samples, the reaction rate decreased from 3.7 moles D_2/liter-hr at 280°C and 100 psi D_2 partial pressure, for the sample of slurry obtained 19 hr after the addition of MoO_3 to the loop, to 2.5 moles D_2/liter-hr under the same conditions for the loop slurry sample obtained 168 hr later.

The reaction rate (for the first experiments) after 3 hr of pumping under deuterium was 4.6 moles D_2/liter-hr at 280°C and 100 psi D_2 partial pressure, which increased after 307 hr of pumping to 7.3 moles D_2/liter-hr at 217°C and the same deuterium partial pressure (see Table 18.3). The pickup of corrosion products and their reduction may have contributed to the increasing reaction rate.

Table 18.3. Effect of Pumping on Catalytic Activity of ThO_2 Slurries Containing MoO_3

450 g of Th per kg of D_2O, 1600°C-fired ThO_2, loop at 280°C

Total Pumping Time (hr)	Loop Atmosphere	Time of Pumping in Indicated Atmosphere (hr)	Recombination Experiment Temperature (°C)	Recombination Rate, P_{D_2} = 100 psi (moles D_2/liter-hr)
		0.008 m MoO_3		
214	O_2	19	280 280	2.9[a] 3.7[b]
401	O_2	187	280 280	0.1[a] 2.5[b]
488	D_2	3	280	4.6
795	D_2	307	217	7.3
		0.012 m MoO_3		
943	D_2	148[c]	149	4.3
1077	O_2	95	200	4.5
1269	O_2	192	180	4.3

[a]First gas recombination experiment.

[b]Third gas recombination experiment.

[c]MoO_3 concentration increased to 0.012 m and pumping continued 148 hr in D_2 atmosphere.

While under reducing conditions, the MoO_3 concentration was increased to 0.012 m MoO_3 (after 795 hr total pumping time) and pumping continued for 14 hr under deuterium without much effect on the reaction rate. At this point the deuterium atmosphere was replaced with an oxygen atmosphere. The reaction rate after pumping 94.5 hr in the second oxygen atmosphere was 4.5 moles D_2/liter-hr at 200°C and P_{D_2} = 100 psi, and after 192 hr, the rate was 4.3 moles D_2/liter-hr at 180°C and the same partial pressure.

The deactivation of the MoO_3 during the initial pumping under oxygen deserves serious attention if one thinks of using a reactor slurry under oxidizing conditions. Pumping the slurry in a reducing atmosphere did serve to stabilize the catalyst somewhat so that subsequent oxygen treatment did not have a great effect, within the limitations of the experiment, but it is not known how long such a stabilization will be effective. The catalyst was reactivated by the deuterium and oxygen gas mixtures used in the recombination tests, but these were added at total pressures up to 900 psi at room temperature. Lower partial pressures of deuterium and oxygen such as would be present in a reactor slurry might not activate the catalyst at the same rate or to the same extent. An in-pile experiment[7] with a slurry containing MoO_3 showed some reactivation by radiolytic gas, but the slurry attained only about 10% of the recombination activity expected from the results of out-of-pile tests.

18.2.2 Palladium Catalysis

Experiments with palladium catalysts in ThO_2 slurries were carried out with a 515 g of Th per kg of D_2O slurry of solids recovered from a Westinghouse loop run of 552 hr duration carried out at 230°C and in an argon atmosphere. The initial ThO_2 was fired at 650°C and the recovered solids contained 3 wt % U, 122 ppm palladium, 2395 ppm iron, 1400 ppm acid insolubles. The uranium had been added to the loop slurry as UO_3, and the palladium was added from a stock thorium oxide prepared by reducing the palladium on the surface.[8] Reaction rates of stoichiometric D_2-O_2 mixtures (400 psi) in the reconstituted slurry were determined without pretreatment of the slurry and also after heating in deuterium and in argon atmospheres for 20 hr at 270°C. There were no important differences in the results with these slurries; therefore only the results obtained with the slurry preheated in argon prior to the recombination tests will be reported.

The recombination rates with the slurry preheated in argon decreased from 3.7 moles D_2/liter-hr at 200°C and 100 psi D_2 partial pressure to 0.9 mole D_2/liter-hr at 280°C and the same partial pressure (Table 18.4). At 280°C the rate increased rapidly near the end of the reaction (Table 18.5), leading to speculation that the rate might be dependent on either the total gas pressure or the ratio of the reacting gases. Results of changing pressure and D_2/O_2 ratios indicated that the result was probably not the result of a change in total pressure but rather to the presence of an oxygen-rich gas mixture (i.e., $D_2/O_2 < 2$) near the end of the recombination. Decreasing the D_2/O_2 ratio from 2 to 1.25 increased the rate at 280°C and 100 psi D_2 partial pressure from 0.4 mole D_2/liter-hr to 5.1. Deuterium in excess of the stoichiometric amount appeared not to affect the rate.

A joint program with the REED corrosion group is under way to investigate the effect of pumping on the catalytic properties of a slurry containing a palladium catalyst.

Table 18.4. Effect of Variables on Reactivity of a Thorium-Uranium Slurry Containing Palladium

Slurry:[a] 515 g of Th per kg of D_2O, 650°C-fired ThO_2; 15.45 g of U per kg of D_2O as UO_3; 122 ppm Pd (based on solids); slurry treated 20 hr at 270°C in argon (300 psi at room temperature)

Reaction Temperature (°C)	Total Gas Pressure, 25°C (psi)	D_2/O_2 Ratio	Recombination Rate, P_{D_2} = 100 psi (moles D_2/liter-hr)
130	600	2.0	0.9
200	600	2.0	3.7
239	600	2.0	3.0
260	600	2.0	2.2
280	600	2.0	0.9
280	300	2.0	0.3
280	600	2.0	0.9
280	600	2.0	0.4 (major portion of gas) 2.1 (near completion)
280	900	2.0	1.3
280	600	3.0	0.5
280	600	2.0	0.4
280	600	1.5	Explosion
280	600	1.25	5.1
280	600	1.00	Reacting gases consumed below 280°C

[a]Slurry reconstituted with solids recovered from Westinghouse loop slurry pumped at 230°C in argon atmosphere for 552 hr.

Table 18.5. Effect of Firing Conditions on Leaching of Uranium in Thorium-Uranium Oxide Slurries at 280°C

Slurry: 450 g of Th per kg of H_2O; U/Th = 0.08; prepared by carbonate method; 1050°C firing; heated 20 hr at 280°C

Firing Time (hr)	Firing Atmosphere	U in Supernatant (ppm)	
		Slurry as Prepared	With 400 ppm Cr
2	Air	108	1870
8	Air	53	1520
72	Air	19	1050
4	H_2	20	1750

18.3 URANIUM LEACHING STUDIES

Appreciable quantities of uranium have been leached from thorium-uranium oxide pumped as aqueous slurries in high-temperature loop studies, presumably the result of a buildup of soluble chromium and a decrease in pH accompanying the corrosion process. A laboratory investigation was initiated to determine the effect of oxide preparation method and electrolyte concentration on the leaching of uranium from mixed oxides by aqueous solutions at reactor temperature. With a thorium-uranium oxide containing U/Th = 0.08, fired 72 hr at 1050°C, a negligible amount of uranium was solubilized by treating the mixed oxides with water alone at 280°C, but a solution containing a few hundred ppm of chromate (added as chromic acid) leached uranium from the solid at 280°C, the amount increasing with increasing chromium concentration from 125 to 1330 ppm. The ratio of ppm U to ppm Cr in the supernatant over this concentration range was about 2.6. The amount of uranium leached depended to some extent on the oxide-firing conditions. There was also evidence from the laboratory studies that the past history of the autoclave, toroid, or loop in which the thorium-uranium oxide slurry is handled may considerably affect the amount of uranium which appears in the supernatant during high-temperature operation.

The thorium-uranium oxide was prepared by the "carbonate" preparation method[1] in the laboratory, the uranium being deposited on a 650°C-fired oxide from ammonium uranyl carbonate solution (solution decomposed by heating) and the resulting mixture fired at 1050°C. A long-term leaching study at 200 and 280°C was carried out in a 1-liter stainless

steel autoclave with a 300 g Th/kg H_2O slurry (no chromic acid added) of the oxide fired 4 hr at 1050°C. Samples were withdrawn at approximately 20-hr intervals over a 230-hr operation, 170 hr at 280°C followed by 60 hr at 200°C. Short-term runs – 20 hr at 200°C with 300 psi O_2 overpressure (added at room temperature) – were carried out in small stainless steel autoclaves with 450 g of Th per kg of H_2O slurries of the mixed oxide as prepared and after the addition of chromic acid.

A sample of supernatant withdrawn from the long-term operations at 210°C during the initial heating of the autoclave (2.3 hr) showed 15 ppm of soluble uranium in the slurry supernatant, but samples withdrawn at 20-hr intervals, to 170 hr, with the slurry at 280°C showed only 2 ppm of soluble uranium. Subsequent heating for an additional 60 hr at 200°C appeared not to increase the amount of soluble uranium.

In the short-term leaching experiments with slurries of the mixed oxide fired 72 hr at 1050°C (450 g of Th per kg of H_2O) in chromic acid solutions, about 80% of the added chromate remained in the slurry supernatant after 20 hr of heating at 280°C, and the ratio of soluble uranium to chromium was 2.6 ± 0.4 over the supernatant chromium-concentration range of 125 to 1330 ppm. Final pH values ranged from 2.1 (for the high chromium concentration) to 4.0. With 2- and 8-hr oxide firing at 1050°C and firing in H_2 as opposed to air, the amount of uranium leached from the solid increased (Table 18.5). Heating slurries, to which no chromic acid was added, in used autoclaves resulted in soluble uranium contents high as compared with those in the long-term study (Table 18.5). Chemical analysis of these supernatants showed less than 3 ppm chromium, and the high uranium solubilities are at present unexplained.

18.4 BORON ADSORPTION STUDIES[9]

In the startup of a homogeneous one-region slurry reactor it would be advantageous to keep the system noncritical under all conditions until all the slurry had been added and operating conditions reached. One technique would be to add enough soluble poison, such as boron, to the slurry to prevent criticality, the boron being removed when operating conditions were reached. Calculations based on the current slurry reactor concept indicate that if the mole ratio of boron to total thorium plus uranium is 0.02 in a slurry of mixed oxide with U/Th = 0.1 the reactor will not go critical.[10] To investigate the possibilities of using such a method of reactor operation, the adsorption of boron, added as boric acid, on thorium-uranium oxide slurry solids was studied over the temperature range 100 to 300°C, using mixed oxides fired at 650 and 1100°C.

With a slurry (270 g of Th per kg of H_2O) of the 650°C fired mixed oxide and initial boron concentration some 33% in excess of the amount required for noncriticality (370 ppm boron in supernatant) the minimum solids/supernatant distribution (see Fig. 18.4) was at about 200°C, the expected reactor operating temperature. At this temperature the ratio,

grams of boron per gram of solid to grams of boron per gram of water, was 0.6 and the solids boron content was 0.017 mg per gram of solid. With the 1100°C-fired oxide and the same temperature and slurry composition, the boron content of the solids was negligible and very much less than the 0.029 milligrams of boron per gram of solids which could be tolerated during reactor operation, i.e., 1% neutron loss (Fig. 18.4). Below 100°C where significant amounts of boron were adsorbed, the amounts adsorbed were approximately proportional to the decrease in surface area of the oxide.

The mixed oxides were prepared by the carbonate preparation method, with 4-hr firings at 650 and 1100°C. Boric acid was added to a slurry (270 g of Th per kg of H_2O) of the mixed oxide, and the slurry was brought to temperature in a stainless steel autoclave. A preliminary experiment indicated that distribution of the boron at 100°C reached equilibrium in 16 hr, and distribution data in the temperature range 100 to 300°C were obtained after 16 hr heating at temperature.

The amounts of boron adsorbed in the slurry solids are plotted in Fig. 18.4 as a function of the temperature at which the slurry was equilibrated. The equilibrium amounts adsorbed in the 1100°C-fired oxide at temperatures above 60°C are less than the minimum permissible amount for reactor operation. The soluble uranium in all supernatants from both the 650 and 1100°C-fired mixed-oxide slurry equilibrations contained less than 2 ppm of soluble uranium; the pH's of the supernatants were between 7.3 and 7.65.

Desorption studies with the 650°C-fired oxide are in progress. At around 200°C, equilibrium desorption was attained in about 2 hr, with approximately 30% of the boron appearing in the supernatant. It appears from these preliminary data that the use of boron as a soluble poison in slurries of low-fired mixed oxide would not be feasible. It should be possible, however, to readily remove a boron poison from a reactor slurry system of 1100°C-fired mixed oxide.

18.5 OXIDE PREPARATION DEVELOPMENT

Oxide preparation development studies included further work on particle-size control in the oxide production facility at the Pilot Plant, continued development of flame denitration methods for the production of mixed thorium-uranium oxides, and further work on the production of thoria spheres by the fluidized-bed denitration of thorium nitrate solutions.

18.5.1 Particle Size Control

In order to gain better control over the particle size of the thorium oxide prepared by the Thorium Oxide Facility for the Homogeneous Reactor Project, operating conditions have been standardized for the

past several months.[11] This program has resulted in the consistent production of thorium oxide in the desired 2- to 3-micron average particle size.

All the runs tabulated were made in the regular Thorium Oxide Facility equipment located in Building 3019. The equipment is essentially as described in a previous report.[12]

Since particle size is known to be dependent on solution concentration, precipitation temperature, reagent mixing rate, and degree of agitation, and possibly other conditions, it was desirable to fix all the known variables except one. For simplicity of operation, the rate of addition of oxalic acid to the thorium nitrate solution was chosen as the variable. A list of the fixed conditions follows.

Oxalic acid solution: 257 gal, 0.7 ± 0.02 M

Thorium nitrate solution: 117 gal, 0.7 ± 0.02 M

Precipitation temperature: 30 ± 1°C

Agitation: 431 rpm, 8-in. semi-turbine impeller in draft tube with side slots completely open and bottom area 50% open (see p 12, ref. 12)

After precipitation, the oxalate slurry was digested for either 48 hr at 85°C or 6 hr at 95°C. The slurry was then filtered and the thorium oxalate cake converted to the oxide by calcination at either 650 or 800°C, depending on the end use.

The geometric mean particle sizes for various oxalic acid flow rates are given in Table 18.6 and plotted in Fig. 18.5. The present operating procedure and controls used in the Thorium Oxide Facility can produce 185-lb batches of thorium oxide having geometric mean particle diameters within ±0.3 μ of any chosen size between 2 and 3 μ. The geometric standard deviation of the product will be approximately 1.30. It is believed that the present data can be successfully extrapolated to cover the size range 1.5 to 4.0 μ with only oxalic acid flow rate as the variable.

18.5.2 Flame Denitration

Preparation of test quantities of thorium-uranium oxide (U/Th = 0.08) by the flame denitration of alcohol solutions of thorium-uranium nitrates continued. Flame temperatures were varied between 800 and 1600°C at 200°C intervals. In some runs, palladium as palladium nitrate and molybdenum as a nitrate solution of ammonium molybdate were added to the feed. The mixed oxide products had surface areas between 6.2 and 7.8 m^2/g and average particle sizes between 0.8 and 3.1 μ (Table 18.7).

Table 18.6 Particle Size Control in Large-Scale Production of Thorium Oxide

Run	Oxalic Acid Flow (gpm)	Mean Size (μ)	Standard Deviation
30	1.6	3.7	1.29
31	3.1	2.5	1.34
32	3.1	2.8	1.36
33	3.6	3.1	1.29
34	3.5	2.6	1.37
35	4.3	2.5	1.27
36	5.5	2.2	1.30
37	4.1	2.7	1.30
39	4.7	2.8	1.40
40	6.6	2.1	1.39
41	6.5	2.0	1.42
42	6.4	2.0	1.35
43	6.6	2.1	1.40
44	6.0	2.1	1.43
45	6.0	2.2	1.34
46	5.9	2.1	1.28
47	5.9	2.0	1.30
48	5.8	2.0	1.30
49	6.3	1.9	1.37
50	6.0	2.1	1.28
51	6.0	2.1	1.31

Table 18.7. Flame Denitration Preparation of Thorium-Uranium Oxide

CH_3OH solution of 158 g $Th(NO_3)_4 \cdot 4H_2O$, 12 g $UO_2(NO_3)_2 \cdot 6H_2O$ per liter

Feed rate, 15 to 25 ml/min

Fuel gases, C_3H_8 with air or cylinder O_2

Reflector, MgO

Run	Estimated Reflector Temperature (°C)	Reflector Position	Calculated Additive Concentrations in Product (ppm)	Product		
				Amount (g)	d_{50} (μ)	Surface Area (m^2/g)
41	1550	Horizontal	None	27.5	2.7	6.5
42	1500	Horizontal	None	190	2.7	6.3
43	1000	Horizontal	None	70	3.1	6.7
44	800	Horizontal	None	15	1.8	6.9
45	1200	Horizontal	None	312	0.77	---
46	1000	Vertical	None	233	3.1	7.6
47	800	Vertical	None	161	2.5	6.5
48	1400	Vertical	5000 ppm MoO_3*	162	2.5	6.2
49	1200	Vertical	5000 ppm MoO_3*	262	2.5	7.7
50	1400	Vertical	300 ppm Pd**	143	2.5	7.7
51	1200	Vertical	300 ppm Pd**	244	2.5	7.8

*Added as an ammonium molybdate solution

**Added as palladium nitrate

Initial toroid tests were carried out by the REED slurry-corrosion group at slurry concentrations of 170 and 340 g of Th per kg of D_2O, with a thorium-uranium oxide prepared by flame denitration at 1550°C. Under O_2 overpressure, the 347 stainless steel corrosion rates at 280°C and 26 fps linear velocity were 3.8 and 2.3 mpy, respectively (Table 18.8); particle size distribution was not significantly affected, and uranium solubilities in the supernatants were 12 and 18 ppm. With a D_2 atmosphere, the corrosion rates for similar slurries were 7.4 and 4.8 mpy, and the uranium solubility in the supernatant with the more concentrated slurry was 42 ppm. Agglomeration occurred in the D_2 runs, the size fraction >3 μ increasing from 1 to 70% in the dilute slurry and the size fraction 1-3 μ increasing from 52 to 82% in the more concentrated slurry.

Two significant equipment improvements were made. The reflector was raised from a horizontal to a vertical position, eliminating plugging caused by the settling of large particles from the combustion-gas stream to the bottom of the reflector. The burner was also redesigned so that the entering alcohol stream was directed into the point of highest flame turbulence. The improvement obtained may be appreciated by comparing the quantities of material obtained between duplicating runs (Table 18.7: runs 43 vs 46, and 44 vs 47). Improved control of the average particle size of the product is also evident.

18.5.3 Fluidized-Bed Denitration

Fluidized-bed denitration of $Th(NO_3)_4$ was studied for producing dense 50-to 500-μ ThO_2 particles. Porous agglomerations of small ThO_2 particles were produced for all conditions tested, instead of growth by addition of dense ThO_2 layers on particles. Bed "bogging" or caking was also a problem, particularly at temperatures of 500°C or lower.

A 3-in.-dia IPS Inconel reactor was installed with feed, exhaust, and control systems (Fig. 18.6). The $Th(NO_3)_4$ was fed as a solution to a spray nozzle with a flow of atomizing-aspirating gas below the surface of the fluidized bed. A solids feed tank, a continuous product classifier-takeoff and sintered-metal filters with blowback connections were part of the reactor installation.

Normal operating procedure was to spray 10 to 15 ml/min of feed solution into the 400 to 700°C fluidized bed. Sintered ThO_2 agglomerates larger than 325 mesh (d_{50} of about 75 μ) were used as the fluidized bed for initial tests. This irregular, high-density material fluidized poorly, and 53- to 250-μ-dia sand was used for later studies. Superficial air velocities in the bed were 0.8 to 1.3 fps.

Porous agglomerations of small ThO_2 particles were produced under all conditions tested. This is believed to be the result of denitration of the solution before it could form a fluid coating on bed particles. When temperatures were lowered to lower the rate of

Table 18.8. Toroid Results* on Th-U Mixed Oxides: 1550°C-Fired Oxide

Toroid conditions: operating temperature, 280°C; exposure time, 300 hr; velocity, 25.9 fps; U/Th ratio, 0.044

Atmosphere	Slurry Conc. (g of Th per kg of D_2O)	Particle Size Distribution, % in Indicated Size Range				Corrosion Rate (mpy)				Uranium Solubility in Supernatant (ppm)
		>3 μ	1-3 μ	0.5-1 μ	<0.5 μ	347 SS	Ti-75A	Inconel	Zr-2	
Initial		5	52	31	12					
O_2	170	1	54	36	9	3.8	0	36	+ (wt gain)	12
D_2	170	70	26	4	0	7.4	2.8	1.3	+	
O_2	340	7	49	37	7	2.3	+	16	+	18
D_2	340	8	82	7	3	4.8	1.3	1.3	+	42

*Performed by REED Slurry-Corrosion Group.

denitration, bed bogging or caking occurred. Caking occurred at any temperature tested for the ThO_2 bed and 1.5 M $Th(NO_3)_4$ in H_2O. Use of 1.5 to 1.8 M $Th(NO_3)_4$ in CH_3OH-H_2O solutions supplied heat as a result of the combustion of the CH_3OH by the fluidizing air, thus apparently eliminating the caking problems. With 1.85 M $Th(NO_3)_4$ in H_2O, the fluidized sand bed operated well at 700°C, poorly at 500°C, and caked quickly at 400°C. The formation of ThO_2 fines was also indicated by rapid plugging of the off-gas filters during use of CH_3OH-H_2O solution feeds or during use of the aqueous feed solution at 700°C.

The ThO_2 product from operation with the sand bed contained 550, 3400, 5100 ppm of nitrate at temperatures of 700, 500, and 400°C. About 75% of the ThO_2 formed at 700°C was present in 20- to 270-mesh fractions, according to screen analyses; however, these agglomerations were easily broken up in H_2O to release 0.5- to 20-μ particles of ThO_2.

18.6 THORIUM OXIDE PRODUCTION

Eighteen 30°C-precipitations, DT-36 through DT-55, were made in order to prepare approximately 3461 lb of calcined thorium oxide.

One precipitation (run 38) was made at 70°C to prepare 95 lb of product, for a total of approximately 3556 lb of thorium oxide. Seven hundred fifty pounds was calcined at 1600°C and classified to 95% less than 5 μ. Approximately 2800 lb of the 650°C-calined thorium oxide was used for preparing mixed oxide, containing approximately 8% of depleted uranium, calcined to 1050°C and classified to 95% less than 5 μ. The intended particle size of all runs except that of run 38 was 2.5 ± 0.3 μ. The run-38 product was approximately 7.0 μ in average particle size. The average particle size was satisfactorily controlled throughout the entire set of runs by maintaining an oxalic acid flow to the precipitator of 4.5 to 5 gal/min.

Twenty-two hundred pounds of thorium oxide was shipped to Y-12: 1200 lb of pure thorium oxide, 100 lb of coprecipitated, 0.5% natural uranium, and 900 lb of mixed oxide, approximately 8% in depleted uranium. Ammonium hydroxide replaced oxalic acid as the dispersing agent in classification.

REFERENCES

1. J. P. McBride, et al., HRP Quar. Prog. Rep. October 31, 1958, ORNL-2654, p 202.

2. Final Report, Houdry Process Corporation, Subcontract 904 under W-7405-eng-26, 58-OCR-15, p 42.

3. R. M. Hubbard and G. G. Brown, "The Rolling Ball Viscometer," Ind. and Eng. Chem., Analytical Ed. Vol. 15, No. 3, p 212-218.

4. J. C. Williams and E. I. Fulmer, "The Evaluation of Yield Value with the Sphere Viscometer," J. App. Phys. 9 (Dec. 1938).

5. The PAR Project ceased operation in December, 1958.

6. J. P. McBride, et al., HRP Quar. Prog. Rep. October 31, 1958, ORNL-2654, p 204-205; E. L. Compere, et al., ibid., p 125-126.

7. In-Pile Slurry Autoclave Experiment L6Z-127S: see Sec. 12.3.2, this report.

8. D. E. Byrnes and W. O. Fletcher, PAR Quar. Prog. Rep., May 31, 1958, WCAP-900, p 51. (Cf. also S. A. Reed and J. P. McBride, HRP-58-461).

9. D. W. Jeffrey and W. L. Brassert, MIT student problem, Report EPS-X-401.

10. R. N. Lyon, personal communication.

11. K. O. Johnsson and C. V. Ellison, Control of Thorium Oxide Particle Size, ORNL-CF-59-1-101.

12. R. L. Pearson et al., Preparation of ThO_2 for Homogeneous Reactor Blanket Use, ORNL-2509

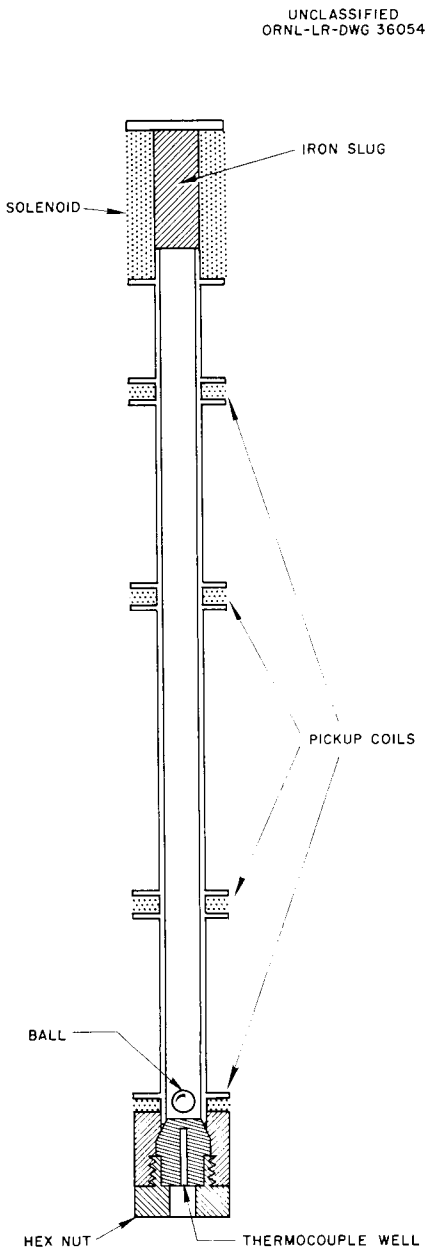

Fig. 18.1. Cross-Sectional Drawing of Viscometer.

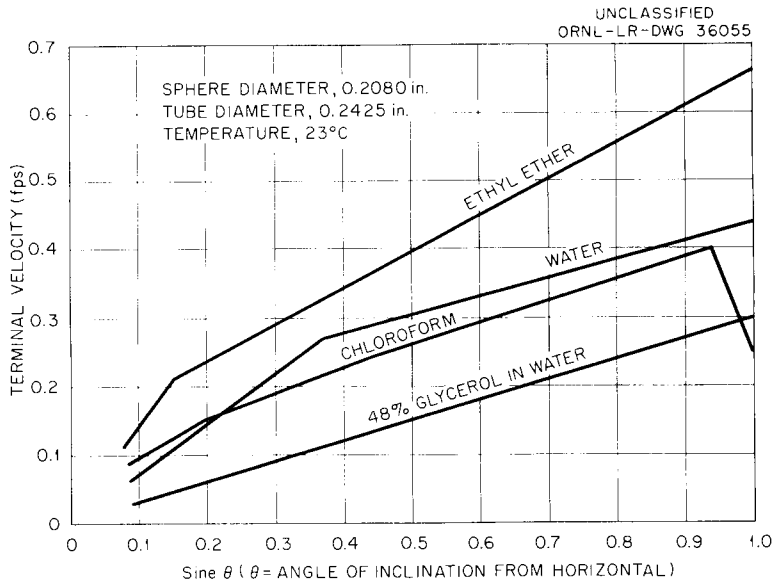

Fig. 18.2. Effect of Angle of Inclination, θ, on the Terminal Velocity of a Sphere Falling Through Newtonian Fluids.

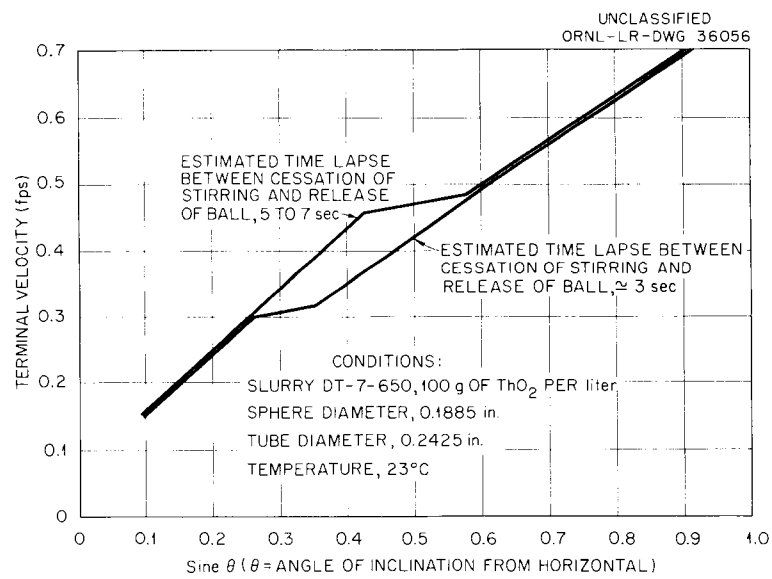

Fig. 18.3. Effect of Angle of Inclination on the Terminal Velocity of a Sphere Falling Through a Thoria Slurry.

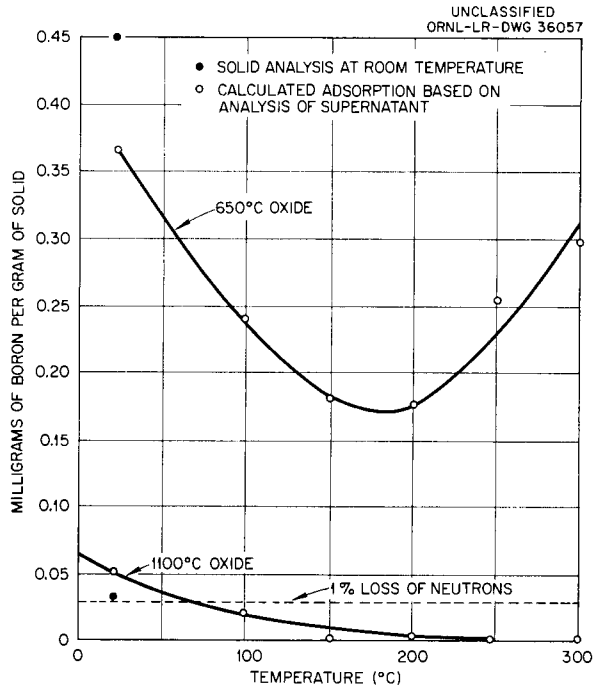

Fig. 18.4. Boron Distribution in Thorium-Uranium Oxide Slurries. Conditions: U/Th = 0.08; 270 g of Th per kg of H_2O; 370 ppm of boron per kg of H_2O.

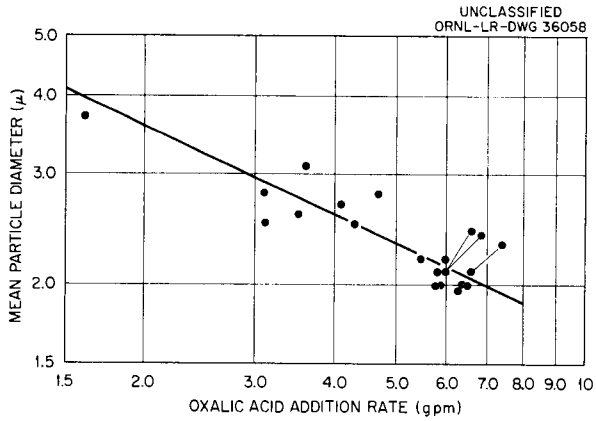

Fig. 18.5. Particle-Size Control in Oxide Production: 650–800°C-Fired Oxide.

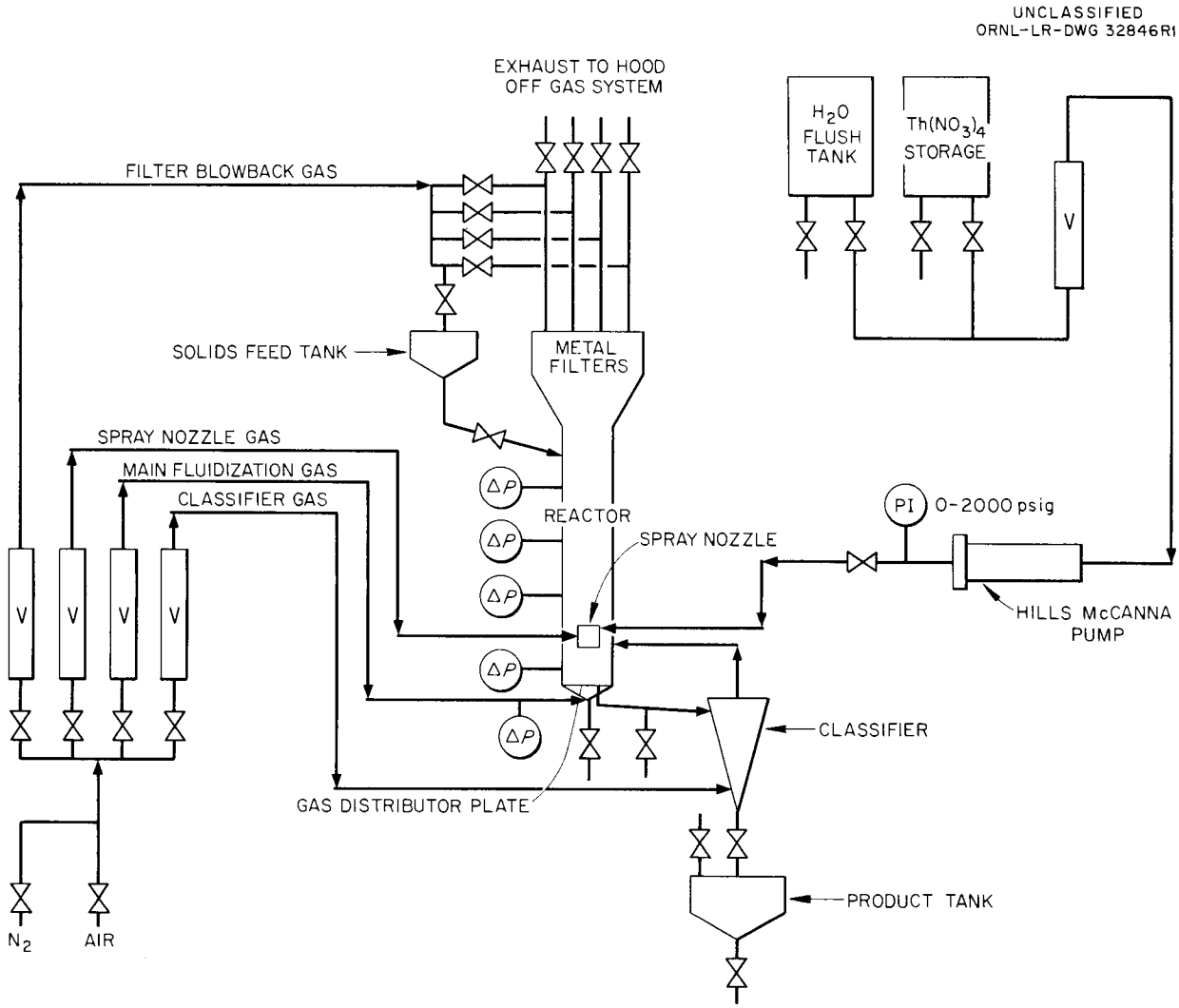

Fig. 18.6. Process Flowsheet for the Fluidized-Bed Denitration of Thorium Nitrate.

19. IN-PILE SLURRY LOOP

W. E. Unger

T. A. Arehart
J. W. Brown, Jr.
P. A. Haas
L. J. King
B. B. Klima
W. F. Schaffer, Jr.
L. B. Shappert
J. W. Snider
W. M. Woods

19.1 STATUS OF LOOP AND AUXILIARIES

Consequent to the decision of the PAR project (Westinghouse, Pennslyvania Power and Light) to stop development of their proposed slurry reactor, Westinghouse discontinued work on the in-pile slurry loop. The loop and its auxiliaries, approximately 75% complete, were assembled in one area at Westinghouse, pending crystallization of plans for its disposition. PAR is preparing a detailed design report, essentially a revised version of the Safety Report (WCAP-669), containing a complete schedule of all pertinent drawings and sketches. Reproducible prints of all drawings are to be forwarded to ORNL.

Preparations to accommodate the loop at ORNL were stopped immediately after the Westinghouse announcement. These included design and construction of the facilities at the face of the ORR, estimated to be about 75% complete (excluding the loop unloading cubicle, cell D, which was scheduled for completion in March 1959), and the design and fabrication of specialized tools and equipment for cutting the loop in the segmenting facility.

19.2 LOOP FILLING AND DISCHARGING SYSTEMS

The filling of the in-pile loop with slurry displaced from a tank by gas pressure was not consistently satisfactory during tests at Westinghouse. Discharge of the loop by simple drain-and-flush procedures removed only about 90% of the slurry and required substantial volumes of flush water. Both the loading and the unloading operations basically involve the transfer of the oxide from one tank to another, which can be most practically accomplished with hydroclones operated on a bypass circuit connecting the tanks. Development of such a transfer system would enable the loop operators to charge, remove, and replace

a circulating slurry without discontinuing loop operations.

A three-hydroclone cascade (Fig. 19.1) was selected for mockup testing after a comparison of the computed performance of several simple systems. The charge tank and loop volumes were each represented by stoppered 9-liter glass bottles, agitated by recirculating pumps. The charge tank was filled with 500-g/liter 1600°C-fired ThO_2, and the rest of the system was filled with water. The final charge-tank concentration after 1 hr of operation was 0.52 g/liter, compared with the 2.5 g of ThO_2 per liter computed (Fig. 19.2).

It is believed entirely practical to design a charge system for a slurry loop with a single pump and the three-hydroclone cascade. Satisfactory charge times and end concentrations can be obtained. (See ORNL CF-58-10-90, Chemical Technology Division Unit Operations Section Monthly Progress Report, October 1958 for a more complete discussion of the system.)

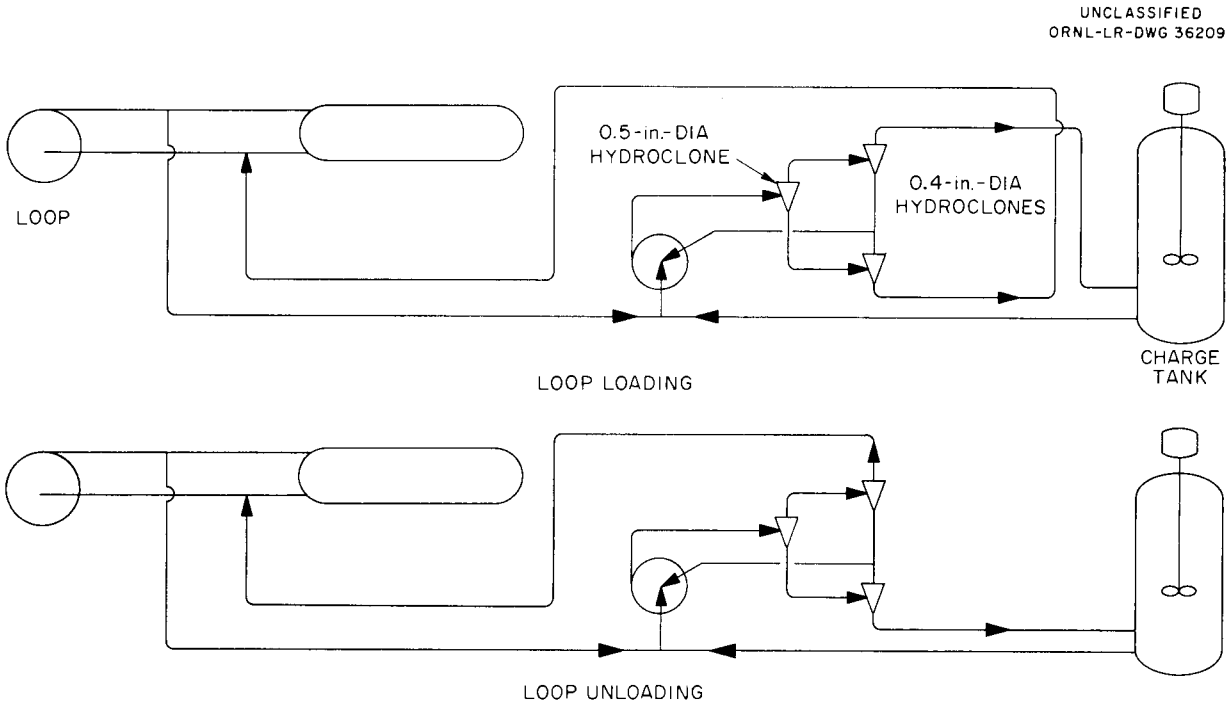

Fig. 19.1. Schematic Diagram of Slurry Transfer by Three-Hydroclone Cascade.

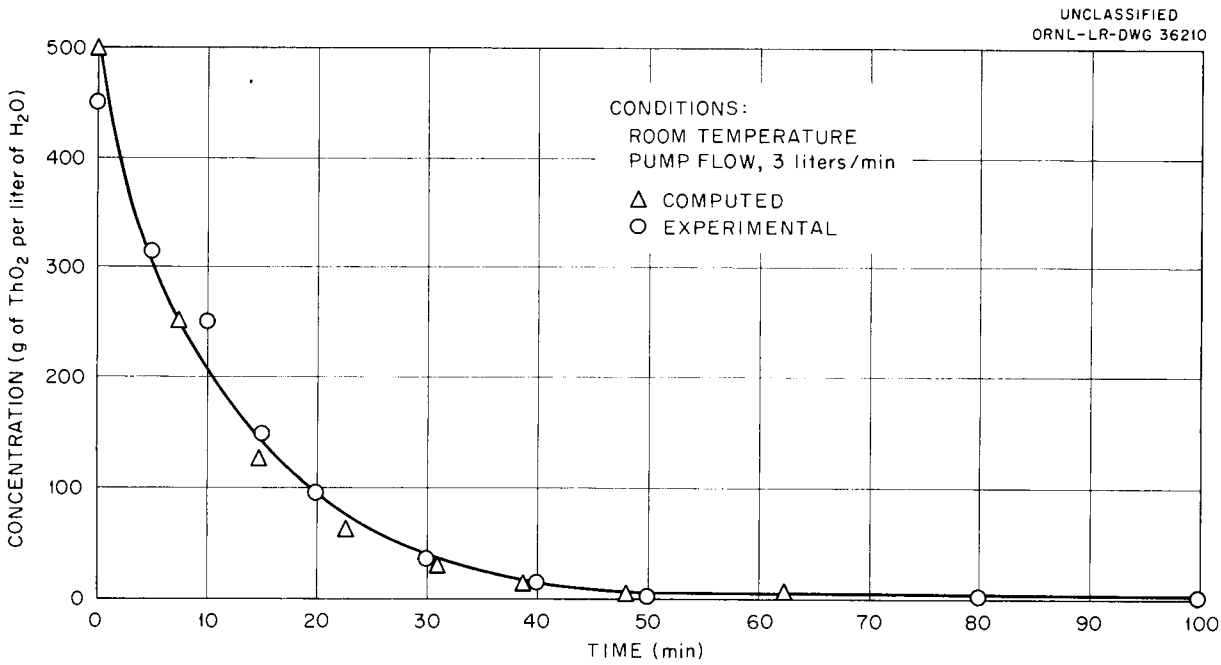

Fig. 19.2. Computed and Experimental Concentrations of ThO_2 in Charge Tank After 1 hr of Operation.

PART VI

SUPPORTING CHEMICAL RESEARCH

H. F. McDuffie

20. AQUEOUS SYSTEMS AT ELEVATED TEMPERATURES

W. L. Marshall

J. S. Gill
G. M. Hebert
E. B. Jones
R. Slusher

Experimental work during the past two quarters has been directed toward the following research programs:

1. the investigation and interpretation of phase-equilibrium data for the five-component system UO_3-CuO-NiO-SO_3-H_2O (D_2O) at 300°C;

2. exploratory and short-range applied studies on aqueous reactor fuel compositions; the effect of extreme temperature gradients within the solutions;

3. comparative solubilities in H_2O and D_2O at high temperature;

4. the investigation of liquid-liquid immiscibility in the system UO_3-SO_3-H_2O from 300 to 350°C;

Detailed reports on several of the above topics are to be issued in the near future. A summary of the current status of each program is given below.

20.1 THE SYSTEM UO_3-CuO-NiO-SO_3-H_2O (D_2O) AT 300°C

Since the summer of 1958, the following approach has been taken in the problem of establishing phase equilibria for the five-component system, UO_3-CuO-NiO-SO_3-H_2O (D_2O), at 300°C. First, a skeletal structure for the solubility relationships is determined, and later the structure is filled in with experimental data if so desired. The mode of attack has been to study those portions of the system in which the degrees of freedom are restricted so that, with a requisite number of identifiable solids, the system equilibrium is defined.

Experimental Approach.--By use of pressure vessels and sampling techniques discussed in previous HRP progress reports, various solutions

were equilibrated with solid phases at 300°C, sampled at temperature through capillary tubing, and analyzed for the solution components. If a particular experimental part of the over-all program consisted in the definition of a ternary curve (i.e., a curve over which solution compositions are in equilibrium with three solids as a function of total SO_3 concentration), then excess amounts of solids were added to solutions of varying SO_3 concentration in order to achieve three solid phases at equilibrium. For these studies of a particular ternary curve the solids at equilibrium were established to be $NiSO_4 \cdot H_2O$, $3CuO \cdot SO_3 \cdot 2H_2O$ (antlerite), and $UO_3 \cdot UO_2SO_4$ (zippeite). Subsequent studies were extended to three four-component systems, UO_3-NiO-SO_3-H_2O, UO_3-CuO-SO_3-H_2O, and CuO-NiO-SO_3-H_2O, to determine binary curves as a function of m_{SO_3}. Over-all skeletal models are being established, incorporating previous data for the three-component systems, CuO-SO_3-H_2O, NiO-SO_3-H_2O, and UO_3-SO_3-H_2O.

The pressure vessels which contain the solution-solid mixtures are rocked for 16 to 20 hr before sampling; however, samples taken at 2 to 3 hr after constant temperature is reached are, for the most part, in agreement with samples taken at the later times. Additional samples have been taken after three days at temperature with no indications that equilibrium was not attained after the 16-hr period. Apparently, supersaturation of solution is not observed since solid phases are always present and rates of equilibrium attainment are faster than at lower temperature. In earlier work at 190°C considerable supersaturation was observed in solutions initially not containing solids. After a run the pressure vessels are cooled, and the solids are removed and are identified by x-ray diffraction.

Experimental runs have been made with both light and heavy water. Heavy-water solutions are prepared from solids or solutions which have been crystallized or concentrated several times from D_2O. Below SO_3 concentrations of 0.1 m there appears to be little difference between H_2O or D_2O in the solubility relationships expressed as saturation moles per mole SO_3.

Experimental data have been obtained for the ternary curve and for three of the binary curves from 0.04 to 0.2 m total SO_3. Data for curves in which one solid phase is present have been obtained from previous investigations of the system UO_3-SO_3-H_2O and from the present investigation of the systems CuO-SO_3-H_2O and NiO-SO_3-H_2O. These data will be included in a report to be issued shortly.

Discussion.--To attempt to calculate precisely the solubility interactions and also to determine which solid will form from a particular composition are formidable if not impossible tasks. Many additional data would be needed to provide assurance that a method of calculation would be successful. Therefore, after critical examinations of all our current and past solubility data, a rough empirical rule is being used to define approximate solution saturation limits. This rule is based upon a concept that HSO_4^- species are the predominant anionic species in solution and

that uranium behaves roughly as a dimer at the higher temperature. The empirical rule follows: If

$$R = \frac{m_{1/2\ UO_3} + m_{CuO} + m_{NiO}}{m_{SO_3}}$$

is less than 0.5 for a specific composition, then this composition remains a complete solution at least to 300°C. This rule is violated at excessively high values of

$$\frac{m_{NiO}}{m_{1/2\ UO_3} + m_{CuO} + m_{NiO}} = R_{NiO}.$$

In cases where R_{NiO} is not excessively high (in all of our HRT applied conditions), the solutions are phase-stable to the liquid-liquid immiscibility temperature. In fact, solutions of HRT composition have been observed to 500°C with no appearance of a solid phase although the second liquid phase does appear at the expected temperature.

Of course the ultimate criteria for solution stability is the actual phase diagram. The solubility data as a function of total SO_3 concentration are used to construct five-component phase diagrams at various fixed concentrations of total SO_3, two of which are shown in Figs. 20.1 and 20.2. Figure 20.1 shows a cube in which the CuO-UO_3 face is in the front plane and $m_{SO_3} = 0.06$ is constant throughout the volume model. For application of a volume model of this sort the initial composition of fuel solution is specified on the front face (i.e., a composition in which nickel as a corrosion product is not present). As corrosion occurs the composition of solution moves into the cube volume (Fig. 20.1) and, depending upon the initial composition point, any one of several solids may be the first to appear at the saturation point. One prime consideration involves picking the composition of the starting solution so that the saturating solid will be $NiSO_4 \cdot D_2O$ or $3CuO \cdot SO_3 \cdot 2D_2O$. In this event, no uranium would be removed from solution but only nickel or copper compounds depending upon the over-all starting composition.

Figure 20.2 shows a projection on the UO_3-CuO plane of a cube volume representing the system UO_3-CuO-NiO-SO_3-D_2O at 0.08 m total SO_3 and at 300°C. The outer curve is on the UO_3-CuO plane, whereas the inner curve originates on the CuO-NiO and UO_3-NiO planes and projects into the cube volume to the ternary point. Saturation concentrations of nickel are indicated in parentheses. A series of curves of this type at different total SO_3 concentrations are used for direct application of the phase-

diagram data. Upon satisfactory completion of this aspect of the research program, better knowledge will be in hand to predict the nature of the solid phases which might be expected to form at saturation and also to state the saturation limits in solution.

20.2 INVESTIGATIONS OF PROBLEMS PERTINENT TO HRT OPERATIONS

Several types of experiments have been performed in order to obtain quick answers to problems directly pertinent to HRT operations. These experiments, for the most part, are short range at this stage and are concerned chiefly with the specific HRT fuel compositions both in the core and in the blanket.

Stability of HRT Fuels from 200 to 500°C.--Experiments were performed to determine the phase stability of particular HRT fuel solutions from 200 to 500°C. The solution compositions were those corresponding to the core and blanket concentrations used in the recent HRT operations. These were 0.025 m UO_3, 0.013 m CuO, 0.003 m NiO, and 0.063 m SO_3 for the core and 0.0079 m UO_3, 0.0042 m CuO, 0.0010 m NiO, and 0.0207 m SO_3 for the blanket. The compositions were investigated in H_2O as well as D_2O to observe any appreciable deviations in behavior. The experiments were carried out both in the absence and presence of an oxygen overpressure. The oxygen overpressure was attained by adding a small amount of cp 30% hydrogen peroxide solution to a quartz capillary tube containing a solution of a particular composition, sealing the tube, and vibrating it at 250°C until UO_4, which precipitated initially, had decomposed to UO_3 and subsequently redissolved in solution. The resulting oxygen pressure was of the order of magnitude of 200 psi. All experiments were carried out in quartz tubes of 2 mm inside diameter. An automatically timed on-off vibrator unit was used for efficient mixing of the solutions. Phase transitions were observed by use of a short-range telescope according to our conventional methods.

The experimental observations indicate that in the presence of an oxygen overpressure a solid phase or phases did not occur in the temperature range of the experiments (200 to 500°C) for either the core or blanket composition. In the absence of an oxygen overpressure a very small amount of a reddish solid or haze appeared in several of the solutions upon cooling the solution from 500°C to room temperature. There is no reason to believe, however, that the reddish solid would not have appeared at a lower temperature on heating if the tubes containing solution were heated at a slower rate. The important point, however, is that in the presence of oxygen, which is an expected condition in the HRT, no solid phases appeared upon rising the temperature at a rate of 3°C per minute to 500°C and after holding the temperature for 16 hr at 500°C. The heavy-liquid phase remained a clear yellow liquid. The critical temperature of the light phase occurred in the expected range, 374°C, as did also the temperature of appearance of the heavy liquid phase (345-350°C for both the core and blanket compositions). A tube containing an HRT core-composition solution with oxygen overpressure was cooled slowly

and also quenched rapidly 8 to 10 times, and no reddish haze or solid was observed under any condition of treatment.

With regard to HRT fuel compositions with oxygen overpressure, these observations indicate the absence of solid precipitates at temperatures considerably in excess of 250 to 300°C if there are no large temperature gradients and subsequent local boiling, thereby causing water transfer within the reactor solution.

Effect of ΔT on Solid-Liquid and Liquid-Liquid Equilibria.-- Suppose that, by means of local boiling or some other deposition mechanism, a concentrated solution or a solid phase, either one containing uranium, appears in solution or on the metal surfaces in the region of high neutron flux. In this event, the temperature of the concentrated solution or solid increases owing to the higher fission density within its volume. The over-all vapor pressure on the system is maintained at a constant value by the saturated water vapor pressure within the pressurizer. When the water vapor pressure from the solid or liquid particle becomes greater than the saturated water vapor pressure in the pressurizer, a vapor space appears around the particle until sufficient water from the particle is transferred to the bulk of the solution to equalize the vapor pressure. The ultimate particle temperature is determined by the rate of heat transfer from the particle through the "vapor lock" to the bulk of solution. If, before pressures are equalized, the liquid or solid particle loses all free water, the rate of heat transfer from particle to liquid will also determine the ultimate temperature of the particle.

Experiments to duplicate the ΔT for these cases have been carried out in inverted U tubes. In one leg of an inverted U tube is placed the solution which will conceivably rise to a higher temperature within the reactor. In the other leg is placed a solution approximating a composition which represents the bulk of the solution. The leg containing the solution bulk is held at a constant temperature to simulate a constant vapor pressure, and the other leg initially containing the same composition is raised in temperature. The ΔT is observed at which a solid crystallizes from solution as a result of its having become concentrated at the higher temperature.

In order to make a preliminary evaluation, H_2O was placed in one leg and was held at 270°C in order to approximate a constant vapor pressure for the bulk of the solution. A UO_2SO_4 solution was placed in the other leg. A solid appeared in the UO_2SO_4 solution at 290-300°C, thus indicating that for aqueous UO_2SO_4 solutions pressures cannot be equalized between a concentrated and dilute solution to a greater extent than about 25°C in temperature equivalency before a solid phase will appear from concentrated solutions. The temperature of UO_2SO_4 solid was raised to 880°C and held at that temperature for 36 hr (in the presence of 270°C water vapor pressure) with only a slight decomposition to U_3O_8. Several runs of this nature have been performed.

The results of these exploratory experiments show that if a temperature gradient between a concentrated solution and a very dilute uranium solution (which simulates the HRT composition) becomes greater than 20 to 30°C above the temperature of the pressurizer, then the second liquid phase in all probability cannot exist. Instead a solid phase or phases will be formed. If then the temperature goes above approximately 800 to 900°C, the solid UO_2SO_4 (anhydrous) (and perhaps the other salts) within the solid mixture will most certainly convert to oxides, thus liberating any $SO_4^{=}$ to the solution bulk.

The above research problem reduces to a study of the vapor pressure of concentrated liquid and liquid-liquid systems from moderate concentrations to the boundary limits for solid-liquid equilibria. Additional work is planned in this direction.

20.3 COMPARATIVE SOLUBILITIES IN D_2O AND H_2O SYSTEMS; SYSTEM UO_3-SO_3-H_2O (D_2O)

In order to make a comparison between solubility behavior in D_2O and H_2O systems, a set of comparative solubilities at 300°C (Fig. 20.3) were determined for the system UO_3-SO_3-H_2O (D_2O). The solid phase in both H_2O and D_2O was shown to be $UO_3 \cdot H_2O$ (D_2O) by x-ray diffraction analysis. After a consideration of these results and the comparative results with D_2O being used in the five-component system UO_3-CuO-NiO-SO_3-H_2O (D_2O), there does not appear to be much difference at 300°C between H_2O and D_2O in solubility relationships in the 0.01 to 0.1 m SO_3 acid range.

20.4 THE TWO-LIQUID PHASE REGIONS OF THE SYSTEM UO_3-SO_3-H_2O

Most of the previous investigations on the two-liquid phase regions of the system UO_3-SO_3-H_2O have been concerned with temperature boundary limits. Now the study is being directed toward the determination of the compositions of the two phases in equilibrium with each other. One problem in the attainment of experimental data of this type lies in the fact that the heavy-liquid phase, although fluid at the equilibrium temperatures, becomes a gel at lower temperatures and therefore is not easily sampled by conventional sampling techniques. Also, in sampling the light phase at temperature, there is the possibility that the heavy phase will interfere. Consequently, a cool-down method is being used in which a volume of solution is sealed in a 25-cm length pyrex or silica tube of 1.5 mm inside diameter. The tube containing solution is vibrated at temperature in a vertical aluminum cylindrical thermostat, during which time the two phases appear and equilibrate with each other. After sufficient time has elapsed the tube is dropped through a hole in the bottom of the thermostat into a dry ice-trichloroethylene bath from which it is later removed. Separate tube segments containing the heavy liquid and the light liquid are cut from the tube and the contained

solutions are analyzed for uranium and sulfate.

Another method currently being investigated involves the use of a high-pressure vessel having a 100-cc volume capacity. Eight pyrex or quartz tubes of 6 mm inside diameter and 8 mm outside diameter containing appropriate solutions are placed inside the pressure vessel. A small volume of water is added to the pressure vessel to counterbalance the large water vapor pressure within the tubes at temperature. The sealed pressure vessel is rocked at constant temperature. After sufficient equilibration time has elapsed, the pressure vessel is placed in a vertical position and is lowered slowly into a wet ice bath. Cooling to room temperature is complete within 5 to 10 min, after which time the eight tubes can then be removed and placed in an ethanol-water-ice bath to wait to be segmented. This latter approach gives considerably larger quantities of solution for analysis, but the slow cool-down period lends an element of doubt to the validity of results.

Some of the present experimental data, along with curves representing past and present data,[1,2] are shown in Fig. 20.4. Present values for analytical compositions of the heavy and light phases in liquid-liquid equilibrium at 300°C and for the heavy phase at 325 and 350°C are shown and indicate the scatter of the data. Our present analytical values for the compositions of the light phases at 325 and 350°C show considerable scatter and are used for the most part in the establishment of the "tie" lines. At the present time the considered best values for the light-phase compositions at 300, 325, and 350°C have been obtained from the previous boundary-curve investigation.[1] This previous investigation, when coupled with the present analytical values for the heavy and light phases, gives connecting relationships between the two phases.

A conventional triangular three-component phase diagram could be presented for these data. However, in this case all data fall very near the curve for stoichiometric UO_2SO_4, which makes the interpretation difficult. The lines in Fig. 20.4 connecting the concentrated solutions to the dilute solutions are not "tie" lines in the usual sense, since these lines do not intersect the composition of the original solutions. The indicated connecting lines cover the range of analytical results obtained from original solutions varying in composition from 0.5 m to 2.52 m UO_2SO_4 and containing from 0 to 10 mole % excess H_2SO_4. The experimental data so presented at this time give an over-all picture of the nature and composition of light and heavy phases in the liquid-liquid immiscibility regions. Refinement of technique and many additional data must be obtained before a complete, definitive picture can be drawn. The applied aspect of this investigation lies in the solution equilibria in the liquid-liquid region for the multicomponent system, UO_3-CuO-NiO-SO_3-H_2O (D_2O) and the interconnection to the solid-liquid equilibria at lower temperature for the same system.

REFERENCES

1. H. W. Wright and W. L. Marshall, HRP Quar. Prog. Rep. Oct. 1, 1952, ORNL-1424.

2. W. L. Marshall, Anal. Chem. 27, 1923 (1954).

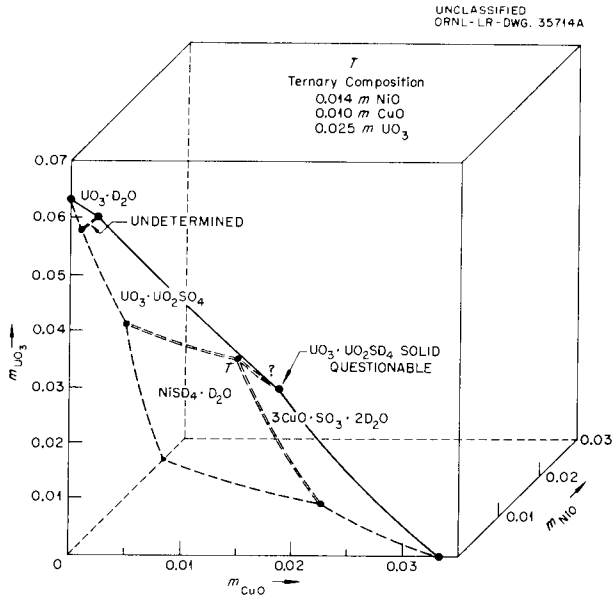

Fig. 20.1. System UO_3-CuO-NiO-SO_3-D_2O at 300°C; 0.06 *m* SO_3.

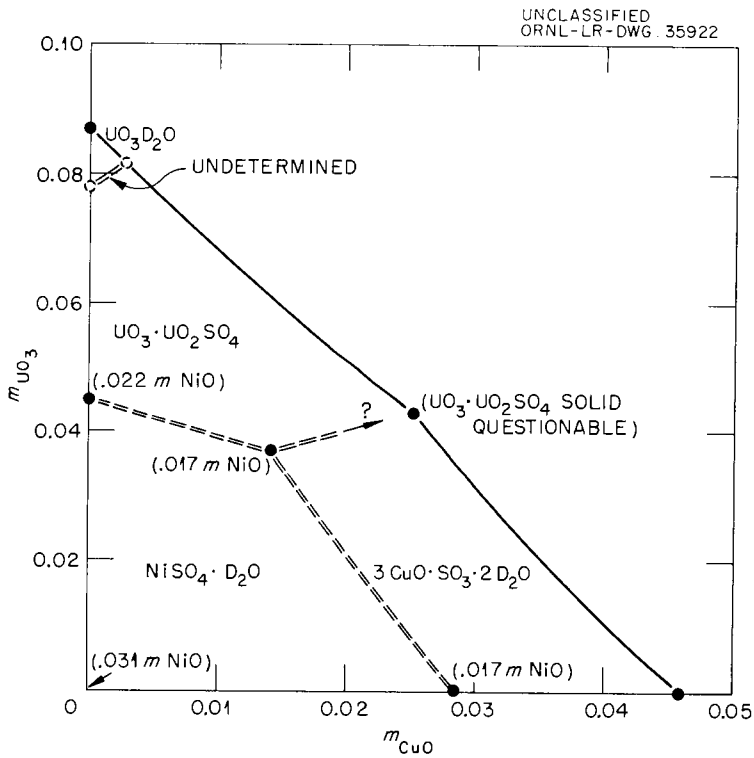

Fig. 20.2. Projection on the UO_3-CuO Base; System UO_3-CuO-NiO-SO_3-D_2O at 300°C; 0.08 *m* SO_3.

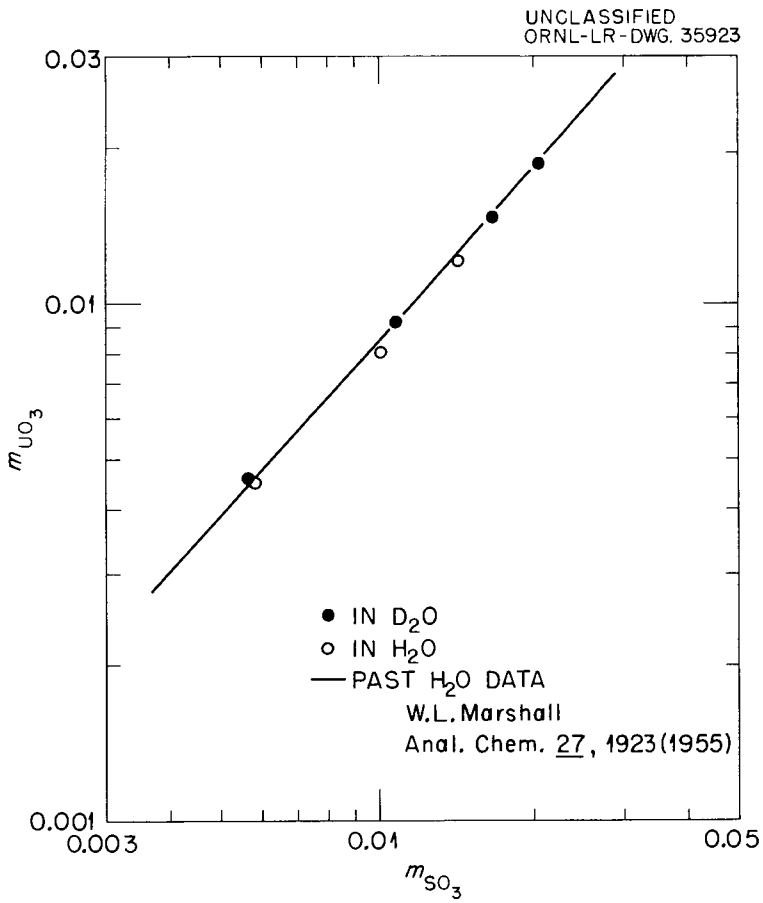

Fig. 20.3. Comparative Solubilities of UO_3 in H_2SO_4-H_2O and D_2SO_4-D_2O at 300°C.

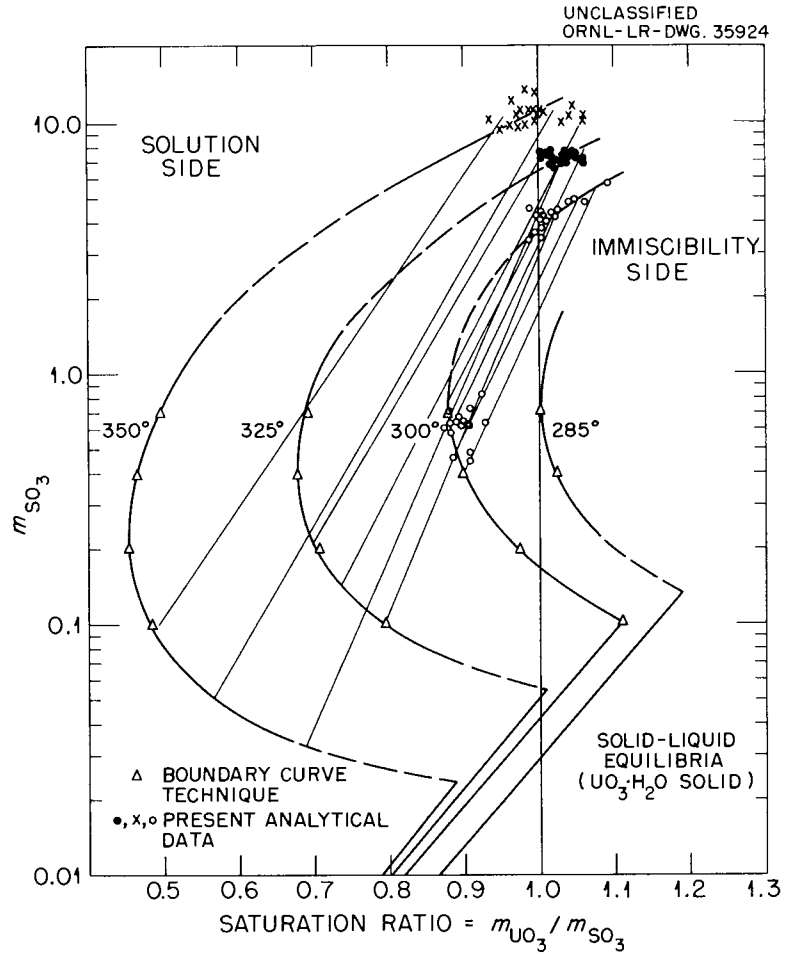

Fig. 20.4. Two-Liquid Phase Regions, System UO_3-SO_3-H_2O.

21. REACTIONS IN AQUEOUS SOLUTIONS

H. F. McDuffie

L. O. Gilpatrick H. H. Stone

21.1 CHEMICAL STUDIES RELATED TO HRT ANALYTICAL PROBLEMS

In the previous quarterly report[1] reference was made to the difficulties encountered in obtaining consistently reliable determinations of the free acid in reactor solution samples. The presence of peroxide was shown to interfere, and the pH titration of the cooled analytical slurry in the usual procedure was found to give erratic results. During the past quarter these observations were confirmed, and the results were reported to the Analytical Chemistry Division.[2]

The analytical control data for the period of the HRT run 17-A were reviewed to see whether they would confirm the chemical evidence that the free-acid determination was unsatisfactory.[3] A standard statistical technique (analysis of variance)[4] was used to determine whether the day-to-day changes in the average free-acid content reported for control solution K-4 were significantly larger than was consistent with the precision indicated by the variations between different results on the same day. This type of analysis was also applied to the uranium, copper, nickel, and total sulfate determinations. Table 21.1 presents a summary of the results of the statistical analyses. The free-acid method was found to have a highly significant variance ratio; the significance may be stated as follows — if there were truly no greater difference between results taken on different days than results obtained on the same day, then we would expect to obtain a set of data showing such a large deviation from a variance ratio of 1.0 not more than five times out of one thousand such sets of data. With such an improbable situation we may confidently reject the hypothesis that there was no day-to-day effect on the results, leaving the conclusion that there was actually <u>some</u> substantial day-to-day bias being introduced. Similarly, the total-sulfate method was shown to contain some day-to-day bias, though at not quite so high a significance level, and the uranium method was shown to contain a day-to-day variation at a level (0.05) which is normally taken by chemists as one requiring investigation. The copper and nickel results were not demonstrably biased during the period surveyed. It is obvious that, in the interpretation of HRT behavior by the use of the results

Table 21.1. Summary of Variance Analysis of HRT K-4 Control Samples

Determination	Variance Between Days / Variance Within Days	Degrees of Freedom	Level of Significance
Uranium	3.09	9/10	0.05
Copper	1.38	9/10	Not significant
Nickel	1.0	6/7*	Not significant
Free acid	7.92	8/9*	0.005
Total sulfate	6.11	9/10	0.01

*The data from days with less than two determinations were not used in these analyses.

of chemical analysis of solution samples, some effects of changes in operating procedures may be obscured if the analytical results contain a day-to-day bias.

A new procedure for free-acid determination was devised which appeared to be free from the most objectionable features of the prior method and also amenable to use with remotely operated facilities.[5] When a solution sample was passed over a cationic ion exchange resin initially in the lithium form, with subsequent flushing of the column by a standard volume of dilute lithium sulfate, the normally interfering ions of uranium, copper, and nickel were found to be strongly adsorbed on the column, displacing lithium ions, but the acidic hydrogen ions were washed through the column. The combined eluate, then, contained sulfuric acid in a dilute lithium sulfate solution; the free acid in this solution can be determined without interference in a number of ways. When preliminary tests of this method confirmed its expected behavior, the method was referred to the Analytical Chemistry Division for consideration as a new procedure and for such further development as was necessary. The use of the lithium form of a cation resin may find application in other chemical systems where the determination of free acid is important.

21.2 THE MECHANISM OF HOMOGENEOUS CATALYSIS

A mechanism for the homogeneous catalysis of the oxidation of dissolved hydrogen by dissolved cupric salts was proposed by Halpern[6] as follows:

$$H_2 + Cu^{++} \underset{k_{-1}}{\overset{k_1}{\rightleftharpoons}} CuH^+ + H^+$$

$$CuH^+ + Cu^{++} \xrightarrow{k_2} 2Cu^+ + H^+$$

$$2Cu^+ - 2e \xrightarrow[\text{Oxidation}]{\text{Rapid}} 2Cu^{++}$$

This mechanism was based on the interpretation of the effects of changes in acidity and copper concentration in the cupric perchlorate-perchloric acid system at 110°C. As previously suggested by Professor P. H. Emmett,[7] this mechanism would give rise to isotope exchange if deuterium gas were used in connection with a light-water solution of the catalyst; any D^+ formed in the first step would immediately exchange with the H_2O to form H^+ which, in the K_{-1} reaction would regenerate HD instead of DD. If no isotope exchange were observed, or if it were substantially less than calculated, the adequacy of this mechanism would be challenged. Tests of the mechanism by an isotope-exchange procedure have been initiated,[8] and some production of HD has been observed. For accurate calculations of the expected amount of exchange it is necessary to have estimates of the rates of the various component reactions, or at least the appropriate ratios of their rates:

$$H_2 + Cu^{++} \longrightarrow CuH^+ + H^+$$

$$D_2 + Cu^{++} \longrightarrow CuD^+ + D^+$$

$$D^+ + CuH^+ \longrightarrow Cu^{++} + HD$$

$$H^+ + CuD^+ \longrightarrow Cu^{++} + HD$$

$$D^+ + CuD^+ \longrightarrow Cu^{++} + DD$$

$$H^+ + CuH^+ \longrightarrow Cu^{++} + HH$$

$$CuH^+ + Cu^{++} \longrightarrow 2Cu^+ + H^+$$

$$CuD^+ + Cu^{++} \longrightarrow 2Cu^+ + D^+$$

To this end, measurements are being made under Halpern's experimental conditions, using the four combinations of heavy and light hydrogen with heavy- and light-water solutions of the catalyst. As a check on the adequacy of our experimental technique, the effect of temperature was measured for a solution tested by Halpern, and the results are compared with Halpern's equation for the temperature dependence in Fig. 21.1. The observed discrepancies are considered to be well within the usual range of agreement for kinetic data obtained in different laboratories.

REFERENCES

1. H. F. McDuffie, L. O. Gilpatrick, and H. H. Stone, HRP Quar. Prog. Rep. Oct. 31, 1958, ORNL-2654, p. 226-227.

2. Memorandum of January 16, 1959, from L. O. Gilpatrick and H. F. McDuffie to M. T. Kelley, "Observations on the HRT Free-Acid Determination."

3. Memorandum from H. F. McDuffie to M. T. Kelley dated September 24, 1958, "HRT Analytical Controls."

4. K. A. Brownlee, Industrial Experimentation, 2d ed., Chapter VII, "The Analysis of Variance," London, HMSO 1947.

5. Memorandum of December 12, 1958, from L. O. Gilpatrick and H. F. McDuffie to M. T. Kelley, "Free-Acid Determination in Uranyl Sulfate Solutions by the Dowex-50 Resin Separation Procedure."

6. J. Halpern, E. R. Macgregor, and E. Peters, J. Phys. Chem., 60, 1455 (1956).

7. H. F. McDuffie and H. H. Stone, HRP Quar. Prog. Rep. Jan. 31, 1957, ORNL-2272, p. 170-171.

8. These studies were initiated by H. R. Jolley, S. J., Department of Chemistry, Loyola University, New Orleans, La., during the summer of 1958, at ORNL.

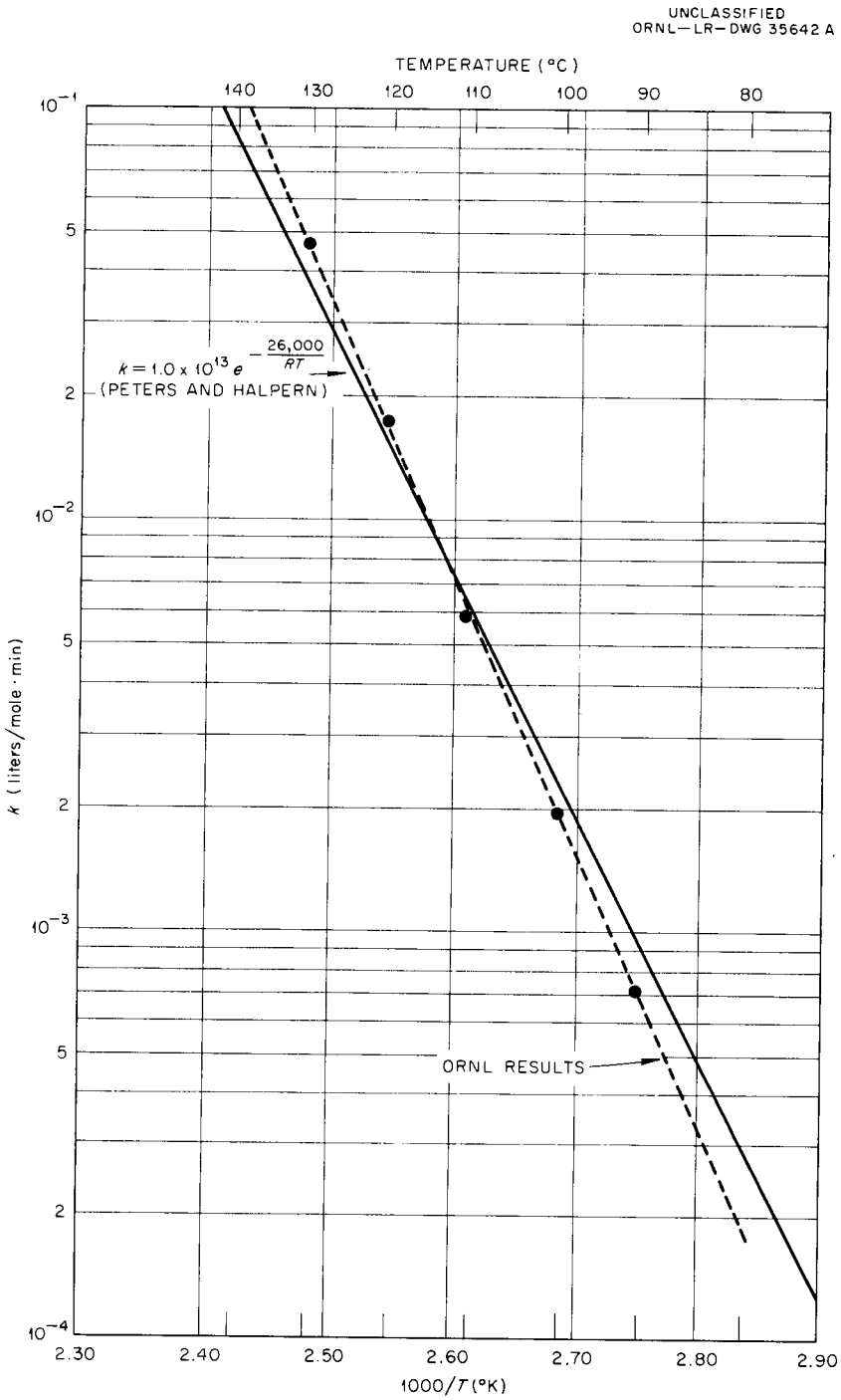

Fig. 21.1. Temperature Dependence of Hydrogen-Cupric Ion Reaction.

PART VII

ANALYTICAL CHEMISTRY

M. T. Kelley

22. ANALYTICAL CHEMISTRY

O. Menis

C. M. Boyd
G. Goldstein
H. P. House
D. L. Manning
T. C. Rains
I. B. Rubin

22.1 DETERMINATION OF U(IV) IN THORIUM OXIDE - URANIUM OXIDE MIXTURES

A method was devised for the determination of U(IV) in mixtures of thorium oxide and uranium oxide which contain from 3 to 30% uranium. The sample is dissolved under reflux conditions in 7 M H_3PO_4 which contains a small amount of HF and standard $K_2Cr_2O_7$ in excess of the amount required to oxidize U(IV) to U(VI). After dissolution, excess dichromate is titrated with standard $FeSO_4$, using diphenylamine sulfonate as the indicator. Uranium(IV) is calculated on the basis of the difference between the amount of dichromate added and the excess found by titration.

A different dissolution procedure is required for certain contaminated, high-fired samples which are insoluble in 7 M H_3PO_4. These samples are dissolved by refluxing them in concentrated HCl under an inert, argon atmosphere to prevent air oxidation of the U(IV). The solution is then diluted, after which H_3PO_4 and an excess of standard $K_2Cr_2O_7$ are added. The determination is then completed as described previously.

Any components which reduce dichromate under the conditions used in this procedure will interfere with the U(IV) determination. In these mixtures, however, only microgram quantities of impurities are encountered, so that no significant error is introduced. The coefficient of variation of the method for U(IV) within the range of 25 to 50 mg is about 1%.

22.2 DETERMINATION OF NEODYMIUM BY FLAME PHOTOMETRY

A flame-photometric method was developed for the determination of neodymium in solutions of UO_2SO_4 which contain copper and corrosion products of stainless steel. The neodymium is extracted into a 0.1 M

solution of 2-thenoyltrifluoroacetone (TTA) in 4-methyl-2-pentanone (hexone) in order (1) to separate it from interferences, and (2) to transfer it to an organic medium prior to the flame-photometric determination because the radiant intensity is about 30-fold greater in an organic rather than aqueous medium. Uranium, copper, nickel, and iron are also extracted with TTA in hexone; these elements, therefore, are removed prior to extraction of the neodymium, by the addition of sodium diethyldithiocarbamate (DDTC) to a 2 M acetate solution of the sample at pH 6 and then extracting with CCl_4. The neodymium is then extracted from the raffinate with TTA in hexone, after which the radiant intensity of the neodymium in the organic phase is measured at a wave length of 663 mμ, using a flame photometer equipped with a photomultiplier tube. In this medium, amounts as low as 0.4 μg of neodymium per milliliter can be estimated whereas, if an aqueous solution is used, the minimum concentration that can be evaluated is of the order of 10 μg/ml. The interferences of a number of other elements, including all rare-earth elements, were evaluated. From the analysis of standard solutions of uranium containing known amounts of neodymium, it was indicated that recovery of neodymium is practically complete. For samples which contain varying amounts of uranium and neodymium within the range of 20 to 100 μg/ml, the coefficient of variation was found to be about 10%.

22.3 SEPARATION OF CHLORIDE BY FUSION PYROLYSIS

A further study was made of the fusion-pyrolysis technique for the separation of small amounts of chloride for analytical purposes, utilizing $Na_2Mo_3O_{10}$ as the flux. It was established that as much as 2 mg of chloride, as NaCl, can be completely removed by pyrolysis with this flux at 800°C in about 2 hr (see Fig. 22.1). From test results, set forth in Table 22.1, the fusion-pyrolysis method is shown to be satisfactory for the separation of chloride from high-fired ThO_2, even at concentrations as low as 1 to 3 ppm.

Table 22.1. Recovery of Chloride by Fusion Pyrolysis

Flux: $Na_2Mo_3O_{16}$, 16 g
Sample: ThO_2, ignited at 1600°C

Sample Weight, g	Chloride, μg		
	Added	Found	Net/g ThO_2
0	11	11	
5	0	6	1.2
10	0	14	1.4
10	0	16	1.6
10	11	26	1.5
		Av.	1.4
		S =	0.2
		V =	10%

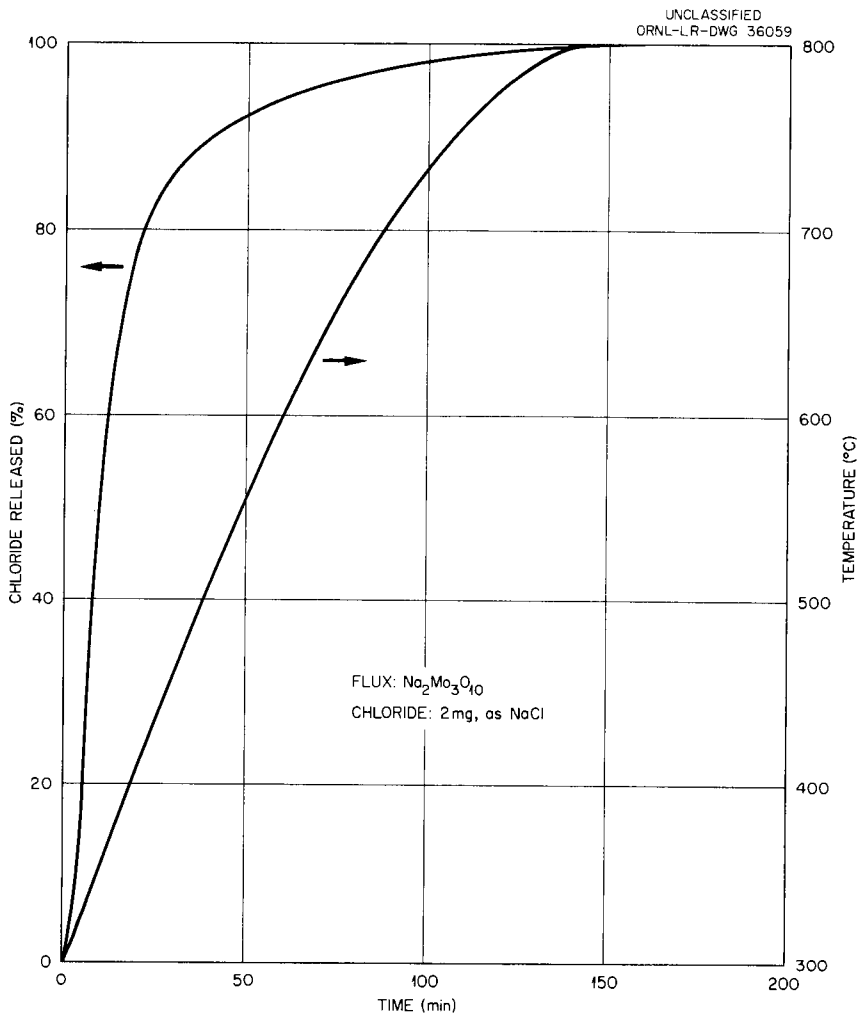

Fig. 22.1. Fusion Pyrolysis of Chloride.

OAK RIDGE NATIONAL LABORATORY
HOMOGENEOUS REACTOR PROJECT

FEBRUARY 2, 1959

PROJECT DIRECTOR
R. B. BRIGGS — D

ASSOCIATE PROJECT DIRECTOR
C. E. WINTERS** — O
A. L. GUNNELS, SEC. — REE

TECHNICAL ASSISTANT
F. KERTESZ — REE

PROJECT EDITOR
W. D. REEL — TI

DESIGN AND ENGINEERING
R. N. LYON, ASSOCIATE DIRECTOR — REE
T. S. CARLSMITH,* SEC. — REE

DESIGN
W. R. GALL, SECTION CHIEF — REE
M. I. LUNDIN, ASSISTANT SECTION CHIEF — REE
J. R. McWHERTER, ASSISTANT SECTION CHIEF — REE

SPECIAL PROBLEMS
C. L. SEGASER — REE

HRP DESIGN
J. R. McWHERTER, ASSISTANT SECTION CHIEF — REE
R. H. CHAPMAN, GROUP LEADER — REE
R. E. SCHAPPEL — REE
L. A. HAACK — REE
E. H. GIFT — REE

MECHANICAL DESIGN, DRAFTING AND SPECIFICATIONS
M. I. LUNDIN, ASSISTANT SECTION CHIEF — REE
F. C. ZAPP, GROUP LEADER — REE
C. A. BURCHSTED — REE
J. E. JONES — REE
W. ROBINSON — REE
H. H. BRADFORD — REE
R. L. CAUBLE — REE
J. P. DILORENZO — REE
F. GINNESS — REE
T. E. HAYNES — REE
A. R. KERR — REE
W. B. KRICK — REE
C. A. ROBERTS — REE
R. D. SATTERFIELD — REE
R. H. SIGLER — REE
W. G. STERLING — REE

RESEARCH AND ANALYSIS
P. R. KASTEN, SECTION CHIEF — REE

REACTOR ANALYSIS
M. W. ROSENTHAL, GROUP LEADER — REE
S. JAYE — REE
B. E. PRINCE — REE

REACTOR PHYSICS
M. TOBIAS, GROUP LEADER — REE
R. CHALKLEY — REE
C. W. NESTOR, JR. — REE

PROGRAMING
T. B. FOWLER — REE
M. P. LIETZKE — REE
H. A. MACCOLL — REE

TRANSPORT PROPERTIES OF SLURRIES
D. G. THOMAS, GROUP LEADER — REE
P. H. HAYES — REE
R. M. SUMMERS — REE

PHYSICAL CHEMISTRY OF SLURRIES
C. S. MORGAN, GROUP LEADER — REE
B. G. SUTTON — REE

STRESS ANALYSIS AND CLOSURE RESEARCH
R. D. CHEVERTON, GROUP LEADER — REE
T. H. MALNEY — REE

COMPONENT DEVELOPMENT
I. SPIEWAK, SECTION CHIEF — REE

MAINTENANCE DEVELOPMENT
J. S. CULVER, GROUP LEADER — REE
R. BLUMBERG — REE
B. D. DRAPER — TVA
P. P. HOLZ — REE
T. L. CASTILE — REE
C. JONES — REE

CIRCULATING PUMPS, HEAT EXCHANGERS
C. H. GABBARD, GROUP LEADER — REE
J. C. MOYERS — REE
I. K. NAMBA — REE
H. R. PAYNE — REE
C. C. HURTT — REE
R. J. LOCKETT — REE

FEED PUMPS AND VALVES
E. C. HISE, GROUP LEADER — REE
H. C. ROLLER — REE
J. P. HURST — REE
G. A. WINDLE — REE

CORE AND BLANKET, CHEMICAL ENGINEERING PROBLEMS
C. G. LAWSON, GROUP LEADER — REE
T. G. CHAPMAN — REE
B. A. HANNAFORD — REE
J. E. MOTT† — REE
R. P. WICHNER — REE
R. GOODMAN — REE
S. R. WEST — REE

SLURRY PROBLEMS
D. M. EISSENBERG — REE
B. J. YOUNG — REE

SYSTEMS DEVELOPMENT
R. B. KORSMEYER, SECTION CHIEF — REE
F. N. PEEBLES, ASSISTANT SECTION CHIEF — REE

SLURRY SYSTEMS DEVELOPMENT I
R. VAN WINKLE, GROUP LEADER — REE
H. B. PIPER — REE
C. A. McLAUGHLIN — REE

SLURRY SYSTEMS DEVELOPMENT II
L. F. PARSLY, JR., GROUP LEADER — REE
R. J. KEDL — REE
M. RICHARDSON — REE
R. E. CARNES — REE

HRT CORE MOCKUP
P. H. HARLEY, GROUP LEADER — REE
L. E. PENTON — REE
T. R. WILSON — REE

OPERATIONS
A. N. SMITH, GROUP LEADER — REE
T. L. BOSWELL — REE
B. R. CHILCOAT — REE
J. T. DICKIE — REE
C. A. GIFFORD — REE
H. G. MOORE — REE
D. H. WALLACE — REE

INSTRUMENTATION AND CONTROLS
D. S. TOOMB, SECTION CHIEF — I&C

REACTOR I&C SYSTEM DESIGN
J. R. BROWN, GROUP LEADER — I&C
S. J. BALL* — I&C
R. W. BORGERS — I&C

HRP SUPPORTING SERVICES
O. G. DAVIS, GROUP LEADER — I&C
J. D. GRIMES — TVA
P. G. HERNDON — I&C
H. D. WILLS — I&C
R. M. BURNETT — I&C
P. E. SMITH — I&C

VALVES AND ACTUATORS
A. M. BILLINGS,** GROUP LEADER — I&C
E. H. BELL** — I&C
B. J. JONES — I&C

INSTRUMENT DEVELOPMENT
R. L. MOORE, GROUP LEADER — I&C
J. L. REDFORD** — I&C
T. M. CATE — I&C

REACTOR MATERIALS RESEARCH
E. G. BOHLMANN, ASSOCIATE DIRECTOR — REE
T. S. CARLSMITH,* SEC. — REE
R. HOWELL, SEC. — REE
R. E. WACKER, RECORDS — REE

SOLUTIONS
J. C. GRIESS, ASSISTANT SECTION CHIEF — REE

LOOPS
R. S. GREELEY, GROUP LEADER — REE
E. S. SHAVELY — REE
W. H. HINDS — REE

LABORATORY STUDIES
J. L. ENGLISH, GROUP LEADER — REE
D. N. HESS — REE
P. D. NEUMANN — REE
L. L. FAIRCHILD — REE
H. L. BARKER — REE
J. E. JACKSON — REE
B. L. JOHNSON — REE
H. R. TINCH — REE
J. L. UNDERWOOD — REE

SLURRIES
E. L. COMPERE, SECTION CHIEF — REE

LOOPS
S. A. REED,* GROUP LEADER — REE
OUT-OF-PILE STUDIES
R. B. GALLAHER — REE
H. F. HENDERSON — REE
F. E. McDANIEL — REE

TOROIDS
S. A. REED,* GROUP LEADER — REE
OUT-OF-PILE STUDIES
L. RICE — REE
R. F. BENSON — REE
B. H. PARKS — REE
G. G. WARNER — REE

IN-PILE BOMBS
L. F. WOO — REE

ENGINEERING
H. C. SAVAGE, SECTION CHIEF — REE

SOLUTIONS
S. E. BOLT, GROUP LEADER — REE
A. J. SHOR — REE
W. C. ULRICH — REE

IN-PILE MOCKUPS
C. H. BURBAGE — REE
J. R. HART — REE
J. W. MOSIER — REE
R. W. RAY — REE
T. R. RAYBURN — REE

100A LOOP OPERATIONS
J. F. WINESETTE* — REE
C. M. BURCHELL — REE
C. L. FRANCIS — REE
J. B. FRENCH — REE
J. W. GOOCH — REE

SLURRIES
D. T. JONES, GROUP LEADER — REE
J. M. BAKER — REE
D. G. GATES — REE

100A LOOP OPERATIONS
J. F. WINESETTE* — REE
L. L. ALLEN — REE
C. R. BENSON — REE
V. R. BULLINGTON — REE
G. A. MOORE — REE
L. G. PHELPS — REE
A. E. PUGH — REE

IN-PILE OPERATIONS
R. A. LORENZ, GROUP LEADER — REE
V. A. DECARLO — REE
J. P. GORDON — REE
E. H. QUINN — REE
R. A. JONES — REE
J. W. MYERS — REE
D. G. PEACH — REE
C. E. ROBERTS — REE
R. G. ROSS — REE
D. M. SMITH — REE
A. L. SUTTON — REE
W. E. TEICHERT — REE
R. M. WALLER — REE

RADIATION
G. H. JENKS, SECTION CHIEF — REE

IN-PILE LOOPS
M. D. SILVERMAN, GROUP LEADER — C
J. E. BAKER — REE
S. H. WHEELER — REE

IN-PILE BOMBS
R. J. DAVIS, GROUP LEADER — C
K. S. WARREN — C
J. L. RUTHERFORD — REE

SUPPORTING RESEARCH
A. L. BACARELLA — C
J. C. BANTER — REE
W. C. YEE — C

REMOTE EVALUATION
A. R. OLSEN — REE
B. W. McCOLLUM, SHIFT LEADER — REE
C. M. FITZPATRICK — REE
W. J. SCHILL — REE
W. H. SMITH, JR. — REE

METALLURGY
G. M. ADAMSON, SECTION CHIEF — M

METALLURGICAL RESEARCH
M. L. PICKLESIMER, LEADER — M
S. G. NELSON — M
P. L. RITTENHOUSE — M
R. L. STEPHENSON — M
P. J. JONES — M
G. C. NELSON — M
J. J. WOODHOUSE — M

METALLURGICAL ENGINEERING
E. S. BOMAR, LEADER — M
F. W. COOKE — M
W. J. LEONARD — M
J. J. PRISLINGER — M
J. K. WHITE — M
C. H. WODTKE — M
C. M. SMITH — M
M. A. WHEELER — M

METALLOGRAPHY
R. S. CROUSE,** LEADER — M
T. M. KEQLEY, JR. — M
E. R. BOYD — M
B. F. DAY** — M
R. L. FITZGERALD** — M
T. J. HENSON** — M

RADIATION DAMAGE
R. G. BERGGREN — SS
J. C. WILSON** — SS
F. B. GRIZZEL — SS

INDUSTRIAL PARTICIPATION

JAPANESE ATOMIC ENERGY RESEARCH INSTITUTE
TENNESSEE VALLEY AUTHORITY

SUBCONTRACTS

FRANKLIN INSTITUTE
RICE INSTITUTE
STANFORD RESEARCH INSTITUTE
UNIVERSITY OF UTAH

AC — ANALYTICAL CHEMISTRY DIVISION
C — CHEMISTRY DIVISION
CT — CHEMICAL TECHNOLOGY DIVISION
D — DIRECTOR'S DIVISION
E&M — ENGINEERING AND MECHANICAL DIVISION
I&C — INSTRUMENTATION AND CONTROLS DIVISION
M — METALLURGY DIVISION
RC — REACTOR CHEMISTRY DIVISION
REE — REACTOR EXPERIMENTAL ENGINEERING DIVISION
SS — SOLID STATE DIVISION
TI — TECHNICAL INFORMATION DIVISION
* — DUAL CAPACITY
** — PART TIME ON PROJECT
† — ATTENDING ORSORT

CHEMICAL TECHNOLOGY
O. E. FERGUSON,* PROBLEM LEADER — CT
I. LOOPE, SEC. — CT

CHEMICAL DEVELOPMENT
D. E. FERGUSON,* SECTION CHIEF — CT

FUEL PROCESSING
R. A. McNEES, GROUP LEADER — CT
M. H. LLOYD — CT
S. PETERSON — CT
W. B. HOWERTON — CT

THORIUM BLANKET STUDIES
J. P. McBRIDE, GROUP LEADER — CT
R. L. PEARSON, PROBLEM LEADER — CT
OXIDE PREPARATION
A. T. KLEINSTEUBER — CT
C. E. SCHILLING — CT
C. W. GREENE — CT
H. A. KROHN, PROBLEM LEADER — CT
IRRADIATION STUDIES
K. H. McCORKLE — CT
L. E. MORSE — CT
P. P. HAYDON — CT
W. L. PATTISON — CT
H. F. SOARD — CT

SURFACE CHEMISTRY
C. H. SECOY, GROUP LEADER — CT
H. F. HOLMES — CT
F. H. SWEETON — CT

DESIGN
W. E. UNGER, ASSISTANT SECTION CHIEF — CT

TiO_2 DEVELOPMENT DESIGN
J. C. SUDDATH — CT

HRT-CP DESIGN SUPPORT
H. D. WEEREN — CT
F. C. McCULLOUGH — CT

INSTRUMENTATION
C. S. LISSER — I&C

ENGINEERING AND DRAFTING
B. F. BOTTENFIELD** — CT
G. B. BERRY** — E&M
E. E. BRIDGES** — E&M
J. D. CUPP — E&M
J. W. DAY — E&M
H. W. FALLON** — E&M
L. C. HUBBARD — E&M
J. H. MANNEY** — E&M
J. D. PHILLIPS** — E&M
F. L. PIESHEL** — E&M
J. H. THOMPSON — E&M
J. N. WHEELER** — E&M

PILOT PLANT
R. B. LINDAUER,** SECTION CHIEF — CT

IN-PILE LOOP OPERATIONS
W. O. BURCH,* GROUP LEADER — CT
L. J. KING, PROBLEM LEADER — CT
J. W. BROWN — CT

SLURRY PREPARATION
W. H. LEWIS,** GROUP LEADER — CT
C. Y. ELLISON, PROBLEM LEADER — CT
K. D. JOHNSSON — CT

UNIT OPERATIONS
P. A. HAAS, GROUP LEADER — CT

SLURRY PREPARATION DEVELOPMENT
S. D. CLINTON — CT
C. C. HAAS, JR. — CT
R. D. ARTHUR — CT
V. L. FOWLER — CT

ENGINEERING ASSISTANCE STUDIES
E. L. YOUNGBLOOD — CT
W. M. WOODS — CT
F. N. McLAIN — CT
D. A. McWHIRTER — CT

CHEMICAL RESEARCH
H. F. McDUFFIE,* ASSISTANT DIRECTOR — RC
I. W. HODGE, SEC. — RC

HETEROGENEOUS EQUILIBRIA IN AQUEOUS SYSTEMS
W. L. MARSHALL, GROUP LEADER — RC
C. J. BARTON — RC
J. S. GILL — RC
G. M. HEBERT — RC
E. V. JONES — RC
R. E. MOORE — RC
R. SLUSHER — RC

REACTIONS IN AQUEOUS SOLUTIONS
G. M. WATSON, SUPERVISOR — RC
H. F. McDUFFIE,* GROUP LEADER — RC
L. O. GILPATRICK — RC
H. H. STONE — RC

RADIATION EFFECTS
G. W. KEILHOLTZ, SUPERVISOR — RC
W. E. BROWNING, GROUP LEADER — RC
R. D. ACKLEY — RC
R. E. ADAMS — RC

ANALYTICAL CHEMISTRY
MYRON T. KELLEY,** DIRECTOR
C. D. SUSANO,** ASSOCIATE DIRECTOR
K. A. ODOM,** SEC. — AC
H. E. ZITTEL, COORDINATOR, HRP ANALYTICAL CHEMISTRY — AC

CORROSION ANALYTICAL LABORATORY
O. MENIS,* SECTION CHIEF — AC
H. P. HOUSE, ASST. SECTION CHIEF — AC

RESEARCH
O. MENIS,* GROUP LEADER — AC
C. M. BOYD — AC
D. L. MANNING, GROUP LEADER — AC
R. G. BALL — AC
G. GOLDSTEIN — AC

DEVELOPMENT AND SPECIAL ANALYSES
T. C. RAINS, GROUP LEADER — AC
N. M. FERGUSON — AC

SERVICE
C. K. TALBOTT, SUPERVISOR — AC
D. E. CARPENTER — AC
F. L. LAYTON — AC
T. P. BACON — AC
W. O. CLAPP, JR. — AC
C. A. CLARK — AC
P. S. GOODWIN — AC
B. D. HICKS — AC
A. H. MATTHEWS — AC
T. O. MILLER — AC
V. S. NORMAN — AC
E. ONKST — AC
C. M. WILSON — AC

SPECTROCHEMICAL SERVICES
C. FELDMAN,** SUPERVISOR — AC
W. R. MUSICK** — AC
A. H. MARSHALL** — AC
J. A. NORRIS,** GROUP LEADER — AC
J. J. MUNDZAK** — AC

HRT AND IN-PILE LOOP ANALYSIS
U. KOSKELA, SUPERVISOR — AC
L. G. FARRAR, ASST. SUPERVISOR — AC
J. E. ATTRILL — AC
C. P. BAKER — AC
R. E. CORCORAN — AC
S. R. DINSMORE — AC
J. L. MOTTERN — AC
G. M. CAMPBELL — AC
G. I. GAULT — AC
F. K. HEACKER — AC
M. H. McCORKODDALE — AC
J. L. SHARP — AC
J. SLESSINGER — AC
W. R. WARREN — AC
H. L. WEBB — AC
H. L. WHITTINGTON — AC

RADIOCHEMICAL ANALYSIS
E. I. WYATT,** SUPERVISOR — AC

HRT DEVELOPMENT
P. F. THOMASON,** GROUP LEADER — AC
R. E. BIGGERS** — AC
F. J. MILLER** — AC
S. A. REYNOLDS,** GROUP LEADER — AC
J. S. ELDRIDGE** — AC
Y. H. HANDLEY** — AC

HIGH RADIATION LABORATORY
J. E. MORTON,** SUPERVISOR — AC

NUCLEAR ANALYSIS LABORATORY
G. W. LEDDICOTTE,** SUPERVISOR — AC
L. C. BATE** — AC
W. J. HAMPTON** — AC
R. W. HARVEY** — AC

OPTICAL AND ELECTRON MICROSCOPY
T. E. WILLMARTH,** GROUP LEADER — AC

HOMOGENEOUS REACTOR TEST
S. E. BEALL, PROJECT ENGINEER — REE
B. EUBANK, SEC. — REE
M. SWANK, SEC. — CT
P. S. WARD, STENO. — REE

J. W. HILL, JR.,* ASSISTANT SECTION CHIEF — REE

REACTOR PLANNING
S. I. KAPLAN,† GROUP LEADER — REE
J. R. BUCHANAN — CT

PLANT OPERATIONS
J. W. HILL, JR.,* CHIEF — REE
J. O. FLYNN — REE
R. H. GUYMON — CT
D. SCOTT, JR. — REE
R. J. HARVEY, SHIFT SUPERVISOR — REE
R. SMITH, JR., CONTROL ROOM SUPERVISOR — REE
D. T. GODWIN — REE
A. L. JOHNSON — REE
L. P. PUGH — REE
W. H. WAGNER — REE
H. F. BAUMAN, SHIFT SUPERVISOR — CT
E. W. BROWN, CONTROL ROOM SUPERVISOR — CT
J. D. BARNES — REE
E. D. BOLLING — REE
W. T. BOSTIC — CT
T. G. HILL — REE
D. F. FRECH, SHIFT SUPERVISOR — REE
R. J. SHANNON, CONTROL ROOM SUPERVISOR — CT
P. B. DAVIS — REE
J. E. EVE — REE
L. J. SHERSKY — CT
J. E. WOLFE — REE
N. C. BRADLEY, SHIFT SUPERVISOR — CT
J. L. STEPP, CONTROL ROOM SUPERVISOR — REE
H. O. CURTIS — REE
H. L. BROWN — REE
T. W. HODGE — REE
F. L. ROUSER — REE

MAINTENANCE PLANNING
W. TERRY, SUPERVISOR — REE
G. H. JOHNSTONE — REE

INSTRUMENTATION
K. W. WEST, GROUP LEADER — I&C
S. J. BALL* — I&C

P. N. HAUBENREICH,* ASSISTANT SECTION CHIEF — REE

REACTOR MATERIALS AND CHEMISTRY
D. M. RICHARDSON, GROUP LEADER — REE
J. E. SUTHERLAND — REE
J. D. JONES — REE

REACTOR ANALYSIS
P. N. HAUBENREICH,* GROUP LEADER — REE
S. R. BUXTON — REE
J. R. ENGEL — CT
J. HIROTA — JAPANESE ATOMIC ENERGY RESEARCH INSTITUTE
J. O. KOLB — REE
J. A. WATTS — REE

CHEMICAL PLANT
W. D. BURCH,* GROUP LEADER — CT
R. H. WINGET — CT
O. O. YARBRO — CT
W. A. LINDSEY — CT
M. O. SMITH — CO-OP STUDENT, UNIV. OF TENN.

PERSONNEL SUMMARY

	FULL TIME	PART TIME	INDUSTRIAL PARTICIPATION	TOTAL
ADMINISTRATION	8	3		11
ANALYTICAL CHEMISTRY	37	18		55
CHEMICAL RESEARCH	14			14
CHEMICAL TECHNOLOGY	41	10		51
DESIGN AND ENGINEERING	95	3	2	100
HOMOGENEOUS REACTOR TEST	43		1	44
REACTOR MATERIALS RESEARCH	94	5		99
TOTAL	332	39	3	374

INTERNAL DISTRIBUTION

1. C. E. Center
2. Biology Library
3. Health Physics Library
4. Metallurgy Library
5-6. Reactor Experimental Engineering Library
7-9. Central Research Library
10-14. Laboratory Records Department
15. Laboratory Records, ORNL R.C.
16. G. M. Adamson
17. T. A. Arehart
18. A. L. Bacarella
19. J. E. Baker
20. R. G. Ball
21. S. J. Ball
22. R. D. Baybarz
23. S. E. Beall
24. L. L. Bennett
25. R. G. Berggren
26. G. B. Berry
27. R. E. Biggers
28. A. M. Billings
29. D. S. Billington
30. E. P. Blizard
31. R. Blumberg
32. E. G. Bohlmann
33. S. E. Bolt
34. C. J. Borkowski
35. B. F. Bottenfield
36. G. E. Boyd
37. J. C. Bresee
38. N. A. Brown
39. F. R. Bruce
40. J. R. Buchanan
41. W. D. Burch
42. C. A. Burchsted
43. S. R. Buxton
44. A. D. Callihan
45. T. A. Carlson
46. W. L. Carter
47. G. H. Cartledge
48. R. H. Chapman
49. R. A. Charpie
50. R. D. Cheverton
51. J. M. Chilton
52. C. J. Claffey
53. H. C. Claiborne
54. W. E. Clark
55. S. D. Clinton
56. T. E. Cole
57. C. W. Collins
58. E. L. Compere
59. R. S. Crouse
60. F. L. Culler
61. J. S. Culver
62. D. G. Davis
63. R. J. Davis
64. V. A. DeCarlo
65. B. D. Draper
66. J. S. Drury
67. W. K. Eister
68. L. B. Emlet (K-25)
69. J. L. English
70. D. E. Ferguson
71. J. D. Flynn
72. D. F. Frech
73. J. H. Frye, Jr.
74. C. H. Gabbard
75. J. L. Gabbard
76. W. R. Gall
77. R. B. Gallaher
78. E. H. Gift
79. H. E. Goeller
80. R. S. Greeley
81. A. T. Gresky
82. J. C. Griess
83. W. R. Grimes
84. E. Guth
85. R. H. Guymon
86. L. A. Haack
87. P. A. Haas
88. J. Halperin
89. B. A. Hannaford
90. P. H. Harley
91. R. J. Harvey
92. P. N. Haubenreich
93. D. N. Hess
94. J. W. Hill

95. E. C. Hise
96. A. Hollaender
97. P. P. Holz
98. H. P. House
99. A. S. Householder
100. S. Jaye
101. G. H. Jenks
102. D. T. Jones
103. E. V. Jones
104. K. O. Johnsson
105. W. H. Jordan
106. S. I. Kaplan
107. P. R. Kasten
108. C. P. Keim
109. M. T. Kelley
110. F. Kertesz
111. S. S. Kirslis
112. J. O. Kolb
113. R. B. Korsmeyer
114. U. Koskela
115. K. A. Kraus
116. N. A. Krohn
117. J. A. Lane
118. C. G. Lawson
119. R. E. Leuze
120. S. C. Lind
121. R. B. Lindauer
122. C. S. Lisser
123. R. S. Livingston
124. M. H. Lloyd
125. R. A. Lorenz
126. M. I. Lundin
127. R. N. Lyon
128. J. L. Marsh (C&CC, South Charleston)
129. W. L. Marshall
130. J. P. McBride
131. F. C. McCullough
132. H. F. McDuffie
133. H. A. McLain
134. R. A. McNees
135. J. R. McWherter
136. O. Menis
137. E. C. Miller
138. C. S. Morgan
139. K. Z. Morgan
140. L. E. Morse
141. J. P. Murray (Y-12)
142. I. K. Namba
143. M. L. Nelson
144. P. D. Neumann
145. R. H. Nimmo
146. A. R. Olsen
147. L. F. Parsly
148. R. L. Pearson
149. F. N. Peebles
150. Sigfred Peterson
151. H. O. Phillips
152. M. L. Picklesimer
153. R. H. Powell
154. B. E. Prince
155. J. J. Prislinger
156. L. R. Quarles
157. S. A. Reed
158. W. D. Reel
159. P. M. Reyling
160. S. A. Reynolds
161. L. Rice
162. D. M. Richardson
163. A. E. Richt
164. R. C. Robertson
165. W. Robinson
166. H. C. Roller
167. A. M. Rom
168. M. W. Rosenthal
169. H. C. Savage
170. W. F. Schaeffer
171. C. E. Schilling
172. H. E. Seagren
173. H. K. Search
174. C. H. Secoy
175. C. L. Segaser
176. E. M. Shank
177. E. D. Shipley
178. M. D. Silverman
179. M. J. Skinner
180. A. N. Smith
181. E. S. Snavely, Jr.
182. A. H. Snell
183. J. W. Snider
184. D. L. Snyder
185. I. Spiewak
186. H. H. Stone
187. R. W. Stoughton
188. C. D. Susano
189. J. E. Sutherland
190. J. A. Swartout
191. E. H. Taylor
192. W. Terry
193. D. G. Thomas
194. P. F. Thomason

195. M. Tobias
196. D. S. Toomb
197. W. E. Unger
198. W. C. Ulrich
199. R. Van Winkle
200. D. W. Vroom
201. R. E. Wacker
202. F. J. Walter
203. K. S. Warren
204. B. Weaver
205. H. O. Weeren
206. A. M. Weinberg
207. S. H. Wheeler
208. J. K. White
209. E. P. Wigner (consultant)
210. H. D. Wills
211. G. C. Williams
212. J. C. Wilson
213. R. H. Winget
214. C. E. Winters
215. L. F. Woo
216. W. C. Yee
217. F. C. Zapp
218. ORNL - Y-12 Technical Library, Document Reference Section
219. HRP Director's Office, Y-12

EXTERNAL DISTRIBUTION

220. Division of Research and Development, AEC, ORO
221-802. Given distribution as shown in TID-4500 (14th ed.) under Reactors-Power category (75 copies - OTS)

Reports previously issued in this series are as follows:

ORNL-527	Date Issued, December 28, 1949
ORNL-630	Period Ending February 28, 1950
ORNL-730	Feasibility Report - Date Issued, July 6, 1950
ORNL-826	Period Ending August 31, 1950
ORNL-925	Period Ending November 30, 1950
ORNL-990	Period Ending February 28, 1951
ORNL-1057	Period Ending May 15, 1951
ORNL-1121	Period Ending August 15, 1951
ORNL-1221	Period Ending November 15, 1951
ORNL-1280	Period Ending March 15, 1952
ORNL-1318	Period Ending July 1, 1952
ORNL-1424	Period Ending October 1, 1952
ORNL-1478	Period Ending January 1, 1953
ORNL-1554	Period Ending March 31, 1953
ORNL-1605	Period Ending July 31, 1953
ORNL-1658	Period Ending October 31, 1953
ORNL-1678	Period Ending January 31, 1954
ORNL-1753	Period Ending April 30, 1954
ORNL-1772	Period Ending July 31, 1954
ORNL-1813	Period Ending October 31, 1954
ORNL-1853	Period Ending January 31, 1955
ORNL-1895	Period Ending April 30, 1955
ORNL-1943	Period Ending July 31, 1955
ORNL-2004	Period Ending October 31, 1955
ORNL-2057	Period Ending January 31, 1956
ORNL-2096	Period Ending April 30, 1956
ORNL-2148	Period Ending July 31, 1956
ORNL-2222	Period Ending October 31, 1956
ORNL-2272	Period Ending January 31, 1957
ORNL-2331	Period Ending April 30, 1957
ORNL-2379	Period Ending July 31, 1957
ORNL-2432	Period Ending October 31, 1957
ORNL-2493	Period Ending January 31, 1958
ORNL-2561	Periods Ending April 30 and July 31, 1958
ORNL-2654	Period Ending October 31, 1958